CRANFIELD INSTITUTE OF TECHNOLOGY

SCHOOL OF MECHANICAL ENGINEERING

PhD Thesis

Academic Year 1985-86

A. I. OBANOR

Simulation of the Performance of HVAC Systems and Central Plant for Energy Calculations: A Component Based Modelling Approach

Supervisor A. M. Jones

November 1985

SUMMARY

In recent years, operational prediction and optimisation of heating, ventilating and air conditioning (HVAC) systems and central plant to minimise the energy required to maintain building indoor conditions have become increasingly important. To effectively design and implement an energy management program for building energy systems, a simulation study must be performed.

This thesis describes research conducted into the development of a modular simulation program for analysing the performance of HVAC systems and central plant. The computer program uses a quasi-steady state modelling approach and is able to simulate a wide variety of systems which are configured using available component models.

Steady state mathematical models of HVAC components are developed using fundamental heat and mass transfer principles, laws of conservation of mass and energy and where appropriate empirical data. The component models are formulated to allow for the effects of various control strategies on the performance of systems and plant to be investigated.

The program is applied to simulate a part of the Collins' Building variable air volume (VAV) air conditioning system and a hypothetical central cooling plant. The results of the simulation exercises are presented and analysed. The issue of validation and building energy simulation models is discussed. Conclusions are drawn and recommendations for further work are made.

ACKNOWLEDGEMENTS

The author is very grateful to Dr. A. M. Jones for all his help and guidance throughout the duration of the project.

Special thanks are due to the staff of Amazon Energy Limited for providing the facilities for conducting this study and particularly Mr Suresh Nalluri for his work on the graphical routine package.

I am grateful to the Association of Commonwealth Universities and the University of Benin for providing financial support for this work. The study leave granted by the latter is also highly appreciated.

Finally, sincere thanks are due to Miss D. J. Roberts for producing some of the diagrams and Mrs Jenny Eveling for typing this thesis.

LIST OF CONTENTS

LIST OF FIGURES

LIST OF TABLES

CHAPTER 1

INTRODUCTION

1.1 BACKGROUND

With growing energy problems facing the world, it is important that we use our natural energy resources as efficiently as possible. The implementation of a rational energy conservation policy, apart from reducing the depletion rate of our energy resources, will extend the time available to develop alternative energy supplies to replace fossil fuel combustion.

One of the main fields of primary energy consumption is heating and cooling of buildings. A Building Research Establishment report (Ref. 1) estimates that about 40 to 50% of the consumption of primary energy in the United Kingdom takes place in building services and that over half of this energy is consumed in the domestic sector. In the United States of America, buildings account for about one third of total energy consumption (Ref. 2). Generally wasteful building design and operating procedures have been followed in the past. Consequently, there is a significant potential for energy savings. Energy experts have indicated that by exploiting currently available technology, the energy consumption in new buildings can be reduced by 30 to 50% and 10 to 30% in existing buildings, with no significant loss in standard of living, comfort, or convenience (Ref. 3). For non residential buildings, the United States Federal Energy Administration (Ref. 4) estimates that savings of up to 40% can be achieved by altering the buildings, their heating, ventilating and air conditioning (HVAC) systems and equipment, and their operating procedures. This potential for savings has been verified by various groups (Refs. 5 and 6).

The key to improving the thermal performance of buildings and the efficient use of energy for heating and cooling is the ability to accurately predict at the pre-construction stage, the performance of the building envelope and plant, and to assess the consequences of operating the building in different ways.

This type of information is required at many levels of the building industry; from the individual designer wishing to test the performance of a particular building to government policy makers wishing to evaluate the likely effectiveness of proposed incentive schemes or mandatory requirements aimed at reducing energy consumption.

1.2 ESTIMATING BUILDING ENERGY USAGE

The energy usage of a building is affected by a complex interaction between its design, operation, and the local environment. The effects of changing individual design features or operational parameters cannot usually be isolated and have to be studied in relation to the overall design and operation of the building.

A building with a specified range of indoor conditions will have a net heat and moisture gain or loss because of internal loads and the building's interaction with the environment. This results in a heating or cooling load on the building. The purpose of the HVAC system is to compensate for the building load so that the specified range of indoor conditions can be maintained. The HVAC system in turn impose requirements on the primary heating and cooling system (central plant) serving the building. Thus energy is utilised in the building to operate the environmental control system and other service equipment (e.g. lighting, elevators or escalators).

Estimating the energy requirements of a building involves the following steps, namely loads calculation, secondary system simulation and primary system simulation. The loads calculation step involves the estimation of the loads experienced by the building spaces. The secondary system simulation step involves calculation of the energy or thermal requirements of the secondary system as they respond to the building loads calculated previously. The primary system simulation step involves the calculation of the amount of fossil fuel or electrical energy required by the primary system and its auxiliaries to satisfy the loads imposed by the secondary system.

Each of these calculation steps may be carried out very simply to achieve approximate results, or they may be performed with increasing degree of complexity and sophistication as more accurate and more refined determination of system performance is desired. Numerous building energy calculation procedures are currently available and they encompass methods from simple degree day procedures to comprehensive and computerised procedures which simulate building heat transfer and system/equipment performance on a minute by minute basis. A detailed review of various building energy calculation procedures is carried out in Chapter 2. However, it is the opinion of the author that for routine energy analysis, computer programs carrying out these calculations on a minute by minute basis are too sophisticated. Their application require the use of large scale computer systems, input preparation time and computer usage costs. Thus, there is a definite need for a procedure that is simple to use, reasonably accurate and which accounts for the significant parameters affecting building energy usage.

1.3 OBJECTIVE OF CURRENT RESEARCH

The objective of the current research is to develop a set of techniques which can be used to produce more energy efficient and cost effective buildings in terms of the provision of internal environmental conditions. These techniques should give analytically significant results for buildings with a wide variety of building characteristics, HVAC systems and equipment, and operational parameters.

The developed system should be capable of being used efficiently by building or HVAC designers. It must therefore be relatively simple and straight forward to use and be capable of running on a modestly priced computer.

1.4 OUTLINE OF THE THESIS

The work carried out in accomplishing the above tasks has been laid out as follows:

A review of various procedures for estimating the energy usage of buildings is given in Chapter 2. These procedures range from single measure methods, such as the degree day method for estimating heating energy requirements of buildings to detailed simulation methods for estimating the energy consumption of the various components of building energy systems.

Component models of building energy systems are presented in the next two chapters. Steady state mathematical models of components of secondary or HVAC systems are presented in Chapter 3 while those for primary systems or central plant are described in Chapter 4. The philosophy behind the development of these models is not to attempt a highly accurate and complex analysis, but a simple, practical and reasonably accurate simulation of the thermal performance of the components of HVAC systems and central plant.

Component based system simulation techniques are reviewed in Chapter 5. Using the component models developed in Chapters 3 and 4, a modular quasi-steady state simulation program, SYSPAN, was developed for use in simulating the performance of HVAC systems and central plant. Results obtained using SYSPAN to simulate a part of the Collins' Building Variable Air Volume Air Conditioning System and a hypothetical central cooling plant are presented and analysed. The issue of validation and building energy simulation models is discussed.

Conclusions and recommendations for further work are presented in Chapter 6.

REFERENCES FOR CHAPTER ONE

1) BUILDING RESEARCH ESTABLISHMENT — "Energy Consumption and Conservation in Buildings", Building Research Establishment Report 191, July 1976.

2) HIRST, E. — "Buildings Energy Use: 1950 - 2000", Energy Conservation in Commercial and Residential Buildings, Chapter. 1.

3) CHIOGIOJI, M. H. OURA, E.N. — Energy Conservation in Commercial and Residential Buildings", 1982. Published by Marcel Dekker, Inc.

4) FEDERAL ENERGY ADMINISTRATION — "Energy Conservation on Campus, Volume 1 Guidelines", Federal Energy Administration, Office of Energy Conservation and Environment, Stock No. 041-018-00125-5, Superintendent of Documents, U.S. Government Printing Office, Washington D.C., December 1976.

5) "Energy Conservation Retrofit for Existing Public and Institutional Facilities", Prepared for NSF/RANN by Public Technology Incorporated, Washington D.C., 1977.

6) "Energy Management for Colleges and Universities", ACE/APPA/NA CUBO Energy Task Force, Washington D.C., 1977.

CHAPTER 2

REVIEW OF PROCEDURES FOR ESTIMATING THE ENERGY USAGE OF BUILDINGS

NOMENCLATURE

Symbol	Description	Unit
a	average temperature rise in building which is maintained by miscellaneous gains alone.	K
C_C	annual energy cost for cooling	£
C_D	empirical correction factor for heating effect vs. 18.3°C degree days	
C_h	annual energy cost for heating	£
COP	coefficient of performance	
CV	calorific value of fuel	MJ/kg
c	intercept on the y-axis as defined by Equation 2.7.	kW
D_d	seasonal degree day total for base d.	
$D_{15.5}$	standard seasonal degree day total	
$D_{18.3}$	seasonal degree day total for base 18.3°C	
E	fuel or energy consumption for the estimate period.	m^3 or kWh
E'	average hourly energy demand	kW
E_l	uncorrected equivalent hours of full load operation	h

Symbol	Description	Unit
E_2	corrected equivalent hours of full load operation	h
F	fuel cost per unit mass	£/kg
F_d	ratio of degree days for base d to the degree days for base 15.5°C	
F_1	factor allowing for the length of the working week as used in Equation 2.5	
F_2	factor allowing for response of building and plant as used in Equation 2.5.	
F_3	factor allowing for the length of the working day as used in Equation 2.5	
f	percentage frequency of occurence of climate factor	%
G	electricity cost per kWh	£/kWh
H_L	design heat loss	kW
h	hours of plant operation	h
k	correction factor as defined in Equation 2.1	
m	slope as defined by Equation 2.7	kW/°C
m_f	amount of fuel consumed	kg
Q_r	net annual heat requirement	kWh

Symbol	Description	Unit
t_b	base temperature	^oC
t_i	design indoor dry bulb temperature	^oC
t_{ic}	intermediate cooling temperature bin midpoint	^oC
t_{ih}	intermediate heating temperature bin midpoint	^oC
t_o	design outdoor dry bulb temperature	^oC
t_{pc}	peak cooling temperature bin midpoint	^oC
t_{ph}	peak heating temperature bin midpoint	^oC
V	heating value of fuel, units consistent with E	
X	outside air dry bulb temperature	^oC
Y	load	kW
η_b	boiler firing efficiency	%
η_s	seasonal efficiency of heating plant	%
ø	plant load	kW

2.1 INTRODUCTION

Effective energy conservation in buildings requires the availability of energy estimating procedures that can quantitatively evaluate the effects of various design and operational parameters. There are a variety of energy estimating procedures presently available with differing level of sophistication (Ref. 1). The sophistication of the calculation procedure can often be inferred from the number of separate ambient conditions and/or time increments used in the calculations. Thus a simple procedure may use only one measure, such as annual degree days, and will be appropriate only for simple systems and applications. Such methods are called single-measure methods. Improved accuracy may be obtained by the use of more information, such as the number of hours anticipated under particular conditions of operation. These methods of which the "bin method" is the most well known are referred to as simplified multiple-measure methods. The most elaborate methods currently in use perform energy balance calculations at each hour over some period of analysis, typically one year. These are called the detailed simulation methods, of which there are a number of variations. These methods require hourly weather data as well as hourly estimates of building operational parameters. Although not widely accepted as necessary, some procedures carry out the calculations at even smaller time intervals.

2.2 SINGLE MEASURE METHODS

Single-measure methods may be divided into those applicable to estimating (1) heating energy requirements and (2) cooling energy requirements. Generally speaking, those for heating are of longer standing and are more refined than those for cooling.

2.2.1 Heating Energy

The traditional degree day procedure for estimating heating energy requirements has been in use for about 50 years. It is based on the assumption that, on a long-term average, solar and internal gains will offset heat loss when the mean daily outdoor temperature is 18.3°C and that fuel consumption will be proportional to the difference between the mean daily temperature and 18.3°C. This basic concept can be represented in an equation stating that energy consumption is directly proportional to the number of degree days in the estimation period. The equation has undergone several stages of refinement **(Refs. 2, 3 and 4)** in an attempt to make it agree as closely as possible with the available measured data on an average basis. The currently recommended form is

$$E = \frac{H_L \times D_{18.3} \times 24 \times C_D}{(t_i - t_o) \times k \times V} \qquad (2.1)$$

where

E = fuel or energy consumption for the estimate period (m^3 or kWh)

H_L = design heat loss (kW)

$D_{18.3}$ = number of 18.3°C degree days for the estimate period.

t_i = design indoor dry bulb temperature (°C).

t_o = design outdoor dry bulb temperature (°C)

k = a correction factor which includes the effects of rated full load efficiency, part load performance, oversizing and energy conservation devices.

V = heating value of fuel, units consistent with that of E.

C_D = empirical correction factor for heating effect vs. 18.3°C degree days

Traditionally, degree days for heating are calculated at a base temperature of 18.3°C. In theory, the degree-day base temperature should equal the building's balance point temperature which is defined as the exterior temperature at which the heat losses through the shell of the building at the specified indoor temperature exactly match its internal gains with no contribution from the heating system. With the advent of increasing energy prices, building owners are reducing thermostat settings and increasing insulation levels. As a result, the heating balance temperatures of buildings may begin to differ from the traditional 18.3°C degree-day base. This difference may result in underestimating the effect of conservation retrofits or overestimating the annual heating requirements for new buildings.

Recognising this deficiency, the United States National Climatic Centre has published degree days to a wide range of base temperatures (Ref. 5). The degree days can be used in Equation 2.1 with the C_D factor eliminated. Kusuda et al. (Ref. 6) have compared energy requirements for residential buildings calculated using the variable-base degree day procedure and DOE-2 building energy analysis program and found close agreement between them.

For application in Britain, the IHVE Guide Section B18 (Ref. 7) describes a scheme of calculation suggested by Billington (Ref. 8) for estimating fuel consumption for space heating. This entails modifying degree days to allow for different base temperatures, calculating the equivalent hours of operation at full load and making allowances for such factors as the length of the working week, the response of the building and plant and the length of the working day. The annual heat requirement is then calculated by multiplying the corrected equivalent hours of operation at full load by the building heat loss rate. The calculation scheme is outlined below.

Degree day reports used by the Department of Energy show the monthly total of degree days in each month of the heating season calculated from a base of 15.5°C. The base temperature is given by

$$t_b = t_i - a \qquad (2.2)$$

where

t_b = base temperature (°C)

a = average temperature rise in building which is maintained by miscellaneous gains alone (K).

The seasonal degree day total for the building is given by

$$D_d = F_d D_{15.5} \qquad (2.3)$$

where

D_d = seasonal degree day total for base d.

$D_{15.5}$ = standard seasonal degree day total for the region in Britain in which the building is sited.

F_d = ratio of degree days for base d to the degree days for base 15.5°C and can be obtained from Table B 18.13 of Ref. 7.

The uncorrected equivalent hours of full load operation is given by

$$E_1 = \frac{24 \times D_d}{t_i - t_o} \qquad (2.4)$$

where

E_1 = uncorrected equivalent hours of full load operation (h).

Further allowances can be made for the length of the working week (F_1), response of building and plant (F_2) and the length of the working day (F_3). The factors F_1, F_2 and F_3 can be obtained from Ref. 7. The corrected equivalent hours of full load operation is given by

$$E_2 = F_1 \times F_2 \times F_3 \times E_1 \qquad (2.5)$$

where

E_2 = corrected equivalent hours of full load operation (h).

The net annual heat requirements is given by

$$Q_r = H_L \times E_2$$

where

Q_r = net annual heat requirement (kWh). To obtain the annual fuel requirement, we must know the seasonal plant efficiency and calorific value of the fuel. The amount of fuel consumed over the heating season is given by

$$m_f = \frac{Q_r \times 360}{\eta_s \times CV} \qquad (2.6)$$

where

m_f = amount of fuel consumed (kg)
η_s = seasonal efficiency of heating plant (%)
CV = calorific value of fuel (MJ/kg).

The degree day method gives fairly reliable results for buildings, for example, dwellings, where the envelope transmission and infiltration are the dominant factors contributing to the building load. In those buildings with highly varying internal loads, sophisticated control systems, complex air conditioning systems or plant arrangements, this method is inadequate.

2.2.2 Cooling Energy

Single - measure methods for estimating cooling energy are less well established than those for heating. This is because the indoor-outdoor temperature difference under cooling conditions is typically much smaller than under heating conditions. As a result, cooling loads depend more strongly on such factors as solar gain and internal loads (besides temperature) than do heating loads. Since these loads are highly dependent on specific building features, attempts to correlate cooling energy requirements against a single climate parameter have not been highly successful.

None-the-less two procedures, the Equivalent Full Load Hours Method and the Cooling Degree Day Method have emerged and are widely used (Ref. 1).

2.2.2.1 Equivalent Full Load Hours Method

This procedure consists of using an estimate, based on the local experience, of the ratio of annual cooling energy requirements to the rated capacity of the cooling equipment. Equivalent full load hours is equal to the number of hours that the cooling equipment will have to operate at full load to consume the same amount of energy when operated under typical conditions for a complete year.

Equivalent hours of operation for cooling equipment have been measured in office buildings (Ref. 9) while for various locations in the United States of America, equivalent full load hours based on an indoor temperature of 23.89°C have been published (Ref. 1). The annual cooling energy consumption of the building is calculated by multiplying the peak cooling load by the equivalent full load hours. However, Stamper (Ref. 10) has suggested that reasonable estimates of the annual kilowatt-hour cooling consumption for the particular system can be obtained by multiplying the number of hours by the air conditioner name plate rating.

This procedure ignores all the operational control parameters of the particular systems serving the building which heavily influence energy usage in non-residential buildings. However, it provides crude estimates of the energy usage of buildings.

2.2.2.2 Cooling Degree Day Method

The cooling energy requirement for residential buildings is estimated in the same manner as described in section 2.2.1 for predicting heating energy requirement. Cooling degree days to base temperature 18.3°C and for other base temperatures for various locations in the United States of America are available (Ref. 5).

2.3 SIMPLIFIED MULTIPLE MEASURE METHODS

The fact that single measure methods do not consider all factors that significantly affect energy use in buildings have led to the development of more sophisticated methods. These methods including the Basic Bin Method, Modified Bin Method and the Simplified Graphical Procedure are known as Simplified Multiple-Measure Methods. They consider more than one environmental parameter when estimating building energy use and are generally adequate in the early phases of a building design.

2.3.1 Basic Bin Method

The basic bin method consists of performing an instantaneous energy calculation at many different outdoor dry bulb conditions and multiplying the result by the number of hours of occurence of each condition (Ref. 1). The bins are usually 2.78°C in size and are often collected in three daily 8-h shifts. The procedure can account for the part load performance of HVAC equipment and has been specifically used for analysis of heat pump systems. Additionally by performing separate calculations for different time periods, variations of indoor loads with time and operating schedules of HVAC systems can be considered

The envelope loads at the midpoint of each of the temperature bins can be obtained by linear interpolation between the design heating and cooling envelope loads. Refinements to the procedure include separate consideration of indoor loads and the use of mean coincident wet bulb temperature data, for each temperature bin, to calculate the latent cooling loads for infiltration and ventilation.

The principal drawback of this procedure is the interpolation between end points corresponding to the summer and winter design envelope loads. The summer loads are based on the design hour and do not account for the variation in the transmission and solar loads which, on the average, are much lower than the design hour values. These loads could be further reduced by cloud cover and other effects. Conversely the winter design envelope loads ignore solar effects which could significantly reduce the total losses through the envelope.

Because of these limitations, the standard bin method has limited applicability in estimating building energy usage, particularly for commercial buildings. A refinement of the standard bin method, the Modified Bin Method (Ref. 11), which addresses the questions of time dependent and solar loads has been developed.

2.3.2 Modified Bin Method

A detailed description of the modified bin method is given in Ref. 11. The method recognises that the building and zone loads consist of time dependent loads (solar and scheduled loads) and temperature dependent loads (conduction and infiltration). To compute the energy consumption, two or more computational periods are selected, normally representing the occupied and unoccupied periods. For each period, the time dependent loads are averaged and added to the conduction loads such that the load is characterized as a function of outside air temperature for the calculated period.

The modified bin method utilises bin weather data. This data may be obtained from Air Force Manual 88-29, Engineering Weather Data (Ref. 12).

In expressing building loads as a function of outdoor temperature, the following assumptions are made:

(i) All exterior loads can be expressed as a linear function of outdoor temperature. The exterior loads include transmission (including structural storage effects), infiltration and solar loads. The transmission and infiltration loads are assumed to be a "piecewise" linear function (Fig. 2.1) of outdoor temperature, while the solar load is assumed to have a linear dependence on outdoor temperature over the entire outdoor temperature range for the location.

(ii) On a daily basis the interior loads can be averaged over the "system on" or "system off" time periods. Time dependencies resulting from scheduling are either averaged over a selected period or multiple calculation periods are established. The duration of a calculation period determines the number of bin hours included in it. Normally, two calculation periods, representing occupied and unoccupied hours, are sufficient, although any number can be used.

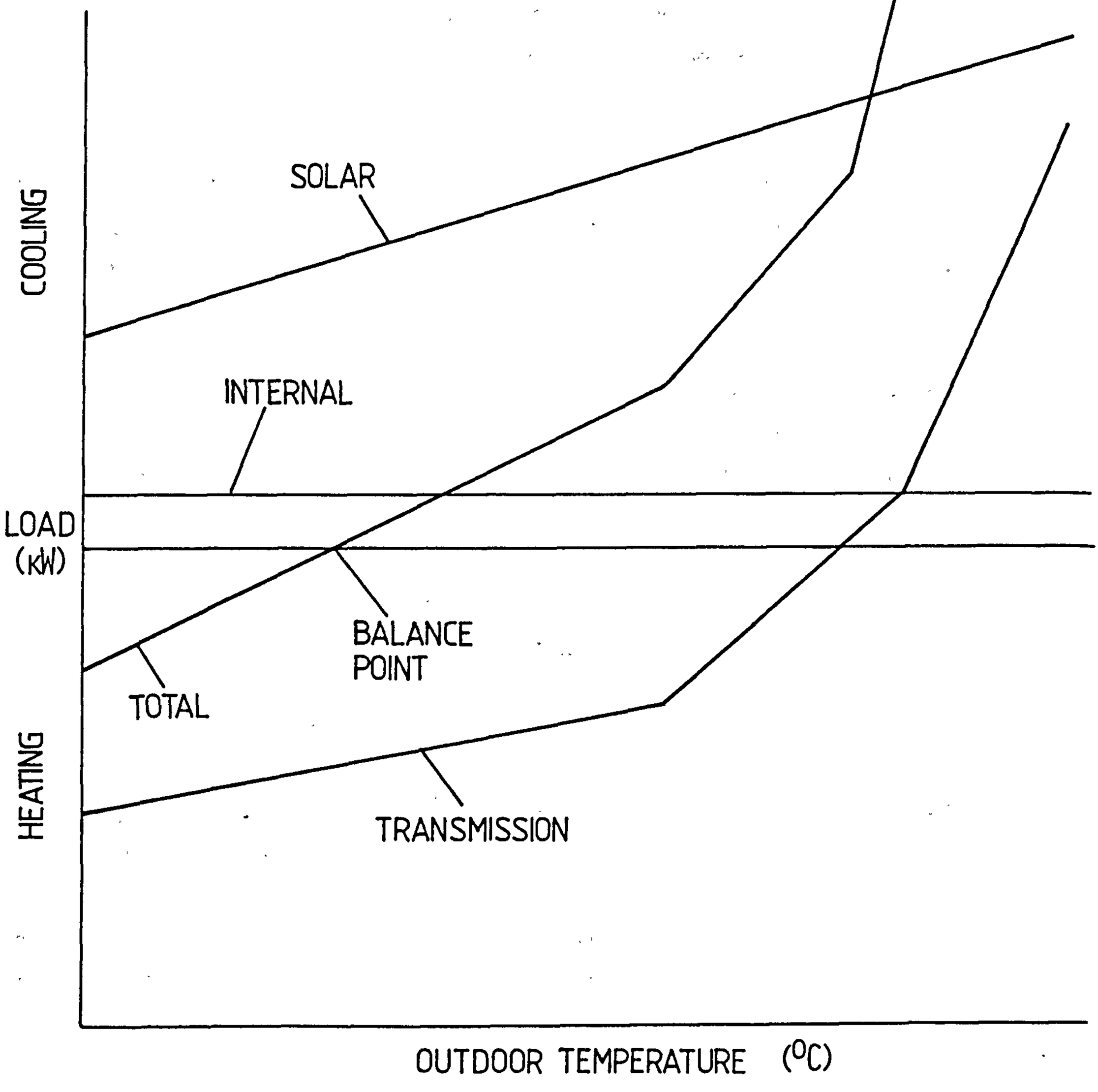

FIG. 2·1 VARIATION OF LOADS WITH OUTDOOR TEMPERATURE

The "occupied" period is defined as the operating period when the systems are operating normally and providing heating and cooling. The "unoccupied" period is the operating mode when the cooling equipment has been turned off and the heating has been set back to a lower temperature. The procedure assumes that the interior loads experienced during each of these periods can be averaged over the duration of the respective period.

The procedure begins with a load estimation for the occupied and unoccupied operating modes. Although these calculations are similar to the design type calculations, they use averaged internal and solar loads, and are also performed at intermediate temperatures.

The load calculations are performed at four temperature bins judged to be significant for the given building and location. The bins are identified by their midpoint temperatures (e.g the 31.94 - 34.72^{o}C bin is identified as the 33.33^{o}C bin), and represent the following four temperature bins.

- Peak Cooling, t_{pc}
- Intermediate Cooling, t_{ic}
- Intermediate Heating, t_{ih}
- Peak Heating, t_{ph}

Peak Cooling, t_{pc}, is usually the midpoint of the highest temperature bin occurring at the location.

Intermediate Cooling, t_{ic}, represents the lowest temperature bin in which the envelope transmission and outdoor air sensible loads impose cooling loads on the building.

Intermediate Heating, t_{ih}, represents the midpoint of a temperature bin where the net building loads change from heating to cooling loads. It is near the balance point for exterior zones, and also the temperature where an economizer cycle is adequate for meeting any building cooling loads.

Peak Heating, t_{ph} is usually the midpoint of the lowest temperature bin occuring at the location.

An alternate approach to developing the loads is to develop an equation of the load profile. This results in a system of linear equations of the form

$$Y = mX + c \qquad (2.7)$$

where

Y represents load
m is slope
X is outside air temperature
c is the intercept

To calculate the average or "diversified" building loads, the internal loads are averaged over the occupied and unoccupied time periods. Loads resulting from solar gains through glazings are calculated by determining a weighted-average solar load for a summer day and a winter day, each of average cloudiness, and then establishing a linear relationship of this solar load as a function of outdoor temperature. The effect of heat transfer through sunlit roofs and walls is included in the transmission load by using the 24 hour time averaged values of the solar component of the cooling load temperature difference (CLTD). The CLTD's approximate the transient effects of building mass.

Once a total load profile as a function of outdoor temperature is determined for the occupied and unoccupied periods, the performance of the HVAC system is simulated. This results in an estimation of the heating and cooling coil loads and fan energy consumption. With the coil loads known as a function of outside air temperature, the primary system input (ie chillers, boilers, etc) is computed for each load with component models which include the effects of part load operation and ambient conditions. The annual energy consumption is then determined by multiplying the frequency of occurence of bin weather data at each ambient conditions by the primary system power input and summing for all bins.

comparative studies have shown that the modified bin method gives results that are comparable to those obtained from comprehensive computer programs **(Refs. 6, 13 and 14).** However, the inability to adequately address the effects of shading and building mass and the approximate nature of correlating time-dependent parameters to the outside temperature are significant limitations of this method.

2.3.3 Simplified Graphical Method

Graphical procedures that simplifies the estimation of annual energy requirements for intermediate and large-sized commercial and institutional buildings have been developed **(Refs 15 and 16).** The graphical method is based on three sets of graphs that correspond to the three elements of any valid energy estimating procedure namely, the loads calculation, the secondary system simulation and the primary equipment simulation. A separate set of graphs is required for each weather zone, building type and size range, HVAC system type, and a heating or cooling requirement. The simplified graphical procedure considers parameters given in Table 2.1.

TABLE 2.1

Parameters considered in Simplified Graphical Procedure

1) Building location and size
2) Peak envelope heating and cooling loads
3) Space temperature control settings (summer and winter)
4) All internal heat gains (including lighting)
5) Operating schedule for HVAC system
6) Type of HVAC system and its method of control
7) Outdoor air ventilation quantities
8) Heating and cooling equipment characteristics.
9) Auxiliary equipment characteristics

The procedure starts with the specification of building location, type and size. This identifies a set of graphs applicable to the building-size range and to a weather zone. From the selected graph set, the initial determination would be of the structural heating and cooling energy requirements using items 2 to 5 of Table 2.1 as input data.

The annual structural energy requirements represent the necessary heat gain or removal to maintain the prescribed temperatures for the building. They form the input to the next set of graphs, which are used to determine the required output of the heating and cooling equipment. The additional input information required in this step are items 6 and 7 of Table 2.1

A determination of the required output from the heating and cooling equipment serves to determine an annual equivalent coefficient of performance (COP) for that equipment. The COP is then used to determine the annual input energy requirement for the heating and cooling equipment.

The energy required by the auxiliary equipment, such as fans and pumps, is a function of HVAC system type, control and operation. The sum of HVAC equipment, the auxiliary, lighting and internal loads energy usage determines the total annual building energy use.

Although the simplified graphical procedure can provide analytically useful results when used for building energy analysis, the authors warn that it is not intended for use in situations requiring a high level of precision and accuracy.

2.3.4 Other Methods

Legg (Ref. 17) has developed a method originally described by Robertson (Ref. 18) to calculate the energy demands of air conditioning systems. The method is to establish the relationship between energy demands and an appropriate climate factor and then to integrate this with the annual frequency distribution of the climate factor.

This is illustrated in Fig 2.2 where plant, load $\emptyset$, is plotted against the climate factor for which there is a known percentage frequency of occurence, f. The average hourly energy demand, E' is then given by the numerical integration:

$$E' = \frac{1}{100} \Sigma(f \times \emptyset) \qquad (2.8)$$

where

E' = average hourly energy demand (kW)

f = percentage frequency of occurence of climate factor (%)

$\emptyset$ = plant load (kW)

From this calculation, the annual energy costs may be obtained, e.g. for heating using fossil fuel:

$$C_h = \frac{E' \times h \times F \times 360}{\eta_b \times CV} \qquad (2.9)$$

and for a refrigeration plant:

$$C_c = \frac{E' \times h \times G}{COP} \qquad (2.10)$$

where

C_h = annual energy cost for heating (£)

h = hours of plant operation (h)

F = fuel cost per unit mass (£/kg)

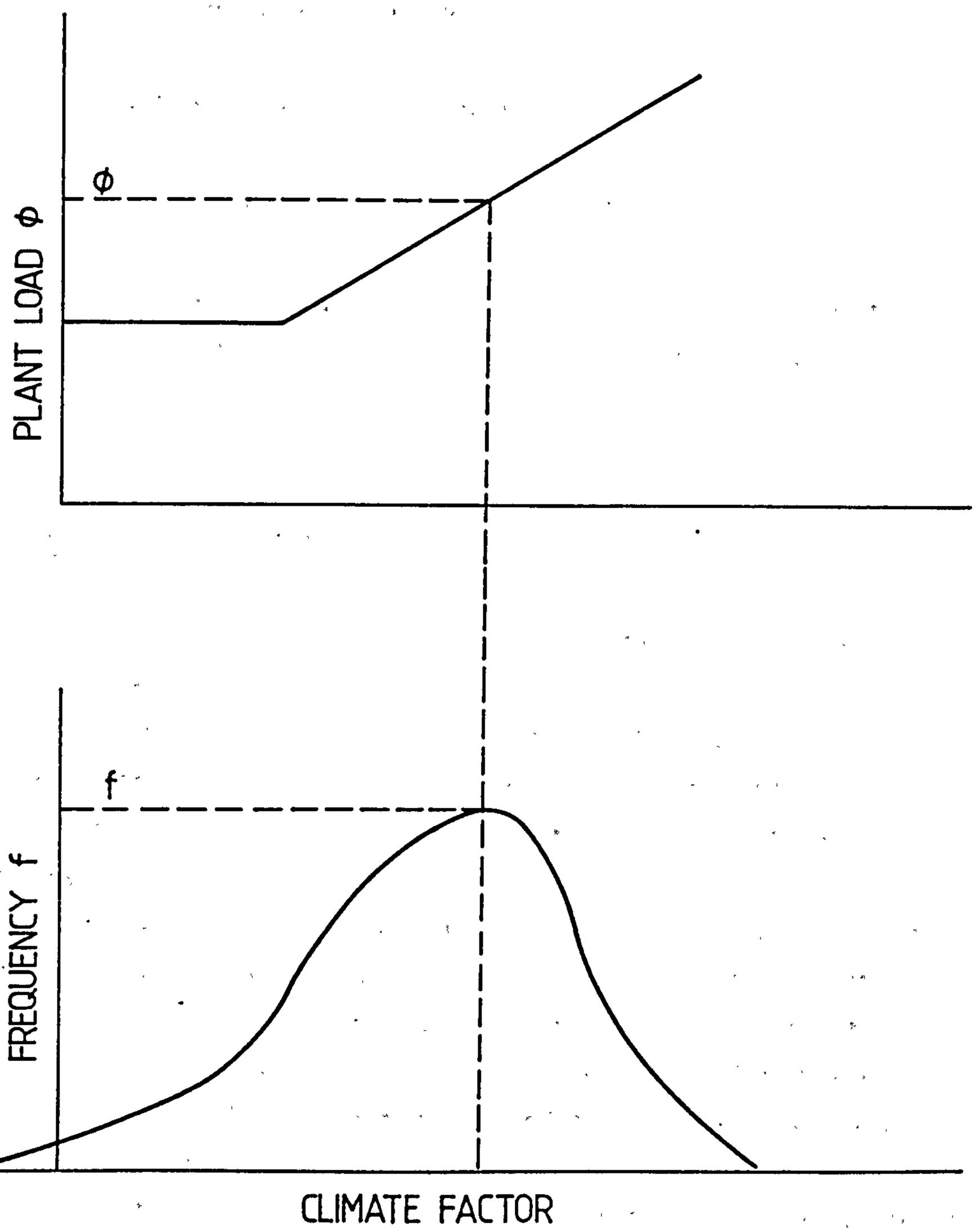

FIG. 2.2 PLANT LOAD Φ AND FREQUENCY OF OCCURENCE f vs CLIMATE FACTOR.

CV = calorific value of fuel (MJ/kg)

G = electricity cost per kWh (£/kWh)

COP = Coefficient of performance

C_C = annual energy cost for cooling (£)

As this method has some similarity with the bin method, it can only provide approximate estimates of the energy consumption of buildings.

2.4 DETAILED SIMULATION METHODS

The wide-ranging and constantly changing internal and external factors which determine the thermal loads on commercial and industrial buildings suggest the need for frequent evaluation of those factors to obtain reasonably accurate estimates of annual energy consumption. The high peak internal heat loads in many commercial modern buildings make it necessary to look at these load patterns at every hour of the day and for each different type of day during the year to evaluate the changing relationship between internal and external loads. The diversity and sophistication of modern energy distribution and control systems further contribute to energy consumption differences. Detailed simulation methods allow the engineer to account for the effect of these changing conditions and system complexities on the estimated energy usage. These methods require large amounts of complex and repetitive calculations. The computational requirements are too extensive to be performed manually, making computer applications of the procedures a necessity.

2.4.1 Building Energy Analysis Programs

A wide variety of building energy analysis computer programs based on the detailed simulation method, have been developed by governmental organizations, utilities, manufacturers, educational institutions and private consultants (Refs. 19, 20, 21 and 22). Analysis of building energy demands and consumption generally involves three major steps, namely thermal loads calculations, system simulation and central plant simulation. Most building energy analysis programs are organised in such a way that each of these steps is analysed by a separate subprogram. Some energy programs carry the program even one step further, into the economic analysis, and thus, consist of four principal computational programs: LOADS, SYSTEMS, PLANT and ECONOMIC analysis.

Lau et. al (Ref. 23) have reviewed the calculational methodologies employed by these building energy simulation programs. The LOADS program uses the building description information with weather data to calculate the heating and cooling loads of the building on an hourly (or smaller time increments) basis throughout an entire year. These heating and cooling loads, both sensible and latent components are responsive to the outside temperature, humidity, wind velocity, and solar conditions; schedules of people lights and equipment; infiltration; time delay of heat transfer resulting from massive walls, roofs and floors; and to the effect of building shading on solar radiation. The LOADS program prints out a set of reports including peak heating and cooling loads by zone and building and also generates an hourly file which will be used by the SYSTEMS program.

The SYSTEMS program uses the hourly load file output by the LOADS program as well as the user input system description to determine the heating and cooling demands of the secondary HVAC systems. In the simulation, the program takes into account the fresh air requirement, the HVAC system control schedules, supply and return fan power and the operating characteristics of the system in maintaining the space temperature and humidity set points. It is these hourly demands of heating and cooling that are passed on to the primary HVAC equipment or central plant.

The PLANT sub-program takes the output of the SYSTEMS sub-program and the user input of specific equipment to calculate the fuel and electrical requirements of the building and its energy systems. The simulation takes into account the part load characteristics of the primary equipment, user specified priorities for distribution of the tasks among the several components, and their operational schedules.

The ECONOMIC sub-program combines the energy consumption by the building and its energy systems with pertinent economic input to perform the life cycle analysis. The input data generally includes building and equipment cost, maintenance costs, utility, interest, and inflation rates. The final output gives the capital investment and the present value of the operational costs for each year over the project lifetime.

Fig 2.3 represents a simplified flow diagram for an energy analysis computer program. The diagram shows the basic function of each major model element on an input/output basis. It is worth noting the system "control interaction" path in this diagram representing the fact that capacity limits and/or control characteristics of the HVAC system can affect the space load. This implies that any variation in space temperature allowed by the system will cause the space sensible load to vary. Also, capacity limits and control characteristics of the central plant can cause variation in the performance of the HVAC system, and hence on loads.

2.4.2. Calculating Space Sensible and Cooling Loads

The calculation of space sensible and cooling loads is a key step in any building energy simulation. There are two widely used methods for doing these calculations:

1) The Heat Balance Method.
2) The Weighting Factor Method.

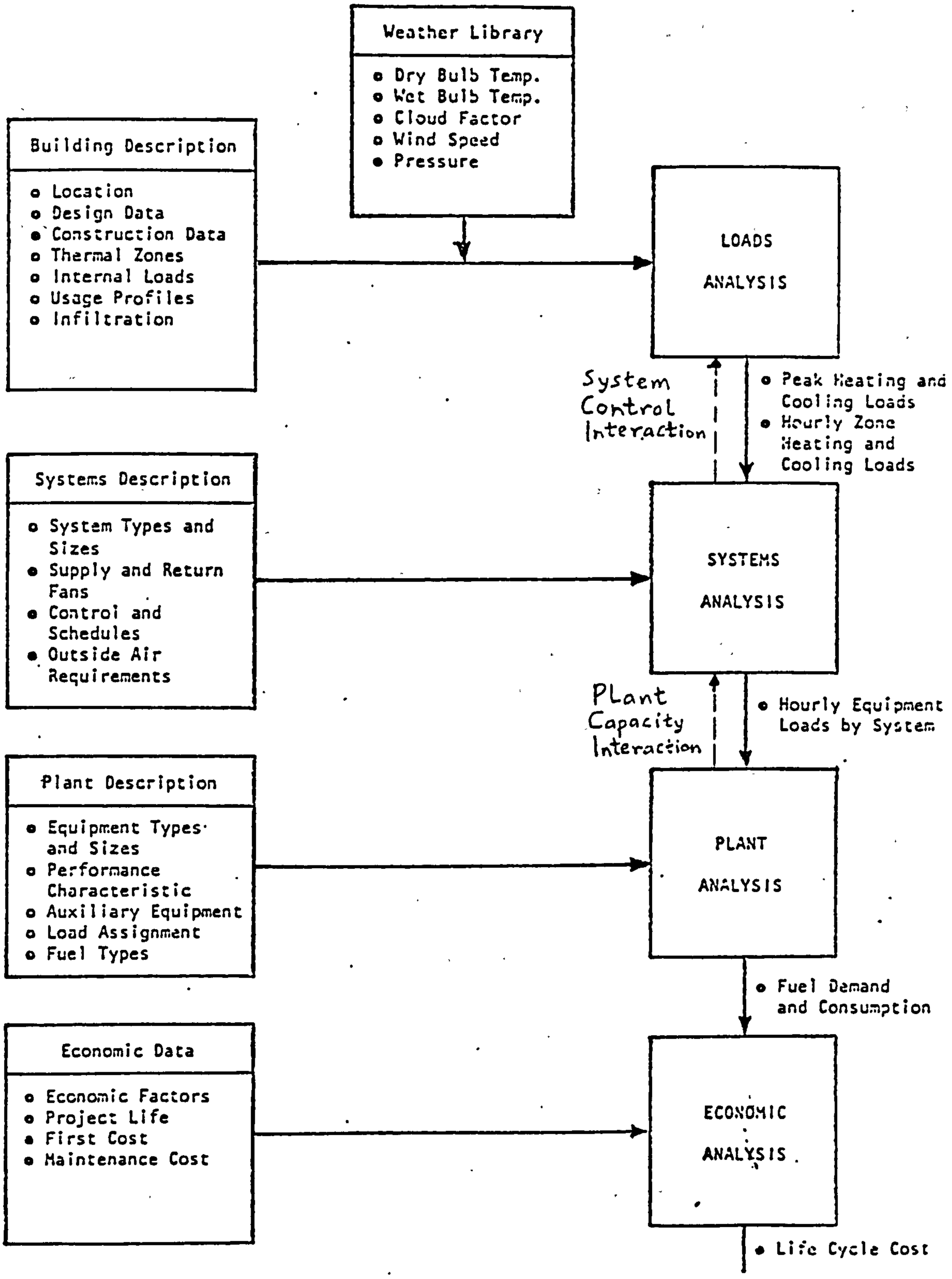

FIG. 2·3 SIMPLIFIED BUILDING ENERGY ANALYSIS COMPUTER PROGRAM FLOW DIAGRAM

The heat balance method for calculating net space sensible loads is the more fundamental of the two methods. Its development relies on the first law of thermodynamics (conservation of energy) and the principles of matrix algebra. Since there are fewer assumptions required than for the weighting factor method, it is also the more flexible of the two. However, the heat balance method requires more calculations at each point in the simulation process, and therefore is more costly in terms of computer resources.

The purpose of the heat balance method is to allow calculation of the net sensible heating/cooling load on the space air mass. The approach is to write a heat balance equation for each enclosing surface, and one for the room air. This set of equations take account of the conduction, convection and radiation heat exchange between the room air, surrounding surfaces, infiltration and internal energy sources. They are then solved for the unknown surface and air temperatures. Once these temperatures are known, they can be used to calculate the convective heat flow to or from the space air mass. The latter constitutes the heating or cooling load which must be met by the space conditioning equipment.

The weighting factor method of calculating space sensible load, first introduced by Mitalas and Stephenson, **(Refs. 24 and 25)**, is a simple but flexible technique that accounts for the important parameters affecting building energy flow. It represents a compromise between simpler methods, such as a steady-state calculation that ignores the ability of building mass to store energy, and more complex methods, such as complete energy-balance calculations. With this method, space heat gains at constant space temperature are determined from the building architectural data, the ambient weather conditions, and internal load profiles. These space heat gains are used, along with the characteristics and availability of heating and cooling systems for the building, to calculate air temperatures and heat extraction rates.

The weighting factor method is based on the assumption that the heat transfer processes occuring in a room can be described by linear equations; and thus that the superposition principle can be used for the calculation of cooling load and space temperature.

This means that the relationship between any excitation (e.g. power input to lights) and the corresponding component of the cooling load can be expressed in the form of a characteristic transfer function. Once all the transfer functions have been determined for a room, they can be used to calculate the response to any excitation. The weighting factors are a convenient way of representing these characteristic transfer functions of a room: they relate the Z-transforms of the excitations to the Z-transforms of the corresponding cooling load components.

Two sets of weighting factors are used: heat gain and air temperature. Heat gain weighting factors represent transfer functions which relate space cooling load to instantaneous heat gains. Air temperature weighting factors represent transfer functions that relates room air temperature to the net energy load of the room.

In the weighting factor method, a two-step process is used to determine the air temperature and heat extraction rate of a room or building zone for a given set of conditions. In the first step, the room's air temperature is assumed to be fixed at some reference value. This reference temperature is usually chosen to be the average air temperature expected for the room over the simulation period. Instantaneous heat gains are calculated on the basis of this constant air temperature. A space sensible cooling load for the room, defined as the rate at which energy must be removed from the room to maintain the air temperature fixed at its reference value, is calculated for each type of instantaneous heat gain. The cooling load generally differs from the instantaneous heat gain because some of the energy from the heat gain can be absorbed by walls or furniture and stored for later release to the air. At the end of the first step, the cooling loads from the various heat gains are summed to give a total cooling load for the room.

In the second step, the total cooling load is used - along with information on the HVAC system attached to the room and a set of air temperature weighting factors - to calculate the actual heat extraction rate and air temperature.

The actual heat extraction rate differs from the cooling load because, in practice, the air temperature can vary from the reference value used to calculate the cooling load or because of the HVAC system characteristics.

2.4.3 Simulating HVAC Systems and Central Plant

The purpose of simulating the HVAC system is to mathematically relate the rate of heating and/or cooling energy delivery to the space loads while the purpose of simulating the central plant or HVAC equipment is to calculate the energy used to meet the heating, cooling, and/or electrical loads of a building. Depending on whether relevant economic data is available, the costs associated with operating the central plant can also be determined. The dynamic performance of HVAC system and central plant under part load condition is the key factor for estimating the energy consumption of buildings.

Kusuda (Ref. 26) has reviewed the methodologies used for simulating the performance of HVAC systems and equipment and placed them in three major categories:

(1) The Truly Dynamic Simulation
(2) Detailed Heat and Mass Balance Simulation
(3) Quasi - Dynamic Simulation

In the truly dynamic performance simulation method, differential equations governing the time-dependent performance characteristics of building construction, control equipment, heat exchangers, fans, pumps, boilers and chillers are solved for very small time increments (in the magnitude of a minute) to represent the duty cycling of control equipment such as thermostats, humidistats and pressurestats. Exact minute-by-minute performance of the building thermal environment as well as the energy consumption and demand pattern of the HVAC systems and equipment is produced.

After the governing differential equations are set up, the finite difference solution must be obtained for each time step, requiring a large amount of computer time. Due to the small time increment and exact nature of the modelling concept used in the simulation algorithms, this is the only procedure by which the transient effect of HVAC control equipment, as well as the heat exchanger time response can be effectively simulated.

The detailed heat and mass balance simulation technique is to solve quasi-steady heat and mass balance equations for all of the major components of the HVAC systems for every hour; for example, leaving air temperature, specific humidity from the cooling coil, with the inputs being entering air temperature, specific humidity and flow rate, entering water temperature and flow rate. The degree of complexity required to determine the leaving air temperature, which depends upon the physical characteristics of the cooling and dehumidifying coils (such as the number of rows, number of face tubes, number of fins per metre, and the type of circuitry) varies with respect to the intent of the specific energy analysis procedure. In many cases, empirical algebraic equations to represent the approximate relationship among input and output are used. The same is true for other equipment, such as chillers, boilers, fans and pumps.

In the quasi-dynamic simulation method, the temperature and flow rate of water and air are assumed to be set at designated design values, so that no calculations are performed to determine the actual balance of the systems and equipment. For example, with this type of calculation, it may be assumed that the leaving air temperature from a set of cooling and dehumidifying coils is regulated to stay at a set value such as 13.0^{o}C, regardless of the flow rates and temperatures of air and water past the coils. Likewise, leaving water temperature of the chilled water from the cooling plant or cooled water from the cooling tower is always assumed to be known.

Most of the quasi-dynamic simulation procedures accurately balance the heating and cooling capacity of the equipment, the heating and cooling distribution capability of the HVAC systems, and the heating and cooling requirements of the spaces.

These procedures tacitly assume that the HVAC system is capable of self-balancing. This type of simplified assumption is, in many cases, reasonably accurate as long as the systems and equipment are properly sized and operated within their respective design limits. However, if the system is exceptionally oversized or undersized, such that the presumed temperature and flow at some of the components deviate from the actual balance point, this simplified method will fail. Because of its simplicity, this method has been used in the simulation procedures recommended by ASHRAE and adopted by the majority of existing HVAC system simulation procedures (Ref. 27)

Public domain building energy analysis programs such as BLAST (Ref. 28) and DOE-2 (Ref. 29) utilise elements of the modelling concepts described in the detailed heat and mass balance simulation and quasi-dynamic simulation techniques. The basic approach used in simulating the performance of building energy systems in these two programs can appropriately be called the fixed schematic technique. This technique consists of writing a calculational procedure which defines a given set of HVAC systems. The system schematic then is fixed (inherent in the source-code), with the user having some options usually limited to equipment performance characteristic, fuel types, and the choice of using or not certain components and control strategies. In modelling a system, the user defines only those parts required; the other components and subsystems are then deactivated and not included in the analysis.

The drawback of this approach is that distinct system schematics must be programmed separately. As additional systems are incorporated, the program's size increases and it costs more to run. This extra code must be maintained, thereby furthering the expense of the program. The fixed schematic technique, by its nature restricts the evaluation of innovative system configurations.

These disadvantages in the fixed schematic approach to system simulation and increased interest in special and innovative systems have led researchers to use the component based modelling approach in simulating building energy systems.

The component based modelling technique differs from the fixed schematic technique in that it is organised around components rather than systems. Each of the components is described mathematically and placed in a library for use in constructing systems. The user input includes definition of the system schematic in addition to equipment characteristics and capacities. Once all the components of a system have been identified and a mathematical model for each has been formulated, the components are connected together to form a network. The set of equations derived from the network formation are solved and the state of the air at the inlet and outlet boundaries of the components of the HVAC system are known. The energy required to satisfy the thermal demands of the coils and auxiliary equipment can be determined from the simulation of the central plant. System simulation computer programs, most of them proprietary, using the component based modelling technique have been developed or are being developed (Refs. 30, 31 and 32).

REFERENCES FOR CHAPTER TWO

1) ASHRAE — ASHRAE Handbook, 1981 Fundamentals Volume, Chapter 28, Energy Estimating Methods.

2) ASHRAE — ASHRAE Handbook and Product Directory, 1976 Systems Volume, Chapter 43, Energy Estimating Methods.

3) REEVES, G.A. — "Degree-Day Correction Factors - Basis for Values", ASHRAE Transactions, 1981, Volume 87 Part 1.

4) KELNHOFER, W.J. — "Evaluation of the ASHRAE Modified Degree Day Procedure for Predicting Energy Usage by Residential Gas Heating Systems", American Gas Association, 1979.

5) — "Degree Days to Selected Bases for First-Order Type Stations", United States Department of Commerce, National Climatic Centre, Asheville North Carolina, 1973.

6) KUSUDA, T. SUD, I. ALEREZA, T. — "Comparison of DOE-2 Generated Residential Design Energy Budgets with those Calculated by the Degree-Day and Bin Methods", ASHRAE Transactions, 1981, Volume 87 Part 1, pp 491-506.

7) IHVE — IHVE Guide Section B18-Owning and Operating Costs, IHVE 1970.

8) BILLINGTON, N.S. — "Estimation of Annual Fuel Consumption", Journal of the Institution of Heating and Ventilating Engineers, November 1966, Volume 34.

9) MILBANK, N.O. DOWDALL, J.P. SLATER, A. — "Investigation of Maintenance and Energy Costs for Services in Office Buildings", Journal of the Institution of Heating and Ventilating Engineers, October 1971, Volume 39.

10) STAMPER, E. "Air Conditioning Usage Study-Equivalent Rated Load Hours", ASHRAE Journal, June 1979, Volume 21 No. 6, pp. 43-45.

11) KNEBEL, D.E. "Simplified Energy Analysis Using the Modified Bin Method", Prepared for ASHRAE, 1983.

12) "Air Force Manual 88-29, Engineering Weather Data", Superintendent of Documents, Government Printing office, Washington, D.C. 26402.

13) KUSUDA, T. "A Comparison of Energy Calculation Procedures", ASHRAE Journal August 1981, Volume 24 No. 8, pp. 21-24.

14) SUD, I.
KUSUDA, T. "The Proposed TC4.7 Simplified Energy Analysis Procedure", ASHRAE Transactions 1982, Volume 88 Part 2, pp. 263-277.

15) SUD, I.
WIGGINS, R.W.
CHADDOCK, J.B.
BUTLER, T.D. "Development of the Duke University Building Energy Analysis Method (DUBEAM) and Generation of Plots for North Carolina", November 30, 1979, Report No. NCEI-0009.

16) SUD, I.
WIGGINS, R.W. "Development of a Simplified Graphical Procedure for Estimating the Energy Usage in Non-Residential Buildings", ASHRAE Transactions, 1983, Volume 89 Part 2A, pp. 29-48.

17) LEGG, R.C. "Analysis of Energy Demands of Air Conditioning Systems", The Heating and Ventilating Engineer, July/August 1977, pp.6-14.

18) ROBERTSON, P. "Evaluation of Air Conditioning Energy Costs", Building Services Engineer, Volume 42, November 1974.

19) ASHRAE "Bibliography on Available Computer Programs in the General Area of Heating, Ventilating, Air Conditioning and Refrigeration", Compiled and Prepared by Ronald H Howell and Harry J Sauer for ASHRAE, July 1980.

20) GROOMS, D.N. "A Directory of Computer Software Application: Energy", Report No. PB 264200, NTIS 1977.

21) "Proceedings of the Third International Symposium on the Use of Computers for Environmental Engineering Related to Buildings", Held at Banff, Alberta, Canada, May 10-12, 1978.

22) BSRIA "Directory of Building Services Technical Software", BSRIA Special Publication 1984.

23) LAU, H. AYRES, J.M. "Building Energy Analysis Programs", IEEE Winter Simulation Conference, Held at San Diego, California, December 3-5, 1979, pp 283-289.

24) MITALAS, G.P. STEPHENSON, D.G "Room Thermal Response Factors", ASHRAE Transactions, 1967 Volume 73 Part 1.

25) MITALAS, G.P. "An Experimental Check on the Weighting Factor Method of Calculating Room Cooling Load", ASHRAE Transactions, 1969, Volume 75 Part 2

26) KUSUDA, T. "Standards Criteria for HVAC Systems and Equipment Performance Simulation Procedures", ASHRAE Journal, October 1981, Volume 23 No. 10, pp. 25-28.

27) STOECKER, W.F. "Procedures for Simulating the Performance of Components and Systems for Energy Calculation", ASHRAE Task Group on Energy Requirements for Heating and Cooling of Buildings, 1975.

28) HITTLE, D.C. "BLAST, The Building Loads Analysis and System Thermodynamics Program, Version 2.0: User's Manual", Volume 1 Report E-153, United States Army Construction Engineering Research Laboratory, June 1979.

29) YORK, D.A.
TUCKER, E.F. "DOE-2 Reference Manual, Version 2.1", Los Alamos Scientific Laboratory; Report LA-7689-M/Report LBL-8706, Rev. 1, Lawrence Berkeley Laboratory, May 1980).

30) KELLY, G.E.
PARK, C.
CLARK, D.R.
MAY, W.B. "HVAC SIM +, A Dynamic Building/HVAC/Control Systems Simulation Program", Paper No. 14, Proceedings of the Workshop on HVAC Controls Modelling and Simulation, Held at the Georgia Institute of Technology, Georgia U.S.A. from February 2-3, 1984.

31) SOWELL, E.F.
TAGHAVI, K.
LEVY, H.
LOW, D.H. "Generation of Building Energy System Models", ASHRAE Transactions 1984, Volume 90 Part 1, pp. 573-586.

32) QUICK, J.P.
IRVING, S.J. "Computer Simulation for Predicting Building Energy Use", Proceedings of the 3rd CIB Symposium on Energy Conservation in the Built Environment, Dublin, April 1982.

CHAPTER 3

SIMULATION OF THE COMPONENTS OF HEATING, VENTILATING AND AIR CONDITIONING (HVAC) SYSTEMS

NOMENCLATURE

Symbol	Description	Unit
A_a	face area	m^2
A_{aa}	second virial coefficient for dry air	m^3/kg
A_{aw}	interaction coefficient for moist air	m^3/kg
A_c	minimum free-flow cross-sectional area	m^2
A_d	duct surface area	m^2
A_f	fin surface area	m^2
A_i, A_{ti}	inside surface areas	m^2
A_o, A_{to}	external surface areas	m^2
A_{tm}	tube mean surface area	m^2
A_{ww}	second virial coefficient for water vapour	m^3/kg
a	tube horizontal spacing	m
a,b,c,d	fan part load model coefficients (see Equation 3.126)	
B	See Equation 3.83	
BF	bypass factor of cooling coil	
C, C_c, C_h	capacity rate ratios	
C_{ac}, C_{ah}	airstream thermal capacities	kW/K
C_{max}	maximum of air or water thermal capacities	kW/K
C_{min}	minimum of air or water thermal capcities	kW/K
C_1, C_2	airside heat transfer coefficient constants	
c	tube vertical spacing	m
c_{pc}	cold fluid specific heat capacity	kJ/kg K
c_{pda}	specific heat capacity of dry air	kJ/kg K
c_{pma}	specific heat capacity of moist air	kJ/kg K
c_{ps}	specific heat capcity of water vapour	kJ/kg K
c_{pw}	specific heat capacity of water	kJ/kg K
D_h	coil hydraulic diameter	m
D_i	inside diameter of tube	m
D_o	outside diameter of tube	m
E, E_c, E_h	effectiveness of cooling or heating coil	

Symbol	Description	Unit
E_{hu}	effectiveness of recirculating water humidifier	
F_h	fin height	m
F_s	fin spacing	m
F_t	fin thickness	m
FFLP	fraction of full load power	
f_s	enhancement coefficient	
G	mass velocity	kg/m^2s
g	moisture content	kg/kg
g_{ai}	moisture content of inlet air to component	kg/kg
g_{ao}	moisture content of outlet air from component	kg/kg
g_{ma}	moisture content of mixed air	kg/kg
g_{oa}	moisture content of outside air	kg/kg
g_{ra}	moisture content of return air	kg/kg
g_{sa}	moisture content of supply air	kg/kg
g_{sm}	saturated air moisture content at t_{sm}	kg/kg
g_{ss}	moisture content of saturated air	kg/kg
g_z	zone air moisture content	kg/kg
g_1, g_2, g_3	moisture content of airstreams 1, 2 and 3 respectively	kg/kg
h	specific enthalpy of moist air	kJ/kg
h_a	specific enthalpy of dry air	kJ/kg
h_{ai}	specific enthalpy of moist air entering a component	kJ/kg
h_{ao}	specific enthalpy of moist air leaving a component	kJ/kg
h_{ffi}	fouling heat transfer coefficient	kW/m^2 K
h_{fg}	latent heat of evaporation	kJ/kg
h_{fgz}	latent heat of evaporation at zone conditions	kJ/kg
h_{fw}	specific enthalpy of water at t_w	kJ/kg
h_g	specific enthalpy of water vapour	kJ/kg
h_i	inside surface heat transfer coefficient	kW/m^2K
h_o, h_{of}, h_{ot}	outside surface heat transfer coefficients	kW/m^2K

Symbol	Description	Unit
h_{sm}	specific enthalpy of saturated air at t_{sm}	kJ/kg
h_{st}	specific enthalpy of steam	kJ/kg
h_w	water-side average film heat transfer coefficient	kW/m^2K
h_{wi}	specific enthalpy of air at t_{wi}	kJ/kg
h_{wsl}	specific enthalpy of water at t_{sl}	kJ/kg
h_1, h_2, h_3	specific enthalpies of airstreams 1, 2 and 3 respectively	kJ/kg
I_o, I	modified Bessel functions of the first kind and order 0 and 1 respectively	
J	Colburn J-factor	
K_o, K_1	modified Bessel functions of the second kind and order 0 and 1 respectively	
k	thermal conductivity	kW/m K
k_f	thermal conductivity of fin material	kW/m K
k_t	thermal conductivity of tube material	kW/m K
L	flow length of the heat exchanger	m
m_a	mass flow rate of air	kg/s
m_{a1}, m_{a2}, m_{a3}	mass flow rates of airstreams 1, 2 and 3 respectively	kg/s
m_c	mass flow rate of cold fluid	kg/s
$m_{c,max}$	maximum mass flow rate of cold fluid	kg/s
m_h	mass flow rate of hot fluid	kg/s
$m_{h,max}$	maximum mass flow rate of hot fluid	kg/s
m_{ma}	mass flow rate of mixed air	kg/s
m_{oa}	mass flow rate of outside air	kg/s
$m_{oa,min}$	minimum mass flow rate of outside air	kg/s
m_{ra}	mass flow rate of return air	kg/s
m_{sa}	mass flow rate of supply air	kg/s
m_{st}	mass flow rate of steam injected into the airstream	kg/s
m_w	mass flow rate of water	kg/s
$m_{wc,max}$	maximum mass flow rate of chilled water	kg/s
$m_{wh,max}$	maximum mass flow rate of hot water	kg/s
N_r	number of rows of tubes	

Symbol	Description	Unit
N_t	number of tubes per row	
NTU	number of transfer units	
NTU_c	number of transfer units for a heat exchanger using chilled water	
NTU_h	number of transfer units for a heat exchanger using hot water	
Nu_D	Nusselt number	
$P_{fa,s}$	fan static pressure	N/m^2
$P_{fa,t}$	fan total pressure	N/m^2
$P_{fa,v}$	fan velocity pressure	N/m^2
PLR	part load ratio (see Equation 3.126)	
Pr	Prandtl number	
p_b	barometric pressure	kN/m^2
p_s	vapour pressure	kN/m^2
p_{si}	saturation vapour pressure over ice	kN/m2
p_{ss}	saturation vapour pressure	kN/m^2
p_{ssl}	saturation vapour pressure at t_{sl}	kN/m^2
p_{sw}	saturation vapour pressure over water	kN/m^2
Q_{fa}	volumetric flow rate of air	m^3/s
$Q_{fa,d}$	volumetric flow rate of air at full load	m^3/s
$\dot{q}$	rate of heat transfer	kW
q_{cs}	rate of sensible heat transfer from airstream to coolant	kW
q_{ct}	rate of total heat transfer from airstream to coolant	kW
q_d	rate of heat transfer to/from airstream from/to duct	kW
q_{fin}	actual rate of heat transfer through fin	kW
q_h	rate of heat transfer from hot fluid to airstream	kW
q_{ideal}	ideal rate of heat transfer through fin	kW
$q_{zc,crit}$	sensible cooling load of critical zone	kW
$q_{zh,crit}$	heating load of critical zone	kW
q_{zs}	zone sensible cooling load	kW
q_{zl}	zone latent cooling load	kW

Symbol	Description	Unit
N_t	number of tubes per row	
NTU	number of transfer units	
NTU_c	number of transfer units for a heat exchanger using chilled water	
NTU_h	number of transfer units for a heat exchanger using hot water	
Nu_D	Nusselt number	
$P_{fa,s}$	fan static pressure	N/m^2
$P_{fa,t}$	fan total pressure	N/m^2
$P_{fa,v}$	fan velocity pressure	N/m^2
PLR	part load ratio (see Equation 3.126)	
Pr	Prandtl number	
p_b	barometric pressure	kN/m^2
p_s	vapour pressure	kN/m^2
p_{si}	saturation vapour pressure over ice	kN/m2
p_{ss}	saturation vapour pressure	kN/m^2
p_{ssl}	saturation vapour pressure at t_{sl}	kN/m^2
p_{sw}	saturation vapour pressure over water	kN/m^2
Q_{fa}	volumetric flow rate of air	m^3/s
$Q_{fa,d}$	volumetric flow rate of air at full load	m^3/s
$\dot{q}$	rate of heat transfer	kW
q_{cs}	rate of sensible heat transfer from airstream to coolant	kW
q_{ct}	rate of total heat transfer from airstream to coolant	kW
q_d	rate of heat transfer to/from airstream from/to duct	kW
q_{fin}	actual rate of heat transfer through fin	kW
q_h	rate of heat transfer from hot fluid to airstream	kW
q_{ideal}	ideal rate of heat transfer through fin	kW
$q_{zc,crit}$	sensible cooling load of critical zone	kW
$q_{zh,crit}$	heating load of critical zone	kW
q_{zs}	zone sensible cooling load	kW
q_{zl}	zone latent cooling load	kW

Symbol	Description	Unit
R_a	air-side film thermal resistance	m^2K/kW
Re_a, Re_D	Reynolds number	
R_f	fin thermal resistance	m^2K/kW
R_{ffi}	inside surface fouling thermal resistance	m^2K/kW
R_i	inside surface thermal resistance	m^2K/kW
R_{ic}	coolant film thermal resistance	m^2K/kW
R_{mt}	tube wall thermal resistance	m^2K/kW
R_t	total thermal resistance	m^2K/kW
R_t	modified overall thermal resistance	m^2K/kW
S	sigma heat	kJ/kg
SHR	sensible heat ratio	
St	Stanton number	
T	absolute dry bulb temperature	K
t	dry bulb temperature	^oC
t_a	dry bulb temperature of air	^oC
t_{ai}	dry bulb temperature of air at inlet to component	^oC
t_{amb}	ambient temperature	^oC
t_{ao}	dry bulb temperature of air at outlet from component	^oC
t_b	mean bulk temperature of fluid	^oC
t_{ccsp}	cooling coil discharge air temperature setpoint	^oC
t_{ci}	temperature of coolant entering coil	^oC
t_{co}	temperature of coolant leaving coil	^oC
t_{dp}	dew point temperature of moist air	^oC
t_{fb}	fin base temperature	^oC
t_h	hot fluid temperature	^oC
t_{hi}	temperature of hot fluid entering coil	^oC
t_{ho}	temperature of hot fluid leaving coil	^oC
t_{ma}	mixed air dry bulb temperature	^oC
$t_{ma,sp}$	set point temperature of mixed air	^oC
t_{oa}	outside air dry bulb temperature	^oC
$t_{oa,co}$	change over temperature from minimum outdoor air to 100% outdoor air	^oC
t_{ra}	return air dry bulb temperature	^oC

Symbol	Description	Unit
t_{rc}	throttling range of cooling coil air temperature controller	K
t_{rh}	throttling range of heating coil air temperature controller	K
t_s	tube wall temperature	^oC
t_{sa}	supply air temperature	^oC
t_{sl}	sling wet bulb temperature	^oC
t_{sm}	mean coil surface temperature	^oC
t_{spc}, t_{sph}	setpoint or desired value of the temperature of the controlled air	^oC
t_{ti}	tube inside surface temperature	^oC
t_{to}	tube outside surface temperature	^oC
t_w	condensate water temperature	^oC
t_{wi}	temperature of water entering a component	^oC
t_{wm}	mean water temperature	^oC
t_{wo}	temperature of water leaving a component	^oC
t_x	temperature at which outdoor air damper closes to minimum flow position	^oC
t_z	zone air dry bulb temperature	^oC
$t_{zc,crit}$	temperature of zone requiring coldest supply air temperature	^oC
$t_{zh,crit}$	temperature of zone requiring warmest supply air temperature	^oC
t_1, t_2, t_3	dry bulb temperatures of airstreams 1, 2 and 3 respectively	^oC
t_{oa1}, t_{oa2}	outside air temperatures corresponding to	^oC
t_{oa3}, t_{oa4}	t_{sp1}, t_{sp2}, t_{sp3} and t_{sp4} respectively	
t_{sp1}, t_{sp2},	temperature setpoints one, two three and	^oC
t_{sp3}, t_{sp4}	four respectively	
U_d	overall heat transfer coefficient for duct	kW/m^2K
U_o	overall heat transfer coefficient for coil	kW/m^2K
U'_o	modified overall heat transfer coefficient for coil	kW/m^2K
u_b	see Equation 3.84	
u_e	see Equation 3.85	

Symbol	Description	Unit
$V_{fa,o}$	fan outlet velocity	m/s
V_w	water velocity in tubes	m/s
$W_{fa,a}$	air power	W
$W_{fa,m}$	fan motor power input	W
$W_{fa,sh}$	fan power	W
$W_{fa,shd}$	fan power at full load	W
x_a	mole fraction for dry gas	
x_b	fin base radius	m
x_e	external radius of fin	m
x_t	tube wall thickness	m
y_b	half thickness of fin	m
β	fin area/air side area	
Δt_m	mean temperature difference	K
Δt_m	mean temperature different between airstream and mean coil surface temperature	K
$\Delta t_{m,cfc}$	mean temperature difference for a counter flow chilled water coil	K
$\Delta t_{m,cfh}$	mean temperature difference for a counterflow hot water coil	K
Δt_{md}	mean temperature difference between duct and ambient air	K
Δt_{fa}	airstream temperature rise due to fan gains	K
η_{ac}	air efficiency of a counterflow chilled water coil	
η_{ah}	air efficiency of a counterflow hot water coil	
η_f	fin efficiency	
$\eta_{fa,m}$	efficiency of motor/drive system	%
$\eta_{fa,t}$	fan total efficiency	%
η_{hu}	humidifying efficiency	%
η_{wc}	water efficiency of a counter flow chilled water coil	
η_{wh}	water efficiency of a counter flow hot water coil	
ϕ	relative humidity	%
σ	free-flow area/face area	

Symbol	Description	Unit
μ	dynamic viscosity	kg/ms
μ_s	dynamic viscosity at temperature t_s	kg/ms
μ'	percentage saturation	%
ν	specific volume	m^3/kg
ρ_a	density of moist air	kg/m^3
ω_c	cooling coil mass flow rate ratio	
ω_h	heating coil mass flow rate ratio	

3.1 INTRODUCTION

To simulate the performance of HVAC systems, it is necessary to understand the performance characteristics of the components used in the systems. An HVAC system is required to provide heating, cooling and/or ventilation to the various zones in a building to produce acceptable occupancy conditions.

Fundamental heat and mass transfer processes such as airstream mixing, sensible heating and cooling, humidification and dehumidification, etc. occur in these components. To meet the space needs, components are assembled and controlled to modify the airstream properties. The following components are modelled for the purpose of determining their thermodynamic performance when combined into the total system:

Mixing Boxes
Heating Coils
Cooling Coils
Fans
Humidifiers
Ducts

The psychrometric processes are analysed using the principles of conservation of mass and energy. The approach generally used in modelling the components is to integrate the control profiles of the components with their mathematical models under steady state conditions.

3.2 PSYCHROMETRIC FORMULAE

In modelling HVAC systems, it is necessary to determine the state of the moist air within the system. In normal air conditioning practice, a psychrometric chart or a set of psychrometric tables is generally used to obtain and analyse the data concerning the state of the moist air. For computer applications, mathematical formulae for calculating the thermodynamic properties of moist air must be developed. The formulae and algorithms given in CIBS publications **(Refs. 1 and 2)** and ASHRAE Handbook of Fundamentals **(Ref. 3)** have been adopted for calculating most of the thermodynamic properties of moist air.

3.2.1. Saturation Vapour Pressure

From Ref. 1, the saturation vapour pressure over water at temperature t is given by:

$$\log p_{sw} = 30.590511 - 8.2 \log T + (2.4804 \times 10^{-3})\, T - \frac{(3142.31)}{(T)} \qquad (3.1)$$

where

$$T = t + 273.15 \qquad (3.2)$$

p_{sw} = saturation vapour pressure over water (kPa)

t = dry bulb temperature (^{o}C)

T = absolute dry bulb temperature (K)

and the saturation vapour pressure over ice at temperatures below $0^{o}C$ is given by:

$$\log p_{si} = 9.5380997 - \frac{(2663.91)}{(T)} \qquad (3.3)$$

where:

p_{si} = saturation vapour pressure over ice at temperatures below $0^{o}C$ (kPa)

Due to the complexity of Equations 3.1 and 3.3, Equations 3.4 and 3.5 relating saturation vapour pressure to temperature are preferred. They are based on the work by Tetens **(Ref. 4)** and Weiss **(Ref. 5)**. Tettens' relationship between p_{sw} and t is given by:

$$p_{sw} = 0.61078 \exp \frac{(17.2693882t)}{(t + 237.30)} \qquad (3.4)$$

and is applicable in the temperature range 0 to 100°C.

Weiss relationship between p_{si} and t is given by:

$$p_{si} = 0.61078 \exp \frac{(21.8745584t)}{(t + 265.50)} \qquad (3.5)$$

and is applicable for temperatures below 0°C

3.2.2 Relative Humidity

Relative humidity is defined as the ratio of the actual vapour pressure of moist air to the saturation vapour pressure at the same temperature and is usually expressed as a percentage. It is given by:

$$\phi = \frac{p_s \times 100.0}{p_{ss}} \qquad (3.6)$$

where

ϕ = relative humidity (%)

p_s = vapour pressure (kPa)

p_{ss} = saturation vapour pressure (kPa)

3.2.3. Moisture Content or Specific Humidity

This is defined as the mass of water vapour associated with unit mass of dry air in an air-water vapour mixture. It is given by:

$$g = \frac{0.62197\ f_s\ p_s}{p_b - f_s p_s} \qquad (3.7)$$

where:

g = moisture content per unit mass of dry air (kg/kg)

f_s = enhancement coefficient which is a function of temperature and barometric pressure (Refs. 2, 3 and 6)

p_b = barometric pressure (kPa)

3.2.4 Percentage Saturation

This is defined as the ratio of the moisture content of moist air to the moisture content of saturated air at the same temperature and is usually expressed as a percentage. It is given by

$$\mu' = \frac{g \times 100.0}{g_{ss}} \qquad (3.8)$$

where:

μ' = percentage saturation (%)

g_{ss} = saturation moisture content per unit mass of dry air (kg/kg)

A direct relationship exists between the relative humidity and percentage saturation. It is derived as follows:

From Equation 3.7, $g = \dfrac{0.62197\ f_s\ p_s}{p_b - f_s\ p_s}$

Also $g_{ss} = \dfrac{0.62197\ f_s\ p_{ss}}{p_b - f_s\ p_{ss}}$

$$\mu' = \frac{g}{g_{ss}} = \frac{0.62197\ f_s\ p_s}{p_b - f_s\ p_s} \times \frac{p_b - f_s\ p_{ss}}{0.62197\ f_s\ p_{ss}}$$

$$\mu' = \frac{p_s}{p_{ss}} \times \frac{p_b - f_s\ p_{ss}}{p_b - f_s\ p_s}$$

From Equation 3.6, $p_s = \phi\ p_{ss}$

Thus $$\mu' = \phi\ \frac{(p_b - f_s\ p_{ss})}{p_b - f_s\ p_s}$$

$$\mu'(p_b - f_s\ p_s) = \phi\ (p_b - f_s\ p_{ss})$$

$$\mu'(p_b - f_s \phi\ p_{ss}) = \phi\ p_b - \phi\ f_s\ p_{ss}$$

$$\mu' p_b = \phi\ (p_b - f_s\ p_{ss}\ \{1 - \mu'\})$$

$$\phi = \mu'\ p_b / (p_b - f_s\ p_{ss}\ \{1 - \mu'\}) \qquad (3.9)$$

3.2.5 Specific Enthalpy

This is defined as the enthalpy of moist air per unit mass of dry air. It is given by

$$h = h_a + g\ h_g \qquad (3.10)$$

where:

h = specific enthalpy of moist air per unit mass of dry air (kJ/kg)

h_a = specific enthalpy of dry air (kJ/kg)

h_g = specific enthalpy of water vapour (kJ/kg)

h_a and h_g can be calculated from the algorithms given in Ref. 2 which is applicable for the temperature range - 10.0 to 60.0 °C. However, from Ref. 3, h_a and h_g can be calculated from

$$h_a = 1.006t \quad (3.11)$$

$$h_g = 2501.0 + 1.805t \quad (3.12)$$

3.2.6 Specific Volume

This is defined as the volume occupied by the moist air per unit mass of dry air. It is given by

$$\upsilon = \frac{R_a T}{(P_b - P_s)} - (x^2 A_{aa} + x_a (1 - x_a)\, 2 A_{aw} + (1-x_a)^2 A_{ww}) \quad (3.13)$$

where

$$R_a = \frac{82.0567 \times 101.325}{28966} = 0.28704 \text{ kJ/kg K}$$

$$x_a = \frac{0.62197}{0.62197 + g} \quad (3.14)$$

υ = specific volume per unit mass of dry air (m^3/kg)

R_a = gas constant for air (KJ/kg K)

x_a = mole fraction of dry gas

A_{aa} = second virial coefficient for dry air (Ref. 2) (m^3/kg)

A_{aw} = interaction coefficient for moist air (Ref. 2) (m^3/kg)

A_{ww} = second virial coefficient for water vapour (Ref. 2) (m^3/kg)

3.2.7 Dew Point Temperature

This is defined as the temperature of saturated air which has the same vapour pressure as the moist air under consideration. It can be obtained by manipulating Equations 3.4 and 3.5.

If p_s is less than 0.61078 then

$$t_{dp} = \frac{265.5y}{21.8745584 - y} \qquad (3.15)$$

If p_s is greater than or equal to 0.61078 then

$$t_{dp} = \frac{237.3y}{17.2693882 - y} \qquad (3.16)$$

where:

$$y = \ln \frac{(p_s)}{(0.61078)} \qquad (3.17)$$

t_{dp} = dew point temperature of moist air (^oC)

3.2.8 Sling Wet Bulb Temperature

The wet bulb temperature is the temperature registered by a thermometer when its bulb is covered by a wetted wick and is exposed to a current of rapidly moving air. The sling wet bulb temperature is obtained by whirling the wet bulb thermometer.

The vapour pressure of unsaturated moist air is given by

$$p_s = p_{ssl} - p_b A (t - t_{sl}) \quad (3.18)$$

where:

p_{ssl} = saturation vapour pressure at t_{sl} (kPa)
t_{sl} = sling wet bulb temperature (^oC)
A = 6.66×10^{-4} K^{-1} when $t_{sl} > 0^oC$
= 5.94×10^{-4} K^{-1} when $t_{sl} < 0^oC$

Knowing p_s, p_b and t, t_{sl} can be determined by solving the equation resulting from substituting for P_{ssl} using Equations 3.4 and 3.5. This non-linear equation can be solved iteratively by using the Newton-Raphson method and noting that $t_{dp} < t_{sl} < t$ for unsaturated moist air.

3.2.9 Sigma Heat

This is defined as the enthalpy of moist air less a small enthalpy term. This term is the enthalpy of the water vapour associated with unit mass of dry air, calculated as if the water vapour was present as liquid water at the wet bulb temperature. Sigma heat is given by

$$S = h - gh_{wsl} \quad (3.19)$$

where

S = Sigma heat (kJ/kg)
h_{wsl} = enthalpy of liquid water at t_{sl} (kJ/kg)

Sigma heat is a function only of wet bulb temperature and barometric pressure. McPherson **(Ref. 7)** has derived this relationship and this is outlined below. As S is the enthalpy less the sensible heat of the water component, we have

$$S = c_{pda}t + gh_{fg} + c_{ps} g (t - t_{sl}) \quad (3.20)$$

$$S = c_{pda}t + gh_{fg} + c_{ps}\, g\, (t - t_{sl}) \quad (3.20)$$

where:

c_{pda} = specific heat capacity of dry air (kJ/kg K)
h_{fg} = latent heat of evaporation at t_{sl} (kJ/kg)
c_{ps} = specific heat capacity of water vapour (kJ/kg K)

The term $c_{pda}t$ represents that portion of S due to the sensible heat of moist air while gh_{fg} represents the contribution to S due to the latent heat of evaporation and $c_{ps}\, g\, (t - t_{sl})$ represents the superheated water vapour term.

Transforming Equation 3.20 we have,

$$S = c_{pda}t + g\, \{h_{fg} + c_{ps}\, (t - t_{sl})\} \quad (3.21)$$

The direct relationship $S = f\, \{t_{sl}, p_b\}$ can be obtained from a consideration of the heat balance that exists at the wetted surface of a wet bulb thermometer. A mixture of 1kg of dry air and g kg of water vapour at a dry bulb temperature, t, approaching and passing closely over the wet bulb surface, leaves in a saturated condition with the moisture content increased to g_{ss} and the temperature reduced to t_{sl}. Sensible heat is transferred from the air to the cooler wet bulb, and the evaporation process transfers latent heat from the wet bulb back to the air. At equilibrium, these two are in balance.

Sensible heat lost = Latent heat gained by the air

$$1.0 \times c_{pma} \times (t - t_{sl}) = 1.0 \times h_{fg} \times (g_{ss} - g) \quad (3.22)$$

where:

$$c_{pma} = (c_{pda} + g\, c_{ps}) \quad (3.23)$$

c_{pma} = specific heat capacity of moist air per unit mass of dry air (kJ/kg K)

Substituting for c_{pma} in Equation 3.22 gives

$$(c_{pda} + g\, c_{ps})\ (t - t_{sl}) = h_{fg}\ (g_{ss} - g)$$
$$c_{pda}\ (t - t_{sl}) + g c_{ps}\ (t - t_{sl}) = h_{fg}\ (g_{ss} - g)$$
$$g\ \{h_{fg} + c_{ps}\ (t - t_{sl})\} = h_{fg}\, g_{ss} - c_{pda}\ (t - t_{sl})$$
$$g = \frac{h_{fg}\, g_{ss} - c_{pda}\ (t - t_{sl})}{h_{fg} + c_{ps}\ (t - t_{sl})}$$

Substituting for g in Equation 3.21 gives

$$S = c_{pda}\, t + h_{fg}\, g_{ss} - c_{pda}\ (t - t_{sl})$$
$$S = h_{fg}\, g_{ss} + c_{pda}\, t_{sl} \qquad (3.25)$$

Over the temperature range 0.0 to 70.0°C,

$$h_{fg} = 2501.0 - 2.387\, t_{sl} \qquad (3.26)$$

c_{pda} is approximately equal to 1.006 kJ/kg K and g_{ss} is a function of t_{sl} and p_b as can be seen from Equation 3.7.

Thus S is a function only of t_{sl} and p_b.

3.3 MIXING BOXES

Mixing boxes are used to control the quantity of outside air entering an HVAC system or to control supply air temperatures as in face and by pass dampers or zone dampers of a dual duct/multizone system. Fig. 3.1 shows what happens when two airstreams meet and mix adiabatically. Moist air at state 1 mixes with moist air at state 2 forming a mixture at state 3.

The fundamental equations which apply are the conservation of energy and conservation of mass. These are:

Dry air mass balance

$$\dot{m}_{a1} + \dot{m}_{a2} = \dot{m}_{a3} \qquad (3.27)$$

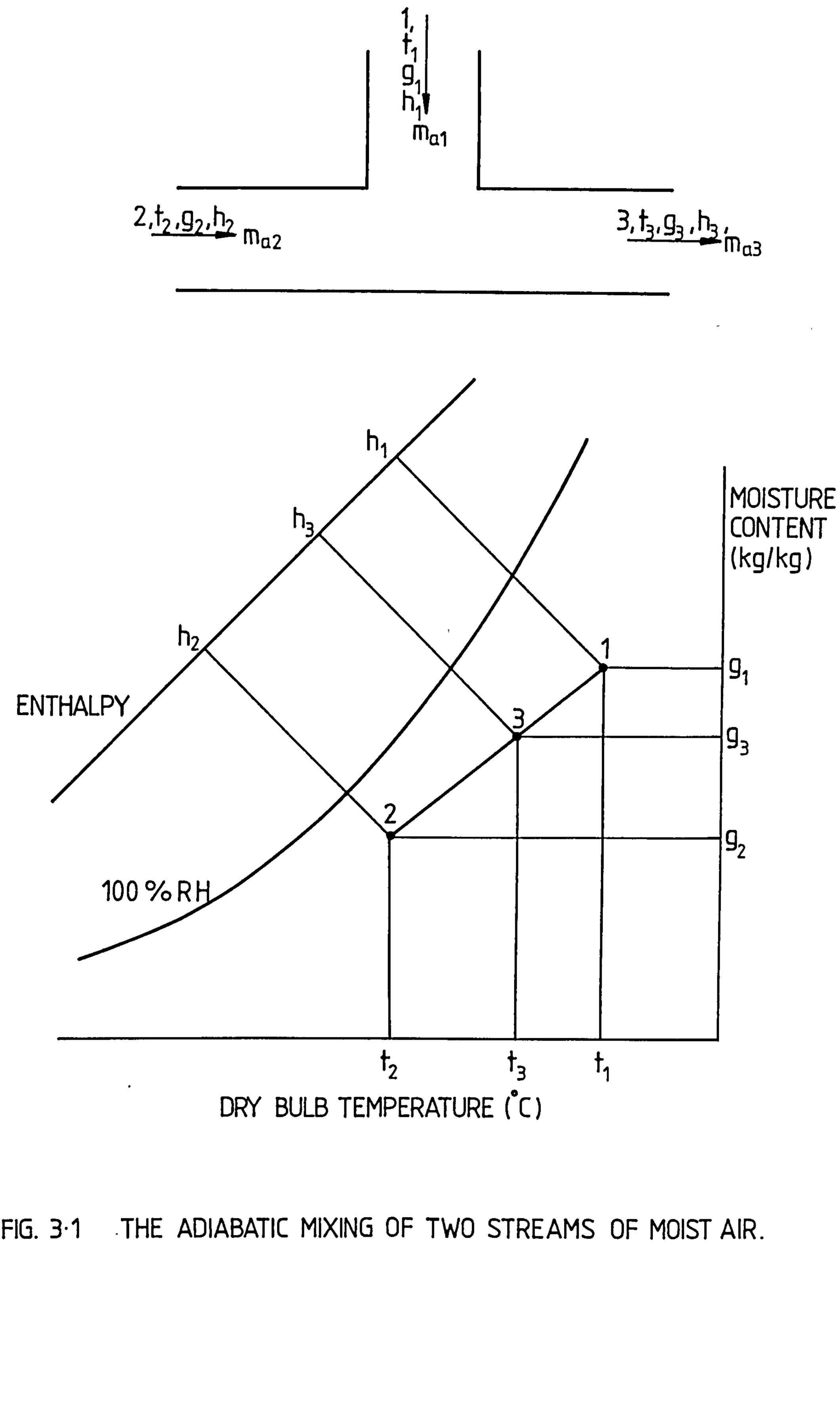

FIG. 3·1 THE ADIABATIC MIXING OF TWO STREAMS OF MOIST AIR.

Water vapour mass balance

$$m_{a1}\, g_1 + m_{a2}\, g_2 = m_{a3}\, g_3 \qquad (3.28)$$

Energy balance

$$m_{a1}\, h_1 + m_{a2}\, h_2 = m_{a3}\, h_3 \qquad (3.29)$$

Assuming the variation of the specific heat capacity of moist air over the working range of interest is so small as to be neglected, Equation 3.29 may be approximated by

$$m_{a1}\, c_{pma}\, t_1 + m_{a2}\, c_{pma}\, t_2 = m_{a3}\, c_{pma}\, t_3$$

$$m_{a1}\, t_1 + m_{a2}\, t_2 = m_{a3}\, t_3 \qquad (3.30)$$

where:

m_{a1}, m_{a2}, m_{a3} = mass flow rates of the dry air portion of airstreams 1, 2 and 3 (kg/s)

g_1, g_2, g_3 = moisture content of airstreams 1, 2 and 3 (kg/kg)

t_1, t_2, t_3 = dry bulb temperatures of air streams 1, 2 and 3 (^{o}C)

Combining Equations 3.27 and 3.28, we have

$$m_{a1}\, g_1 + m_{a2}\, g_2 = (m_{a1} + m_{a2})\, g_3$$
$$m_{a1}\, (g_1 - g_3) = m_{a2}\, (g_3 - g_2)$$

$$\frac{m_{a2}}{m_{a1}} = \frac{g_1 - g_3}{g_3 - g_2}$$

From Equations 3.27 and 3.29 we have

$$\frac{m_{a2}}{m_{a1}} = \frac{h_1 - h_3}{h_3 - h_2}$$

From Equations 3.27 and 3.30, we have

$$\frac{m_{a2}}{m_{a1}} = \frac{t_1 - t_3}{t_3 - t_2}$$

Thus

$$\frac{m_{a2}}{m_{a1}} = \frac{g_1 - g_3}{g_3 - g_2} = \frac{h_1 - h_3}{h_3 - h_2} = \frac{t_1 - t_3}{t_3 - t_2} = \frac{\text{Line 31}}{\text{Line 32}} \qquad (3.31)$$

Equation 3.31 shows that when two airstreams mix adiabatically, the mixture state lies on the straight line which joins the state points of the constituents and the position of the mixture state point is such that the line is divided inversely as the ratio of the masses of dry air in the constituent airstreams.

3.3.1 Outdoor Air Control Systems

The introduction of outside (ventilation) air is necessary when the conditioned space is occupied by people. Outside air dampers are used to control the amount of fresh air introduced into the HVAC system. Depending on the control methods used, a fixed or varying amount of outside air is introduced. Outside air control systems are often designed so that the cooling load on the mechanical refrigerating equipment is minimised as much as possible. The minimum amount of outside air must always be provided. Outdoor air is usually provided in one of the following ways.

a) By means of an outdoor air damper which is fixed and set to minimum outdoor air volume – **Minimum Outdoor Air Control System.**

b) By means of an outdoor air damper which opens to maximum position at all times of system operation i.e. 100% outside air is always used - **Maximum Outdoor Air Control System.**

c) By means of an outdoor air damper which opens to minimum and maximum positions at set temperatures of outdoor air. Between these set temperatures, the damper opens to proportional position depending on the mixed air temperature - Proportional Outdoor Air Control System

d) By means of an outdoor air damper which is controlled by outdoor and return air temperatures so that mixed air temperature may remain at the set value - Temperature Control System.

e) By means of an outdoor air damper which is controlled by outdoor and return air enthalpies so that mixed air temperature may remain at the set value - Enthalpy Control System.

The simulation of outdoor air control systems involves determining the state point of mixed air and the amount of outdoor air introduced into the HVAC system. To do this the following data are required:

From system characteristics:

$m_{oa,min}$ = minimum mass flow rate of outdoor air (kg/s)

m_{ma} = mass flow rate of mixed air to air handling system (kg/s)

From weather data:

t_{oa} = dry bulb temperature of outdoor air (^{o}C)

g_{oa} = moisture content of outdoor air (kg/kg)

From simulation of rest of system:

t_{ra} = dry bulb temperature of return air (^{o}C)

g_{ra} = moisture content of return air (kg/kg)

3.3.1.1 Minimum Outdoor Air Control System

In this system, an outdoor air damper opens to a minimum position when the fan is started and closes when the fan stops as shown in Fig. 3.2. This provides ventilation air to make up for exhaust and exfiltration from the space. A manual return air damper usually provides balancing .

The procedure for calculating the mass flow rate of outdoor air, the temperature and moisture content of mixed air is:

The mass flow rate of outdoor air, m_{oa}, is:

$$m_{oa} = m_{oa,min} \tag{3.32}$$

From Equation 3.27, the mass flow rate of return air m_{ra}, is:

$$m_{ra} = m_{ma} - m_{oa}$$

$$m_{ra} = m_{ma} - m_{oa,min} \tag{3.33}$$

From Equation 3.30, the temperature of mixed air, t_{ma}, is calculated as:

$$m_{ma}\, t_{ma} = m_{oa,min}\, t_{oa} + (m_{ma} - m_{oa,min})\, t_{ra}$$

$$t_{ma} = \frac{(m_{oa,min}\, t_{oa} + (m_{ma} - m_{oa,min})\, t_{ra})}{m_{ma}} \tag{3.34}$$

From Equation 3.28, the moisture content of mixed air, g_{ma}, is calculated as

$$m_{ma}\, g_{ma} = m_{oa,min}\, g_{oa} + (m_{ma} - m_{oa,min})\, g_{ra}$$

$$g_{ma} = \frac{(m_{oa,min}\, g_{oa} + (m_{ma} - m_{oa,min})\, g_{ra})}{m_{ma}} \tag{3.35}$$

where:

m_{oa} = mass flow rate of outdoor air (kg/s)

m_{ra} = mass flow rate of return air (kg/s)

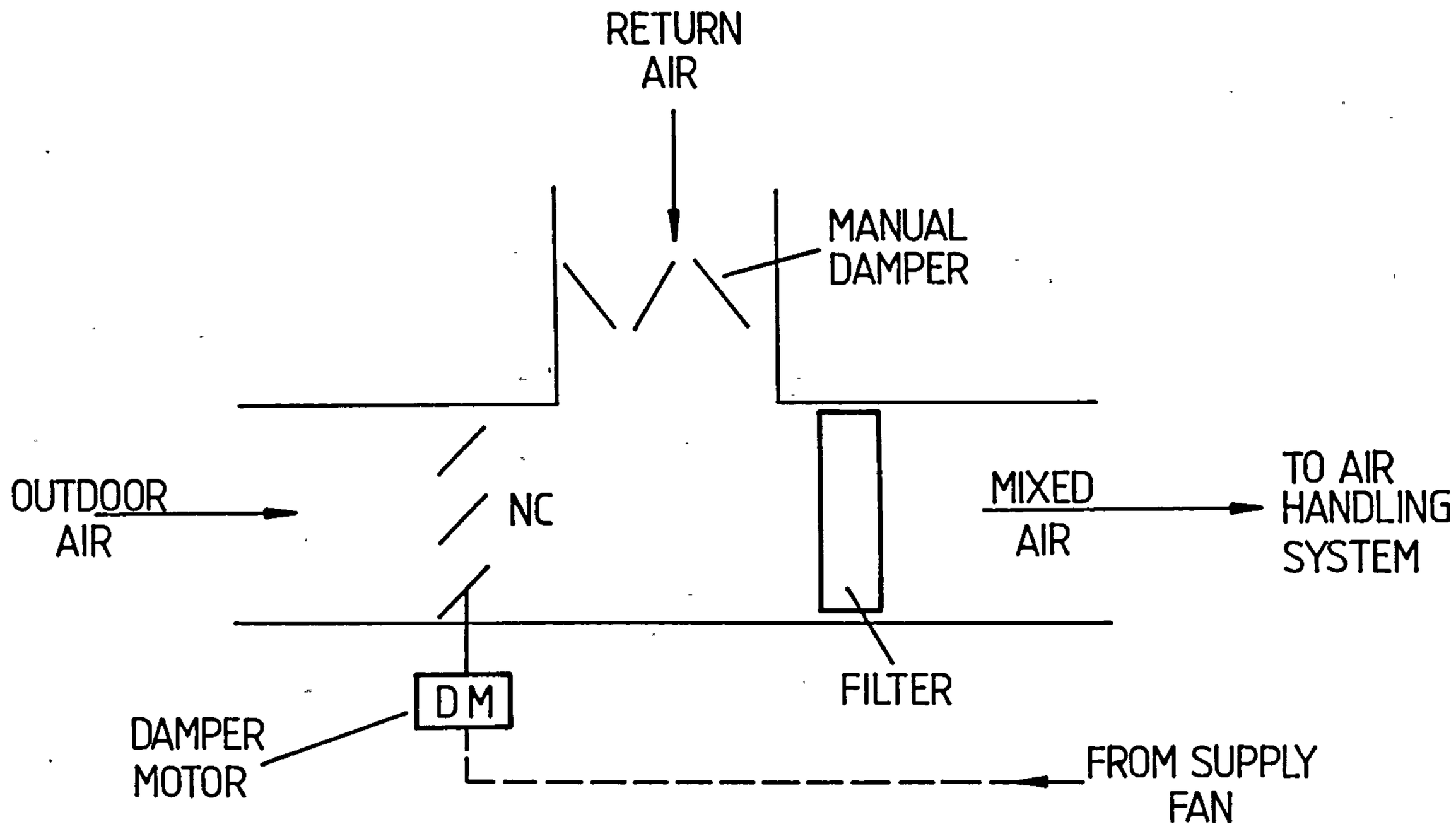

FIG. 3·2 SCHEMATIC DIAGRAM OF MINIMUM OUTDOOR AIR CONTROL SYSTEM

t_{ma} = dry bulb temperature of mixed air (^{o}C)

g_{ma} = moisture content of mixed air (kg/kg)

3.3.1.2 Maximum Outdoor Air Control System

100% outside air is used in buildings with large exhaust air requirements. This often occurs in laboratory buildings or hospital operating rooms. No return air is recirculated in these installations.

For these special applications,

$$m_{sa} = m_{oa} \quad (3.36)$$

$$t_{sa} = t_{oa} \quad (3.37)$$

$$g_{sa} = g_{oa} \quad (3.38)$$

where:

m_{sa} = mass flow rate of supply air to HVAC system (kg/s)

t_{sa} = dry bulb temperature of supply air before being conditioned by the HVAC system (^{o}C).

g_{sa} = moisture content of supply air before being conditioned by the HVAC system (kg/kg)

3.3.1.3 Proportional Outdoor Air Control System

This control system provides a year-round system with a fixed minimum outdoor air damper, which opens whenever the fan is running; a maximum outdoor air damper which is automtically controlled by a mixed air thermostat (proportional control); and a high limit outdoor air thermostat that returns the system to a minimum outdoor air condition.

Whenever the outdoor air is above the setting of the mixed air thermostat ($t_{ma,sp}$) and below the setting of the high limit ($t_{oa,co}$), 100% outdoor air will be used. The proportional outdoor air control system is shown schematically in Fig 3.3. It is also called the dry bulb economiser system.

Apart from the data stated in section 3.3.1, the calculation of the mass flow rate of outdoor air and the state point of mixed air requires:

From system characteristics:

$t_{ma,sp}$ = desired temperature of mixed air (^{o}C)
$t_{oa,co}$ = change over temperature from minimum outdoor air to 100% outdoor air (^{o}C)

Let t_x be the outdoor temperature at which the outdoor air damper closes to minimum flow position.

Applying Equation 3.30 we have

$$m_{oa,min}\ t_x + (m_{ma} - m_{oa,min})\ t_{ra} = m_{ma}\ t_{ma,sp}$$
$$m_{oa,min}\ t_x = m_{ma}\ t_{ma,sp} - (m_{ma} - m_{oa,min})t_{ra}$$

$$t_x = \frac{m_{ma}\ t_{ma,sp} - (m_{ma} - m_{oa,min})\ t_{ra}}{m_{oa,min}} \qquad (3.39)$$

where:

t_x = outdoor temperature at which the outdoor air damper closes to minimum flow position (^{o}C).

Thus the algorithm for determining m_{oa}, t_{ma} and g_{ma} is:

If $t_{oa} \geqslant t_{oa,co}$ or $t_{oa} < t_x$, then
  calculate t_{ma} using Equation 3.34
  calculate g_{ma} using Equation 3.35

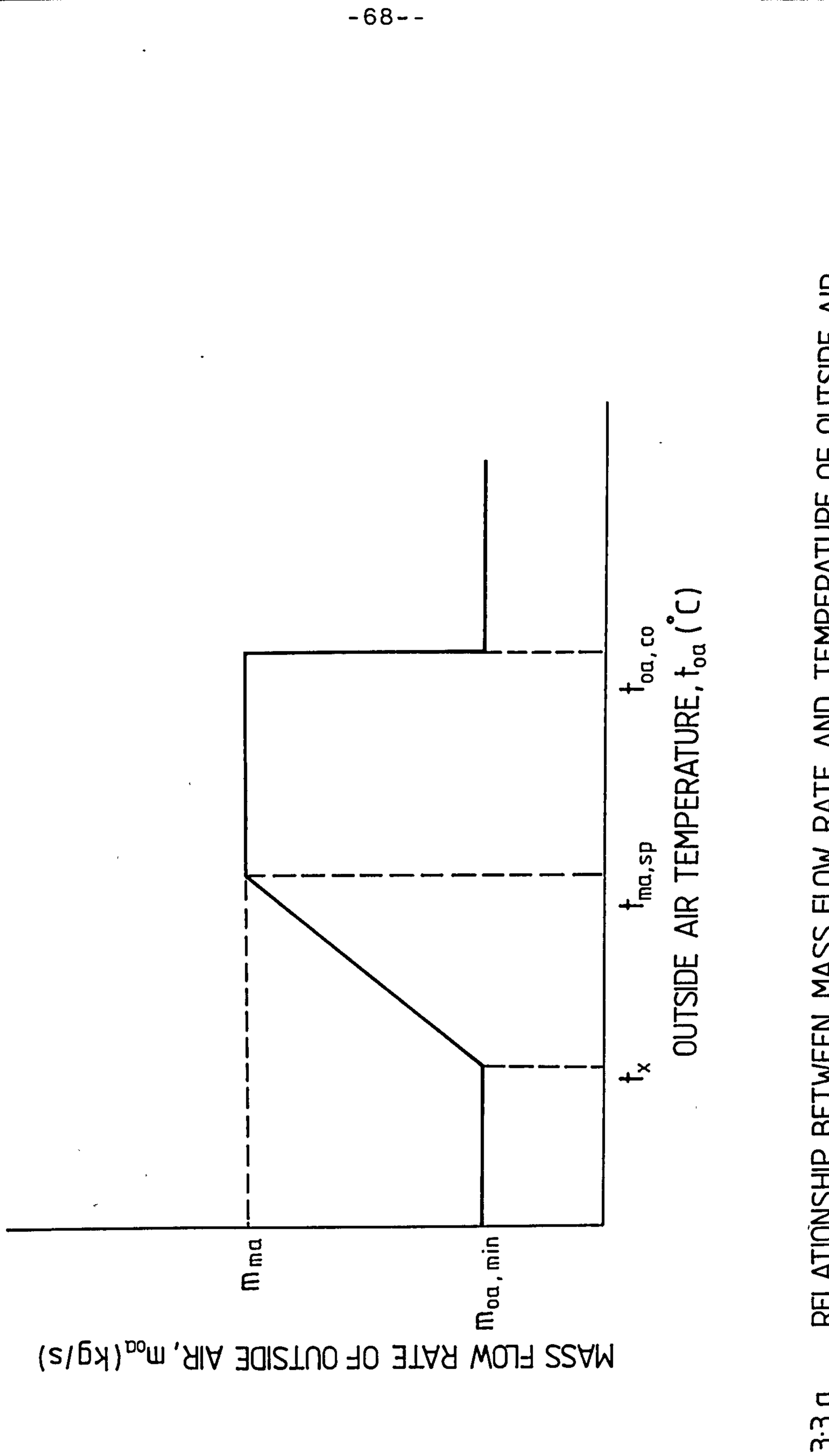

FIG. 3.3 RELATIONSHIP BETWEEN MASS FLOW RATE AND TEMPERATURE OF OUTSIDE AIR FOR PROPORTIONAL OUTDOOR AIR CONTROL SYSTEM.

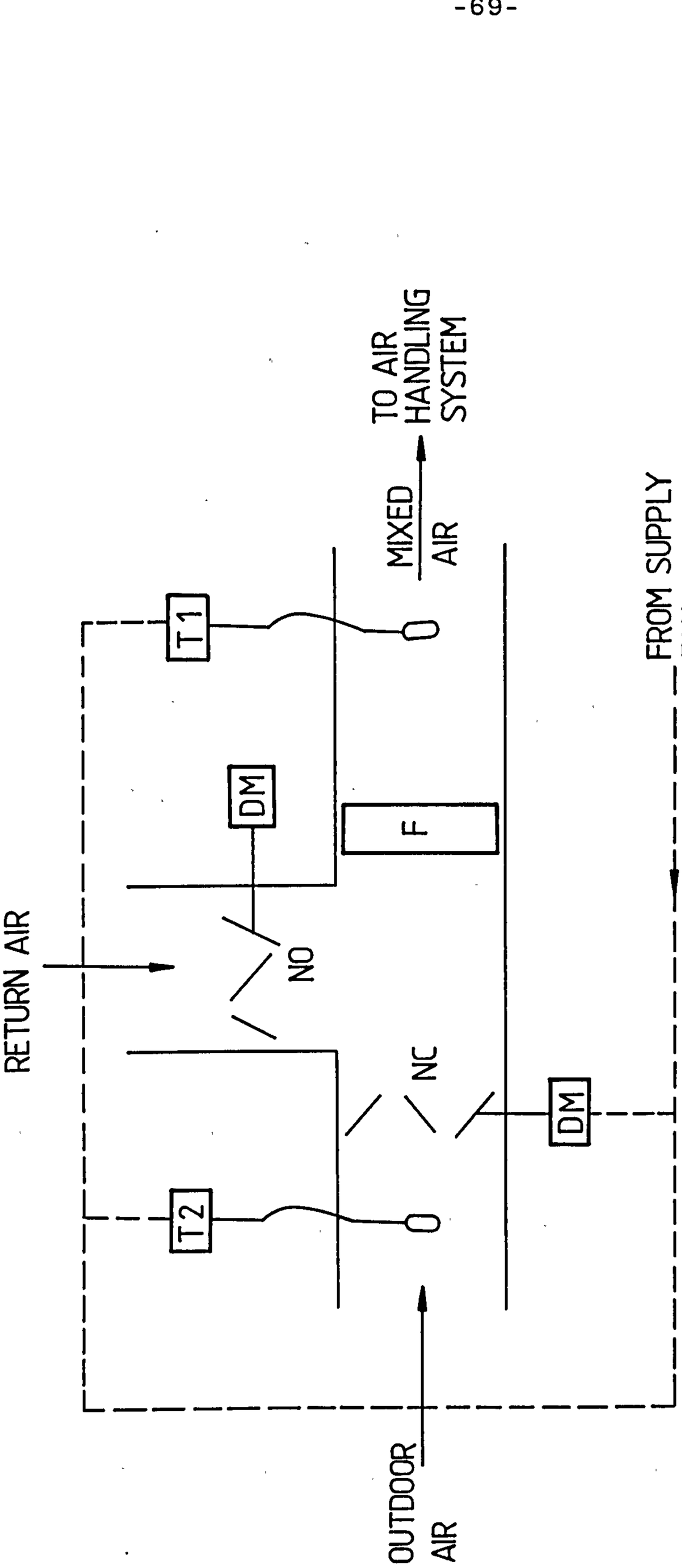

FIG. 3.3b SCHEMATIC DIAGRAM OF PROPORTIONAL OUTDOOR AIR CONTROL SYSTEM

If $t_{ma,sp} \leqslant t_{oa} < t_{oa,co}$, then

$$m_{oa} = m_{ma}$$
$$t_{ma} = t_{oa}$$
$$g_{ma} = g_{oa}$$

If $t_x \leqslant t_{oa} < t_{ma,sp}$, then

$$t_{ma} = t_{ma,sp}$$

m_{oa} is controlled to maintain t_{ma} at $t_{ma,sp}$ by the mixed air proportional thermostat. Applying Equation 3.30, m_{oa} can be calculated as

$$m_{oa}\, t_{oa} + (m_{ma} - m_{oa})\, t_{ra} = m_{ma}\, t_{ma,sp}$$

$$m_{oa}\, (t_{oa} - t_{ra}) = m_{ma}\, (t_{ma,sp} - t_{ra})$$

$$m_{oa} = \frac{(t_{ra} - t_{ma,sp})\, m_{ma}}{t_{ra} - t_{oa}} \qquad (3.40)$$

Applying Equation 3.28, g_{ma} can be calculated as

$$m_{oa}\, g_{oa} + (m_{ma} - m_{oa})\, g_{ra} = m_{ma}\, g_{ma}$$

$$g_{ma} = \frac{m_{oa}\, g_{oa} + (m_{ma} - m_{oa})\, g_{ra}}{m_{ma}} \qquad (3.41)$$

3.3.1.4 Temperature Type Outdoor Air Control System

This system operates by means of an outdoor air damper which is controlled by a differential thermostat sensing the outdoor and return air temperatures and a mixed air thermostat, proportionally controlled so that mixed air temperature may remain at the set value. The system is shown schematically in Fig. 3.4.

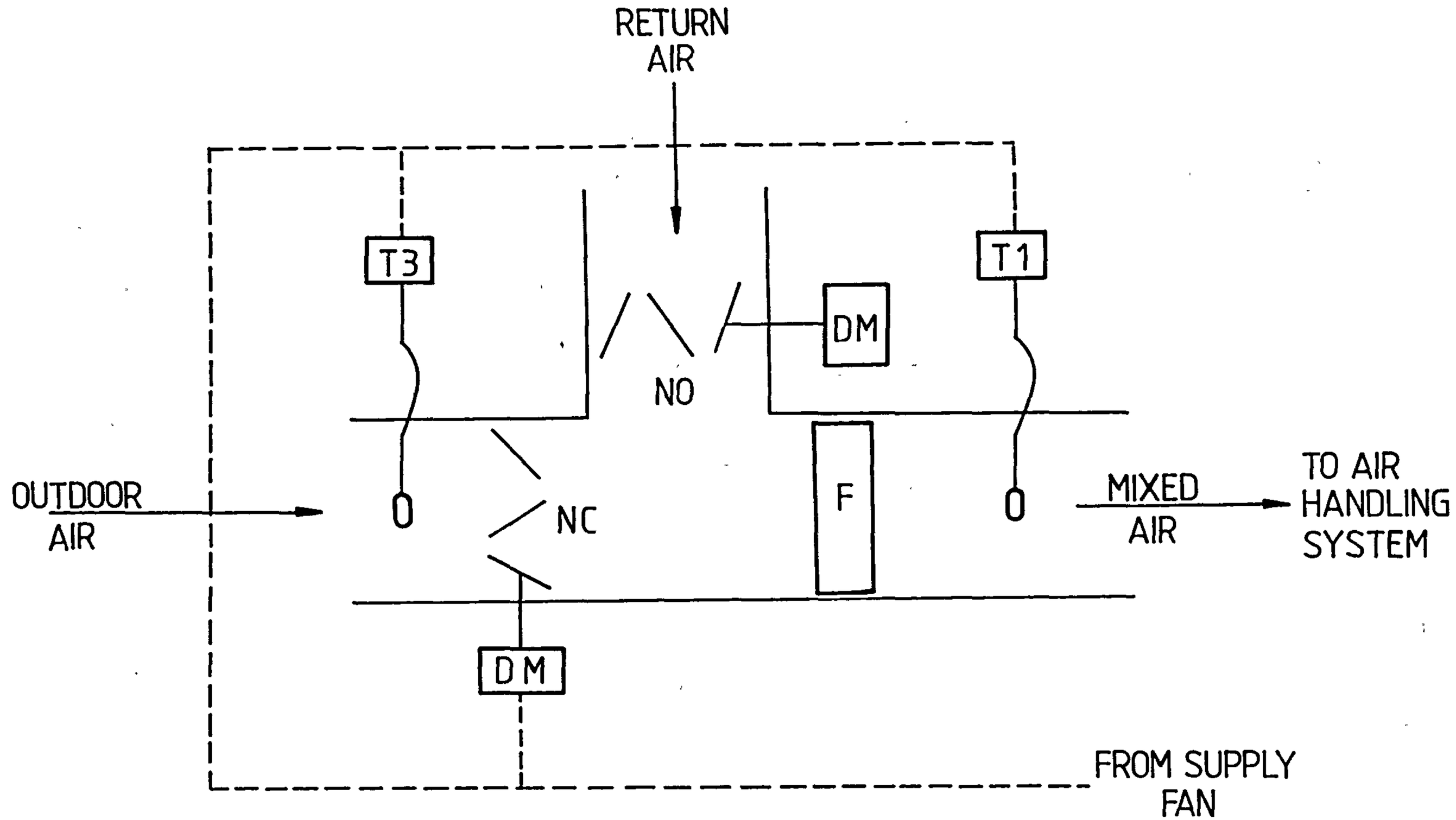

T1 - MIXED AIR THERMOSTAT (PROPORTIONAL)

T3 - DIFFERENTIAL THERMOSTAT

DM - DAMPER MOTOR

F - FILTER

FIG. 3·4 SCHEMATIC DIAGRAM OF TEMPERATURE TYPE OUTDOOR AIR CONTROL SYSTEM

The control program for this system depends on the relative values of t_{oa}, t_{ra} and the desired temperature of mixed air, $t_{ma,sp}$.

The algorithm for determining m_{oa}, t_{ma} and g_{ma} is:

1) If $t_{ma,sp} < t_{oa} < t_{ra}$ then

$m_{oa} = m_{ma}$

$t_{ma} = t_{oa}$

$g_{ma} = g_{oa}$

2) If $t_{oa} < t_{ma,sp} < t_{ra}$ then

$t_{ma} = t_{ma,sp}$

From Equation 3.40, m_{oa} is calculated as

$$m_{oa} = \frac{(t_{ra} - t_{ma,sp})\, m_{ma}}{t_{ra} - t_{oa}}$$

Calculate g_{ma} using Equation 3.41

Check to make sure that $m_{oa,min} < m_{oa} < mma$

If $m_{oa} < m_{oa,min}$ then

$m_{oa} = m_{oa,min}$

Calculate t_{ma} using Equation 3.34

Calculate g_{ma} using Equation 3.35

If $m_{oa} > m_{ma}$ then

$m_{oa} = m_{ma}$

$t_{ma} = t_{oa}$

$g_{ma} = g_{oa}$

3) If $t_{oa} < t_{ra} < t_{ma,sp}$ then

$m_{oa} = m_{oa,min}$

Calculate t_{ma} using Equation 3.34

Calculate g_{ma} using Equation 3.35

4) If $t_{ra} = t_{oa}$ then

$$m_{oa} = m_{ma}$$
$$t_{ma} = t_{oa}$$
$$g_{ma} = g_{oa}$$

5) If $t_{ma,sp} < t_{ra} < t_{oa}$ then

$m_{oa} = m_{oa,min}$

Calculate t_{ma} using Equation 3.34

Calculate g_{ma} using Equation 3.35

6) $t_{ra} < t_{ma,sp} < t_{oa}$ then

Calculate m_{oa}, t_{ma} and g_{ma} in a manner similar to that in step 2.

7) If $t_{ra} < t_{oa} < t_{ma,sp}$ then

$$m_{oa} = m_{ma}$$
$$t_{ma} = t_{oa}$$
$$g_{ma} = g_{oa}$$

3.3.1.5 Enthalpy Type Outdoor Air Control System

The outdoor air damper in this system is controlled by considering the enthalpies of the outdoor and return air streams. For most common applications, the enthalpy optimisation logic is based on the following rules:

1) When the outdoor air dry bulb is below the cooling coil discharge air dry bulb temperature set point, outdoor and return air are mixed to obtain the desired supply air temperature without the use of mechanical cooling. This corresponds to Region 1 on the psychrometric chart of Fig. 3.5.

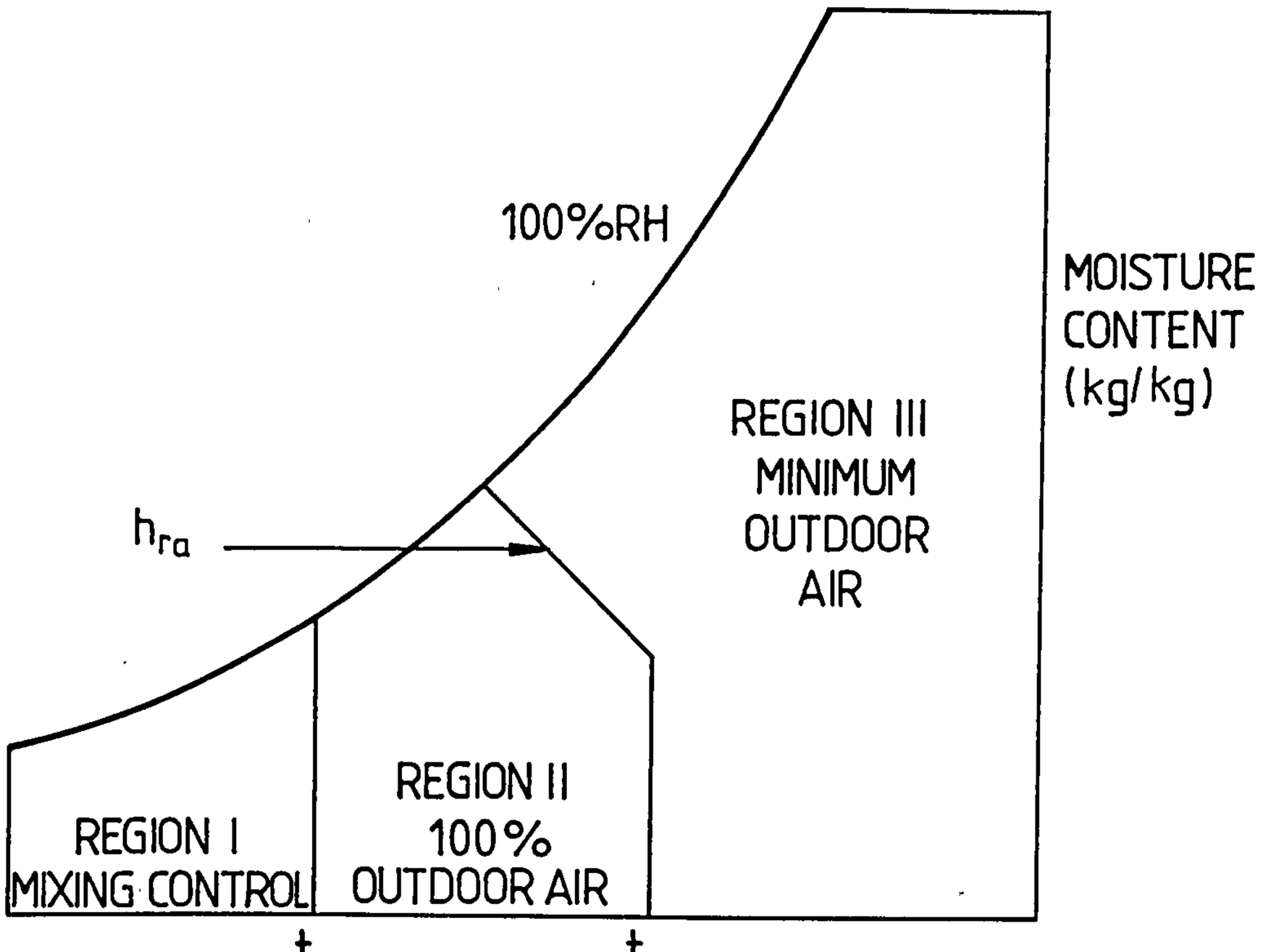

t_{ccsp} = COOLING COIL DISCHARGE AIR DRY BULB TEMPERATURE SETPOINT. (°C)

t_{ra} = RETURN AIR TEMPERATURE. (°C)

h_{ra} = SPECIFIC ENTHALPY OF RETURN AIR. (kJ/kg)

FIG. 3·5 OPERATING REGIONS ON A PSYCHROMETRIC CHART FOR ENTHALPY TYPE OUTDOOR AIR CONTROL SYSTEM.

2) When the outdoor air enthalpy is below the enthalpy of the return air and the outdoor air dry bulb temperature is between the cooling coil discharge air dry bulb temperature set point and the return air dry bulb temperature (Region 11), 100% outdoor air should be used for maximum economy.

3) When the outdoor air enthalpy is greater than the enthalpy of the return air and the outdoor air dry bulb temperature is greater than the return air dry bulb temperature (Region 111), minimum outdoor air should be used.

Thus the algorithm for determining m_{oa}, t_{ma} and g_{ma} is:

Region 1

$$t_{ma} = t_{ccsp}$$

where:

t_{ccsp} = cooling coil discharge air dry bulb temperature setpoint (^{o}C)

$$m_{oa} = \frac{m_{ma}\ (t_{ra} - t_{ccsp})}{t_{ra} - t_{oa}}$$

Calculate g_{ma} using Equation 3.41

Check to make sure that $m_{oa,min} < m_{oa} \leq m_{ma}$ by following the procedure of item 2 Section 3.3.1.4

Region 11

$$m_{oa} = m_{ma}$$
$$t_{ma} = t_{oa}$$
$$g_{ma} = g_{oa}$$

Region 111

$$m_{oa} = m_{oa,min}$$

Calculate t_{ma} using Equation 3.34

Calculate g_{ma} using Equation 3.35

3.3.2 Mixing Boxes for Zone Dampers in Dual Duct/Multizone Systems

Multizone or dual duct systems supply air of a desired temperature to a zone by mixing two airstreams. The mixing proces is analysed in the same way as outlined in Section 3.3.

3.4 HEATING COILS

Heating coils are used as preheat coils located in either the outside or mixed air ducts, hot decks in multizone or dual duct systems, and reheat coils.

The coils consist of banks of bare tubes or banks of tubes which have finned or extended surfaces. Practically all modern coils are of the extended surface type. Fig 3.6 shows two types of finned tubing. Fig. 3.6(a) employs spiral fins while Fig. 3.6(b) shows continuous flat-plate fins. The heating medium passes through the tubes while moist air flows across the tubes and through the fins. The tubes are commonly made of copper, aluminium, or red brass; the secondary surface is made of aluminium or copper. The fins are usually mechanically bonded to the tubes.

3.4.1 Heat Transfer Performance

The heat transmission rate of air passing over a clean tube (with or without extended surface) to a fluid flowing within it, is impeded principally by three thermal resistance. The first is that from the air to the surface of the tube, it is usually called the external surface or air-film thermal resistance. The second is the thermal resistance to the conduction of heat through the fin and tube metal. Finally, there is a tube-side heating fluid film thermal resistance to impede the flow of heat between the internal surface of the metal and the fluid in the tube. For some applications, an additional thermal resistance is included to account for either or both external and internal surface fouling.

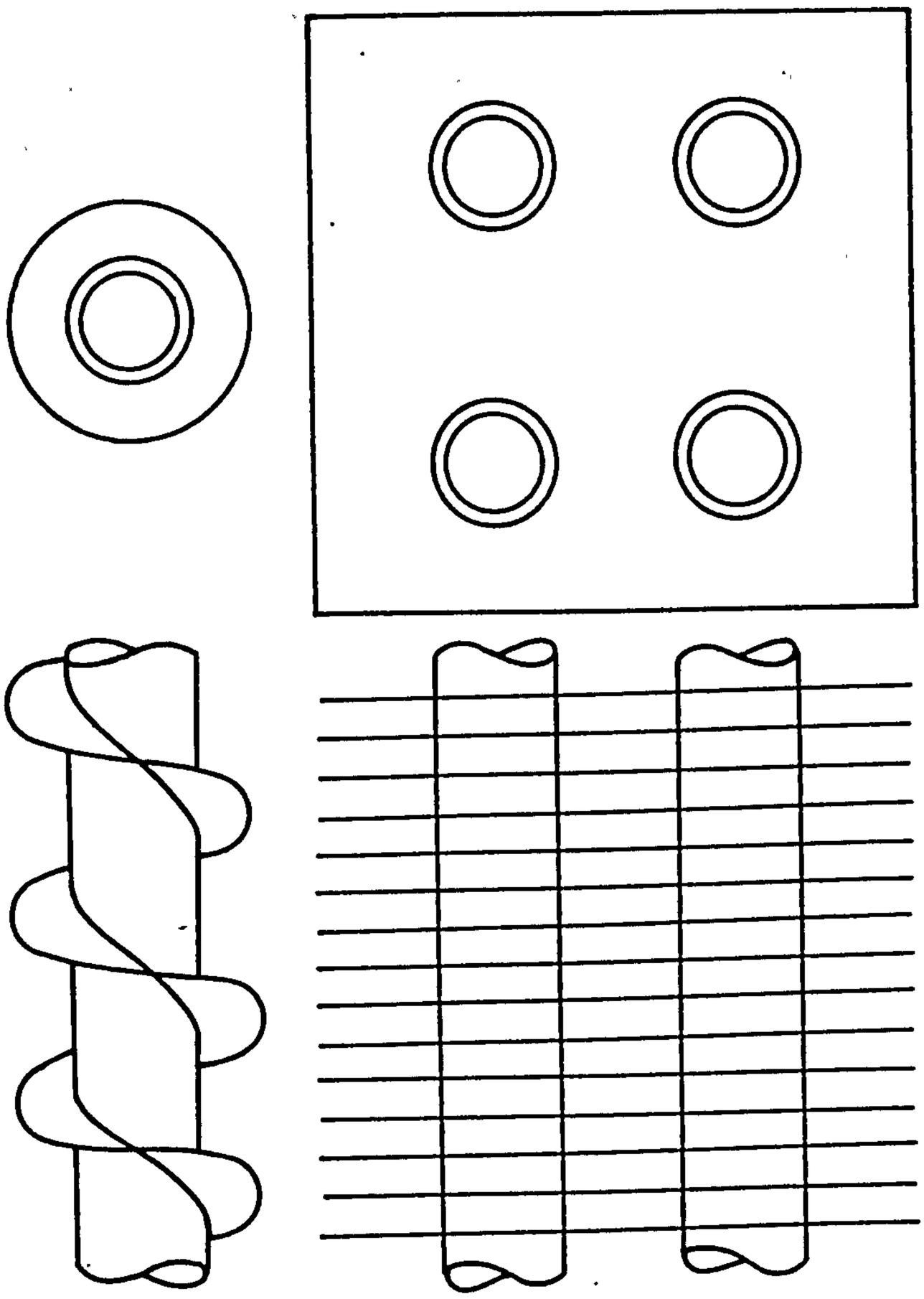

FIG. 3·6 SCHEMATIC ILLUSTRATIONS OF FINNED TUBING.

(a) (b)

The performance of heating coils depends in general on:

1) The overall coefficient (U_o) of heat transfer between moist airstream and the hot fluid.

2) The mean temperature difference (Δt_m) between moist airstream and the hot fluid.

3) The physical dimensions of and data for the coil (such as face area A_a and total external surface area A_o) with characteristics of the heat transfer surface.

The rate of heat transfer from the hot fluid to the airstream is expressed by the following basic equation:

$$q_h = U_o A_o \Delta t_m \qquad (3.42)$$

where:

q_h = rate of heat transfer from the hot fluid to the airstream (kW).

U_o = overall coefficient of heat transfer between the airstream and hot fluid (kW/m^2K)

A_o = total external surface area (m^2)

Δt_m = mean temperature difference between the airstream and hot fluid (K)

Assuming no extraneous heat losses, the same amount of heat is gained by the airstream:

$$q_h = \dot{m}_a c_{pma} (t_{ao} - t_{ai}) \qquad (3.43)$$

where:

m_a = mass flow rate of air (kg/s)

t_{ao} = dry bulb temperature of air leaving the heating coil (^oC).

t_{ai} = dry bulb temperature of air entering the heating coil (^oC).

The same amount of heat is lost by the hot fluid.

$$q_h = m_h\, c_{ph}\, (t_{hi} - t_{ho}) \qquad (3.44)$$

where:

m_h = mass flow rate of hot fluid (kg/s)

c_{ph} = specific heat capacity of hot fluid (kJ/kg K)

t_{hi} = temperature of hot fluid entering the coil (^oC)

t_{ho} = temperature of hot fluid leaving the coil (^oC)

The most economical heat exchanger is usually the finned-tube employing some form of crossflow arrangement. Fig. 3.7 shows two schematic arrangements. Fig 3.7(a) shows a pure crossflow heat exchanger with two rows of tubes. This type with one or two rows of tubes is commonly used in steam coils for heating air. Fig. 3.7(b) shows a counter-crossflow arrangement with four tube passes. This type with two or more tube passes is commonly used where hot water passes through the tubes.

Threlkeld (Ref. 8) has shown that the mean temperature difference for a crossflow heat exhanger is equivalent to that for a counterflow heat exchanger when one fluid temperature remain constant e.g. condensing steam. However, in this thesis, the multirow counter crossflow heat exchanger will be approximated by the multirow counterflow heat exchanger.

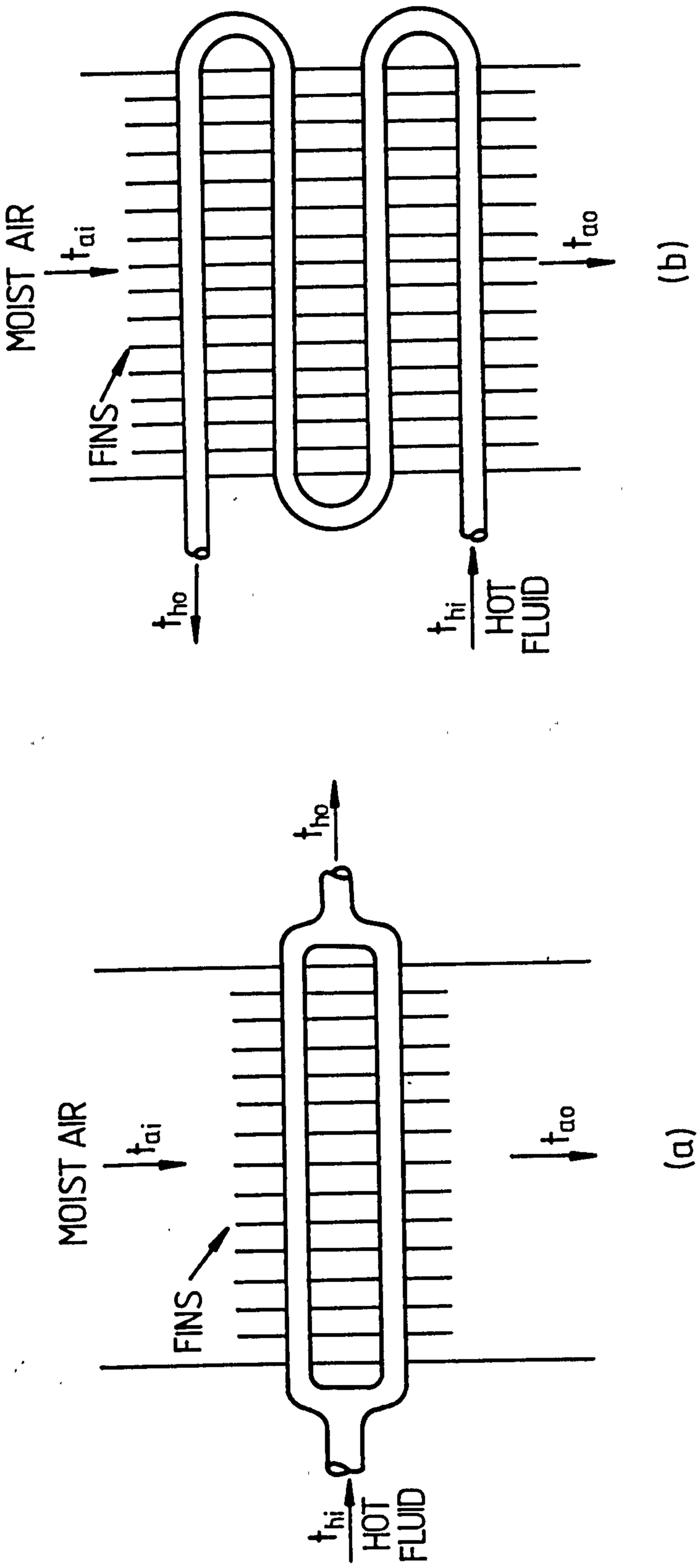

FIG. 3·7 SCHEMATIC CROSS-FLOW ARRANGEMENTS.

For a counterflow heat exchanger using hot water as the heating medium, the mean temperature difference is given by

$$\Delta t_{m,cfh} = \frac{(t_{wo} - t_{ai}) - (t_{wi} - t_{ao})}{\ln \frac{(t_{wo} - t_{ai})}{(t_{wi} - t_{ao})}} \qquad (3.45)$$

where:

$\Delta t_{m,cfh}$ = logarithmic mean temperature difference for counterflow (K)

t_{wo} = temperature of water leaving the heating coil (^{o}C)

t_{wi} = temperature of water entering the heating coil (^{o}C)

Fig. 3.8 shows the temperature distribution in a single-pass counterflow heat exchanger.

3.4.2 Effectiveness of a Counter Flow Hot Water Coil

3.4.2.1. Air Efficiency

The highest theoretical temperature to which air passing through a counterflow hot water coil can achieve is the temperature of the entering hot water, t_{wi}. The air efficiency, η_{ah}, is defined as the ratio of the actual increase in energy content of the air to the maximum theoretically possible. Thus

$$\eta_{ah} = \frac{m_a c_{pma} (t_{ao} - t_{ai})}{m_a c_{pma} (t_{wi} - t_{ai})} = \frac{t_{ao} - t_{ai}}{t_{wi} - t_{ai}} \qquad (3.46)$$

3.4.2.2. Water Efficiency

The lowest theoretical temperature to which water can be cooled in a counterflow heating coil is the temperature of the inlet air, t_{ai}.

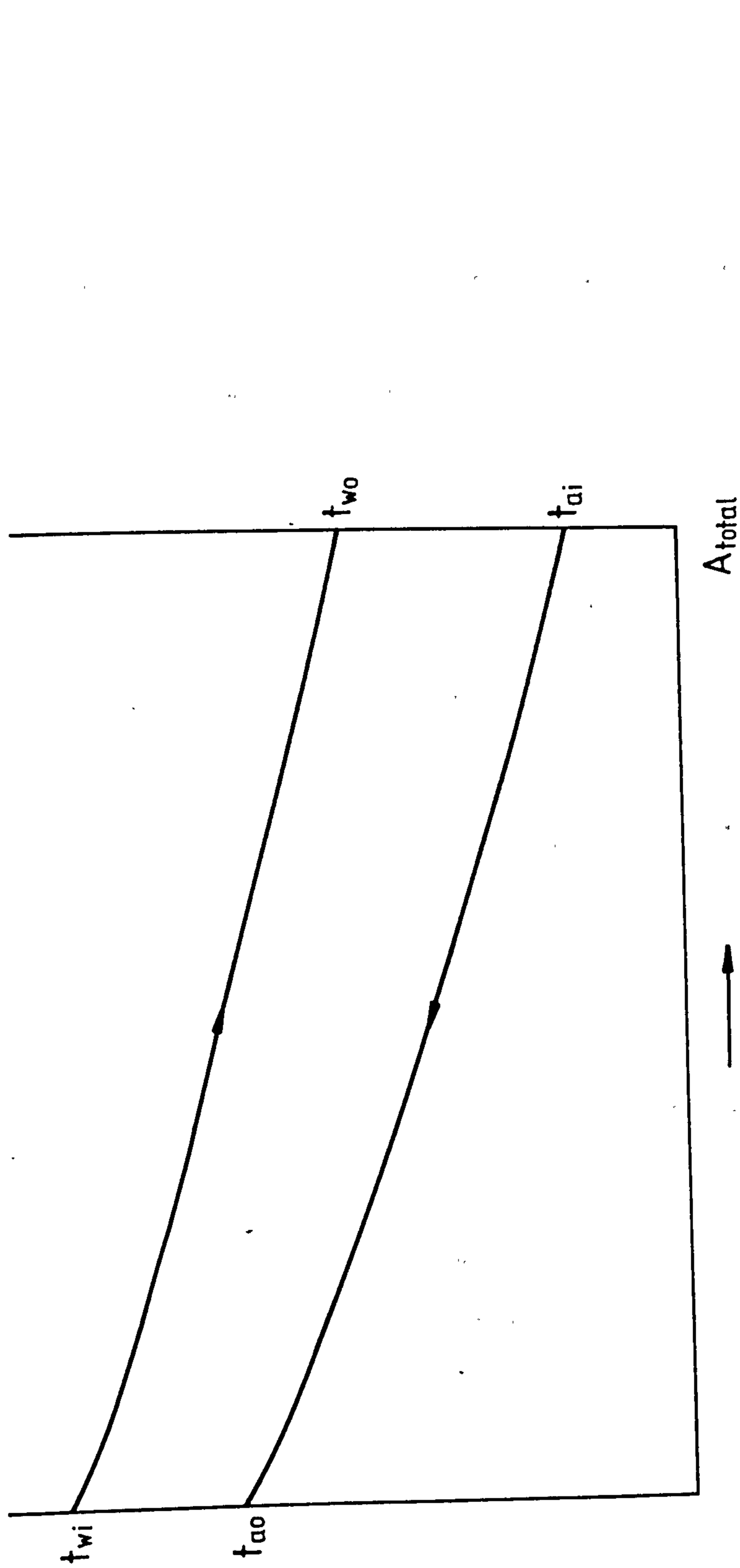

FIG 3·8 TEMPERATURE DISTRIBUTION IN SINGLE-PASS COUNTERFLOW HEAT EXCHANGER

The water efficiency η_{wh}, is defined as the ratio of the actual decrease in energy content of the water to the maximum theoretically possible. Thus

$$\eta_{wh} = \frac{m_w\, c_{pw}\, (t_{wi} - t_{wo})}{m_w\, c_{pw}\, (t_{wi} - t_{ai})} = \frac{t_{wi} - t_{wo}}{t_{wi} - t_{ai}} \qquad (3.47)$$

where:

m_w = mass flow rate of water through the heating coil (kg/s)

c_{pw} = specific heat capacity of water (kJ/kg K)

The effectiveness, E_h, of the hot water coil is defined as the efficiency for the fluid having the smaller thermal capacity. The thermal capacities for the two fluids are defined as follows:

For air, $C_{ah} = m_a\, c_{pma}$

For water, $C_{wh} = m_w\, c_{pw}$

The capacity rate ratio, C_h is the ratio of the smaller to the larger thermal capacity. Thus if:

$C_{ah} > C_{wh}$, then $C_h = \frac{C_{min}}{C_{max}} = \frac{C_{wh}}{C_{ah}} = \frac{m_w c_{pw}}{m_a c_{pma}}$ (3.48a)

and $E_h = \eta_{wh}$ (3.48b)

$C_{ah} < C_{wh}$, then $C_h = \frac{C_{min}}{C_{max}} = \frac{C_{ah}}{C_{wh}} = \frac{m_a c_{pma}}{m_w c_{pw}}$

and $E_h = \eta_{ah}$ (3.49b)

The number of transfer units, NTU_h, for a heating coil will now be defined. As with E_h and C_h, the definition of NTU_h depends on the relative magnitudes of the thermal capacities of the fluid streams.

It is defined as:

$$NTU_h = \frac{U_o A_o}{C_{min}} \qquad (3.50)$$

Thus if:

$$C_{ah} > C_{wh}, \text{ then } NTU_h = \frac{U_o A_o}{m_w c_{pw}} \qquad (3.51a)$$

$$C_{ah} < C_{wh}, \text{ then } NTU_h = \frac{U_o A_o}{m_a c_{pma}} \qquad (3.51b)$$

Expressions for E for several flow configurations have been published (Refs. 9, 10, 11 and 12). For a counter flow heat exchanger, the effectiveness, E, is given by

$$E = \frac{1 - \exp(-NTU\{1-C\})}{1 - C \exp(-NTU\{1-C\})} \qquad (3.52)$$

where $NTU = \frac{U_o A_o}{C_{min}}$ and $C = \frac{C_{min}}{C_{max}}$

Two limiting cases of Equation 3.52 are of particular interest, namely C = 0 and 1.

If C = 0 Equation 3.52 reduces to

$$E = 1 - \exp(-NTU) \qquad (3.53a)$$

If C = 1, then

$$E = \frac{NTU}{NTU + 1} \qquad (3.53b)$$

The derivation of Equations 3.52 and 3.53b is given in Appendix A3.1.

The rate of heat transfer from hot water to the moist airstream is then given by

$$q_h = C_{min}\, E_h\, (t_{wi} - t_{ai}) \qquad (3.54)$$

3.4.3 Overall Heat Transfer Coefficient for a Dry Heat Exchanger

From Equations 3.42 and 3.54, it is evident that the overall coefficient of heat transfer, U_o, must be determined in order to obtain the rate of heat transfer in a heat exchanger. Fig. 3.9 shows a schematic local section of a finned-tube heat exchanger. We will assume (1) steady state heat transfer, and (2) negligible contact resistance between the base of the fin and the tube ($t_{fb} = t_{to}$).

Before deriving an expression for U_o it will be useful, here, to define the fin efficiency η_f. Because the fin does not have a uniform temperature, the fin efficiency is defined as

$$\eta_f = \frac{q_{fin}}{q_{ideal}}$$

where:

q_{fin} = actual rate of heat transfer through fin (kW)

q_{ideal} = ideal rate of heat transfer through fin if entire fin surface were at fin base temperature t_{fb} (kW)

Here q_{ideal} is given by

$$q_{ideal} = A_f\, h_{of}\, (t_{fb} - t_a) \qquad (3.56a)$$

where:

A_f = surface area of fin (m^2)

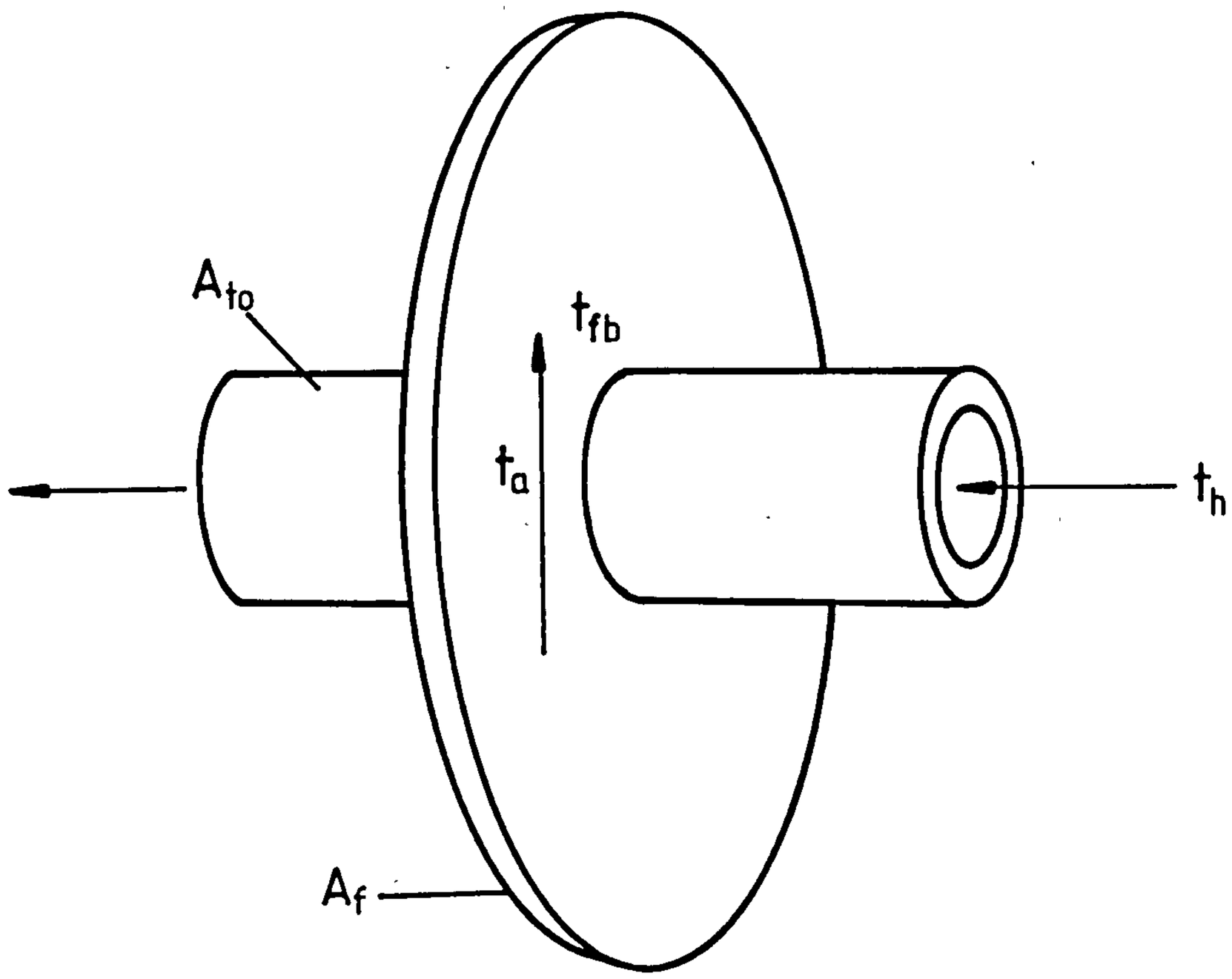

x_t = TUBE WALL THICKNESS (m)
t_a = DRY BULB TEMPERATURE OF AIR (°C)
t_{fb} = FIN BASE TEMPERATURE (°C)
t_{to} = TUBE OUTER SURFACE TEMPERATURE = t_{fb} (°C)
t_{ti} = TUBE INNER SURFACE TEMPERATURE (°C)
t_h = HOT FLUID TEMPERATURE (°C)
A_{ti} = TUBE INSIDE SURFACE AREA (m^2)
A_{to} = TUBE NET OUTSIDE SURFACE AREA (m^2)
A_{tm} = TUBE MEAN SURFACE AREA (m^2)
A_f = FIN SURFACE AREA (m^2)
A_o = TOTAL OUTSIDE SURFACE AREA (m^2)
$A_o = A_{to} + A_f$

FIG. 3·9 SCHEMATIC ILLUSTRATION OF A FINNED-TUBE HEAT EXCHANGER

h_{of} = heat transfer coefficient on the finned side of the heat exchanger (kW/m^2K)

t_{fb} = fin base temperature (^oC)

t_a = dry bulb temperature of air (^oC)

Thus q_{fin} is determined as

$$q_{fin} = \eta_f A_f h_{of} (t_{fb} - t_a) \quad (3.56b)$$

Considering Fig. 3.9, we may write the following equations for the rate of heat transfer

$$q = h_i A_{ti} (t_h - t_{ti}) \quad (3.57)$$

$$q = \frac{k_t A_{tm} (t_{ti} - t_{to})}{x_t} \quad (3.58)$$

$$q = h_{ot} A_{to} (t_{to} - t_a) + \eta_f h_{of} A_f (t_{fb} - t_a) \quad (3.59)$$

$$q = U_o A_o (t_h - t_a) \quad (3.60)$$

Assuming $h_{ot} = h_{of} = h_o$, we have from Equation 3.59,

$$q = h_o (A_{to} + \eta_f A_f) (t_{to} - t_a) \quad (3.61)$$

From Equation 3.57, $t_h - t_{ti} = \frac{q}{h_i A_i}$

From Equation 3.58, $t_{ti} - t_{to} = \frac{q x_t}{k_t A_{tm}}$

From Equation 3.61, $t_{to} - t_a = \frac{q}{h_o (A_{to} + \eta_f A_f)}$

Adding these equations we have,

$$t_h - t_a = \frac{q}{h_i A_i} + \frac{q x_t}{k_t A_{tm}} + \frac{q}{h_o(A_{to} + \eta_f A_f)} \qquad (3.62)$$

From Equation 3.60, $t_h - t_a = \frac{q}{U_o A_o}$

Thus

$$\frac{q}{U_o A_o} = \frac{q}{h_i A_i} + \frac{q x_t}{k_t A_{tm}} + \frac{q}{h_o (A_{to} + \eta_f A_f)} \qquad (3.63a)$$

Dividing throughout by q we have,

$$\frac{1}{U_o A_o} = \frac{1}{h_i A_i} + \frac{x_t}{k_t A_{tm}} + \frac{1}{h_o (A_{to} + \eta_f A_f)} \qquad (3.63b)$$

Multiplying throughout by A_o we have,

$$\frac{1}{U_o} = \frac{A_o}{h_i A_i} + \frac{x_t A_o}{k_t A_{tm}} + \frac{A_o}{h_o (A_{to} + \eta_f A_f)} \qquad (3.63c)$$

Now $A_o = A_{to} + A_f$; considering the last term in Equation 3.63c we have

$$\frac{A_o}{h_o (A_{to} + \eta_f A_f)} = \frac{A_{to} + A_f}{h_o (A_{to} + \eta_f A_f)}$$

$$= \frac{A_{to} + \eta_f A_f + A_f - \eta_f A_f}{h_o (A_{to} + \eta_f A_f)}$$

$$= \frac{1}{h_o} + \frac{A_f (1 - \eta_f)}{h_o (A_{to} + \eta_f A_f)}$$

$$\frac{A_o}{h_o(A_{to} + \eta_f A_f)} = \frac{1}{h_o} + \frac{1 - \eta_f}{h_o (\eta_f + A_{to}/A_f)}$$

Substituting into Equation 3.63c we have

$$\frac{1}{U_o} = \frac{A_o}{A_i h_i} + \frac{A_o x_t}{k_t A_{tm}} + \frac{1 - \eta_f}{h_o (\eta_f + A_{to}/A_f)} + \frac{1}{h_o} \qquad (3.64)$$

Thus $R_t = R_i + R_{mt} + R_f + R_a$

where:

$R_t = \frac{1}{U_o}$ = total thermal resistance (m^2 K/kW)

$R_i = \frac{A_o}{A_i h_i}$ = inside surface thermal resistance (m^2 K/kW)

$R_{mt} = \frac{A_o x_t}{k_t A_{tm}}$ = tube wall thermal resistance (m^2 K/kW)

$R_f = \frac{1 - \eta_f}{h_o(\eta_f + A_{to}/A_f)}$ = fin thermal resistance (m^2 K/kW)

$R_a = \frac{1}{h_o}$ = air-side film thermal resistance (m^2 K/kW)

The thermal resistances R_t, R_i, R_{mt}, R_f and R_a are referred to external area, A_o. For practical problems, Equation 3.64 should be modified to allow for fouling factors.

A minor deposit of a film or scale on the outside surface of a finned coil generally has little effect upon U_o because of the usually large magnitude of $\frac{1}{h_o}$. Sometimes an allowance is made for imperfect bonding of the fins to the tubes but this effect is difficult to evaluate and with good construction, it should be small. It is more important to include a fouling coefficient for the inside surface of the tubes. The thermal resistance ,

R_{mt}, of the tube wall is a very small portion of the total resistance, R_t and may be neglected with very little error. Thus for more cases,

$$\frac{1}{U_o} = \frac{A_o}{A_i h_i} + \frac{A_o}{A_i\ h_{ffi}} + \frac{1- \eta_f}{h_o(A_{to}/A_f+\eta_f)} + \frac{1}{h_o} \qquad (3.65a)$$

where:

h_{ffi} = fouling coefficient of heat transfer on the inside surface of the tubes (kW/m^2 K)

$$\text{Thus } U_o = \frac{1}{\frac{A_o}{A_i h_i} + \frac{A_o}{A_i\ h_{ffi}} + \frac{1 - \eta_f}{h_o(A_{to}/A_f+\eta_f)} + \frac{1}{h_o}} \qquad (3.65b)$$

Let R_{ffi} be the inside surface fouling thermal resistance referred to A_o (m^2 K/kW).

$$R_{ffi} = \frac{A_o}{A_i\ h_{ffi}}$$

Thus

$$U_o = \frac{1}{R_i + R_{ffi} + R_f + R_a} \qquad (3.65c)$$

3.4.4. Evaluating Heat Transfer Coefficients and Fin Efficiency

3.4.4.1. External Surface Heat Transfer Coefficient Or Air-Side Heat Transfer Coefficient

The common finned tube heat exchangers used extensively in HVAC systems are generally compact heat exchangers where a large surface area per unit volume exists. An arbitrary definition has been proposed which states that the ratio of surface area to volume in a compact heat exchanger is greater than about 656 m^2/m^3 (Ref. 10)

The thermal characteristic performance of a finned tube heat exchanger is usually expressed in terms of the relationship between the air side Reynolds number Re_a, and the average heat transfer Colburn J-factor (Ref. 13) as follows:

$$J = \psi (Re_a) \qquad (3.66)$$

Re_a is based on the coil hydraulic diameter D_h and is expressed as:

$$R_{ea} = \frac{G D_h}{\mu} \qquad (3.67)$$

where:

G = mass velocity (kg/m^2s)
D_h = coil hydraulic diameter (m)
μ = dynamic viscosity (kg/ms)

D_h (Ref. 12) is defined as

$$D_h = \frac{4 L A_C}{A_O} \qquad (3.68)$$

where:

L = flow length of the heat exchanger (m)
A_C = minimum free-flow cross-sectional area (m^2)

G is defined as

$$G = \frac{m_a\ (1.0 + g_{ai})}{A_c} \qquad (3.69)$$

The average heat transfer J-factor is a function of the Stanton and Prandtl numbers (St and Pr respectively) and is given by

$$J = St\ Pr^{2/3} \qquad (3.70)$$

where

$$St = \frac{h_o}{G\ c_{pma}} \qquad (3.71)$$

$$Pr = \frac{\mu \times c_{pma}}{k} \qquad (3.72)$$

k = thermal conductivity (kW/mK)

Kays and London **(Ref. 12)** have studied extensively the heat transfer and pressure drop characteristics of a wide variety of compact heat exchanger surfaces. These include compact heat exchangers with tubular surfaces, plate-fin surfaces, surfaces where flow is normal to banks of finned tubes (finned-tube surfaces) and matrix surfaces. They recommend that the fluid properties μ, c_p and k be evaluated at the mean mixed fluid temperature. The finned-tube surface type, especially the family of heat exchangers with staggered tubes and either circular or continuous flat plate fins are widely used in HVAC systems. Experimental heat transfer data for representative coils, when plotted as J-factor against Re_a indicates that the functional relationship given by Equation 3.66 can be expressed as:

$$J = C_1\ Re_a^{C_2} \qquad (3.73)$$

Elmahdy and Biggs **(Ref. 14)** have suggested that over the air side Reynolds number range of 200 to 2000, the quantities C_1 and C_2 are constants for a particular coil. They postulate that C_1 and C_2 are dependent on the physical characteristics of the heat exchanger.

After analysing experimental heat transfer data for twenty different heat exchangers, the parameters C_1 and C_2 were found to be expressible in terms of the physical dimensions of the heat exchangers, namely fin thickness, spacing and height as well as the coil hydraulic diameter.

The expression for C_1 and C_2 according to Elmahdy and Biggs are:

$$c_1 = 0.159 \left\{\frac{F_t}{F_h}\right\}^{0.141} \left\{\frac{D_h}{F_t}\right\}^{0.065} \qquad (3.74)$$

$$c_2 = -0.323 \left\{\frac{F_t}{F_h}\right\}^{0.049} \left\{\frac{F_s}{F_t}\right\}^{0.077} \qquad (3.75)$$

$$F_h = 0.5 \{F_d - D_o\} \qquad (3.76)$$

where:

F_t = fin thickness (m)
F_h = fin height (m)
F_s = fin spacing (m)
F_d = fin diameter (m)
D_o = outside tube diameter (m)

Combining Equations 3.70, 3.71 and 3.73, h_o can be determined from the expression.

$$h_o = G\, c_{pma}\, Pr^{-2/3}\, C_1\, Re_a{}^{C_2} \qquad (3.77)$$

3.4.4.2 Internal Heat Transfer Coefficient

The internal heat transfer coefficient, h_i can be determined from empirical correlations for forced convection.

For fully developed turbulent flow of liquids in smooth tubes, the Dittus-Boelter equation (Ref. 13) is

$$Nu_D = 0.023 \quad Re_D^{0.8} \quad Pr^n \tag{3.78}$$

where:

n = 0.4 for heating ($t_s > t_b$)
n = 0.3 for cooling ($t_s < t_b$)
t_s = tube wall temperature (^oC)
t_b = bulk fluid temperature (^oC)
Nu_D = Nusselt number
Re_D = Reynolds number
Pr = Prandtl number

Equation 3.78 applies under conditions of $Re_D > 10,000$, $0.7 < Pr < 160$ and $L/D > 60$ and for moderate temperature differences between the fluid and the wall. All fluid properties should be evaluated at the arithmetic mean bulk temperature of the fluid, t_b.

For situations involving a large property variation, the Sieder and Tate equation (Ref. 15) is recommended:

$$Nu_D = 0.027 \quad Re_D^{0.8} \quad Pr^{1/3} \quad \left\{\frac{\mu}{\mu_s}\right\}^{0.14} \tag{3.79}$$

Equation 3.79 is applicable for $Re_D > 10,000$, $0.7 < Pr < 16,700$ and $L/D > 60$. All properties are evaluated at the bulk mean temperature t_b, except μ_s which is evaluated at the wall temperature t_s.

The heat transfer coefficient for laminar flow in tubes can be evaluated from an empirical correlation suggested by Seider and Tate (Ref. 15):

$$Nu_D = 1.86 \left\{Re_D \, Pr \, \frac{D}{L}\right\}^{1/3} \left\{\frac{\mu}{\mu_s}\right\}^{0.14} \tag{3.80}$$

Equation 3.80 applies for $\left\{Re_D \, Pr \, \frac{D}{L}\right\} > 10$ and all properties should be evaluated at the arithmetic mean bulk temperature except for μ_s, which is evaluated at the wall temperature.

For all water coils with surface designs employing smooth plain internal tube walls, the tube side water film heat transfer coefficient, h_w can be calculated by the following formula from McAdams (Ref. 13).

$$h_w = \frac{1.0572906\ (1.352 + 0.0198t_{wm})\ V_w^{0.8}}{D_i^{0.2}} \qquad (3.81)$$

where

h_w = water-side average film heat transfer coefficient (kW/m^2K)
t_{wm} = mean water temperature (^oC)
V_w = water velocity in tubes (m/s)
D_i = tube internal diameter (m)

Equation 3.81 is valid for water in the temperature range 4 to 104^oC and where the water-side Reynolds number is greater than 3100. It is recommended by ARI (Ref. 16) and the ASHRAE Handbook of Fundamentals (Ref. 3).

3.4.4.3 Fouling Coefficient

The term, R_{ffi}, in Equation 3.65c makes an allowance for the build-up of scale and dirt which may occur on the inside surface of the coil tubes. $\frac{1}{h_{ffi}}$ is known as the fouling factor. For water coils, this factor varies from a nominal value of about 0.09 up to 0.35 m^2 K/kW depending on the application (Ref. 17).

3.4.4.4 Fin Efficiency

Finned-tube heat exchangers are widely used in HVAC systems to increase the air side conductance and more evenly proportion the thermal resistance on each side of the heat exchanger. Numerous types of fin arrangements are used, the most common being smooth spiral, crimped spiral, flat plate and configurated plate.

Mathematical solution for the temperature distribution and fin efficiency of a large number of finned configurations are available in the literature **(Ref. 18, 19 and 20).** Exact solutions have been derived for constant thickness annular fins **(Ref. 18 and 19)** and tapered annular fins of constant area **(Ref. 19 and 21).**

For an annular fin of constant thickness, Gardner **(Ref. 19)** gives the fin efficiency as:

$$\eta_f = \frac{2}{u_b\left(1 - \left(\frac{\{u_e\}}{\{u_b\}}\right)^2\right)} \times \frac{(I_1\{u_b\} - B\,K_1\{u_b\})}{(I_o\{u_b\} + B\,K_o\{u_b\})} \qquad (3.82)$$

$$B = \frac{I_1(u_e)}{K_1(u_e)} \qquad (3.83)$$

$$u_b = \frac{F_h\sqrt{h_o/k_f}\,y_b}{\left(\frac{\{x_e\}}{\{x_b\}} - 1\right) - 1} \qquad (3.84)$$

$$u_e = \frac{u_b\,x_e}{x_b} \qquad (3.85)$$

$$F_h = x_e - x_b \qquad (3.86)$$

where:

$I_n(u)$ = modified Bessel function of the first kind and order n.
$K_n(u)$ = modified Bessel function of the second kind and order n.
k_f = thermal conductivity of fin material (kW/m K)
y_b = half-thickness of the fin (m)
x_e = $\frac{F_d}{2}$ = external radius of the fin (m)
x_b = fin base radius (m)

The modified Bessel functions I_o, I_1, K_o and K_1 can be evaluated by the polynomial approximation of these functions given by Abramowitz and Stegun (Ref. 22).

The continuous flat plate fin of uniform thickness is commonly used in finned coils in HVAC systems. It is not possible to obtain an exact mathematical solution for the efficiency of such a fin and approximate methods are necessary. Carrier and Anderson (Ref. 21) have shown that an adequate approximation is to assume that the fin area served by each tube is equivalent in performance to an annular fin of equal area and thickness. Fig. 3.10 shows the method where the equivalent outer radius of the annular fin is determined as

$$\pi x_e^2 - \pi x_b^2 = ac - \pi x_b^2$$

$$\pi x_e^2 = ac$$

$$x_e = \sqrt{\frac{ac}{\pi}} \qquad (3.87)$$

where

a = tube horizontal spacing (m)

c = tube vertical spacing (m)

Thus the fin efficiency of a continuous flat plate fin can now be determined by using Equations 3.82 to 3.86.

3.4.5 Heating Coil Control Methods

In various HVAC systems, the temperature of air leaving the heating coil is controlled with one of four control methods (Ref. 23):

1) Fixed Set Point
2) Outside Air Reset
3) Zone Controlled Reset
4) Wild/Uncontrolled Coil

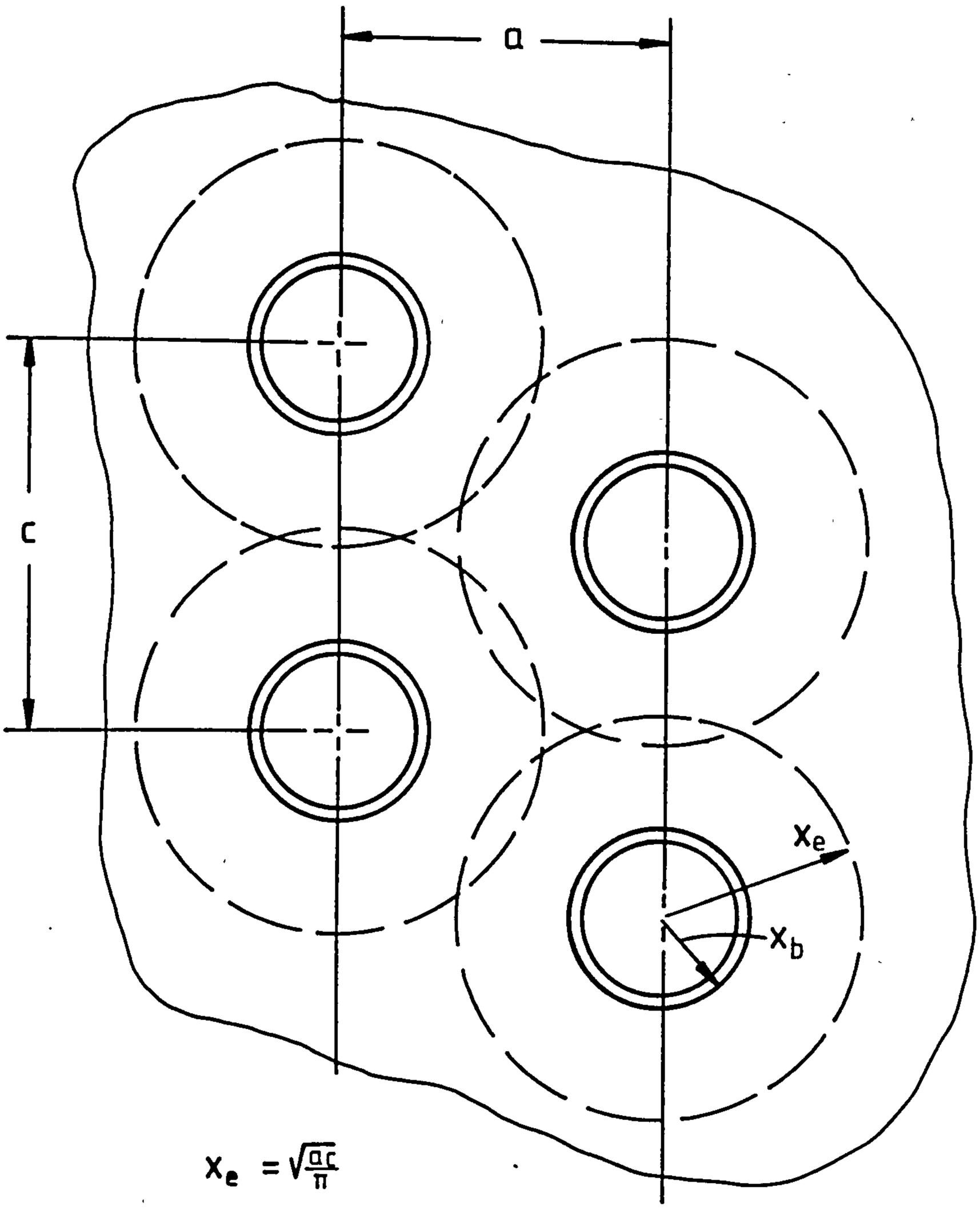

FIG. 3·10. APPROXIMATE METHOD FOR TREATING A CONTINUOUS FLAT PLATE FIN OF UNIFORM THICKNESS IN TERMS OF AN ANNULAR FIN OF EQUAL AREA.

3.4.5.1 Fixed Set Point

With a fixed set point, a heating coil discharge air sensor and controller are used to maintain a fixed leaving air control point. The control point will deviate from the set point depending on the throttling range (proportional band) of the controller and the load on the coil. The throttling range of an air temperature controller is the difference in temperature of the controlled air between the zero and full capacity conditions. Fig. 3.11 shows the basic heating coil control arrangement, assuming the characteristic curve of the controller/valve is linear.

The relationship between heating coil leaving air temperature to load, set point and throttling range can be derived. If

t_{sph} = set point or desired value of the temperature of the controlled air (^{o}C)

t_{rh} = throttling range of the heating coil air temperature controller (K)

ω_h = heating coil mass flow rate ratio - the ratio of mass flow rate of heating medium to its maximum mass flow rate .

then,

$$\frac{t_{ao} - (t_{sph} + 0.5t_{rh})}{\omega_h - 0.0} = \frac{t_{sph} - 0.5t_{rh} - (t_{sph} + 0.5t_{rh})}{1.0}$$

$$t_{ao} - t_{sph} - 0.5\, t_{rh} = - t_{rh}\, \omega_h$$

$$t_{ao} = t_{sph} - t_{rh}\, (\omega_h - 0.5) \qquad (3.88)$$

where:

$$\omega_h = \frac{m_h}{m_{h,max}} \qquad (3.89)$$

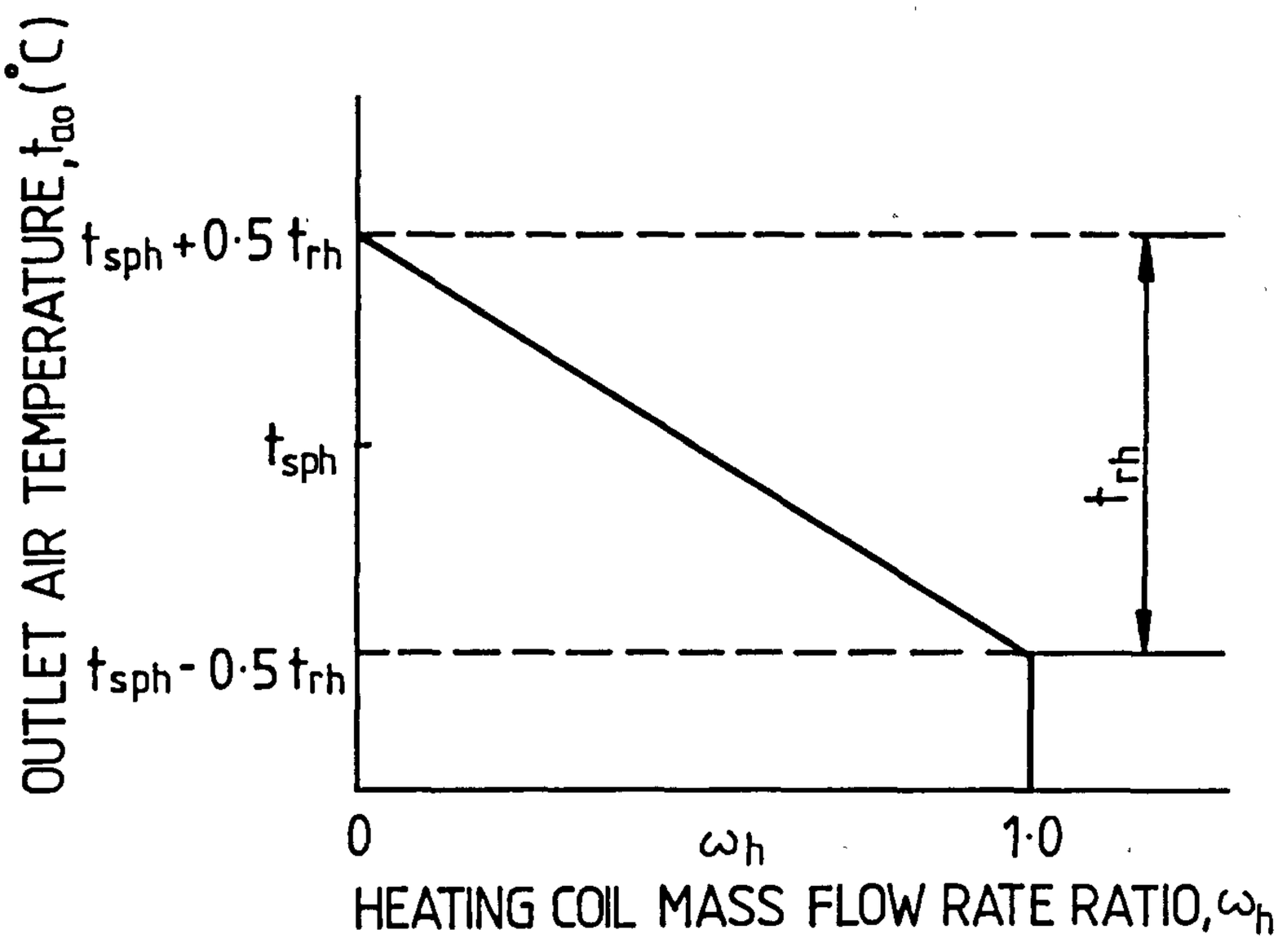

FIG. 3·11. FIXED SETPOINT CONTROL OF HEATING COIL

m_h = mass flow rate of heating medium (kg/s)

$m_{h,max}$ = maximum mass flow rate of heating medium.(kg/s)

For a perfect controller i.e. one in which the throttling range is zero (as might be approximated physically by a finely tuned proportional plus integral controller), Equation 3.88 becomes

$$t_{ao} = t_{sph} \qquad (3.90)$$

Thus, the leaving air temperature can be maintained at a fixed value as long as the capacity of the heating coil is adequate.

3.4.5.2 Outside Air Reset

With outside air reset, a heating coil discharge air controller is reset from a sensor located outdoors. The leaving air sensor maintains a control point based on the controller throttling range and the varying set point provided by the outside air sensor. Fig 3.12 shows the basic heating coil control arrangement.

The heating coil leaving air temperature is computed from Equation 3.88 or Equation 3.89 for a perfect controller where the setpoint varies and may be computed from Equations 3.91a, 3.91b and 3.91c.

If

t_{oa} = outside air temperature (^oC)

t_{oa1} = outside air temperature corresponding to setpoint t_{sp1} (^oC)

t_{oa2} = outside air temperature corresponding to setpoint t_{sp2} (^oC)

t_{sp1} = temperature setpoint one (^oC)

t_{sp2} = temperature setpoint two (^oC)

then,

$$\frac{t_{sp1} - t_{sph}}{t_{oa} - t_{oa1}} = \frac{t_{sp1} - t_{sp2}}{t_{oa2} - t_{oa1}}$$

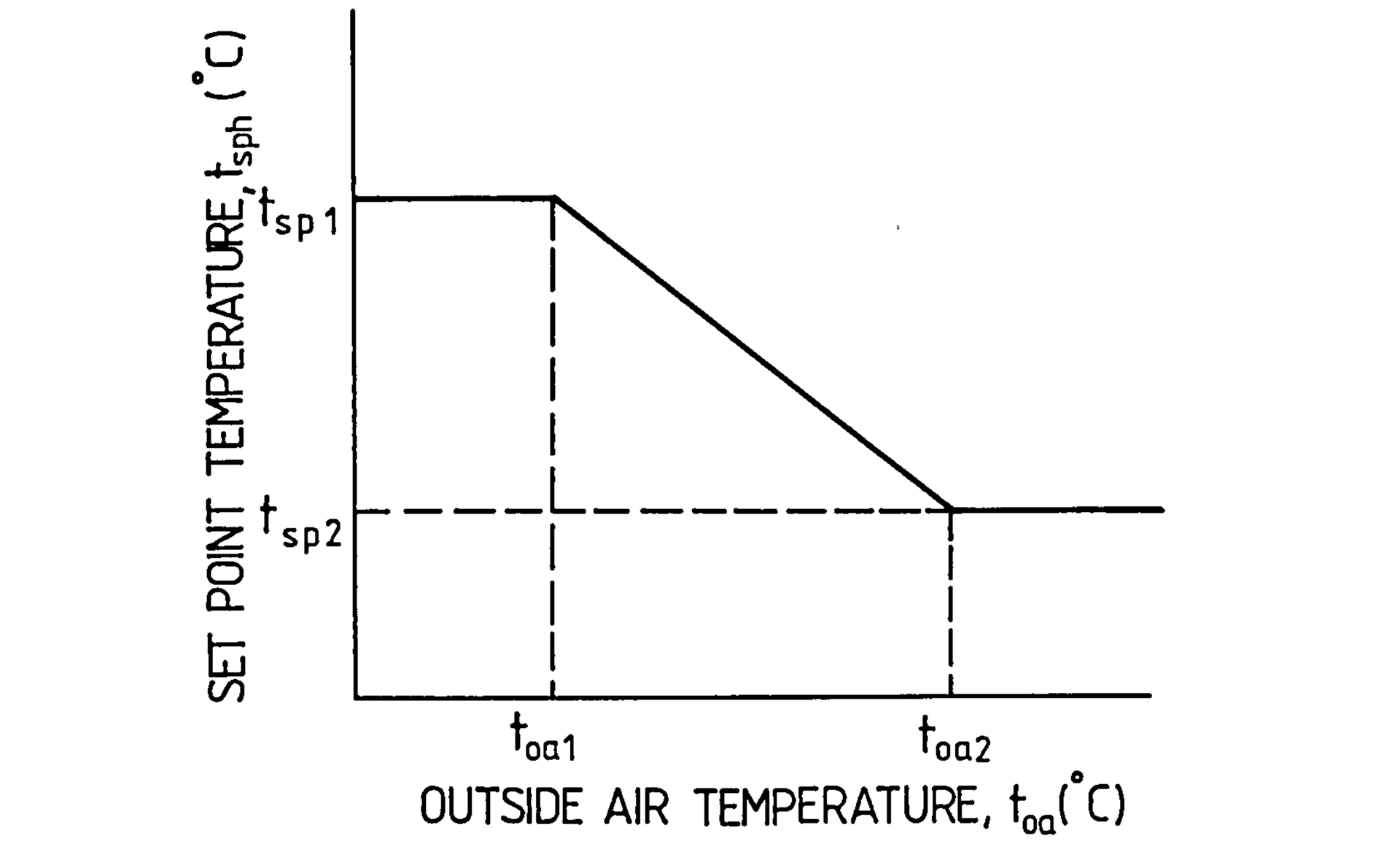

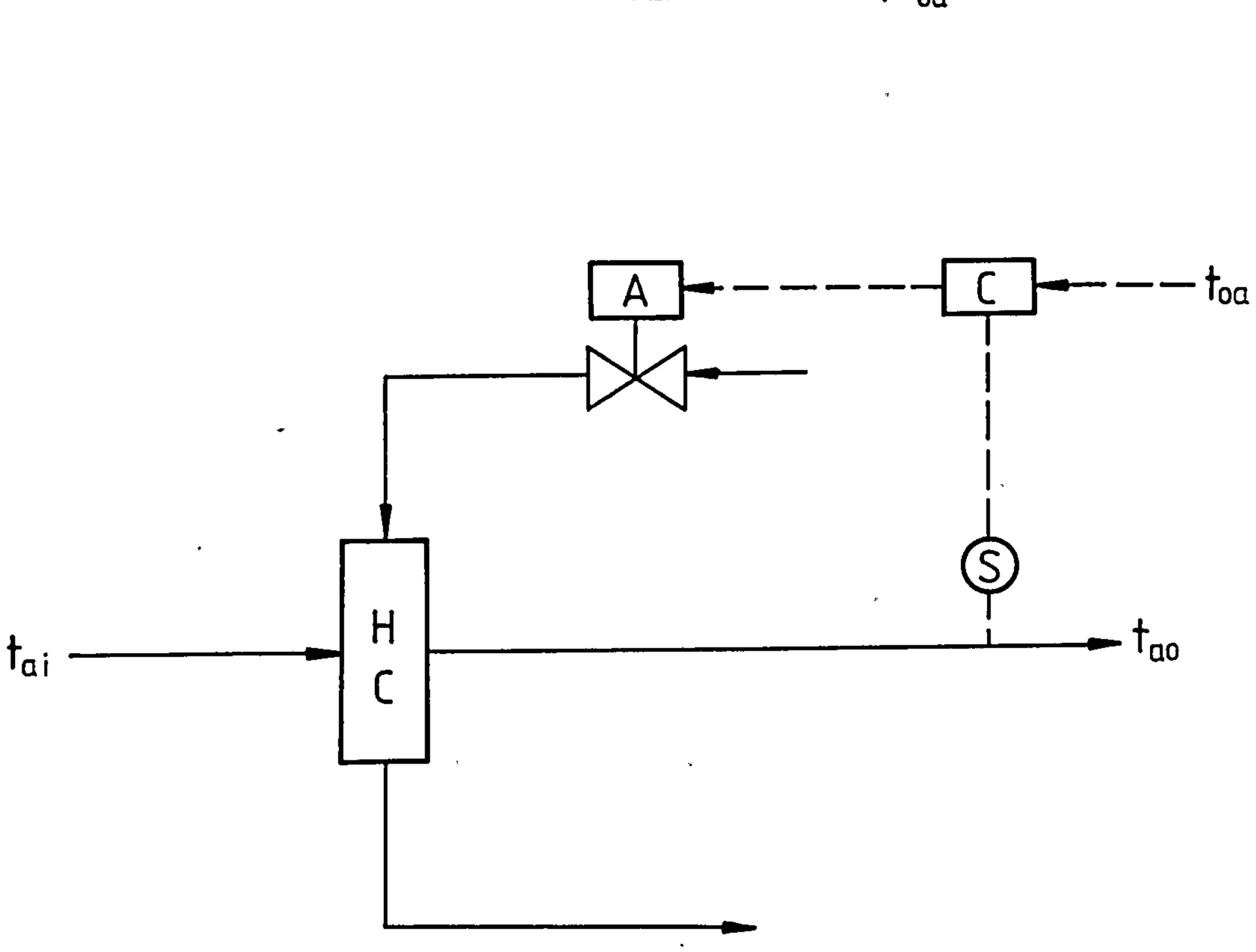

FIG. 3·12 OUTSIDE AIR RESET CONTROL OF HEATING COIL.

$$t_{spl} - t_{sph} = \frac{t_{oa} - t_{oal}}{t_{oa2} - t_{oal}} \quad (t_{spl} - t_{sp2})$$

$$t_{sph} = t_{spl} - \frac{(t_{oa} - t_{oal})}{(t_{oa2} - t_{oal})} \quad (t_{spl} - t_{sp2}) \qquad (3.91a)$$

where:

t_{sph} = temperature setpoint corresponding to t_{oa} (^{o}C)

Thus if:

$t_{oa} \leqslant t_{oal}$, $t_{sph} = t_{spl}$ (3.91b)

$t_{oal} < t_{oa} < t_{oa2}$, calculate t_{sph} from Equation 3.91a.

$t_{oa} \geqslant t_{oa2}$, $t_{sph} = t_{sp2}$ (3.91c)

3.4.5.3 Zone Controlled Reset

With zone controlled reset, a selector relay will determine the zone requiring the highest supply air temperature. This zone will in turn be used to reset the setpoint of the heating coil discharge air. Fig 3.13 shows the basic heating coil control arrangement. The heating coil leaving air temperature is computed from Equation 3.88 or Equation 3.89 for a perfect controller where the setpoint is given by

$$t_{sph} = t_{zh,crit} + \frac{q_{zh,\ crit}}{(m_a \times c_{pma})} \qquad (3.92)$$

where:

$t_{zh,crit}$ = temperature of zone requiring highest leaving air temperature - critical zone (^{o}C)

$q_{zh,crit}$ = heating load of critical zone (kW)

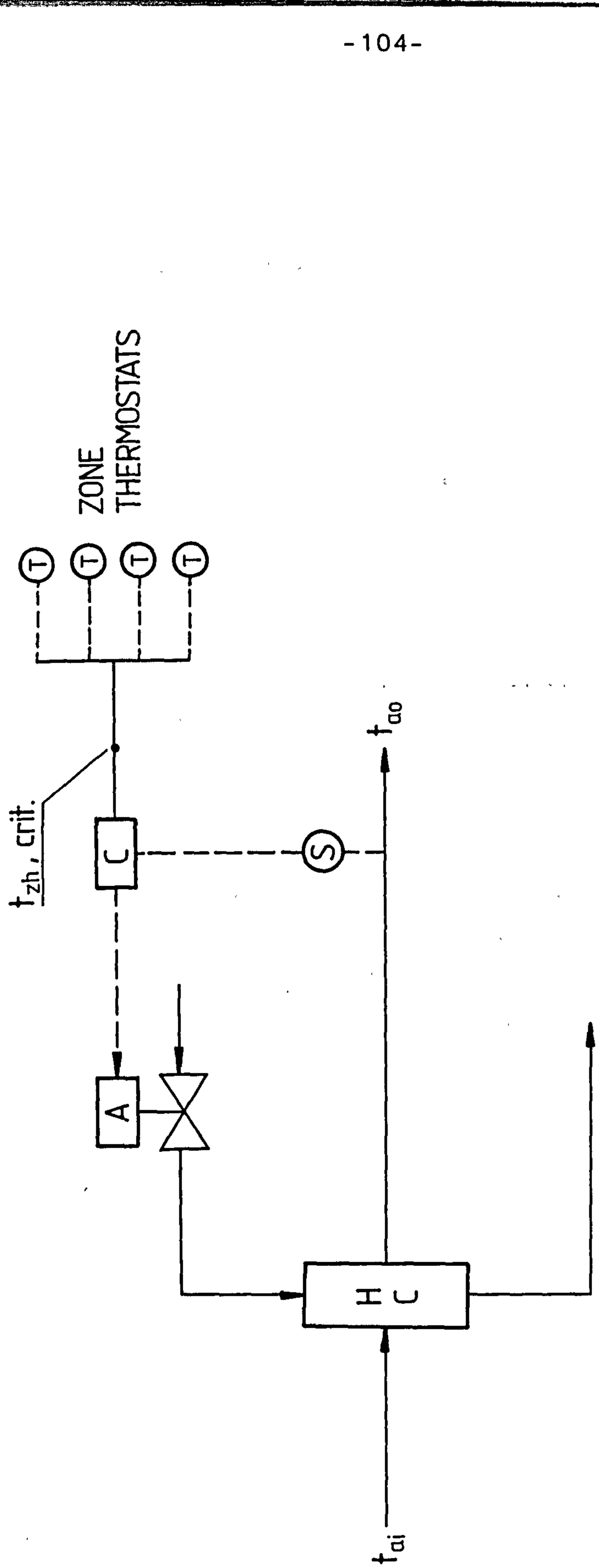

FIG. 3.3·13 ZONE CONTROLLED RESET OF HEATING COIL

3.4.5.4 Wild Or Uncontrolled Coil

A wild or uncontrolled heating coil occurs in two ways. First, if no valve or control is present, the leaving conditions will be a function of the entering fluid stream properties and mass flow rate and the effectiveness of the heat exchanger. Second, if the control valve is wide open, the coil is operating at its limit and the leaving conditions will be constrained by the capacity of the coil.

3.4.6 Algorithm for Simulating the Performance of a Counterflow Hot Water Coil Controlled bya Proportional Discharge Temperature Controller

This algorithm assumes that the hot water coil is a finned-tube heat exchanger with circular or continuous flat plate fins and heat transfer coefficients and surface geometry data are known or can be determined. It utilises the effectiveness and secant methods to determine the state of moist air leaving the coil, the mass flow rate of water through the coil, the rate of heat transferred to the airsteam and the temperature of water leaving the coil.

Input Data

Tube horizontal spacing = a (m)
Tube vertical spacing = c (m)
Tube outside diameter = D_o (m)
Tube inside diameter = D_i (m)
Fin spacing = F_s (m)
Fin thickness = F_t (m)
Hydraulic diameter = D_h (m)
Free - flow area/face area = σ
Fin area/Air side area = β
Face area = A_a (m^2)
Air side area = A_o (m^2)
Water side area = A_i (m^2)
Number of tubes per row = N_t

Number of rows of tubes = N_r

Air side heat transfer coefficient constants C_1 and C_2.

Inlet water temperature = t_{wi} (^oC)

Maximum water mass flow rate = $m_{wh,max}$ (kg/s)

Dry bulb temperature of air entering the coil = t_{ai} (^oC)

Moisture content of air entering the coil = g_{ai} (kg/kg)

Set point temperature = t_{sph} (^oC)

Throttling range of air temperature controller = t_{rh} (K)

Mass flow rate of air through the coil = m_a (kg/s)

Thermal conductivity of fin and tube material = k_f and k_t respectively (kW/mK)

Calculation Steps

1) Check if the heating coil is off.

   If $t_{ai} > t_{sph} + 0.5t_{rh}$, then the heating coil is off

   $t_{ao} = t_{ai}$

   $g_{ao} = g_{ai}$

   $m_{wh} = 0.0$

   $q_h = 0.0$

   $t_{wo} = t_{wi}$

   EXIT

2) Hot water coil is operating. In using the secant method, two starting values of water mass flow rate are required.

   Set $m_{wh1} = 0.0$

   $m_{wh2} = \omega m_{wh,max}$ $(0 < \omega \leq 1)$

3) From controller/valve characteristics (Equation 3.88), compute leaving air temperatures corresponding to m_{wh1} and m_{wh2}. Let these be t_{ao1} and t_{ao2} respectively.

4) Compute error 1, ER1 = $t_{ao1} - t_{ai}$

5) Using t_{ao2}, compute $q_h = m_a\ c_{pma}\ (t_{ao2} - t_{ai})$

6) Using m_{wh2}, compute $t_{wo} = t_{wi} - \dfrac{q_h}{m_{wh2}\ c_{pw}}$

7) Compute mean water temperature $t_{wm} = 0.5\ (t_{wo} + t_{wi})$

8) Compute $\Delta t_{m,cf}$ using Equation 3.45

9) Compute mean mixed air temperature, $t_{am} = t_{wm} - \Delta t_{m,cf}$

10) Compute waterside heat transfer coefficient, h_w. Use Equation 3.81 if water flow inside tubes is turbulent. Use Equation 3.80 if water flow inside tubes is laminar.

11) Compute heat transfer coefficient on the air side, h_a using Equation 3.77.

12) Compute fin efficiency η_f using Equations 3.82 to 3.87

13) Compute overall heat transfer coefficient U_o using Equation 3.64 or 3.65a.

14) Compute coil effectiveness E_h using Equation 3.52.

15) Compute new value for q_h, q_{hn} using Equation 3.54.

16) Compute a new value for t_{ao2}. $t_{ao2} = t_{ai} + \dfrac{q_{hn}}{m_a\ c_{pma}}$

17) Compute error 2, ER2 = $t_{ao1} - t_{ao2}$

18) Check for convergence

TOL = EPS x ABS (t_{aol})

where EPS is a small number

ERROR = ABS (ER2)

If ERROR < TOL go to step 25

19) Check that ER2 ≠ ER1

If ER2 = ER1, check the value of m_{wh2}.

If $m_{wh2} = m_{wh,max}$, simulate the performance of the coil at this condition. Exit.

20) $$A1X = \frac{(m_{wh2} - m_{wh1})}{ER2 - ER1}$$

21) Set $m_{wh1} = m_{wh2}$, ER1 = ER2

22) Compute a new value for m_{wh2}

$m_{wh2} = m_{wh2} - ER2 \times A1X$

23) Compute t_{ao3} using m_{wh2} in Equation 3.88

$t_{ao1} = t_{ao3}$

$t_{ao2} = t_{ao3}$

24) Return to step 5.

25) Compute output data

$t_{ao} = t_{ao1}$

$m_{wh} = m_{wh1}$

$g_{ao} = g_{ai}$

q_h has been previously calculated in step 5.

t_{wo} has been previously calculated in step 6.

26) Exit.

3.5 COOLING COILS

Cooling coils are used for cooling air with or without accompanying dehumidification. In HVAC applications, they are generally plate fin heat exchangers with chilled water or refrigerant on the tube side and air on the fin side; although spirally-wound fins are sometimes used.

When the chilled water or refrigerant in the coil tubes is at a lower temperature than the dew point temperature of the entering air, moisture will condense out of the air onto the tube and fin surfaces. Thus such coils can be used for cooling as well as dehumidification of the airstream. For air undergoing cooling and dehumidification, the psychrometric path of the air flowing through the coil follows one similar to that shown in Fig 3.14.

3.5.1 Heat Transfer Performance

The analysis of coil performance involving simultaneous cooling and dehumidification is complicated by the need to consider latent (or mass) transfer as well as sensible heat transfer. The total heat transfer is not a function of temperature difference alone, but depends also on the humidity of the air passing over the coil surface.

Two commonly used methods for analysing the performance of cooling and dehumidifying coils are the sensible heat ratio and the three line methods **(Refs. 17, 24 and 25).** The three line method is slightly more accurate than the sensible heat ratio method; however it is more complex and takes a longer time for convergence especially for iterative applications like simulating the performance of the coil and its control. Thus the sensible heat ratio method has been preferred in order to enhance the computational efficiency of the cooling coil simulation program.

The rate of heat transfer from the airstream to the coolant is given by

$$q_{ct} = m_a (h_{ai} - h_{ao}) - m_a(g_{ai}-g_{ao})h_{fw} \qquad (3.93)$$

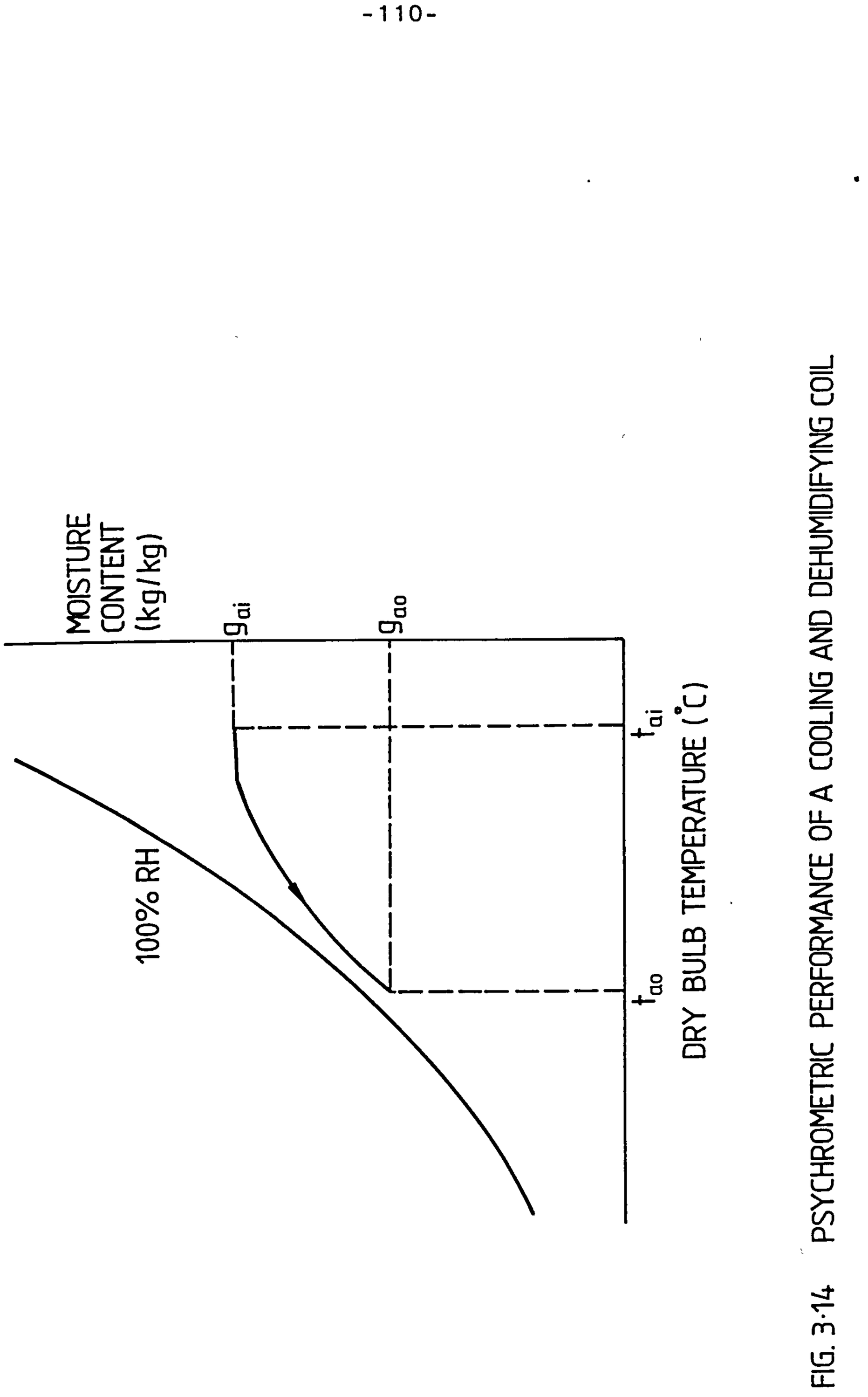

FIG. 3·14 PSYCHROMETRIC PERFORMANCE OF A COOLING AND DEHUMIDIFYING COIL

where

q_{ct} = rate of heat transfer from the airstream to the coolant (kW)

h_{ai} = enthalpy of air entering the cooling coil (kJ/kg)

h_{ao} = enthalpy of air leaving the cooling coil (kJ/kg)

g_{ai} = moisture content of air entering the cooling coil (kg/kg)

g_{ao} = moisture content of air leaving the cooling coil (kg/kg)

h_{fw} = specific enthalpy of water at condensate temperature t_w (kJ/kg)

According to Ref. 17, t_w is subject to substantial variations, depending on the method of coil installation as affected by coil face orientation, air flow direction, and air duct insulation. In practice t_w is frequently the same as the leaving air wet bulb temperature. Within the normal air conditioning range, precise values of t_w are not necessary since the enthalpy of the condensate $m_a (g_{ai} - g_{ao}) h_{fw}$ removed from the air, usually represents about 0.5 - 1.5% of the total cooling load. Thus Equation 3.93 reduces to

$$q_{ct} = m_a(h_{ai} - h_{ao}) \qquad (3.93a)$$

The rate of sensible heat transfer from the airstream to the coolant is given by

$$q_{cs} = m_a c_{pma} (t_{ai} - t_{ao}) \qquad (3.94)$$

where

q_{cs} = rate of sensible heat transfer from the airstream to the coolant (kW)

The sensible heat ratio, SHR, is defined as the rate of sensible transfer to total heat transfer. Thus

$$SHR = \frac{q_{cs}}{q_{ct}} = \frac{m_a c_{pma} (t_{ai} - t_{ao})}{m_a (h_{ai} - h_{ao})}$$

$$SHR = \frac{c_{pma} (t_{ai} - t_{ao})}{h_{ai} - h_{ao}} \qquad (3.95)$$

The sensible heat ratio method compensates for the latent heat transfer between the air and the outside surface of the coil by using the product of (1) the reciprocal of the sensible heat ratio and (2) the temperature difference between air and external coil surface as an equivalent sensible heat transfer temperature difference. In effect this gives an equivalent thermal resistance to be used with the overall mean temperature difference Δt_m. This modified overall thermal resistance is defined as

$$R'_t = SHR\ R_a + R_m + R_{ffi} + R_{ic} \qquad (3.96)$$

where:

R'_t = modified overall thermal resistence (m^2 K/kW)
R_a = air-side film thermal resistance (m^2 K/kW)
R_m = metal (tubing and fins) thermal resistance (m^2 K/kW)
R_{ffi} = inside surface fouling thermal resistance (m^2 K/kW)
R_{ic} = coolant film thermal resistance (m^2 K/kW)

The rate of total heat transfer from the airstream to the coolant is then given by

$$q_{ct} = \frac{A_o \ \Delta t_m}{R'_t} \qquad (3.97)$$

From the coolant side, q_{ct} is given by

$$q_{ct} = m_c c_{pc} (t_{co} - t_{ci}) \qquad (3.98)$$

where:

m_c = mass flow rate of coolant (kg/s)
c_{pc} = specific heat capacity of coolant (kJ/kg K)
t_{co} = temperature of coolant leaving the coil (^oC)
t_{ci} = temperature of coolant entering the coil (^oC)

Multirow finned tube heat exchangers are usually arranged so that the moist airstream flows over the tube banks in a counter-cross flow fashion. However, in this thesis, the counter-cross flow arrangement of a multirow heat exchanger will be approximated by a counterflow passage between moist air and coolant separated by metallic surface.

For a counterflow heat exchanger using chilled water as the coolant, the mean temperature differnce is given by

$$\Delta t_{m,cfc} = \frac{(t_{ai} - t_{wo}) - (t_{ao} - t_{wi})}{\ln \frac{(t_{ai} - t_{wo})}{(t_{ao} - t_{wi})}} \qquad (3.99)$$

where

$\Delta t_{m,cfc}$ = logarithmic mean temperature difference for counterflow (K).

3.5.2 Effectiveness of a Counterflow Chilled Water Coil

3.5.2.1 Air Efficiency

The lowest theoretical temperature to which air passing through a counterflow chilled water coil can achieve is the temperature of the entering chilled water, t_{wi}. The air efficiency, n_{ac} is defined as the ratio of the actual decrease in energy content of the air to the maximum theoretically possible. Thus

$$\eta_{ac} = \frac{m_a (h_{ai} - h_{ao})}{m_a (h_{ai} - h_{wi})} = \frac{h_{ai} - h_{ao}}{h_{ai} - h_{wi}} \qquad (3.100a)$$

where:

h_{wi} = specific enthalpy of air at t_{wi} (kJ/kg)

From Equation 3.95, $h_{ai} - h_{ao} = \frac{c_{pma} (t_{ai} - t_{ao})}{SHR}$

Also $h_{ai} - h_{wi} = \frac{c_{pma} (t_{ai} - t_{wi})}{SHR}$

Thus

$$\eta_{ac} = \frac{c_{pma} (t_{ai} - t_{ao})}{SHR} \times \frac{SHR}{c_{pma} (t_{ai} - t_{wi})}$$

$$\eta_{ac} = \frac{t_{ai} - t_{ao}}{t_{ai} - t_{wi}} \qquad (3.100)$$

3.5.2.2 Water Efficiency

The highest theoretical temperature to which water can be heated in a counterflow cooling coil is the temperature of the inlet air, t_{ai}. The water efficiency, η_{wc}, is defined as the ratio of the actual increase in energy content of the water to the maximum theoretically possible. Thus

$$\eta_{wc} = \frac{m_w c_{pw} (t_{wo} - t_{wi})}{m_w c_{pw} (t_{ai} - t_{wi})} = \frac{t_{wo} - t_{wi}}{t_{ai} - t_{wi}} \qquad (3.101)$$

The effectiveness, E_c, of the chilled water coil is defined as the efficiency for the fluid having the smaller thermal capacity. The thermal capacities for the two fluids are defined as follows:

For air, $C_{ac} = \frac{m_a c_{pma}}{SHR}$

For water, $C_{wc} = m_w c_{pw}$

The capacity rate ratio, C_c, is the ratio of the smaller to the larger thermal capacity. Thus if:

$$C_{ac} > C_{wc}, \text{ then } C_c = \frac{C_{min}}{C_{max}} = \frac{C_{wc}}{C_{ac}} = \frac{m_w\, c_{pw}\, SHR}{m_a\, c_{pma}} \qquad (3.102a)$$

$$\text{and } E_c = \eta_{wc} \qquad (3.102b)$$

$$C_{ac} < C_{wc}, \text{ then } C_c = \frac{C_{min}}{C_{max}} = \frac{C_{ac}}{C_{wc}} = \frac{m_a\, c_{pma}}{SHR\, m_w\, C_{pw}} \qquad (3.103a)$$

$$\text{and } E_c = \eta_{ac} \qquad (3.103b)$$

The number of transfer units, NTU_c, for a cooling coil is defined as:

$$NTU_c = \frac{U_o' A_o}{C_{min}} \qquad (3.104)$$

$$U_o' = \frac{1}{R_t}$$

U_o' = modified overall heat transfer coefficient (kW/m^2K)

Thus if:

$$C_{ac} > C_{wc}, \text{ then } NTU_c = \frac{U_o' A_o}{m_w c_{pw}} \qquad (3.105a)$$

$$C_{ac} < C_{wc}, \text{ then } NTU_c = \frac{U_o' A_o\, SHR}{m_a c_{pma}} \qquad (3.105b)$$

From Equation 3.52, the effectiveness E_c for a counterflow chilled water coil is given by

$$E_c = \frac{1 - \exp(-NTU_c\{1 - C_c\})}{1 - C_c \exp(-NTU_c\{1 - C_c\})} \quad (3.106)$$

If $C_c = 0$, Equation 3.106 reduces to

$$E_c = 1 - \exp(-NTU_c) \quad (3.107a)$$

If $C_c = 1$ then

$$E_c = \frac{NTU_c}{NTU_c + 1} \quad (3.107b)$$

The rate of total heat transfer from the moist airstream to the chilled water is given by

$$q_{ct} = C_{min} E_c (t_{ai} - t_{wi}) \quad (3.108a)$$

$$\text{Also } q_{cs} = q_{ct} \times SHR \quad (3.108b)$$

The derivation of Equations 3.106 and 3.107b is given in Appendix A3.2.

3.5.3 Cooling Coil Control Methods

The cooling coil leaving air temperature may be controlled with one of the following control types (Ref. 23):

1) Fixed Set Point
2) Outside Air Reset
3) Zone Controlled Reset
4) Wild/Uncontrolled Coil

3.5.3.1 Fixed Set Point

With a fixed set point, a cooling coil discharge air sensor and controller are used to maintain a fixed leaving air control point. The control point will deviate from the setpoint depending on the throttling range of the controller and the load on the coil. Fig 3.15 shows the basic cooling coil control arrangement assuming the characteristic curve of the controller/valve is linear.

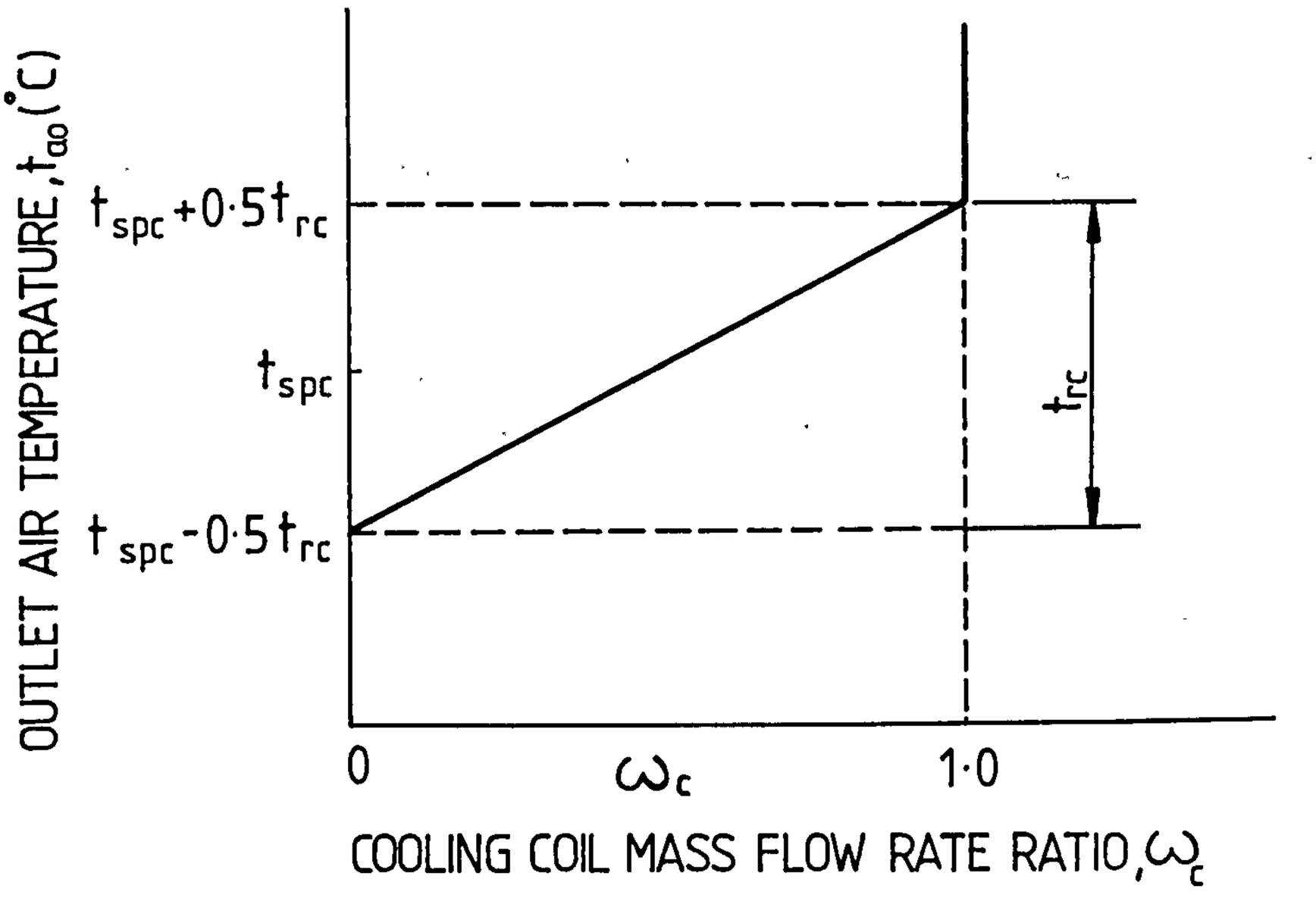

FIG. 3·15. FIXED SET POINT CONTROL OF COOLING COIL.

The relationship between cooling coil leaving air temperature to load, setpoint and throttling range can be derived. If

t_{spc} = setpoint or desired value of the temperature of the controlled air (^{o}C)

t_{rc} = throttling range of the cooling coil air temperature controller (k)

ω_c = cooling coil mass flow rate ratio - the ratio of mass flow rate of coolant to its maximum mass flow rate

then

$$t_{ao} = t_{spc} + t_{rc} (\omega_c - 0.5) \qquad (3.109)$$

where

$$\omega_c = \frac{m_c}{m_{c,max}} \qquad (3.110)$$

$m_{c,max}$ = maximum mass flow rate of coolant kg/s)

For a perfect controller i.e one in which the throttling range is zero, Equation 3.109 becomes

$$t_{ao} = t_{spc} \qquad (3.111)$$

Thus the leaving air temperature can be maintained at a fixed value as long as the capacity of the cooling coil is adequate.

3.5.3.2 Outside Air Reset

With outside air reset, a cooling coil discharge air controller is reset from a sensor located outdoors. The leaving air sensor maintains a control point based on the controller throttling range and the varying setpoint provided by the outside air sensor. Fig. 3.16_a shows the basic cooling coil control arrangement.

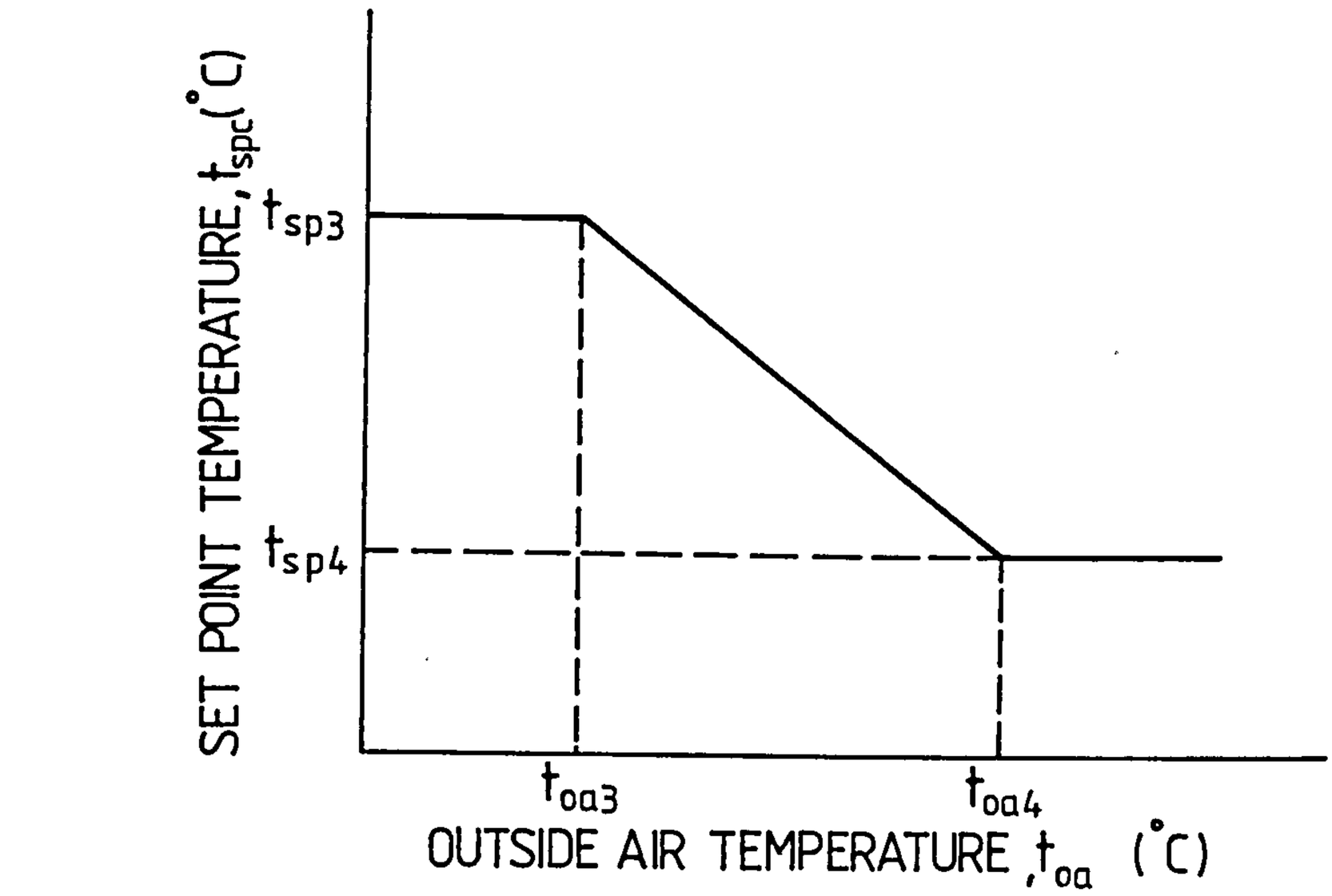

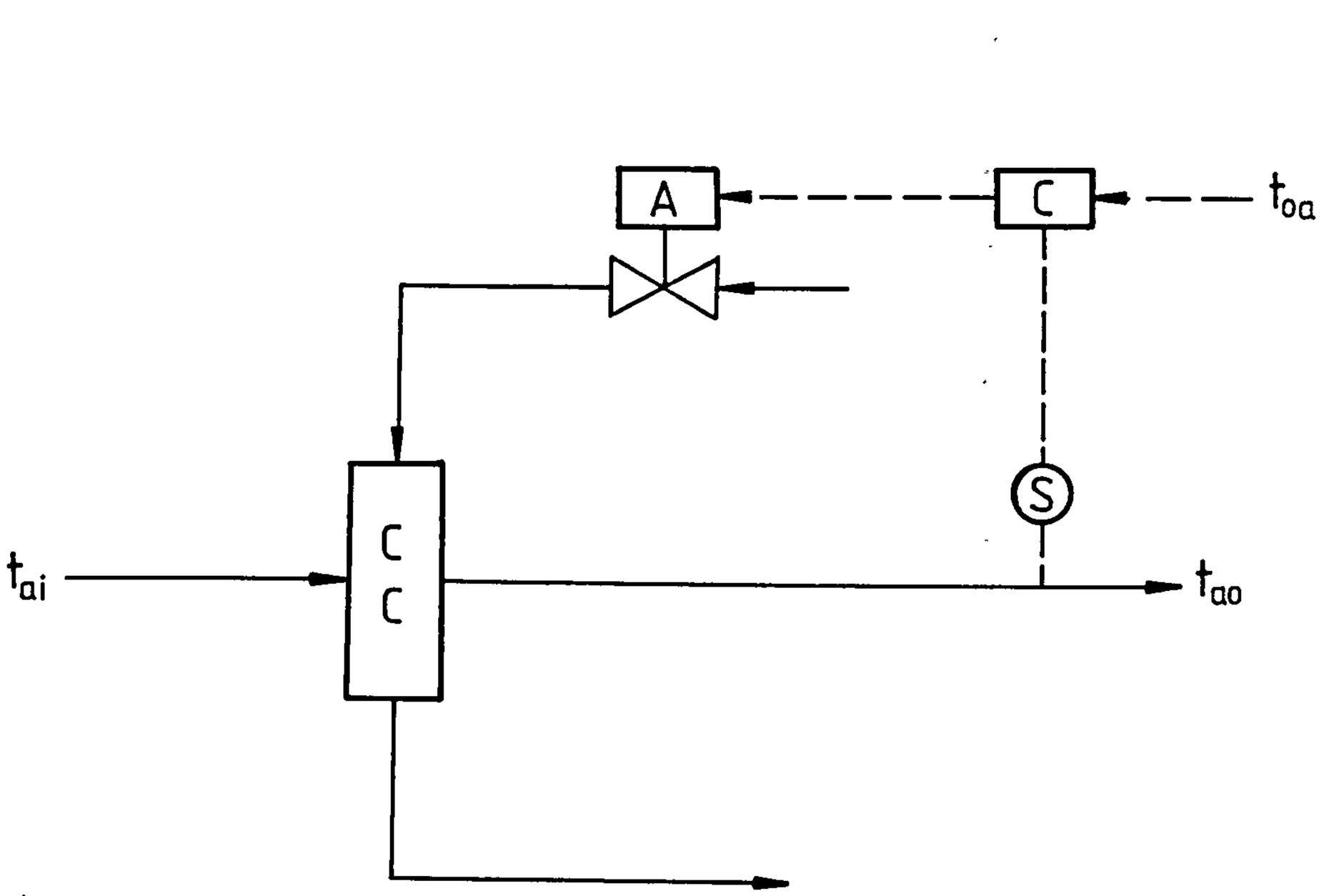

FIG. 3·16.a. OUTSIDE AIR RESET CONTROL OF COOLING COIL.

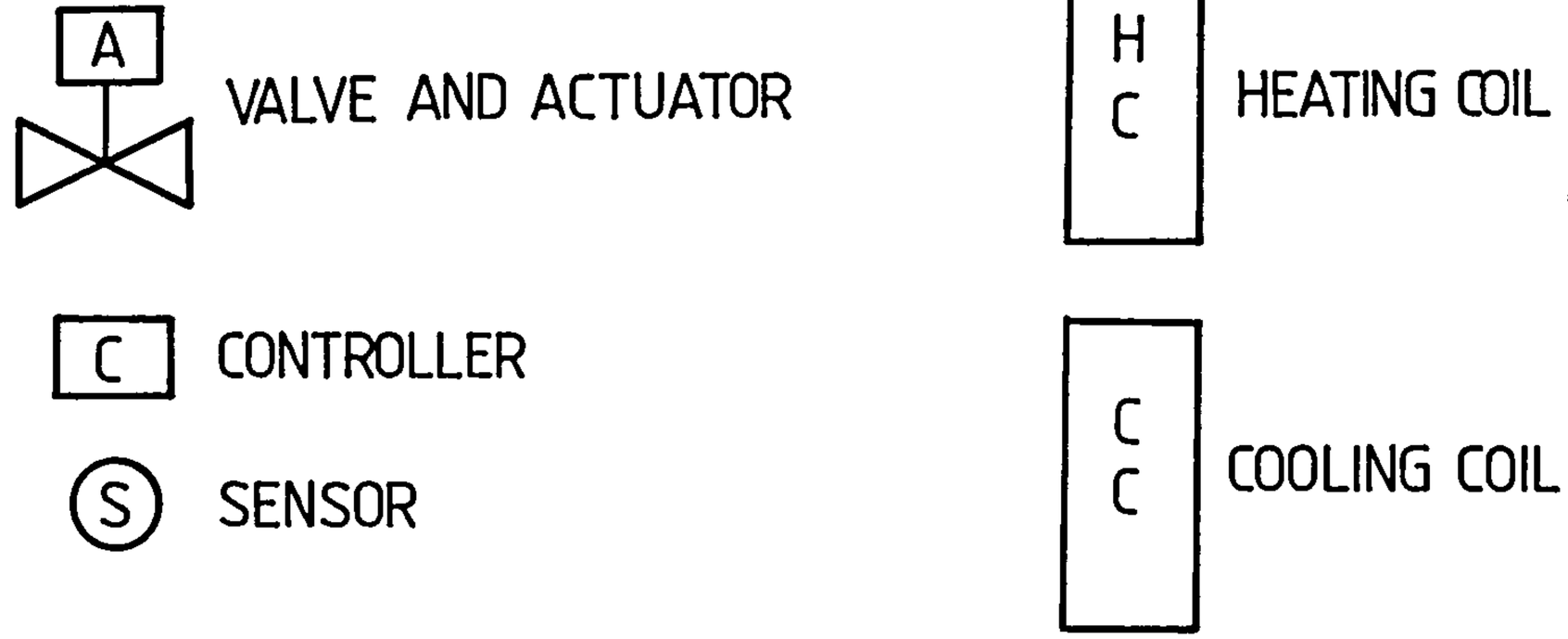

FIG. 3·16 b HEATING AND COOLING COIL CONTROL SCHEMATIC LEGEND

The cooling coil leaving air temperature is computed from Equation 3.109 or Equation 3.111 for a perfect controller where the setpoint varies and may be computed from Equations 3.112a, 3.112b and 3.112c.

$$t_{spc} = t_{sp3} - \frac{(t_{oa} - t_{oa3})\ (t_{sp3} - t_{sp4})}{(t_{oa4} - t_{oa3})} \qquad (3.112a)$$

Thus if:

$$t_{oa} \leqslant t_{oa3},\ t_{spc} = t_{sp3} \qquad (3.112b)$$

$t_{oa3} < t_{oa} < t_{oa4}$, calculate t_{spc} from Equation 3.112a

$$t_{oa} \geqslant t_{oa4},\ t_{spc} = t_{sp4} \qquad (3.112c)$$

where:

t_{oa3} = outside air temperature corresponding to setpoint t_{sp3} (^{o}C)

t_{oa4} = outside air temperature corresponding to setpoint t_{sp4} (^{o}C)

t_{sp3} = temperature setpoint three (^{o}C)

t_{sp4} = temperature setpoint four (^{o}C)

3.5.3.3 Zone Controlled Reset

With zone controlled reset, a selector relay will determine the zone requiring the lowest supply air temperature. This zone will in turn be used to reset the setpoint of the cooling coil discharge air The cooling coil leaving air temperature is computed from Equations 3.109 or Equation 3.111 for a perfect controller where the setpoint is given by

$$t_{spc} = t_{z,crit} - \frac{q_{zc,crit}}{(m_a \times c_{pma})} \qquad (3.113)$$

where:

$t_{zc,crit}$ = temperature of zone requiring lowest leaving air temperature - critical zone (^{o}C).

$q_{zc,crit}$ = cooling load of critical zone (kW).

3.5.3.4 Wild/Uncontrolled Coil

A wild or uncontrolled cooling coil occurs in the same manner as described for heating coils in section 3.4.5.4. Thus the leaving air temperature from the cooling coil will be under similar constraints as stated for heating coils.

3.5.4 Contact - Mixture Principle

The contact-mixture principle **(Ref. 24)** is often used in the analysis of cooling and dehumidifying processes in cooling coils. It assumes that a proportion of the inlet air is in contact with the coil surface and at that temperature, while the rest bypasses the coil and leaves without change in temperature. The bypass factor, BF, of a cooling coil can be derived by considering the rate of sensible heat transfer across the air side of the coil.

From Equation 3.94, $q_{cs} = m_a c_{pma} (t_{ai} - t_{ao})$

Also

$$q_{cs} = \frac{A_o \Delta t'_m}{R_a} \qquad (3.114)$$

$$\Delta t'_m = \frac{(t_{ai} - t_{sm}) - (t_{ao} - t_{sm})}{\ln \frac{(t_{ai} - t_{sm})}{(t_{ao} - t_{sm})}} \qquad (3.115)$$

where:

$\Delta t'_m$ = mean temperature difference between the airstream and the mean coil surface temperature (K)

t_{sm} = mean coil surface temperature (^{o}C)

Thus, Equation 3.114 becomes

$$q_{cs} = \frac{A_o}{R_a} \times \frac{(t_{ai} - t_{ao})}{\ln \frac{(t_{ai} - t_{sm})}{(t_{ao} - t_{sm})}} \qquad (3.116)$$

Thus

$$m_a\, c_{pma}\, (t_{ai} - t_{ao}) = \frac{A_o}{R_a} \times \frac{(t_{ai} - t_{ao})}{\ln \frac{(t_{ai} - t_{sm})}{(t_{ao} - t_{sm})}}$$

$$\ln \frac{(t_{ai} - t_{sm})}{(t_{ao} - t_{sm})} = \frac{A_o}{m_a\, c_{pma}\, R_a}$$

$$\frac{t_{ai} - t_{sm}}{t_{ao} - t_{sm}} = \exp \left(\frac{A_o}{m_a\, c_{pma}\, R_a} \right)$$

$$\frac{t_{ao} - t_{sm}}{t_{ai} - t_{sm}} = \exp \left(\frac{-A_o}{m_a\, c_{pma}\, R_a} \right) \qquad (3.117a)$$

The left hand side of Equation 3.117a is the ratio of bypassed air to total air which is the bypass factor of the cooling coil.

Thus

$$BF = \frac{t_{ao} - t_{sm}}{t_{ai} - t_{sm}} = \exp \left(\frac{-A_o}{m_a\, c_{pma}\, R_a} \right) \qquad (3.117b)$$

$$\text{Thus} \quad t_{sm} = \frac{t_{ao} - BF\, t_{ai}}{1 - BF} \qquad (3.117c)$$

The saturated air enthalpy, h_{sm}, and moisture content, g_{sm} corresponding to t_{sm} is

$$h_{sm} = \frac{h_{ao} - BF\, h_{ai}}{1 - BF} \qquad (3.118)$$

$$g_{sm} = \frac{g_{ao} - BF\, g_{ai}}{1 - BF} \qquad (3.119)$$

where:

h_{sm} = saturated air enthalpy corresponding to t_{sm} (kJ/kg)

g_{sm} = saturated moisture content at t_{sm} (kg/kg)

3.5.5 Algorithm for Simulating the Performance of a Counterflow Chilled Water Coil Controlled by a Proportional Discharge Temperature Controller

This algorithm assumes that the chilled water coil is a finned-tube heat exchanger with circular or continuous flate plate fins and heat transfer coefficients and surface geometry data are known or can be determined. It utilises the sensible heat ratio, effectiveness and secant methods to predict the heat and mass transfer performance and balance point of coil operation. The state of moist air leaving the coil, the mass flow rate of water through the coil, the sensible, latent and total rate of heat transfer and the temperature of water leaving the coil are determined.

Apart from the data specified in Section 3.4.6 for heating coils, the following data are required:

Maximum mass flow rate of water through the coil = $m_{wc,max}$ (kg/s)
Setpoint temperature = t_{spc} (^{o}C)
Throttling range of air temperature controller = t_{rc} (K)

Calculation Step

1) Check if the cooling coil is off.

If $t_{ai} < t_{spc} - 0.5\ t_{rc}$, then the cooling coil is off.

$t_{ao} = t_{ai}$
$g_{ao} = g_{ai}$
$m_{wc} = 0.0$
$q_{cs} = 0.0$
$q_{ct} = 0.0$
$q_{ci} = 0.0$
$t_{wo} = t_{wi}$
Exit

2) Chilled water coil is operating. Use two starting values of water mass flow rate for simulating coil performance

Set $m_{wc1} = 0.0$

$m_{wc2} = \omega\, m_{wc,max}$ $\quad (0 < \omega \leq 1)$

3) From controller/valve characteristics (Equation 3.109), compute leaving air temperatures corresponding to m_{wc1} and m_{wc2}. Let these be t_{ao1} and t_{ao2} respectively.

4) Compute error 1, ER1 $= t_{ai} - t_{ao1}$

5) Compute arithmetic mean air temperature, t_{am}

$t_{am} = 0.5\,(t_{ai} + t_{ao2})$

6) Compute h_a using Equation 3.77 using airstream properties calculated at t_{am}, g_{ai}.

7) Compute R_a

$$R_a = \frac{1}{h_a}$$

8) Compute BF and t_{sm} using t_{ao2} and Equations 3.117b and 3.117c respectively.

9) Compute dewpoint temperature of air entering the coil, t_{dpai}.

10) Determine how coil operates

If $t_{dpai} > t_{sm}$, then coil performs sensible cooling and dehumidification

By tranforming Equations 3.118 and 3.119, computer h_{ao} and g_{ao}

Compute q_{cs} $\quad q_{cs} = m_a\, c_{pma}\, (t_{ai} - t_{ao2})$

Compute q_{ct} $\quad q_{ct} = m_a\, (h_{ai} - h_{ao})$

Compute q_{cl} $\quad q_{cl} = q_{ct} - q_{cs}$

$$SHR = \frac{q_{cs}}{q_{ct}}$$

Else coil performs sensible cooling only.

$g_{ao} = g_{ai}$

Compute h_{ao}. $h_{ao} = f(t_{ao2}, g_{ao})$

$q_{ct} = m_a (h_{ai} - h_{ao})$

$q_{cs} = q_{ct}$

$q_{cl} = 0.0$

SHR = 1.0

11) Compute t_{wo} using m_{wc2}. $t_{wo} = t_{wi} + \dfrac{q_{ct}}{(m_{wc2} \times c_{pw})}$

12) Compute mean water temperature, $t_{wm} = 0.5\ (t_{wi} + t_{wo})$.

13) Compute heat transfer coefficient on the waterside, h_w.

14) Compute heat transfer coefficient on the air side, h_a, using the mean mixed air temperature $t_{aml} = t_{wm} - \Delta t_{m,cfc}$ and g_{ai}

15) Compute fin efficiency, η_f

16) Compute R_t' using Equation 3.96

17) Compute coil effectiveness E_c using Equation 3.106

18) Compute new values for q_{ct} and q_{cs}, namely q_{ctn} and q_{csn} using Equations 3.108a and 3.108b

19) Compute a new value for t_{ao2}, $t_{ao2} = t_{ai} - \dfrac{q_{csn}}{(m_a \times c_{pma})}$

20) Compute error 2, ER2 = $t_{ao2} - t_{aol}$

21) Check for convergence

TOL = EPS x ABS (t_{aol}) where EPS is a small number

ERROR = ABS (ER2)

22) Check that ER2 $\neq$ ER1

If ER2 = ER1, check the value of m_{wc2}. If $m_{wc2} = m_{wc,max}$, simulate the performance of the coil at this condition. Exit.

23) $$AIX = \frac{(m_{wc2} - m_{wc1})}{ER2 - ER1}$$

24) Set $m_{wc1} = m_{wc2}$ and ER1 = ER2

25) Compute a new value for m_{wc2}

$m_{wc2} = m_{wc2} - ER2 \times AIX$

26) Compute t_{ao3} using m_{wc2} in Equation 3.109

$t_{ao1} = t_{ao3}$

$t_{ao2} = t_{ao3}$

27) Return to Step 5

28) Compute output data

$t_{ao} = t_{ao1}$

g_{ao} has been calculated in Step 10

$m_{wc} = m_{wc2}$

q_{cs}, q_{ct}, q_{cl} has been calculated in Step 10

t_{wo} has been calculated in Step 11

29) Exit

3.6 FANS

Basically, a fan is an air pump, a machine which creates a pressure difference and causes air flow. The impeller does work on the air, imparting to it both static and kinetic energy, varying in proportion depending on the fan type. In HVAC systems, three locations of fans are generally used; supply air fan, return air fan, and room or zone exhaust air fan.

Most commercial fans used in HVAC systems may be placed in one of two general types based upon construction and air flow patterns. These two types are centrifugal fans and axial flow fans. Centrifugal fans have flow within the rotating wheel (rotor) that is substantially radial to the shaft, with the rotor operating in a scroll-type housing. Axial fans have flow within the wheel that is substantially parallel to the shaft and operates within a cylinder or ring-type housing.

3.6.1 Fan Performance

The performance of fans is generally given in the form of a graph showing pressure, efficiency, and power as a function of volume flow rate. The following terms are generally used when discussing fan performance:

Fan capacity: The fan capacity, Q_{fa}, is defined as the volume of air, in m^3/s. passing through the fan outlet. In normal applications, the volume leaving the fan is substantially equal to that entering since the change in specific volume of the air between fan inlet and outlet is negligible.

Fan outlet velocity:

The fan velocity, $V_{fa,o}$, is the outlet velocity of a fan obtained by dividing the volume flow rate by the fan outlet area. It is the average velocity that would occur at a point removed from the fan in a discharge duct having the same cross sectional area as the fan outlet.

Fan velocity pressure:

The fan velocity pressure, $P_{fa,v}$, is the pressure corresponding to the fan outlet velocity. It is given by

$$P_{fa,v} = \frac{1}{2} \rho_a V_{fa,o}^2 \qquad (3.120)$$

$P_{fa,v}$ = velocity pressure (N/m^2)
ρ_a = density of air (kg/m^3)
$V_{fa,o}$ = fan outlet velocity (m/s)

Fan total pressure: The fan total pressure, $P_{fa,t}$ is the difference between total pressure at the fan outlet and the total pressure at the fan inlet.

Fan static pressure: The fan static pressure, $P_{fa,s}$, is the fan total minus the fan velocity pressure. It is given by

$$P_{fa,s} = P_{fa,t} - P_{fa,v} \qquad (3.121)$$

where:

$P_{fa,s}$ = fan static pressure (N/m^2)
$P_{fa,t}$ = fan total pressure (N/m^2)

Air Power: The air power, $W_{fa,a}$ is the theoretical power required to drive a fan if there were no losses. It is given by

$$W_{fa,a} = P_{fa,t} \times Q_{fa} \qquad (3.122)$$

where

$W_{fa,a}$ = air power (W)

Fan Power: The fan power, $W_{fa,sh}$, is the actual power required to drive a fan. It is the power input to the impeller or the power input to the fan drive shaft.

Fan total efficiency:

The fan total efficiency, $\eta_{fa,t}$, is the ratio of air power fo fan power. Thus

$$\eta_{fa,t} = \frac{W_{fa,a}}{W_{fa,sh}} \times 100 \qquad (3.123)$$

$\eta_{fa,t}$ = fan total efficiency (%)

$W_{fa,sh}$ = fan power (W)

The power required by the fan motor, $W_{fa,m}$, is given by

$$W_{fa,m} = \frac{W_{fa,sh} \times 100}{\eta_{fa,m}} \qquad (3.124)$$

where

$W_{fa,m}$ = fan motor power input (W)

$\eta_{fa,m}$ = efficiency of motor/drive system (%)

The fan contributes heat to the HVAC system and must be included in the airstream temperature rise.

If the fan and motor are both in the airstream, then the temperature rise is

$$\Delta t_{fa} = \frac{W_{fa,m}}{m_a \times c_{pma}} \qquad (3.125a)$$

where

Δt_{fa} = airstream temperature rise due to fan gains (K)

If the fan only is in the airstream, then the temperature rise is

$$\Delta t_{fa} = \frac{W_{fa,sh}}{m_a \times c_{pma}} \qquad (3.125b)$$

3.6.2 Duct Static Pressure Control

The three most common methods of controlling duct static pressures employ discharge volume dampers, fan inlet vanes, or variable speed motors. Janisse (Ref. 26) has presented the variation of fan power input with fan capacity for these common control methods and this is shown in Fig. 3.17. From a power consumption standpoint, variable speed motors are the most efficient followed by inlet vanes with discharge volume dampers or throttling at the unit being the least efficient. From first cost considerations, the positions are reversed with discharge dampers being the least costly followed by inlet vanes with variable speed motors being the most expensive.

With discharge damper control, dampers are installed to add at the fan the resistance that no longer exists in the duct when air flow decreases.

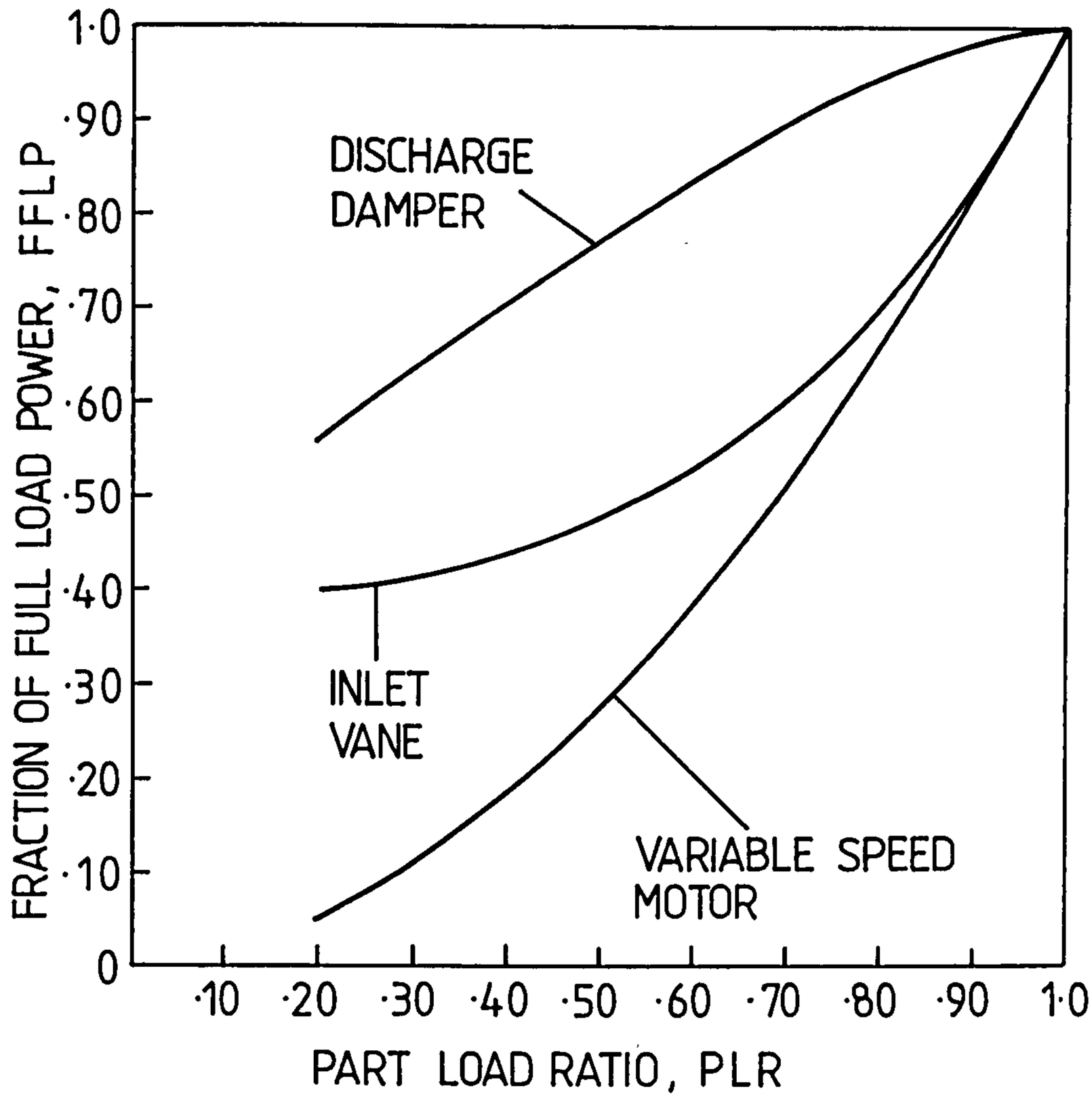

FIG. 3·17 FRACTIONAL FAN POWER Vs. AIR QUANTITY REDUCTION FOR THREE COMMON METHODS OF CONTROLLING DUCT STATIC PRESSURES.

With variable inlet vanes control, vanes are positioned by an actuator in response to a signal from a duct pressure controller. Through action of the actuator, the duct pressure controller repositions the inlet vanes to maintain a relatively constant duct pressure at the point of sensing. For axial-flow fans, the blade pitch angle is changed to facilitate the control of fan capacity.

With variable speed motor control, the motor speed is varied in response to a signal from the duct pressure controller to maintain a relatively constant duct pressure.

The fraction of full load power, FFLP, as shown in Fig. 3.17 may be expressed by the following equation:

$$FFLP = a + b \times PLR + c \times PLR^2 + d \times PLR^3 \qquad (3.126)$$

$$FFLP = \frac{W_{fa,sh}}{W_{fa,shd}} \qquad (3.127)$$

$$PLR = \frac{Q_{fa}}{Q_{fa,d}} \qquad (3.128)$$

where

PLR = part load ratio

$W_{fa,shd}$ = fan power at full load conditions (W)

$Q_{fa,d}$ = fan air volume at full load conditions (m^3/s)

a,b,c,d = fan part load model coefficients which have different values depending on fan capacity control method.

3.6.3 Fan Performance Simulation

The simulation of the fan performance involves calculating the power required by the fan/motor and the airstream temperature rise. For constant air volume systems, Equations 3.122 to 3.125 can be used to determine these quantities if the appropriate data is known. For variable air volume systems Equation 3.122 to 3.128 are used to determine these quantities if the method of control is specified. The moisture content of the air passing through the fan does not change.

3.7 HUMIDIFIERS

Humidifiers are used to increase the moisture content of air passing through an air handling unit. Humidification is required during periods, especially in winter, when the moisture content of outdoor air is low and the mixing of this air with return air might lead to the supply air having low moisture content. Two methods of humidification are in common use; one in which air is brought into intimate and effective contact with recirculated water, giving a process close to that of adiabatic saturation and one in which steam (normally dry saturated) is injected directly into the air.

3.7.1 Recirculating - Water Humidifier

In this type of humidifier, the air is brought into contact with recirculated water by means of either a wetted cell structure or by injecting the water as a finely divided spray (Fig. 3.18); the feed water being supplied at a temperature reasonably close to the wet bulb temperature of the entering air. Both configurations require the use of eliminator plates downstream of the unit to remove any droplets of water escaping from the humidifier. The psychrometric process takes place along a line of constant wet bulb temperature, as indicated in Fig. 3.19, where the latent heat of evaporation of the water is supplied by sensible heat transfer from the airstream.

The effectiveness of the humidifier is given by

$$E_{hu} = \frac{g_{ao} - g_{ai}}{g_{ss} - g_{ai}} \qquad (3.129a)$$

and the humidifying efficiency is

$$\eta_{hu} = E_{hu} \times 100.0 \qquad (3.130)$$

where

E_{hu} = effectiveness of recirculating water humidifier

g_{ao} = moisture content of air leaving the humidifier (kg/kg)

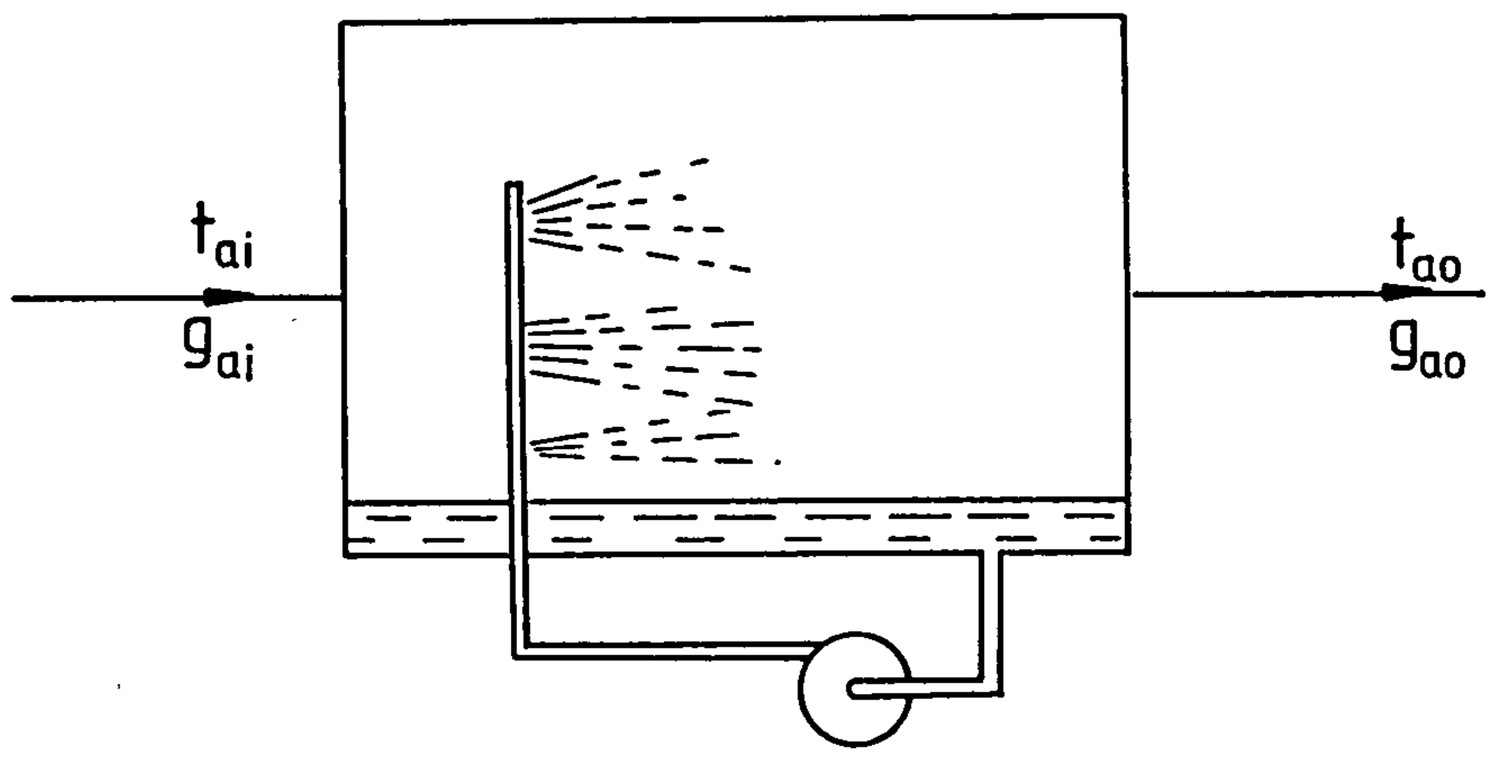

FIG. 3·18 SCHEMATIC DIAGRAM OF A HUMIDIFIER USING DIRECTLY RECIRCULATED SPRAY WATER.

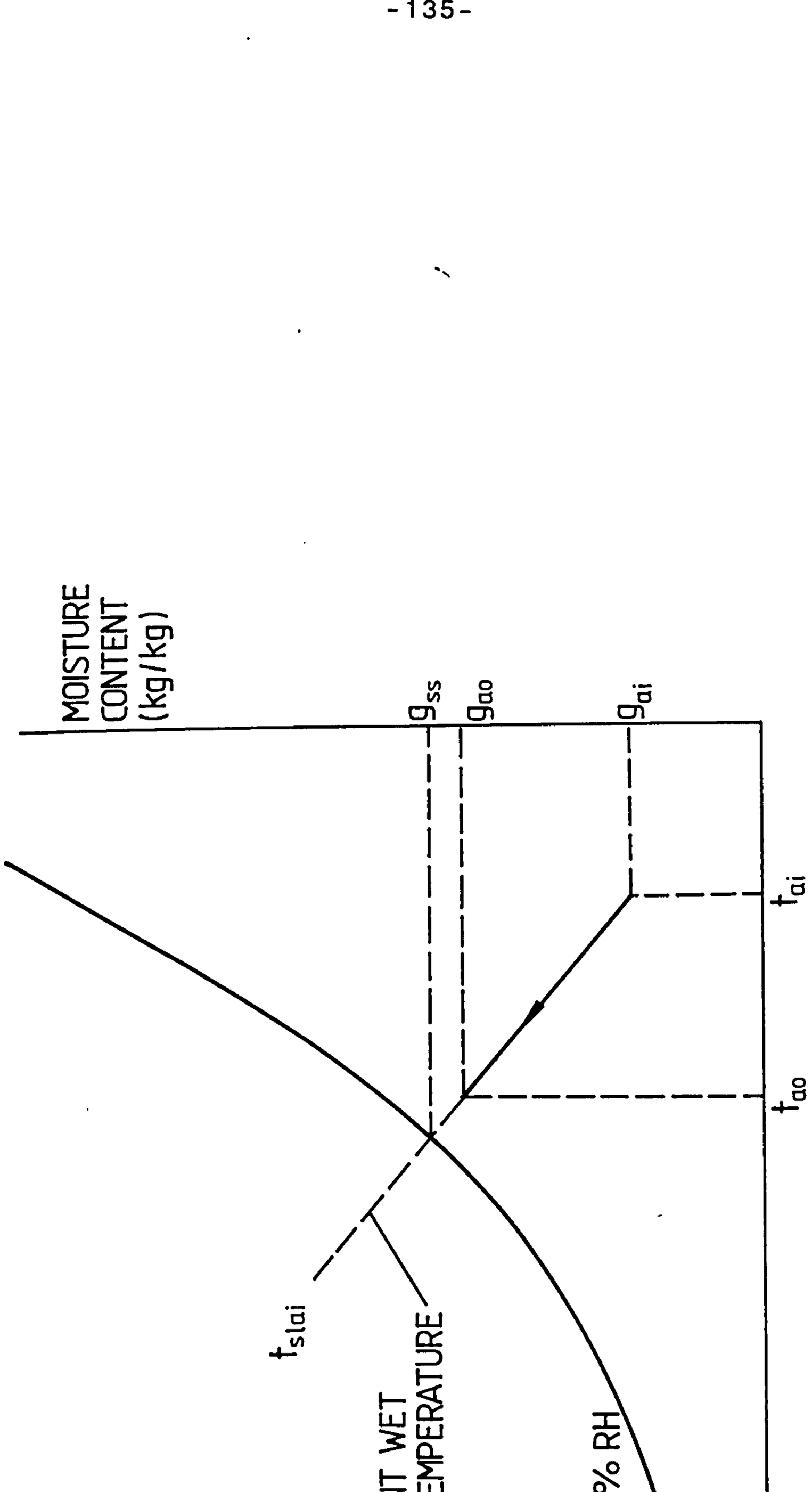

FIG. 3·19 PSYCHROMETRIC PROCESS FOR AIR PASSING THROUGH A HUMIDIFIER USING RECIRCULATED SPRAY WATER.

g_{ai} = moisture content of air entering the humidifier (kg/kg)

g_{ss} = moisture content of saturated air at the wet bulb temperature of entering air, t_{slai} (kg/kg)

η_{hu} = humidifying efficiency (%)

From Equation 3.129a, we have

$$g_{ao} = g_{ai} + E_{hu} (g_{ss} - g_{ai}) \qquad (3.129b)$$

The state of air leaving the humidifier can be determined if the effectiveness of the humidifier and the state of inlet air is known.

Calculation Steps

1) Compute the wet bulb temperature of the inlet air, t_{slai}.
2) Compute the saturated moisture content at t_{slai}, g_{ss}
3) Compute the moisture content of air leaving the humidifier, g_{ao}.
4) Since the change of state of air occurs along a line of constant wet bulb temperature, $t_{slao} = t_{slai}$. Knowing t_{slao} and g_{ao}, the dry bulb temperature of air leaving the humidifier, t_{ao} can be determined from psychrometric relations.

3.7.2 Steam Humidifier

Steam is directly injected into the airstream, thus increasing the moisture content of the air. The dry bulb temperature of air leaving the humidifier is slightly increased, the degree of increase depending on the condition of the injected steam. The psychrometric process for steam humidification is shown in Fig. 3.20.

The state of air leaving the humidifier can be determined by applying the principles of conservation of mass and energy. Assuming none of the injected steam is condensed, we have

$$m_a g_{ai} + m_{st} = m_a g_{ao} \qquad (3.131a)$$

$$m_a h_{ai} + m_{st} h_{st} = m_a h_{ao} \qquad (3.132a)$$

where

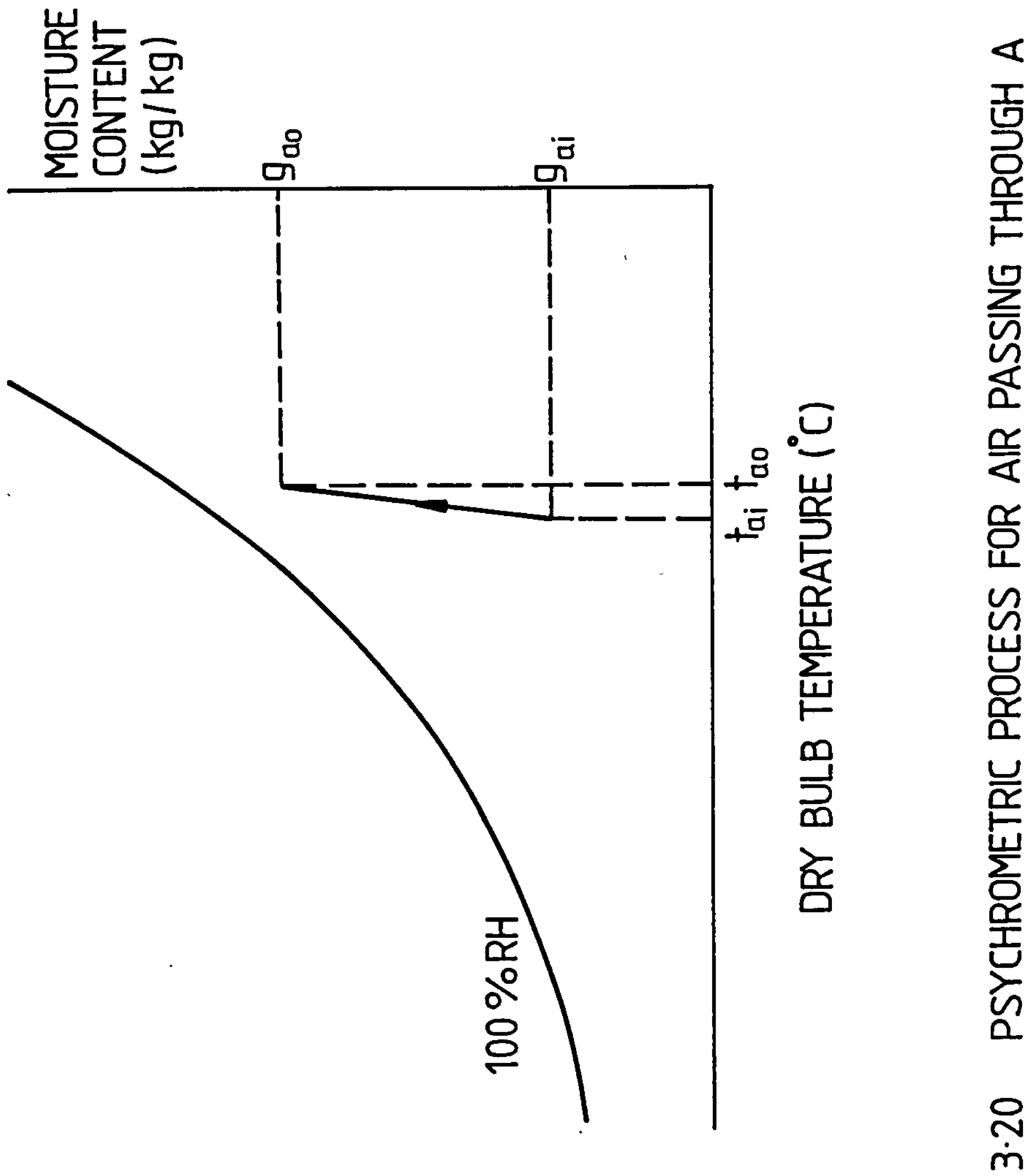

FIG. 3.20 PSYCHROMETRIC PROCESS FOR AIR PASSING THROUGH A STEAM HUMIDIFIER.

m_{st} = mass flow rate of steam injected into the airstream (kg/s)
h_{ai} = specific enthalpy of air entering the humidifier (kJ/kg)
h_{st} = specific enthalpy of steam (kJ/kg)
h_{ao} = specific enthalpy of air leaving the humidifier (kJ/kg)

Transforming Equations 3.131a and 3.132a, we have

$$g_{ao} = g_{ai} + \frac{m_{st}}{m_a} \qquad (3.131b)$$

$$h_{ao} = h_{ai} + \frac{m_{st}\, h_{st}}{m_a} \qquad (3.132b)$$

Thus knowing the condition and mass flow rate of steam injected into the airstream as well as the state of the inlet air, the state of the outlet air can be determined.

Calculation Steps

1) Knowing m_{st}, compute g_{ao} from Equation 3.131b
2) Knowing the condition of the injected steam, e.g. the pressure of dry saturated steam, compute its saturation temperature and hence the enthalpy h_{st}
3) Compute h_{ao} from Equation 3.132b
4) Compute t_{ao} from Equations 3.10 to 3.12

3.8 DUCTS

Ducts are used to convey air form the air handling unit to the spaces to be conditioned as well as returning all or part of the air to the unit from the conditioned zones. Whenever the air inside the duct is at a temperature different from the ambient temperature, heat will be transmitted outwardly or inwardly.

The duct model accounts for the thermal gains/losses from/to the surroundings. The temperature of air leaving the duct, t_{ao}, can be determined if the following data are known.

Entering air temperature t_{ai} (^{o}C)
Ambient temperature, t_{amb} (^{o}C)
Overall heat transfer coefficient for duct, U_d (kW/m^2K)
Duct surface area, A_d (m^2)

Assuming $t_{ai} < t_{amb}$ i.e. duct is carrying cold air, the rate of heat transferred to the airstream from the surroundings, q_d, is from Equation 3.43

$$q_d = m_a\ c_{pma}\ (t_{ao} - t_{ai})$$

Also from Equation 3.42

$$q_d = U_d\ A_d\ \Delta t_{md}$$

$$t_{md} = \frac{t_{ao} - t_{ai}}{\ln \frac{(t_{amb} - t_{ai})}{(t_{amb} - t_{ao})}}$$

Thus

$$\frac{U_d\ A_d\ (t_{ao} - t_{ai})}{\ln \frac{(t_{amb} - t_{ai})}{(t_{amb} - t_{ao})}} = m_a\ c_{pma}\ (t_{ao} - t_{ai})$$

$$\frac{t_{amb} - t_{ai}}{t_{amb} - t_{ao}} = \exp \frac{(U_d\ A_d\ )}{(m_a\ c_{pma})}$$

$$t_{amb} - t_{ao} = \exp \frac{(-U_d\ A_d\ )}{(m_a\ c_{pma})}\ (t_{amb} - t_{ai})$$

Thus

$$t_{ao} = t_{amb} - \exp \frac{(-U_d\ A_d\ )}{(m_a\ c_{pma})}\ (t_{amb} - t_{ai}) \qquad (3.133)$$

Knowing t_{ao}, q_d can be determined.
The moisture content of air leaving the duct does not change.
Thus $g_{ao} = g_{ai}$

If $t_{ai} > t_{amb}$, for ducts carrying hot air, t_{ao} is given by

$$t_{ao} = t_{amb} + (t_{ai} - t_{amb}) \exp \frac{(-U_d A_d)}{(m_a c_{pma})} \qquad (3.134)$$

3.9 ZONES

The air conditioned by the HVAC system is supplied to the various zones in a building to maintain the conditions required within the zones. The relationship between the sensible and latent cooling loads of a zone and the temperature and moisture content maintained within is given by

$$q_{zs} = m_{sa} c_{pma} (t_z - t_{sa}) \qquad (3.135)$$

$$q_{zl} = m_{sa} h_{fgz} (g_z - g_{sa}) \qquad (3.136)$$

where

q_{zs} = zone sensible cooling load (kW)
m_{sa} = mass flow rate of supply air to zone (kg/s)
t_z = zone air dry bulb temperature (^{o}C)
t_{sa} = temperature of supply air to zone (^{o}C)
q_{zl} = zone latent cooling load (kW)
h_{fgz} = latent heat of evaporation at zone conditions (kJ/kg)
g_z = zone air moisture content (kg/kg)
g_{sa} = moisture content of supply air (kg/kg)

REFERENCES FOR CHAPER 3

1) CIBS — "CIBS Guide Sections C1 and C2, Properties of Humid Air, Water and Steam", CIBS, 1975

2) IHVE — "Some Fundamental Data Used by Building Services Engineers", IHVE, 1973

3) ASHRAE — "ASHRAE Handbook, 1985 Fundamentals", ASHRAE.

4) TETENS, O. — "Uber Einige Meteorologische", Begriffe Z Geophys. 1930, Volume 6, pp. 297-309.

5) WEISS, A. — "Algorithms for the Calculation of Moist Air Properties on a Hand Calculator", Transactions of the ASAE, 1977, Volume 20, No. 6 pp. 1133-1136.

6) GOFF, J.A. — "Standardisation of the Thermodynamic Properties of Moist Air", ASHVE Transactions, 1949, Volume 55, pp. 459-484.

7) MCPHERSON, M.J. — "A Direct Relationship Between Sigma Heat and Wet Bulb Temperature", Journal of the Mine Ventilation Society of South Africa, June 1984, Volume 37, No. 6, pp. 71-72

8) THRELKELD, J.L. — "Thermal Environmental Engineering", Second Edition, 1970. Published by Prentice-HallInc., Engelwood Cliffs, N.J.

9) MUELLER, A.C. — "Heat Exchangers", in (Handbook of Heat Transfer, Edited by W.M. Rohsenow and J.P. Hartnett, Chapter 18, Published by McGraw Hill Book Company, Inc.

10) McQUISTON, F.C. PARKER, J.D. "Heating, Ventilating and Air Conditioning, Analysis and Design", Second Edition, 1982. Published by John Wiley and Sons, Inc.

11) STEVENS, R.A. FERNANDEZ, J. WOOLF, J.R. "Mean-Temperature Difference in One, Two and Three-Pass Crossflow Heat Exchangers", ASME Transactions, February 1957, Volume 79 pp. 287-297.

12) KAYS, W.M. LONDON, A.L. "Compact Heat Exchangers", Third Edition, 1984. Published by McGraw-Hill, Inc.

13) McADAMS, W.H. "Heat Transmission", Third Edition 1954. Published by McGraw-Hill Book Company, Inc.

14) ELMAHDY, A.H. BIGGS, R.C. "Finned Tube Heat Exchanger: Correlation of Dry Surface Heat Transfer Data", ASHRAE Transactions, 1979, Volume 85 Part 2 pp. 262-273.

15) SIEDER, E.N. TATE, C.E. "Heat Transfer and Pressure Drop of Liquids in Tubes", Ind. Eng. Chem. 1936, Volume 28.

16) AIR CONDITIONING AND REFRIGERATION INSTITUTE (ARI) "Standard for Forced Circulation Air-Cooling and Air-Heating Coils", ARI Standard 410-81, 1981.

17) ASHRAE "ASHRAE Handbook, 1983 Equipment", ASHRAE.

18) HARPER, D.R. BROWN, W.B. "Mathematical Equations for Heat Conduction in the Fins of Air-Cooled Engines", National Advisory Committee for Aeronautics, Report No. 158, 1922.

19) GARDNER,K.A. "Efficiency of Extended Surface", ASME Transactions, 1945, Volume 67 pp. 621-631.

20) JAKOB, M — "Heat Transfer, Volume 1", Published by John Wiley and Sons, Inc., New York, 1940.

21) CARRIER, W.H. ANDERSON, S.W. — "The Resistance to Heat Flow through Finned Tubing", ASHVE Transactions 1944, Volume 50, pp. 117-152.

22) ABRAMOWITZ, M. STEGUN, I.A. — "Handbook of Mathematical Functions with Formulas, Graphs and Mathematical Tables", National Bureau of Standards Applied Mathematics Series 55, Third Printing March 1965.

23) KNEBEL, D.E. — "Simplified Energy Analysis Using the Modified Bin Method", Prepared for ASHRAE, 1983.

24) CARRIER, W.H. CHERNE, R.E. GRANT, W.A. ROBERTS, W.H. — "Modern Air Conditioning, Heating, and Ventilating", Third Edition 1970. Published by Sir Isaac Pitman and Sons Limited.

25) MCELGIN, J. WILEY, D.C. — "Calculation of Coil Surface Areas for Air Cooling and Dehumidification", Heating, Piping and Air Conditioning, March 1940.

26) JANISSE, N.J. — "How to Control Air Systems", Heating, Piping and Air Conditioning, April 1969. pp. 129-136.

CHAPTER 4

SIMULATION OF THE COMPONENTS OF CENTRAL PLANT

NOMENCLATURE

Symbol	Description	Unit
A1 - A12	full load water chiller model coefficients	
a,b,c,d	water pump part load model coefficients	
B1 - B18	full load water chiller model coefficients	
CPW, c_{pw}	specific heat capacity of water	kJ/kgK
CV_{fu}	calorific value of gaseous fuel	kJ/m^3
C1, C2, C3	reciprocating water chiller part load model coefficients	
D1 - D4	centrifugal water chiller part load model coefficients	
E	effeciveness of cooling tower	
E_{bd}	see Equation 4.3	
E_{bp}	see item 5 of Section 4.3.4	
F_{on}	fraction of the hour that the water chiller is running	
FFLP	fraction of full load power	
FFLPHI	value of FFLP at high capacity step	
FFLPLO	value of FFLP at low capacity step	
FFLP2	see Equation 4.29b	
FOM	factor of merit of cooling tower	
g_{ai}	moisture content of air entering the cooling tower	kg/kg
g_{ao}	moisture content of air leaving the cooling tower	kg/kg
g'	acceleration due to gravity	m/s^2
H_w	total pump head	m. of water
h_{ai}, h_{ao}	specific enthalpies of air entering and leaving the cooling tower respectively	kJ/kg
h_1, h_2	specific enthalpies of refrigerant entering and leaving the evaporator respectively	kJ/kg
h_3, h_4	specific enthalpies of refrigerant entering and leaving the condenser respectively	kJ/kg

Symbol	Description	Unit
MAC	mass flow rate of air entering the condenser	kg/s
MHR	minimum hot gas bypass ratio	
MR	mass flow rate of refrigerant	kg/s
MUR	minimum unloading ratio	
MWC	condenser water mass flow rate	kg/s
MWE	evaporator water mass flow rate	kg/s
m_a	mass flow rate of air through the cooling tower	kg/s
m'_a	see Equation 4.45	kg/s
m_w, m_{wi}	mass flow rates of water entering the cooling tower	kg/s
m'_w	see Equation 4.45	kg/s
m_{wo}	mass flow rate of water leaving the cooling tower	kg/s
P	compressor motor input power	kW
P_i	water pump motor input power	kW
P_{if}	water pump motor input power at full load	kW
P_o	water pump power output	kW
PCT	cooling tower fan motor input power	kW
PCTF	cooling tower fan motor input power at full load	kW
PCWP	condenser water pump motor input power	kW
PLEF	boiler part load efficiency factor	
PLR	part load ratio	
PLRHI	value of PLR at high capacity step	
PLRLO	value of PLR at low capacity step	
PPL	compressor motor input power at part load	kW
PLRS	value of PLR at the surge point S (see Fig. 4.7)	
P_b	barometric pressure	kPa
QBI	rate of heat input to boiler	kW
QBN	boiler net output	kW
QBO	boiler gross output	kW
QBP	boiler gross output required to satisfy building heating load	kW

Symbol	Description	Unit
QBPL1	piping loss	kW
QBPL2	pickup loss	kW
QC	condenser heat rejection load	kW
QCT	cooling tower load	kW
QE	evaporator cooling load	kW
QEPL	evaporator cooling load at part load condition	kW
QL	rate of heat loss from water chiller	kW
R	tower capacity factor	
R*	see Equations 4.51a and 4.51b	
S_{ai}	sigma energy of air entering the cooling tower	kJ/kg
S_{ao}	sigma energy of air leaving the cooling tower	kJ/kg
S_{wi}	sigma energy of air at t_{wi}	kJ/kg
SLF	stop loss factor	
TAC1, TAC2	dry bulb temperatures of air entering and leaving the condenser respectively	^{o}C
TWC1, TWC2	condenser entering and leaving water temperatures respectively	^{o}C
TWE1, TWE2	evaporator entering and leaving water temperatures respectively	^{o}C
t_{amb}	dry bulb temperature of ambient air	^{o}C
$t_{sl,amb}$	sling wet bulb temperature of ambient air	^{o}C
t_{slai}, t_{slao}	sling wet bulb temperatures of air entering and leaving the cooling tower respectively	^{o}C
t_{wi}, t_{wo}	temperatures of water entering and leaving the cooling tower respectively	^{o}C
$(UA)_C$	condenser UA value	kW/K
$(UA)_E$	evaporator UA value	kW/K
V_a	volumetric flow rate of air through the cooling tower	m^3/s
V_{af}	volumetric flow rate of air through the cooling tower at full load	m^3/s
V_{fu}	amount of gaseous fuel consumed	m^3/s

Symbol	Description	Unit
V_w	volumetric flow rate of water discharged by pump	m^3/s
WAR	reference water-air ratio	
X	see Equation 4.38	kW
Y	see Equation 4.40	kW
Δt_c	mean temperature difference across condenser	K
Δt_e	mean temperature difference across evaporator	K
Δt_w	water stream temperature rise, see Equation 4.57	K
η_a	air efficiency of cooling tower	
η_{bd}	distribution efficiency	%
η_{bf}	boiler full load efficiency	%
η_{bp}	part load efficiency of boiler	%
η_c	compressor efficiency	
η_{cwp}	condenser water pump effiency	
η_p	pump efficiency	%
η_w	water efficiency of cooling tower	
ν_a	specific volume of ambient air	m^3/kg
ρ_w	density of water	kg/m^3

4.1 INTRODUCTION

The central plant or HVAC equipment is defined as the mechanical and electrical machines and apparatus used to produce the chilled or heated air or water which will be distributed to the spaces conditioned by the HVAC systems. In meeting the HVAC systems thermal loads, the central plant or primary system components consume fuel and electrical energy. The energy consumed by pumps and fans for distributing heating or cooling fluids must be accounted for to obtain total building energy consumption. The following components of the primary system are modelled:

Boilers
Vapour Compression Chillers
Cooling Towers
Pumps

The approach generally used in the analysis of the components is to determine the steady state performance at the full load or rated condition and then applying correction curves or factors to account for the change in performance at part load conditions.

4.2 BOILERS

A boiler is a pressure vessel designed to transfer heat (produced by combustion) to a fluid. This definition has been expanded (Ref. 1) to include transfer of heat from electrical resistance elements to the fluid by direct action of the electrodes. For HVAC applications, the fluid is usually water in the form of liquid or steam.

For HVAC systems, a boiler is a cast iron or steel pressure vessel heat exchanger designed with fuel burning devices and other equipment to:

1) burn fossil fuels (or use electric current); and
2) transfer the released heat to water (in water boilers) or to water and steam (in steam boilers).

4.2.1 Boiler Performance at Full Load

The heat output of a boiler is used to deliver the building heating load. However, the actual output capacity of the boiler must be greater than the building load because of two factors:

1) There is a constant loss of heat through hot piping to surrounding areas, some of which is not useful heating. Insulation will reduce, but not eliminate this loss. This is called the piping loss, QBPL1.

2) There is an additional heat loss when starting up a cold system. Before the boiler can deliver heat to the building, all the piping, water and equipment of the heating system itself must be heated. This is called the pick up loss, QBPL2.

Because of these losses, the boiler must have excess capacity so that the remaining capacity can handle the building load. This is expressed as follows:

$$QBO = QBN + QBPL1 + QBPL2 \qquad (4.1)$$

where:

QBO = boiler gross output (kW)
QBN = boiler net output (kW)
QBPL1 = piping loss (kW)
QBPL2 = pickup loss (kW)

The net output is the useful load, which is the sum of the requirements for space heating and service hot water, if any. The gross output is the actual heat output of the boiler.

The piping and pick up loses can be calculated if the details of the piping network and equipment are known. However, the usual practice is to make an allowance to be added to the net output. The distribution efficiency can be used to quantify these losses. It is given by

$$\eta_{bd} = \frac{QBN}{QBO} \times 100 \qquad (4.2)$$

where

η_{bd} = distribution efficiency (%)

From Equations 4.1 and 4.2, the term (QBPL1 + QBPL2) is given by

$$QBPL1 + QBPL2 = QBN \times \left(\frac{1}{E_{bd}} - 1 \right) \qquad (4.3)$$

where $E_{bd} = 0.01 \times \eta_{bd}$

The required heat input to a boiler will be greater than the gross output because some of the heat available in the fuel will be lost in the combustion gases at the chimney and from boiler outside surface (radiation and convection losses). The overall or full load efficiency of the boiler is defined as

$$\eta_{bf} = \frac{QBO}{QBI} \times 100 \qquad (4.4)$$

where:

η_{bf} = full load efficiency of boiler (%)

QBI = rate of heat input to boiler (kW)

Modern automatic fired boilers have efficiencies of 75-80% at full load when new or well maintained (Ref.2). However, Bratley (Ref. 3) from a survey of available literature found that the range of full load efficiencies for all types of oil and gas fired, non-condensing boilers is from 70-80%.

Poor maintenance and operating procedures often result in boilers actually operating at 50-60% efficiency or even less. The full load efficiency can be determined precisely only by laboratory test under fixed conditions.

The amount of fuel consumed can be determined if the calorific value is known. For example, for a gaseous fuel,

$$V_{fu} = \frac{QBI}{CV_{fu}} \qquad (4.5)$$

where:

V_{fu} = amount of gaseous fuel consumed (m^3/s)
CV_{fu} = calorific value of gaseous fuel (kJ/m^3)

4.2.2 Boiler Performance at Part Load

Boiler manufacturers do not usually supply the part load efficiency values of boilers. However, a number of researchers have carried out tests to determine the part load performance of various boilers (Refs 4, 5, 6, 7,8 and 9).

One useful way of comparing the part load efficiency curves for different boilers is to introduce the concept of part load efficiency factor, PLEF, which is the ratio of efficiency at part load to that at full load.

Thus,

$$PLEF = \frac{\text{Efficiency at part load}}{\text{Efficiency at full load}} = \frac{\eta_{bp}}{\eta_{bf}} \qquad (4.6).$$

The part load ratio, PLR, for boiler operation is given by

$$PLR = \frac{QBP}{QBO} \qquad (4.7)$$

where

QBP = boiler gross output at part load (kW)

The experimentally determined plots of PLEF against PLR for various boilers are shown in Fig. 4.1.

Bratley (Ref. 3) has used the concept of stop loss factor, SLF, to characterise the performance of boilers at part load conditions. SLF is defined as:

$$SLF = \frac{\text{The stop loss energy consumption over a period}}{\text{Total amount of energy which would be consumed if the burner worked continually during the period}}$$

The part load efficiency factor is a function of the stop loss factor and part load ratio. This functional relationship is:

$$PLEF = \frac{1}{1 + SLF\left(\frac{1}{PLR} - 1\right)} \qquad (4.8)$$

The derivation of Equation 4.8 is given in Appendix A4.1. Bratley also plotted values of PLEF (obtained from Equation 4.8) against PLR for various values of SLF and these are shown in Fig. 4.2.

Superimposing the family of theoretical curves (obtained from Equation 4.8) on the experimental curves (Fig. 4.1) as shown in Fig. 4.3, it can be seen that quite good agreement is obtained between the theoretical and experimentally determined values of PLEF. Thus the part load performance of a fossil fuel-fired boiler can be determined by specifying its stop loss factor.

Values of full load efficiencies and stop loss factors for various boilers using fossil fuels obtained from References 4 to 12 are given in Appendix A4.2.

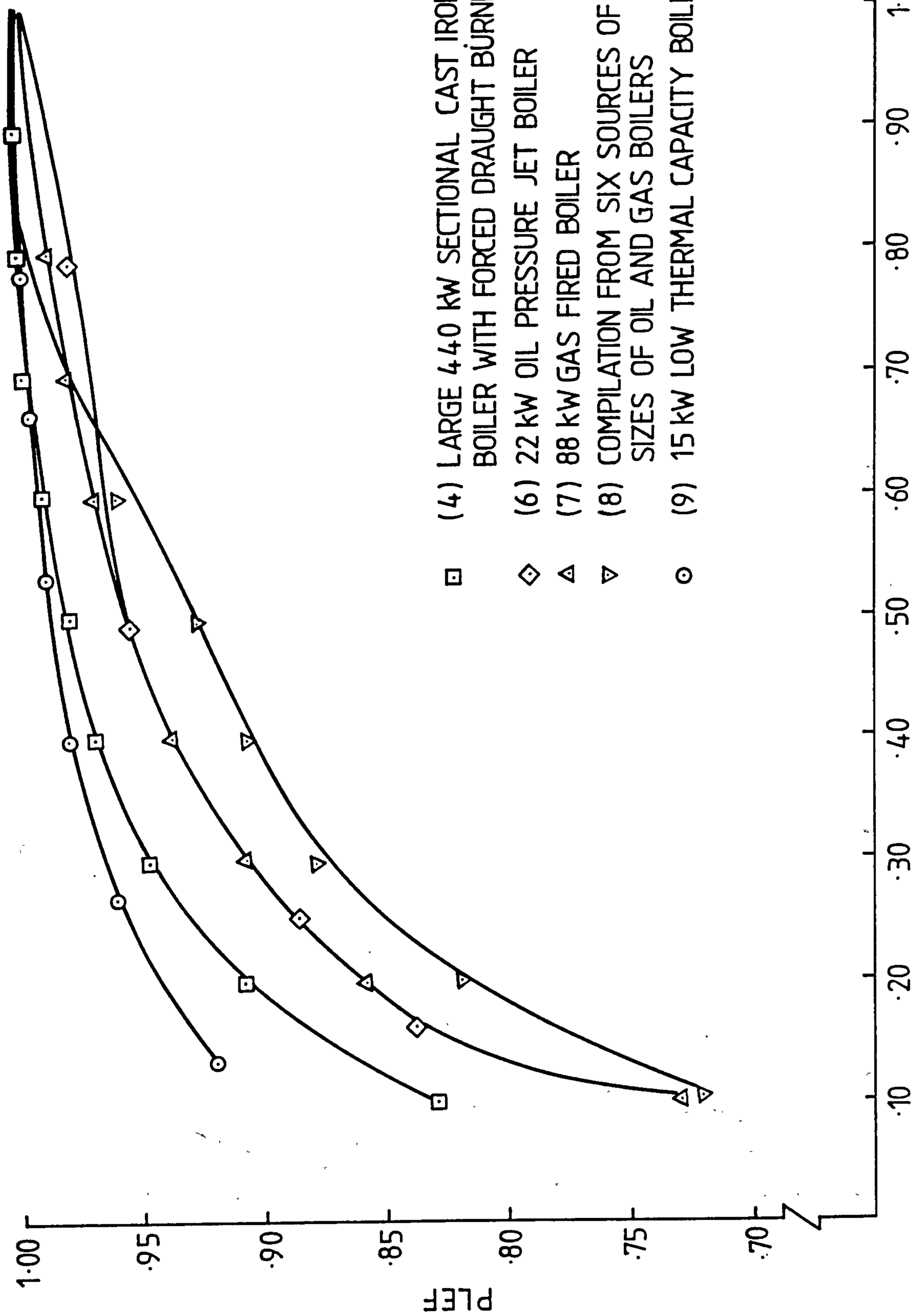

FIG. 4·1 EXPERIMENTAL VALUES OF PLEF Vs. PLR (4,6,7,8,9)

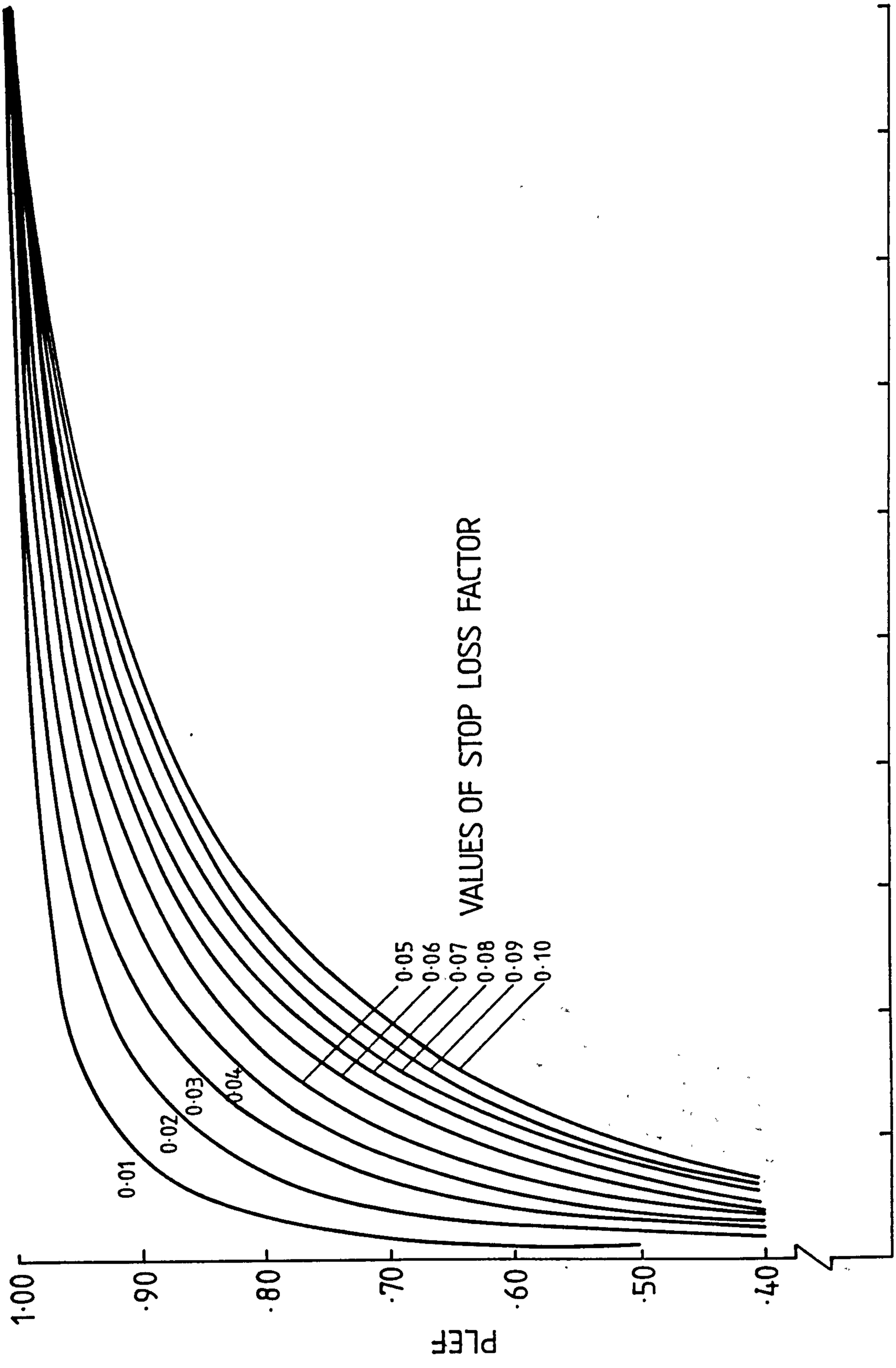

FIG 4·2. FAMILY OF SLF CURVES

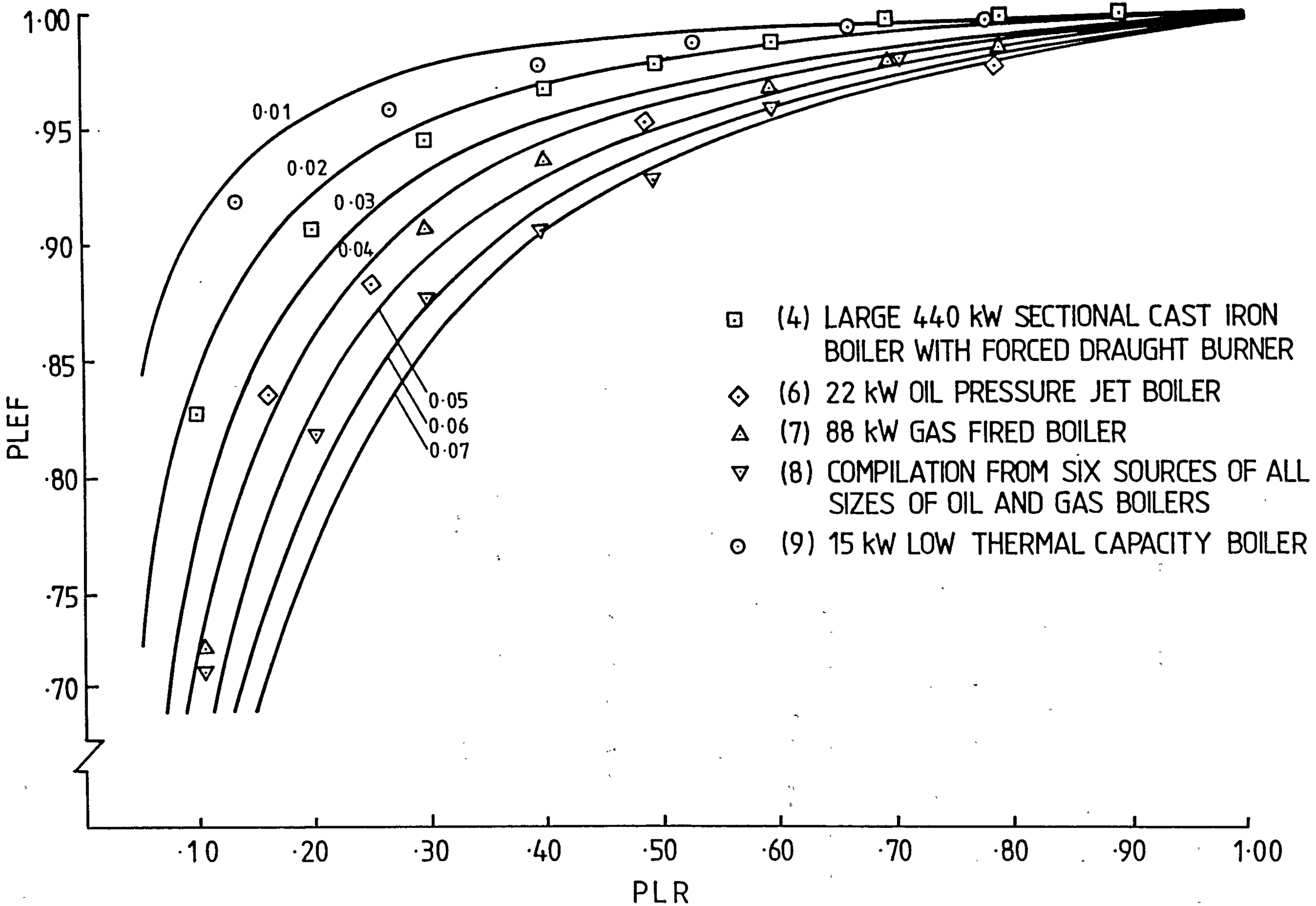

FIG.4·3 EXPERIMENTAL VALUES OF PLEF SUPERIMPOSED ON SLF CURVES

4.2.3 Control of Boiler Input and Output

Boiler controls are designed to control the rate of fuel input (on-off, step-firing, or modulating) in response to some control signal representing load change, so that the average boiler output equals load within some acceptable tolerance (Ref. 1). Boiler controls include safety controls that act to shut off fuel flow when unsafe conditions develop.

Steam boilers are operated by boiler mounted, pressure actuated controls which vary the input of fuel to the boiler. Common examples are on-off, high-low-off, and modulating.

Hot water boilers are operated by temperature actuated controls that are usually mounted on the boiler. Controls are the same as for steam boilers, i.e. on-off, high-low-off, and modulating. Energy conservation can be achieved by resetting the hot water supply temperature to the HVAC system from an outside air thermostat.

4.2.4 Algorithm for Simulating the Performance of a Fossil Fuel-Fired Boiler

.This algorithm determines the rate of heat input to the boiler and the flow rate of fuel consumed to satisfy the heating load imposed on it by the building. The following data are requried:

Boiler capacity, QBO
Boiler full load efficiency, η_{bf}
Stop loss factor, SLF
Building heating load, QBN
Heating system distribution efficiency, η_{bd}
Calorific value of fuel, CV_{fu}

Calculation Steps

1) Compute boiler gross output required to satisfy building heating load, QBP.

$$QBP = \frac{QBN}{E_{bd}} \quad \text{where } E_{bd} = 0.01 \times \eta_{bd}$$

2) Check if the boiler is overloaded. If QBP > QBO, then boiler is overloaded. Print error message and adjust QBP and appropriate variables in HVAC system.

Compute part load ratio, PLR

$$PLR = \frac{QBP}{QBO}$$

3) Compute part load efficiency, PLEF, using Equation 4.8.

4) Compute part load efficiency η_{bp}, using Equation 4.6.

5) Compute rate of heat input to boiler, QBI

$$QBI = \frac{QBP}{E_{bp}} \quad \text{where } E_{bp} = 0.01 \times \eta_{bp}$$

6) Compute flow rate of fuel consumed, V_{fu}, using Equation 4.5.

4.2.5 Multiple Boilers

Multiple boiler installations are used for very large projects. The objective is to maximise the use of the higher efficiency part of the boiler part load characteristic by matching the number of boilers more closely to the heat demand, and so ensuring a higher part load ratio and thereby higher efficiency for the boilers that are operating.

The algorithm given in Section 4.2.4 can be extended to simulate the performance of multiple boilers. For a given building heating load, this involves determining the combination of boilers operating for minimal energy consumption.

Multiple boilers installations offer the user some standby capacity if repair work must be done on any boiler.

4.3 VAPOUR COMPRESSION CHILLERS

Vapour compression refrigeration systems or chillers are widely used for producing refrigeration required for air conditioning. The function of a refrigeration system is to abstract a quantity of heat at one temperature level and to discharge it at a higher temperature level. In effect, a refrigeration system is a heat pump in that it pumps heat from one temperature level to a higher one.

Mechanical compression using reciprocating or centrifugal compressors have found the greatest acceptance for air conditioning work, with reciprocating compressors primarily for the small and intermediate refrigeration loads (up to 420 kW) and centrifugal compressors primarily for larger refrigeration loads (above 280 kW) **(Ref. 1)**. In this thesis only reciprocating and centrifugal compressor water chillers will be considered.

4.3.1 Vapour Compression Water Chillers - Principles of Operation

The water chiller is a mechanical refrigeration device which transfers heat from a low temperature reservoir to a high temperature reservoir with an input of energy. The most efficient thermodynamic cycle for a water chiller is the Carnot cycle; however water chillers use a vapour compression cycle, due to the practical limitations of the working refrigerant.

A pressure enthalpy (p-h) of an ideal saturated vapour compression refrigeration cycle is shown in Fig. 4.4. This cycle consists of a constant pressure heat addition in the evaporator (process 1-2), isentropic compression in the compressor (process 2-3), constant pressure heat rejection in the condenser (process 3-4), and isenthalpic expansion in the expansion valve (process 4-1).

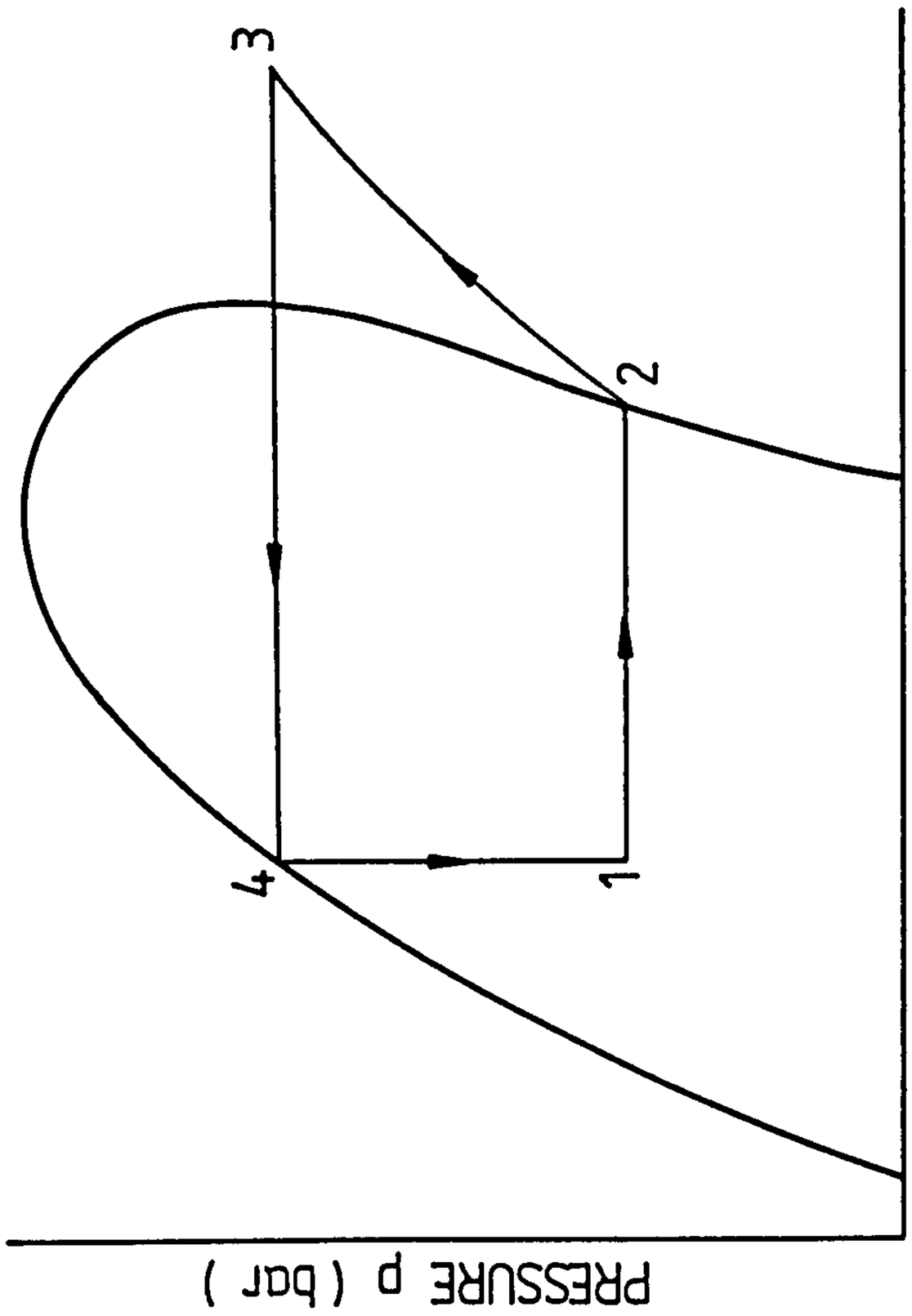

FIG 4.4 IDEAL VAPOUR COMPRESSION REFRIGERATION CYCLE SHOWN ON THE p-h DIAGRAM.

expansion valve (process 4-1).

An actual vapour compression cycle would vary from the ideal case due to several reasons, such as pressure losses in piping, sub cooling/superheating at the exit of the condenser/evaporator respectively, and non-isentropic compression.

A schematic of a water-cooled water chiller is shown in Fig. 4.5. The schematic shows the basic pieces of equipment and the variables labelled as appropriate. The water chiller model developed, here, is a model of the complete system and does not consist of individual component models or involve internal pressures or temperatures.

4.3.2 Reciprocating Compressor Water Chiller Full Load Model

Full load reciprocating compressor water chiller operation occurs when all compressors and cylinders are operating. This type of data is usually provided in manufacturers' equipment catalogues.

Allen and Hamilton (Refs. 13, 14 and 15) have developed steady state models to predict the performance of reciprocating water chillers. By applying basic physical laws to the water-cooled water chiller shown in Fig. 4.5, they obtained the following equations governing the steady state operation of water chillers:

From evaporator water energy balance,

$$QE = MWE \cdot CPW \cdot (TWE1 - TWE2) \qquad (4.9)$$

From evaporator basic heat transfer equation,

$$QE = (UA)_E \cdot \Delta t_E \qquad (4.10)$$

From evaporator refrigerant energy balance,

$$QE = MR \cdot (h_2 - h_1) \qquad (4.11)$$

From compressor energy balance,

$$P = \frac{MR \cdot (h_3 - h_2)}{\eta_c} \qquad (4.12)$$

From condenser water energy balance

$$QC = MWC \cdot CPW \quad (TWC2 - TWC1) \qquad (4.13)$$

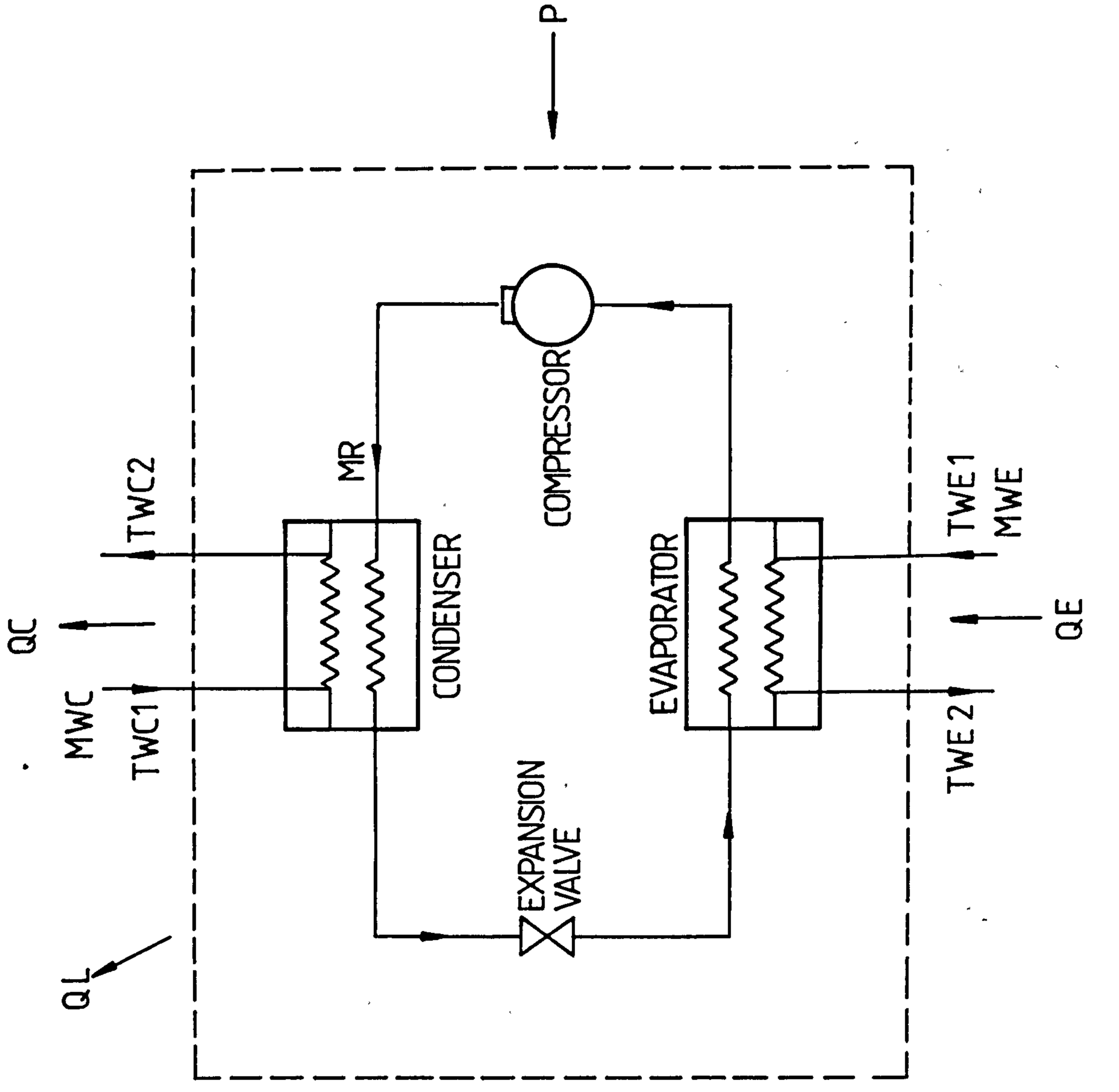

FIG. 4·5 WATER-COOLED WATER CHILLER SYSTEM SCHEMATIC

From condenser basic heat transfer equation,

$$QC = (UA)_C \cdot \Delta t_C \qquad (4.14)$$

From condenser refrigerant energy balance,

$$QC = MR \cdot (h_3 - h_4) \qquad (4.15)$$

Examination of Equations 4.9 through 4.15 show that they contain refrigeration system internal variables such as refrigerant mass flow rate and enthalpy values. The internal variables can be eliminated by utilising functional relationships among variables and examining typical water chiller performance data. Analysis of water chiller data has shown (Ref. 16) that these seven original equations can be replaced by five functional relationships in terms of the water temperatures entering and leaving the evaporator and condenser. These are

$$QE = MWE \cdot CPW\ (TWE1 - TWE2) \qquad (4.9)$$

Combining Equations 4.10 and 4.11 we obtain,

$$QE = \Psi_1\ (TWE2, TWC2) \qquad (4.16)$$

From Equation 4.12 we get,

$$P = \Psi_2\ (TWE2, TWC2) \qquad (4.17)$$

Combining Equations 4.14 and 4.15 we obtain,

$$QC = \Psi_3\ (TWE2, TWC2) \qquad (4.18)$$

$$QC = MC \cdot CPW \cdot (TWC2 - TWC1) \qquad (4.13)$$

From overall water chiller energy balance we get,

$$QL = QE + P - QC \qquad (4.19)$$

Allen and Hamilton (Ref. 13) have analysed available water chiller data and shown that the energy losses, QL are small for the well designed systems currently available from the major manufacturers. The thermal balance equation (Equation 4.18) may be replaced by Equation 4.20 which results from simplifying Equation 4.19.

Thus,

$$QC = QE + P \qquad (4.20)$$

The functional relationships, Ψ_1 and Ψ_2 are determined from regression analysis of available water chiller data. A second order polynomial in two variables requiring six coefficients per equation as shown in Equation 4.21 or 4.22 was considered adequate by Allen and Hamilton to describe the functional relationship. A slightly more accurate representation of the functional relationship is given in Ref. 16 and requires nine coefficients per equation as shown in Equation 4.23 or 4.24.

From Allen and Hamilton

$$QE = A1 + A2 \cdot TWE2 + A3 \cdot TWE2^2 + A4 \cdot TWC2 + A5 \cdot TWC2^2 + A6 \cdot TWE2 \cdot TWC2 \qquad (4.21)$$

$$P = A7 + A8 \cdot TWE2 + A9 \cdot TWE2^2 + A10 \cdot TWC2 + A11 \cdot TWC2^2 + A12 \cdot TWE2 \cdot TWC2 \qquad (4.22)$$

From Ref. 16

$$QE = B1 + B2 \cdot TWE2 + B3 \cdot TWE2^2 + B4 \cdot TWC2 + B5 \cdot TWC2^2 + B6 \cdot TWE2 \cdot TWC2 + B7 \cdot TWE2^2 \cdot TWC2 + B8 \cdot TWE2 \cdot TWC2^2 + B9 \cdot TWE2^2 \cdot TWC2^2 \qquad (4.23)$$

$$P = B10 + B11 \cdot TWE2 + B12 \cdot TWE2^2 + B13 \cdot TWC2 + B14 \cdot TWC2^2 + B15 \cdot TWE2 \cdot TWC2 + B16 \cdot TWE2^2 \cdot TWC2 + B17 \cdot TWE2 \cdot TWC2^2 + B18 \cdot TWE2^2 \cdot TWC2^2 \qquad (4.24)$$

Thus, the full load water-cooled water chiller model can be expressed in terms of five equations (Equations 4.9, 4.13, 4.20, 4.23 and 4.24), nine variables (QE, P, QC, MWE, TWE1, TWE2, MWC, TWC1 and TWC2), and eighteen coefficients (B1 through B18) that are determined from experimental or manufacturers' catalogue data by polynomial regression.

The vast majority of data available to determine Equations 4.23 and 4.24 come from manufacturers' equipment catalogues. Data in these catalogues is generally published under the standards mentioned in References 17 and 18. These data are usually given in a table showing QE and P as functions of TWE2 and TWC2. If the chiller ratings are given as QE and P as functions of TWE2 and TWC1, then for such data, TWC1 replaces TWC2 in Equations 4.23 and 4.24. The standards and industry practice is to generally give the full load data with evaporator and condenser water differential temperatures of 5.56K.

Manufacturers catalogue and experimental data for a nominal 70.3kW water cooled reciprocating water chiller have been presented by Leverenz and Bergan (Ref. 19). The validity of Equation 4.23 and 4.24 was tested by determining eighteen coefficients using regression analysis and recalculating the original catalogue data from which the model coefficients were derived.

These equations approximated the original data with less than 0.5% absolute difference for all of the data points.

The full load model coefficients for the nominal 70.3kW reciprocating water chiller are:

B1	=	82.865644	B2	=	0.690942
B3	=	0.08653425	B4	=	-1.3468568
B5	=	0.0129888	B6	=	0.21566263
B7	=	-0.01576577	B8	=	-4.832048E-03
B9	=	3.7754825E-04			
B10	=	11.527754	B11	=	1.2360555
B12	=	-0.03559041	B13	=	0.34554115
B14	=	-2.1703287E-03	B15	=	-7.785435E-02
B16	=	2.4987552E-03	B17	=	1.4342661E-03
B18	=	-4.0865307E-05			

The catalogue data from which the full load model coefficients were derived is given in Appendix A4.3, Table 1.

For air cooled water chillers, it is necessary to modify the water cooled water chiller model presented above. Examination of manufacturers' catalogue data show that data is not available for MAC and TAC2 in air cooled water chillers. MAC is controlled internal to any given air cooled water chiller, and MAC and QC are not needed to interface with any other equipment model. Therefore the following sets of equations can be used to model the full load performance of an air cooled water chiller.

$$QE = MWE \cdot CPW \cdot (TWE1 - TWE2) \quad (4.9)$$

$$QE = B1 + B2.\ TWE2 + B3.TWE2^2 + B4 \cdot TAC1 + B5 \cdot TAC1^2 + B6 \cdot TWE2 \cdot TAC1 + B7 \cdot TWE2^2 \cdot TAC1 + B8 \cdot TWE2 \cdot TAC1^2 + B9 \cdot TWE2^2 \cdot TAC1^2 \quad (4.25)$$

$$P = B10 + B11 \cdot TWE2 + B12 \cdot TWE2^2 + B13 \cdot TAC1 + B14 \cdot TAC1^2 + B15 \cdot TWE2 \cdot TAC1 + B16 \cdot TWE2^2 \cdot TAC1 + B17 \cdot TWE2 \cdot TAC1^2 + B18 \cdot TWE2^2 \cdot TAC1^2 \quad (4.26)$$

$$QC = QE + P \quad (4.20)$$

The full load air cooled water chiller model consists of four equations and seven variables. Thus three variables will have to be specified in order to solve the system of equations for a particular situation.

4.3.3 Capacity Control of Reciprocating Water Chillers

Water chillers are generally designed to handle the maximum refigeration load of an air conditioning system. For most of the cooling season, the refrigeration load is smaller than the maximum value and this results in the chiller operating at part load for such times. The need for a reduction in refrigerating capacity as the load varies is apparent.

All methods of compressor capacity control function by reducing the amount of compressed refrigerant delivered to the condenser. Less liquid is therefore available to the evaporator, and the system capacity is reduced. Reciprocating compressor capacity can be controlled in the following ways **(Refs. 1 and 20):**

1) On-Off Control
2) Speed Variation
3) Cylinder Unloading
4) Hot-Gas Bypass
5) A combination of some of these methods.

Method 1 refers to simply starting and stopping the compressor in response to demand. This method may be satisfactory with small compressors.

Method 2 refers to changing the speed of the compressor in response to the load. Compressor displacement varies directly with speed.

Method 3 is the most widely used means of controlling capacity of multicylinder reciprocating compressors. The operation of one or more cylinders is controlled so that the refrigerant vapour is not compressed and pumped out of the unloaded cylinders to the condenser, even though the pistons continue to go through their strokes. This reduces the quantity of liquid refrigerant going to the evaporator, reducing compressor capacity.

Method 4 refers to bypassing the compressor hot gas discharge around the condenser. This keeps suction pressure from falling below a set value.

4.3.4 Reciprocating Compressor Water Chiller Part Load Model

Using any or a combination of the methods given in Section 4.3.3, the water chiller can be controlled to satisfy the refrigeration load imposed on it by the HVAC system.

If QEPL is the imposed refrigeration load, the part load ratio, PLR is given by

$$PLR = \frac{QEPL}{QE} \qquad (4.27)$$

The general part load characteristic curve for a reciprocating water chiller employing cycling, hot gas bypass and cylinder unloading for compressor capacity control is shown in Fig. 4.6. The fraction of full load power, FFLP is plotted against the part load ratio for the entire operating range of the chiller. The curve can be broken into three distinct regions depending on the value of part load ratio. It will be useful at this juncture to define certain terms connected with compressor capacity control.

The minimum hot-gas bypass ratio, MHR, is the point expressed as a part load ratio, below which hot gas bypass stops and compressor cycling begins. Below this point, the chiller cycles on and off to meet the load. MHR is always equal to or less than MUR.

The minimum unloading ratio, MUR, is the point expressed as a part load ratio at which the compressor unloading stops and hot gas bypass or cycling begins.

Thus in general if:

$0.0 < PLR < MHR$ (from point 0 to 1), chiller cycles on and off to meet the refrigeration load,

$MHR \leq PLR < MUR$ (from point 1 to 2), hot gass bypass occurs,

$MUR \leq PLR \leq 1.0$ (from point 2 to 3), cylinder unloading occurs.

However, if MHR = MUR, there is no hot gas bypass capability and the chiller moves from unloading immediately to cycling as PLR drops below this ratio. If MHR = MUR = 1.0, the chiller does not unload and cycles from full load down to zero load.

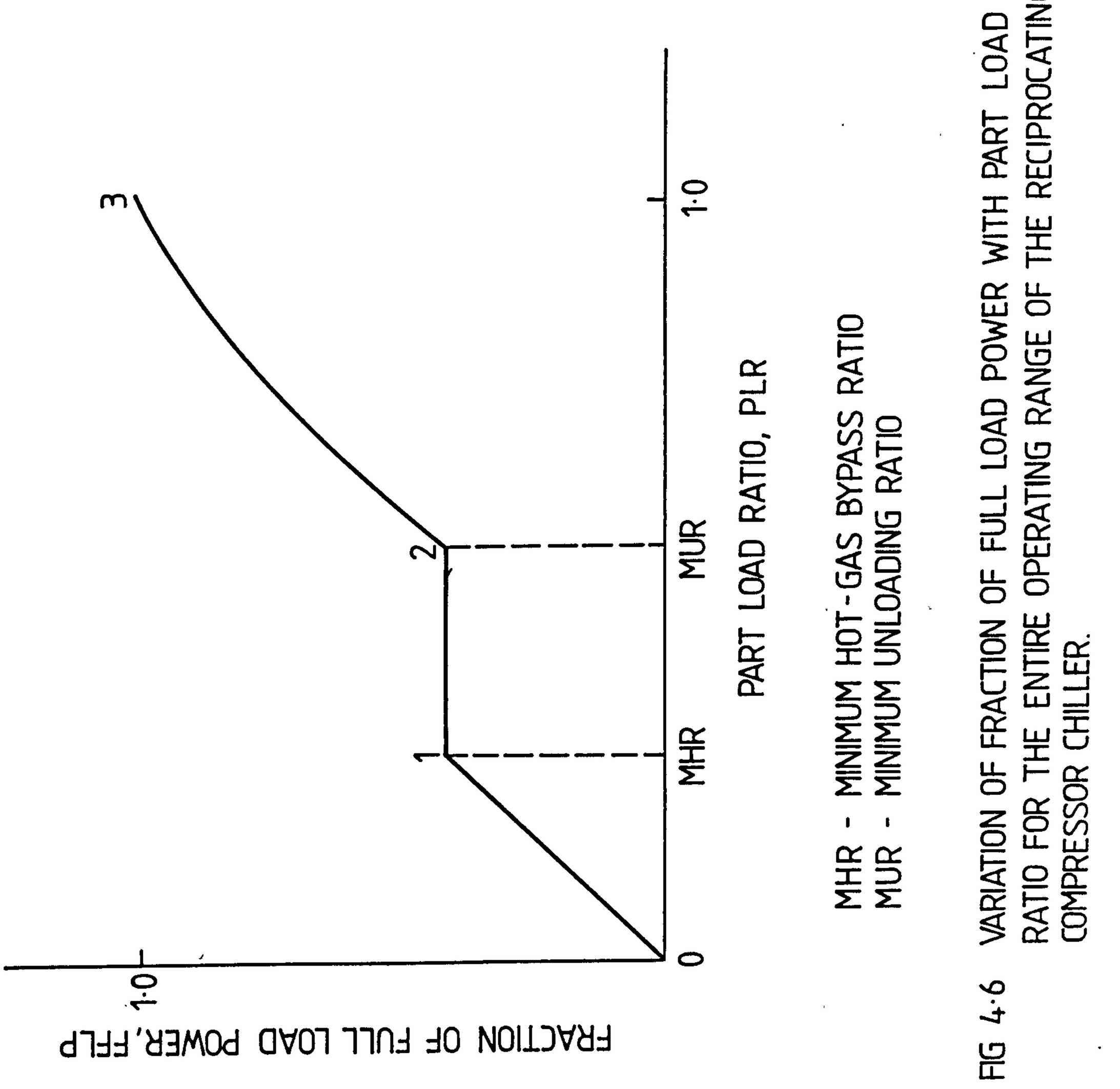

MHR - MINIMUM HOT-GAS BYPASS RATIO
MUR - MINIMUM UNLOADING RATIO

FIG 4·6 VARIATION OF FRACTION OF FULL LOAD POWER WITH PART LOAD RATIO FOR THE ENTIRE OPERATING RANGE OF THE RECIPROCATING COMPRESSOR CHILLER.

Between points 2 and 3, the relationship between FFLP and PLR is

$$FFLP = C1 + C2 \cdot PLR + C3 \cdot PLR^2 \qquad (4.28)$$

Between points 1 and 2, the compressor is operating under a load larger than the external load on the machine. This additional load, called a "false load", causes the compressor to consume as much electricity as if the entire load was external to the chiller. Thus in this region, FFLP can be computed by substituting PLR = MUR in Equation 4.28.

Therefore

$$FFLP = FFLP2 \qquad (4.29a)$$

where

$$FFLP2 = C1 + C2 \cdot MUR + C3 \cdot MUR^2 \qquad (4.29b)$$

Between points 0 and 1, the chiller is cycling. The fraction of on time factor, F_{on} is given by:

$$F_{on} = \frac{QEPL}{MUR \cdot QE} \qquad (4.30)$$

FFLP is given by:

$$FFLP = F_{on} \cdot FFLP2 \qquad (4.31)$$

The power consumed by the chiller at part load, PPL, can now be determined. It is given by:

$$PPL = FFLP \cdot P \qquad (4.32)$$

Leverenz and Bergan (Ref. 19) have carried out tests to determine the part load performance data for a nominal 70.3kW reciprocating water chiller. The water chiller has four cylinders and does not have a hot gas bypass capability. The minimum unloading ratio for the chiller tested is 0.25.

Applying regression analysis to the experimental data, the coefficients C1, C2 and C3, which model the cylinder unloading portion of the part load characteristic curve were determined as:

C1 = 0.147333 C2 = 1.335675 C3 = -0.508362

The experimental part load data from which model coefficients C1, C2 and C3 were derived is given in Appendix A4.3 Table 2.

Manufacturers' catalogues do not usually contain part load performance data in such detail as reported by Leverenz and Bergan. Rather, they are generally available in a form showing the variation of FFLP with PLR for various steps of capacity reduction due to cylinder unloading. For example Table 4.1 shows the part load performance data for a 50 Hz York LCH 50W hermetic reciprocating water chiller **(Ref. 21).** The chiller's compressor has four cylinders and rotates at a speed of 1470 r.p.m.

TABLE 4.1 50Hz York LCH50W Reciprocating Water Chiller Capacity Reduction Steps

PLR	FFLP
1.0	1.0
0.75	0.80
0.50	0.61
0.25	0.40

If the chiller is operating at a part load ratio of 0.6 say, this implies that the compressor is cycling between two and three cylinders in operation; two cylinders sixty percent of the time and three cylinders forty percent of the time.

Thus, the corresponding part load power consumption of the chiller is

$$PPL = (0.6 \times 0.61 + 0.4 \times 0.80)P$$

$$PPL = 0.686P$$

Therefore, it follows that if detailed part load performance data of reciprocating chillers is not available, the limited data from manufacturers catalogues can be used to simulate the part load performance in an approximate manner.

4.3.5 Algorithm for Simulating the Performance of a Water-Cooled Reciprocating Water Chiller

This algorithm determines the power consumed by the compressor of the chiller in satisfying a refrigeration load, and the condenser heat rejection load. It is assumed that the chiller does not have a hot gas bypass control capability and that the following data are known:

Refrigeration load, QEPL
Temperature of water leaving the evaporator, TWE2
Temperature of water leaving the condenser, TWC2
Full load model coefficients, B1 through B18
Part load model coefficients, C1, C2, C3
Minimum unloading ratio, MUR

Calculation Steps

1) Computer full load capacity, QE, at TWE2 and TWC2 using Equation 4.23.

2) Compute part load ratio, PLR.

$$PLR = \frac{QEPL}{QE}$$

3) Compute full load power, P, at TWE2 and TWC2 using Equation 4.24.

4) Compute part load power required, PPL
   If PLR < MUR, compute PPL using Equations 4.30, 4.31 and 4.32
   If PLR = MUR, compute PPL using Equations 4.29a, 4.29b and 4.32
   If PLR > MUR, compute PPL using Equations 4.28 and 4.32

5) Compute condenser heat rejection load, QC

$$QC = QEPL + PPL$$

4.3.6 Multiple Chiller Systems

Multiple chiller systems offer the user some standby capacity if repair work must be done on one chilling machine. Starting inrush current and power costs at part load conditions are reduced. Energy is saved since at system partial load, some of the chillers will be operating close to/or at full load. Maintenance can be scheduled for one chilling machine during part load times and sufficient cooling can still be provided by the remaining unit(s). However, these advantages are gained at a significant increase in installed cost.

The simulation of the performance of multiple chiller systems involves determining the combination of chillers that will satisfy a given refrigeration load for minimal energy consumption.

4.3.7 Centrifugal Water Chiller Full Load Model

The centrifugal water chiller operates on the same vapour compression refrigeration system and cycle as described in section 4.3.1. The system consists of a centrifugal compressor, condenser, flow control device, and evaporator. The evaporator is the flooded liquid chiller type and the condenser is water cooled. The flow control device is either a float valve or orifice. The centrifugal compressor is widely used in large air conditioning systems.

The full load centrifugal water chiller model is similar to the water cooled reciprocating water chiller model. Thus the full load centrifugal water chiller model consists of five equations (Equations 4.9, 4.13, 4.20, 4.23 and 4.24), nine variables (QE, P, QC, MWE, TWE1, TWE2, MWC, TWC1, and TWC2) and eighteen coefficients (B1 through B18) that are determined from experimental or manufacturers' catalogue data by polynomial regression.

4.3.8 Capacity Control of Centrifugal Water Chiller

As stated in Section 4.3.3, the capacity of a compressor must be regulated to meet the load demand.

There are three methods of controlling the capacity of centrifugal compressors (Ref. 20):

1) Suction Pamper Control
2) Speed Control
3) Variable Inlet Guide Vanes

The compressor capacity control is operated from a temperature sensor located in the leaving chilled water line.

The suction damper is a simple one-piece butterfly damper in the suction line, that rotates to throttle the gas flow. When it throttles flow back along the compressor performance curve, operation will eventually reach the unstable surge region. This is at about forty to fifty percent of full load.

The speed control method of varying centrifugal compressor capacity involves the use of variable speed prime movers. If the compressor drive is an electric motor, a variable speed type called a wound rotor motor can be used. For very large installations, steam turbines are used and speed control is accomplished by throttling steam flow to the turbine. Minimum load is limited to forty to fifty percent however, to ensure stable operation above the surge point.

For both suction damper and speed control methods, hot gas bypass is required to reduce capacity below about fifty percent. No reduction in power occurs below this point. Fig. 4.7 shows typical power versus capacity curves for different methods of centrifugal compressor capacity control (Ref. 20).

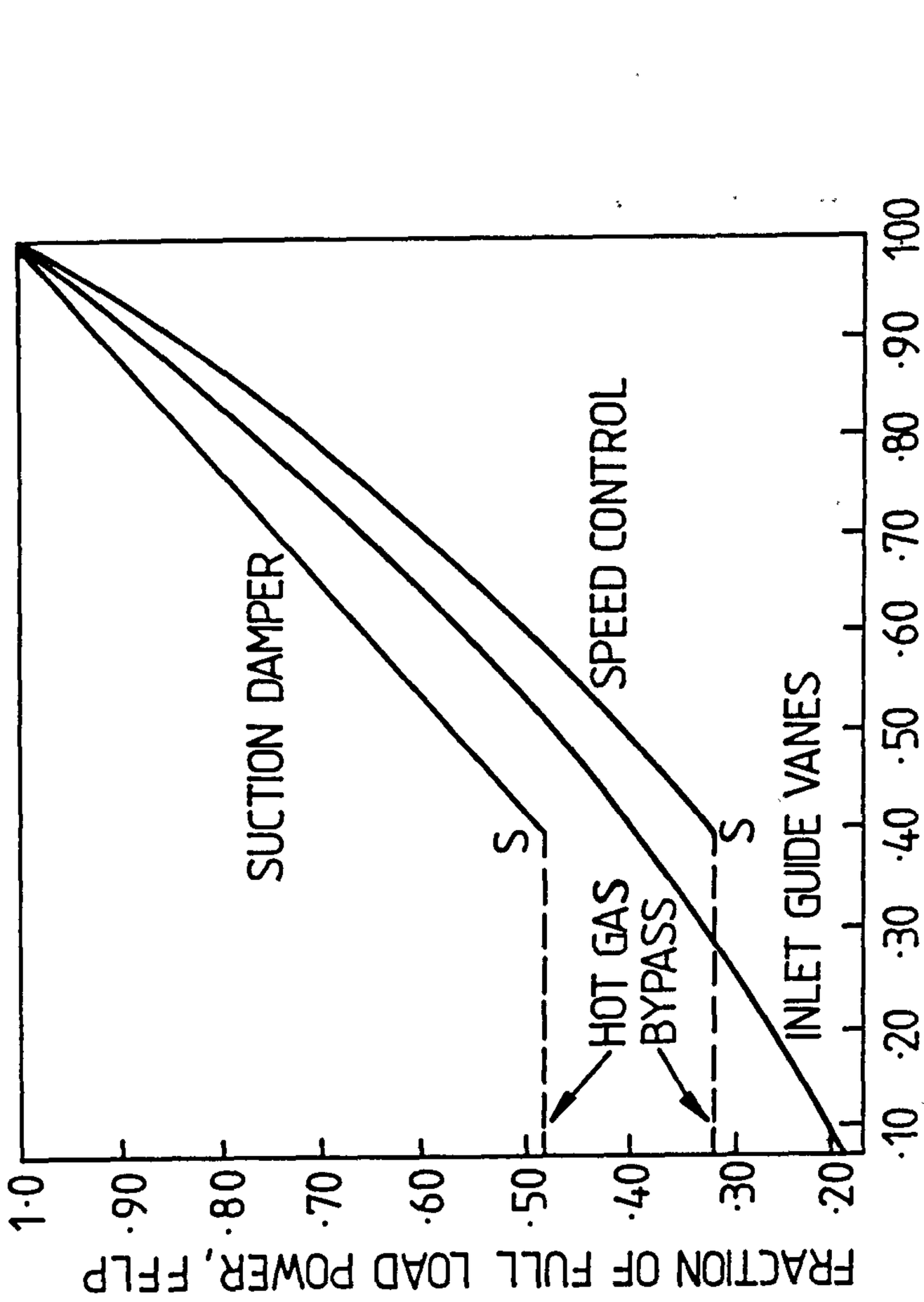

FIG. 4·7 POWER VERSUS CAPACITY OF CENTRIFUGAL COMPRESSORS - COMPARISON OF CONTROL METHODS.

An excellent method of varying compressor capacity uses adjustable inlet guide vanes, also called prerotation vanes. This is a set of adjustable vanes in the compressor suction that are gradually closed to reduce the volume of refrigerant gas compressed, thus reducing the capacity.

4.3.9 Centrifugal Water Chiller Part Load Model

For stability purposes, a centrifugal compressor should not operate below the surge point (point S in Fig. 4.7) unless hot gas bypass control is utilised. The part load performance curve can be divided into two distinct regions depending on the value of part load ratio.

The part load ratio for an imposed refrigeration load, QEPL is given by

$$PLR = \frac{QEPL}{QE} \qquad (4.27)$$

Let the part load ratio corresponding to S be PLRS. Thus if PLR > PLRS, the relationship between FFLP and PLR is

$$FFLP = D1 + D2 \times PLR + D3 \times PLR^2 + D4 \times PLR^3 \qquad (4.33)$$

where D1, D2, D3 and D4 are part load model coefficients having different values depending on the compressor capacity control method.

If the centrifugal compressor possesses a hot gas bypass control mechanism, then the capacity may be controlled below the point S by aritificially loading the suction with hot gas from the compressor discharge. For this operating condition,

$$PLR = PLRS \qquad (4.34a)$$

and

$$FFLP = D1 + D2 \times PLRS + D3 \times PLRS^2 + D4 \times PLRS^3 \qquad (4.34b)$$

The power consumed by the chiller's compressor to satisfy a given refrigeration load is given by

$$PPL = FFLP \times P \qquad (4.32)$$

The algorithm for simulating the performance of centrifugal water chillers is similar to that for reciprocating water chillers with the appropriate equations and model coefficient substituted.

4.4 COOLING TOWERS

The function of a cooling tower is to reduce the temperature of circulating water so that it may be reused in condensers of a refrigeration plant and other heat exchange equipment. Mechanical draught cooling towers are commonly used in HVAC applications. Air can be blown upward through the tower with the fan at the bottom (forced draught), or drawn upwards throught the tower with the fan at the top (induced draught).

Fans may be either the centrifugal or the propeller type. Centrifugal fans create a higher pressure and are therefore more suitable when there is considerable resistance to air flow through the tower. Propeller fans tend to be noisier.

Most towers contain a fill of some type, such as wood slats or latticework. The fill retards the rate of water fall and increases the water surface exposed to the air. Eliminator plates are generally placed at the air outlet to minimise drift or carry over of liquid water in the exhaust air.

When the air and water move in opposite directions, the tower is called a counterflow type. When the air and water move at right angles to each other the tower is called a crossflow type. When the air and the water move in the same direction, the tower is called a parallel flow type, Fig. 4.8 shows the three cooling tower air/water flow types.

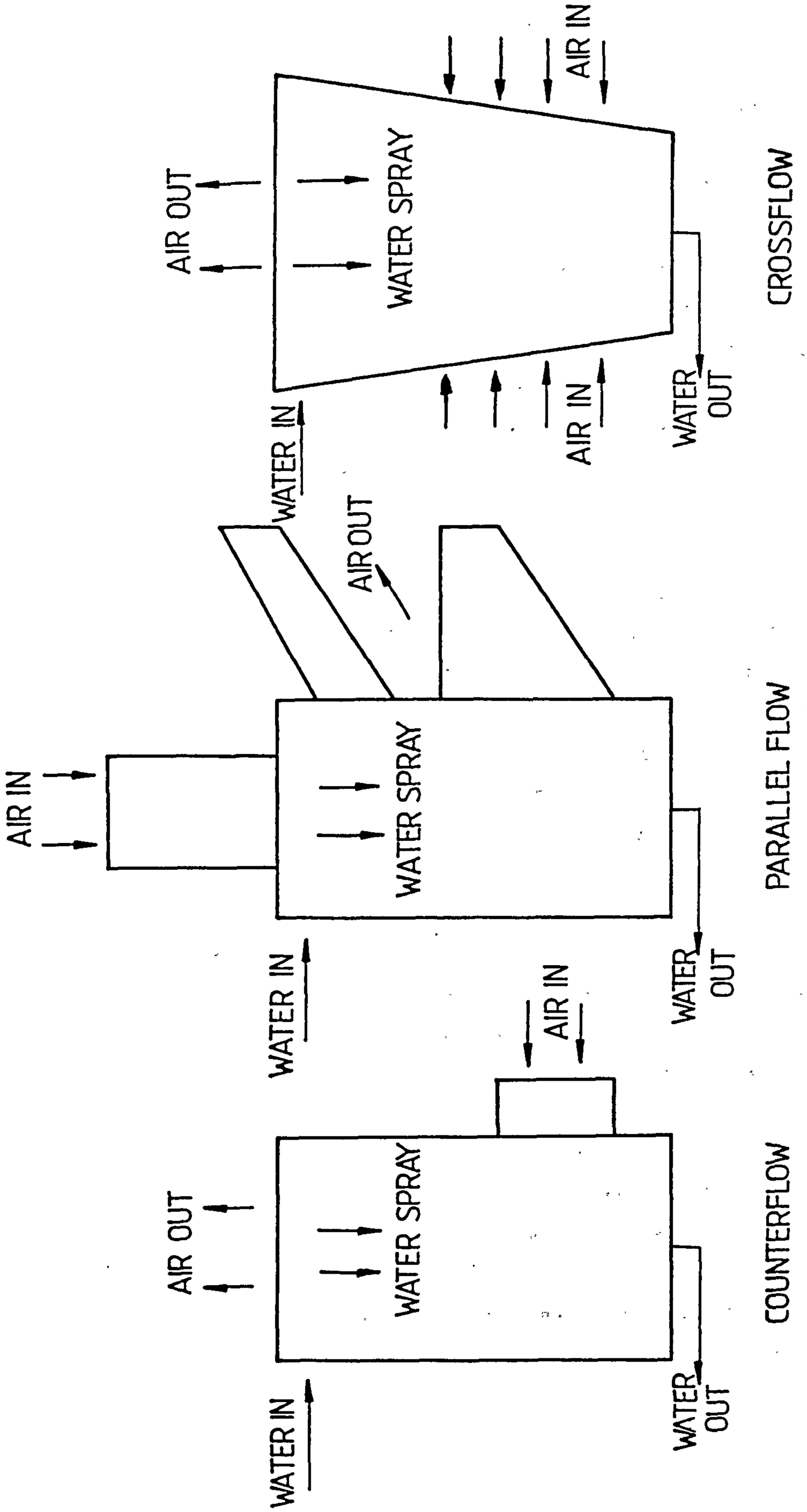

FIG. 4·8 COOLING TOWER AIR/WATER FLOW TYPES

4.4.1 Analysis of Heat Transfer Performance of Cooling Towers: Introduction

The basic theory of cooling tower operation was first proposed in 1923 by Walker et. al. (Ref. 22). However the first practical use of the differential equations was developed by Merkel in 1925 (Ref. 23).

He combined the equations for heat and water vapour transfer and used enthalpy as the driving force to allow for both sensible and latent heat transfer. Heat is removed from the water by a transfer of sensible heat due to a difference in temperature levels and by the latent heat equivalent of the mass transfer resulting from the evaporation of a portion of the circulating water. Merkel combined these into a single process based on enthalpy difference as the driving force.

Merkel's theory requires two main assumptions, namely, that the water loss by evaporation is neglected and the Lewis number for air/water vapour systems is unity. The theory states that all of the heat transfer taking place at any postion in the tower is proportional to the difference between the enthalpy of saturated air at the temperature of the water at that point in the tower and the enthalpy of the air at the point in the tower. Merkel's simplified approach has been almost universally adopted for the calculation of tower performance.

Sutherland (Ref. 24) has presented a method for accurate analysis of mechanical draught counterflow cooling towers and compared his results with those obtained by using Merkel's approximate method. Sutherland relaxed the assumptions made by Merkel and used a fourth-order Range Kutta method to solve the differential equations obtained by carrying out a heat and mass balance over an elemental volume of the counterflow cooling tower. He showed that substantial underestimation of tower volume from 5 to 15 percent are obtained if the approximate method is used.

For building energy analysis computer programs, Sutherland's method is too complex and does not consider the prediction of cooling tower performance at off-design conditions.

A completely different and simpler approach to the simulation of the performance of cooling towers has been presented by Whillier (Refs. 25 and 26). It does not use the Merkel's method of analysis and takes account of the water loss by evaporation. It is reasonably accurate and is readily applicable for simulation of the off-design performance of cooling towers and has therefore been adopted for developing the cooling tower model presented in this thesis.

4.4.2 Energy Balance for a Cooling Tower

In a cooling tower, the moisture content of the air increases from g_{ai} to g_{ao}, so that the rate of evaporation of the water is equal to m_a (g_{ao} - g_{ai}), where

m_a = mass flow rate of dry air (kg/s)
g_{ai} = moisture content of air at inlet (kg/kg)
g_{ao} = moisture content of air at outlet (kg/kg)

As a result of the evaporation taking place in the tower, the mass flow rate of water leaving the tower is

$$m_{wo} = m_{wi} - m_a(g_{ao} - g_{ai}) \qquad (4.35)$$

where

m_{wo} = mass flow rate of water leaving the tower (kg/s)
m_{wi} = mass flow rate of water entering the tower (kg/s)

The energy balance for a cooling tower is obtained by equating the enthalpies of the entering air and water streams to the enthalpies of the leaving air and water streams. Thus,

$$m_a\, h_{ai} + m_{wi}\, c_{pw}\, t_{wi} = m_a\, h_{ao} + (m_{wi} - m_a\,\{g_{ao} - g_{ai}\})\, c_{pw}\, t_{wo}$$

$$m_{wi}\, c_{pw}\, (t_{wi} - t_{wo}) = m_a\, \{(h_{ao} - h_{ai}) - c_{pw}\, t_{wo}(g_{ao} - g_{ai})\} \qquad (4.36)$$

where

c_{pw} = specific heat capacity of water (kJ/kg K)
t_{wi} = temperature of water entering the tower (^{o}C)
t_{wo} = temperature of water leaving the tower (^{o}C)
h_{ao} = specific enthalpy of air leaving the tower (kJ/kg)
h_{ai} = specific enthalpy of air entering the tower (kJ/kg)

From the definition of sigma energy we have

$$S = h - g\, c_{pw}\, t_{sl}$$

Thus

$$h_{ao} = S_{ao} + g_{ao}\, c_{pw}\, t_{slao}$$
$$h_{ai} = S_{ai} + g_{ai}\, c_{pw}\, t_{slai}$$

where

S_{ao} = sigma energy of air leaving the tower (kJ/kg)
S_{ai} = sigma energy of air entering the tower (kJ/kg)
t_{slai} = wet bulb temperature of air entering the tower (^{o}C)

Substituting for h_{ao} and h_{ai} in Equation 4.36 we get,

$$m_w\, c_{pw}\, (t_{wi} - t_{wo}) = m_a\, (S_{ao} - S_{ai}) + X \qquad (4.37)$$

where

$$X = m_a\, c_{pw}\, \{g_{ao}\, (t_{slao} - t_{wo}) + g_{ai}\, (t_{wo} - t_{slai})\} \qquad (4.38)$$

Equation 4.36 may be expressed as

$$m_w\, c_{pw}\, (t_{wi} - t_{wo}) = m_a\, (h_{ao} - h_{ai}) - Y \qquad (4.39)$$

where

$$Y = m_a\, c_{pw}\, t_{wo}\, (g_{ao} - g_{ai}) \qquad (4.40)$$

The left hand side of Equations 4.37 and 4.39 is the rate of heat transfer in the cooling tower.

Whillier (Refs. 24 and 25) has noted that the terms X and Y are small relative to the other terms and both are always positive.

Consideration of a wide range of numerical situations indicates that the numerical value of X is always a little less than half the value of Y, and that the value of X is typically between 2 and 4 percent of the left hand side of Equations 4.37 and 4.39.

The energy balance equation that is used by most authors is Equation 4.39, with the term Y being ignored. Equation 4.37 is preferred by Whillier, with the term X ignored, for the reason that the error involved in ignoring X is a little less than half of the error involved when Equation 4.39 is used with Y being ignored. The reason for ignoring the terms X or Y is to enable the use of simple definitions for the air efficiency and the water efficiency, and to facilitate use of the terms "approach" and "range" in calculations of tower performance.

Subsequent equations for the cooling tower model will hence be developed on the basis of sigma energies, using Equation 4.37 and the term X ignored.

4.4.3 The Efficiency of Cooling Towers

The performance of cooling towers can be expressed in several ways, of which the two most convenient are the water efficiency and the air efficiency.

4.4.3.1 Water Efficiency

The lowest possible temperature to which the water can be cooled in any cooling tower is the wet bulb temperature of the air entering the tower, t_{slai}. The water efficiency is defined as the ratio of the actual energy removed from the water, to the maximum possible amount that could be removed.

Thus

$$\eta_w = \frac{m_w c_{pw} (t_{wi} - t_{wo})}{m_w c_{pw} (t_{wi} - t_{slai})} = \frac{t_{wi} - t_{wo}}{t_{wi} - t_{slai}} \qquad (4.41a)$$

The range of a cooling tower is the reduction in temperature of the water through the cooling tower; the approach is the difference between the temperature of the leaving water and the wet bulb temperature of the entering air.

Thus

$$\text{Range} = t_{wi} - t_{wo} \qquad (4.42)$$

$$\text{Approach} = t_{wo} - t_{slai} \qquad (4.43)$$

Now $t_{wi} - t_{slai} = (t_{wi} - t_{wo}) + (t_{wo} - t_{slai})$

$= \text{Range} + \text{Approach}$

Thus

$$\eta_w = \frac{\text{Range}}{\text{Range} + \text{Approach}} \qquad (4.41b)$$

4.4.3.2 Air Efficiency

The maximum possible wet-bulb temperature that the air passing through a cooling tower can achieve is the temperature of the entering water, t_{wi}. At this condition the sigma energy value of the air will be S_{wi}. The air efficiency is defined as the ratio of the actual increase in energy content of the air, to the maximum possible increase.

Thus,

$$\eta_a = \frac{S_{ao} - S_{ai}}{S_{wi} - S_{ai}} \qquad (4.44)$$

4.4.3.3 Reference Water - Air Ratio, WAR

The ratio of the mass flow rates of water to air, m_w/m_a, may vary from perhaps 0.1 to about 5, although the usual range is between 0.3 and 3 **(Refs. 25 and 26).** Quite, obviously at the extremes of m_w/m_a the fluid having the greater thermal capacity will exhibit a small change in temperature, and hence the efficiency for that fluid will be very low. On the other hand the fluid with very low thermal capacity will exhibit a large change in temperature and hence the efficiency for that fluid will be high.

There exists one combination of water and air mass flow rates, hereafter called the reference water-air ratio, WAR, at which the energy that would be given up by the water in cooling to the air inlet wet-bulb temperature is exactly equal to the energy increase of the airstream when its wet-bulb temperature is increased to the water inlet temperature. At this water-air ratio (and only at this value) the thermal capacities of the water and airstreams would be equal.

The reference water-air ratio may be derived from Equation 4.37 with X neglected, on the basis of the above definition. Thus for this condition,

$$m_w c_{pw} (t_{wi} - t_{slai}) = m'_a (S_{wi} - S_{ai})$$

Thus,

$$WAR = \frac{m'_w}{m'_a} = \frac{S_{wi} - S_{ai}}{c_{pw} (t_{wi} - t_{slai})} \qquad (4.45)$$

It is of considerable importance to note that WAR depends on only three items, namely

1) the inlet water temperature
2) the inlet air wet-bulb temperature
3) the barometric pressure

According to Whillier, WAR is entirely independent of the design of the cooling tower, the efficiency of the tower, and of the actual water and air mass flow rates. It is that ratio of water to air mass flow rates at which the thermal capacities of the two streams would be equal. The reference water-air ratio may vary from about 0.5 at low wet bulb temperatures to about 2.5 at high wet-bulb temperatures.

4.4.3.4 Tower Capacity Factor, R

In any cooling tower the actual water-air ratio will, in general, differ from the reference value, so that the thermal capacities of the water and air streams will seldom be equal. A factor of fundamental importance in evaluating the performance of any tower is hence the ratio of the actual water-air ratio to the reference value, i.e., the ratio of the thermal capacity of the water stream to the maximum thermal capacity of the airstream. This ratio is called the tower capacity factor, R.

Thus,

$$R = \frac{(m_w/m_a)}{WAR} \qquad (4.46)$$

An important relationship between the air and water efficiencies can be derived by manipulating Equations 4.37, 4.41a, 4.44, 4.45 and 4.46.

Neglecting X, Equation 4.37 becomes

$$m_w\, c_{pw}\, (t_{wi} - t_{wo}) = m_a\, (S_{ao} - S_{ai}) \qquad (4.37a)$$

From Equations 4.41a and 4.44 we have

$$\frac{\eta_a}{\eta_w} = \frac{\{t_{wi} - t_{slai}\}}{\{t_{wi} - t_{wo}\}} = \frac{\{S_{ao} - S_{ai}\}}{\{S_{wi} - S_{ai}\}} \qquad (4.47)$$

From Equation 4.37a we have,

$$\frac{S_{ao} - S_{ai}}{t_{wi} - t_{wo}} = \frac{m_w\, c_{pw}}{m_a} \qquad (4.37b)$$

From Equation 4.45 we have,

$$\frac{t_{wi} - t_{slai}}{S_{wi} - S_{ai}} = \frac{1}{WAR \cdot c_{pw}} \qquad (4.45a)$$

Using Equations 4.37b and 4.45a, Equation 4.47 becomes

$$\frac{\eta_a}{\eta_w} = \frac{m_w\, c_{pw}}{m_a} \cdot \frac{1}{WAR \cdot c_{pw}} = \frac{m_w/m_a}{WAR} \qquad (4.47a)$$

Using Equation 4.46, Equation 4.47a becomes

$$\frac{\eta_a}{\eta_w} = R \qquad (4.48a)$$

Thus $\eta_a = R\, \eta_w$ (4.48b)

Equation 4.48 is valid only if the air efficiency is defined in terms of energy ratios. It does not hold if the air efficiency is defined in terms of temperature ratios.

The capacity factor R, in cooling towers specifies the relative thermal capacities of the two fluid streams. Thus it has the same significance as the thermal capacity ratio C_{min}/C_{max}, in conventional heat exchangers (as outlined in Chapter 3). It is an extremely important parameter in that it serves as a basis for rationalisation of the theory of cooling towers and many other types of wet heat-exchange equipment.

4.4.4 Correlation of Experimental Data

At values of the capacity factor R less than 1, that is the thermal capacity of the water stream is less than the thermal capacity of the airstream, the maximum possible value of the water efficiency will be 1, but the maximum possible value of the air efficiency will be R. Similarly, at values of R greater than 1, the maximum possible values of the air and water efficiencies are 1, and 1/R, respectively.

This is illustrated by the upper lines marked FOM = 1 in Figures 4.9a and 4.9b, in which efficiency is plotted against R. These upper lines represent the maximum possible water and air efficiencies attainable in any cooling tower.

An extensive series of tests was carried out by Hemp (Ref. 27) on a packed cooling tower which could be supplied with hot water from the condenser of a refrigeration plant, or with cold water from the evaporator. Thus, in one case the water was cooled in the tower, while in the other the water was heated. The tests covered an extremely wide range of m_w/m_a, from 0.6 to 11.6. The wet-bulb temperature of the air was 34°C, the barometric pressure 119.5 kPa and the inlet water temperature about 12°C and 43°C for the two conditions. The reference water-air ratio, WAR, for these two situations was approximately 0.79 and 1.59 respectively for the two values of inlet water temperature. When the test data are plotted as water efficiency against the water-air ratio, m_w/m_a, the data lie on two distinct curves (Ref. 27). However when plotted as in Figure 4.9a or 4.9b showing water efficiency against the tower capacity factor, R, the data fall on a single curve (Ref. 27).

The effectiveness, E, of a cooling tower is defined as the efficiency for the fluid having the smaller thermal capacity.

$$\text{If } R < I, \quad E = \eta_w \tag{4.49a}$$

$$\text{If } R \geq I, \quad E = \eta_a \tag{4.49b}$$

Whiller (Ref. 26) plotted curves of E against R* for various sets of data and tried three equations for the best fit lines through them. These are Equations 4.50a, 4.50b and 4.50c, and while none is perfect, the third seems to be adequate for all test data examined by him. The equations are:

Straight line equation

$$E = 1 - R^* (1 - FOM) \tag{4.50a}$$

Hyperbolic-type equation

$$E = \frac{1}{1 + R^* (1/FOM - 1)} \tag{4.50b}$$

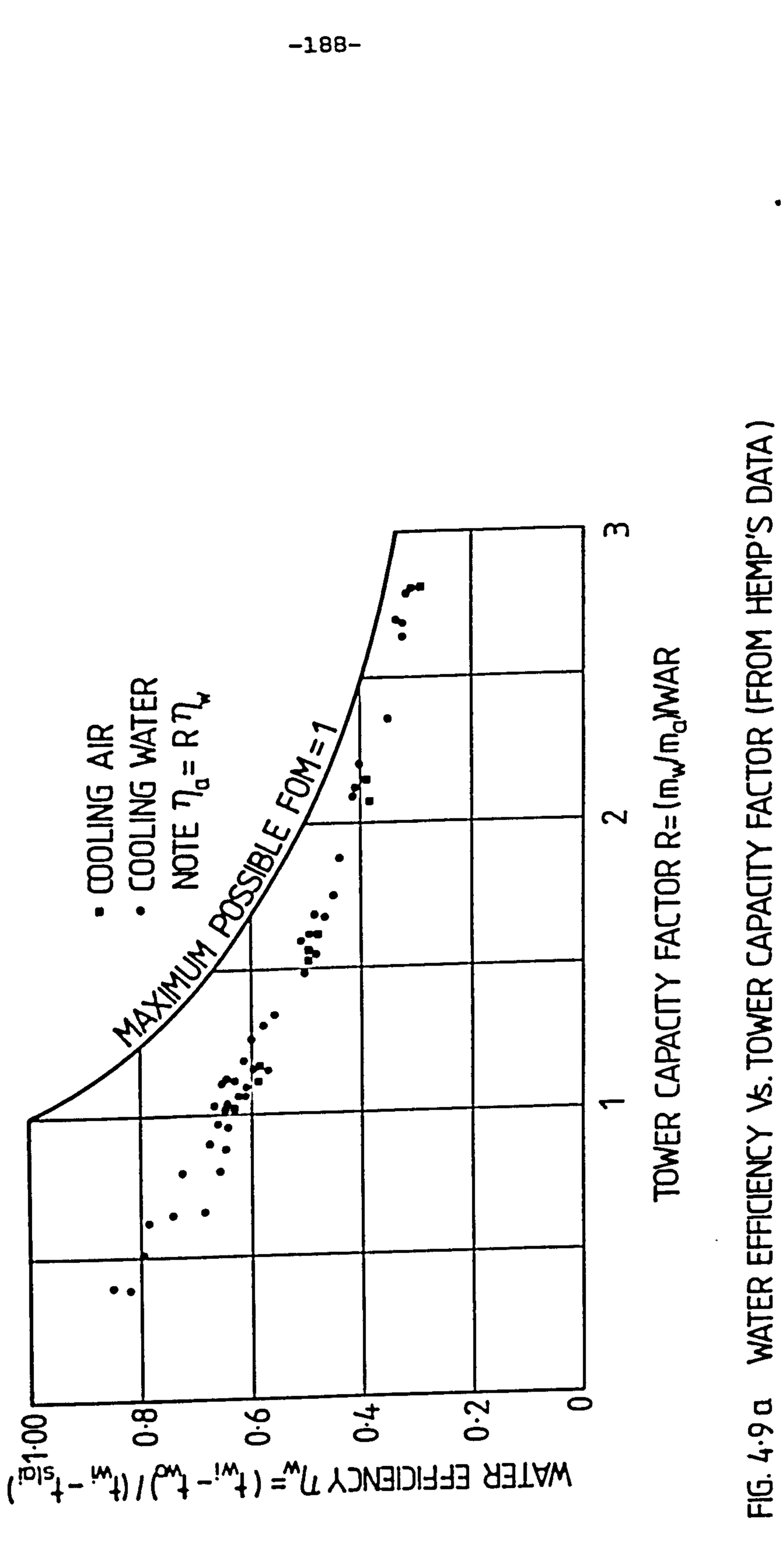

FIG. 4·9 a WATER EFFICIENCY Vs. TOWER CAPACITY FACTOR (FROM HEMP'S DATA)

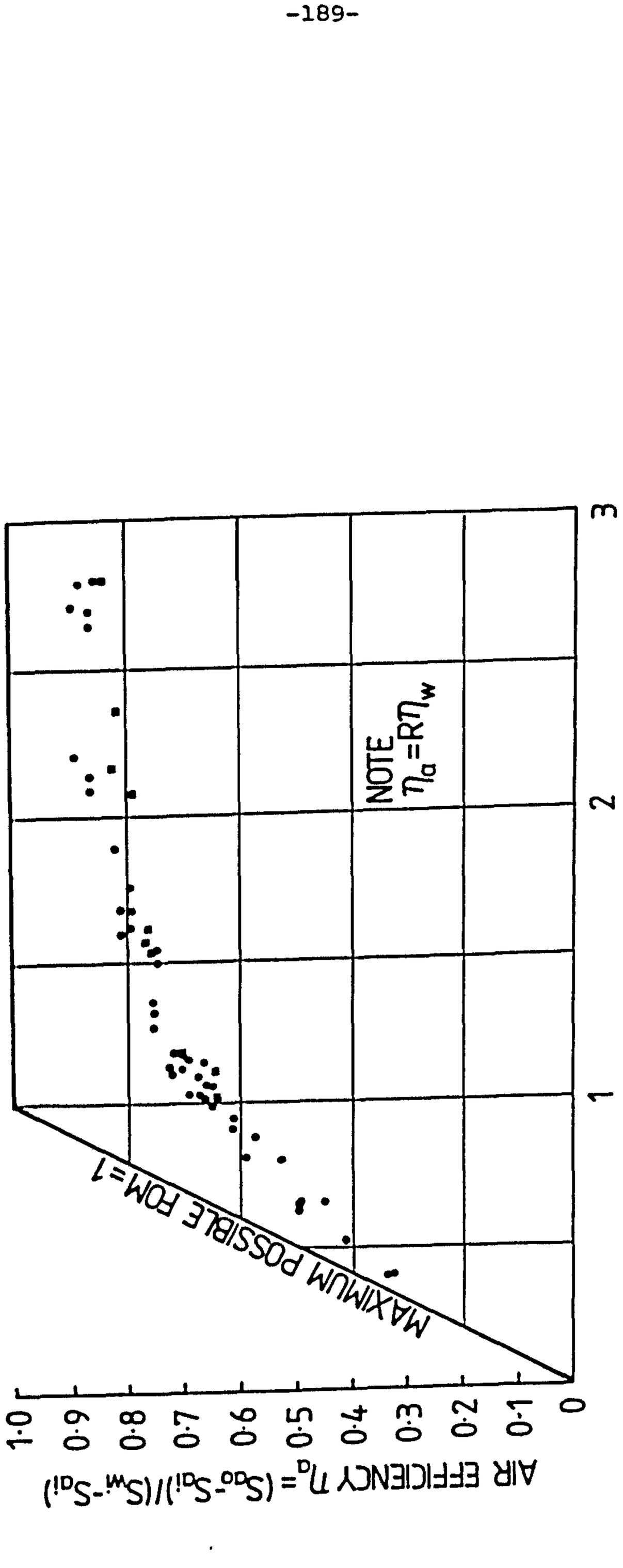

FIG. 4·9b AIR EFFICIENCY Vs. TOWER CAPACITY FACTOR (FROM HEMP'S DATA)

Experimental-type equation

$$E = FOM^{R^*} \qquad (4.50c)$$

In these equations, the term R* is always less than 1. It is defined as follows:

$$\text{If } R < 1,\ R^* = R \qquad (4.51a)$$

$$\text{If } R > 1,\ R^* = 1/R \qquad (4.51b)$$

Thus R* is seen to be equivalent to C_{min}/C_{max} in the theory of conventional heat exchangers. After considering several sets of test data, Whillier (Ref. 26) found that the exponential relation, Equation 4.50c has the widest applicability. The hyperbolic equation, 4.50b, has too much curvature. Hence Equation 4.50c is adopted for developing the cooling tower model.

Lines of constant factor of merit, FOM, based on Equation 4.50c, are shown in Fig 4.10. This figure is most useful when analysing cooling tower test data, since test data plotted on the figure enable an immediate estimate of FOM to be made.

4.4.5 Factor of Merit of Cooling Towers

The value of FOM (which is also the intercept on the R=1 line of the best curve through the data) is known as the factor of merit of the tower. A perfect tower would have a factor of merit, FOM = 1. According to Whillier (Ref. 26), all good commercial cooling towers seem to have a factor of merit between 0.6 and 0.7.

Whillier notes that Equation 4.50 is an empirical one and that data for highly efficient towers (F > 0.7) can often be equally represented by a straight line. However, the data for inefficient towers do not fall on a straight line, but on a line approximated adequately by Equation 4.50c.

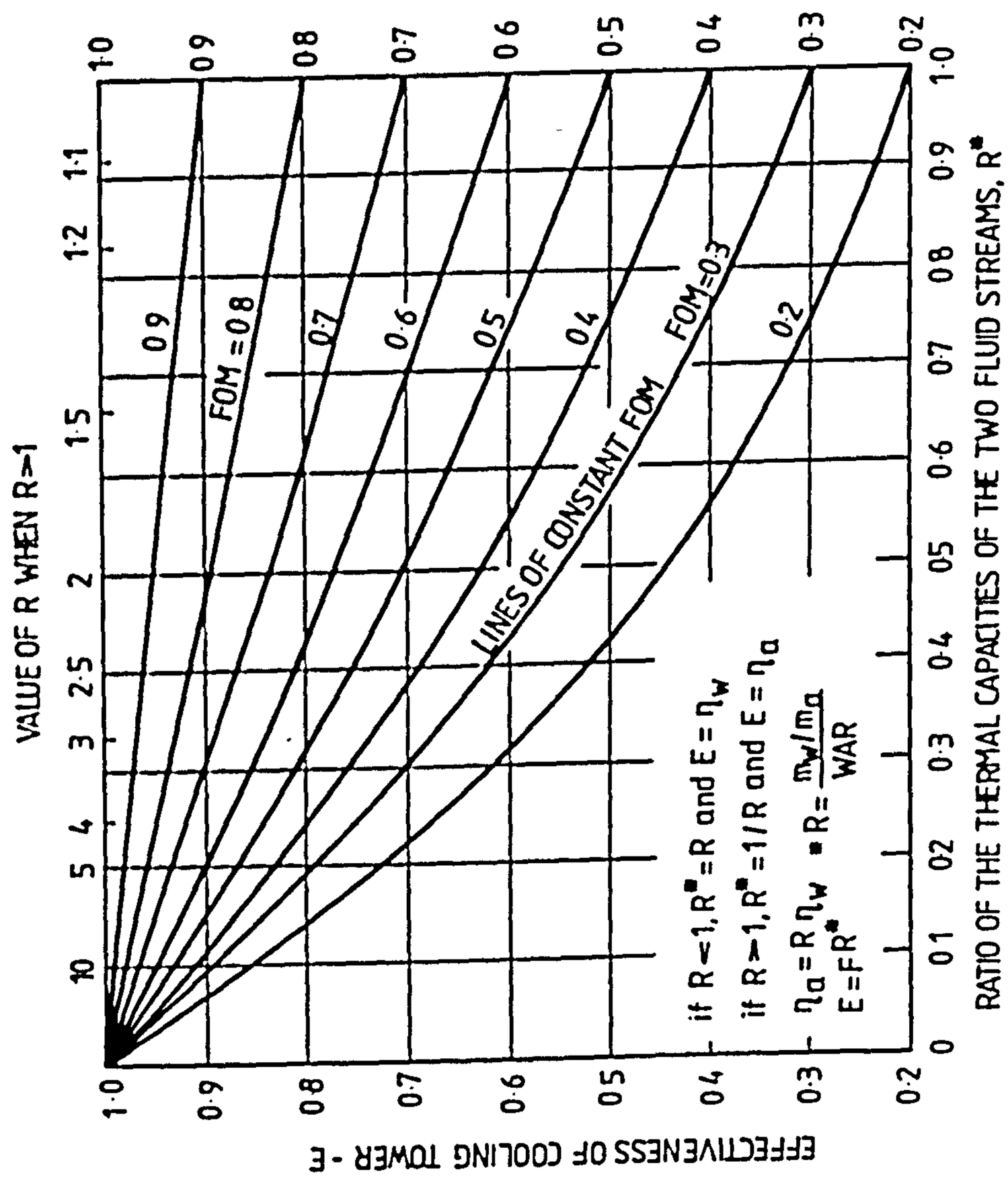

FIG. 4·10 CURVES OF CONSTANT FACTOR OF MERIT

Since test data tend to lie on lines of constant FOM when plotted in Figure 4.10, then it is possible to categorise each cooling tower uniquely by means of its factor of merit, FOM. This represents a significant simplification in the rating of cooling towers. Knowing FOM for a cooling tower is equivalent to knowing the UA factor, and the configuration, of a conventional heat exchanger.

Typical values of factor of merit, FOM for various types of cooling towers are given in Appendix 4.4 Table 1. These values are taken from Ref. 26.

4.4.6 Capacity Control of Cooling Towers

Most cooling tower systems are subjected to substantial changes in ambient wet-bulb temperature and load during the normal operating season. Accordingly, some form of capacity control may be required to maintain prescribed condensing temperatures.

Fan cycling is the simplest method of capacity control on cooling towers and is often used on multiple-unit or multiple cell installations. In non freezing climates where close control of the leaving water temperature is not essential, fan cycling affords an adequate and inexpensive method of capacity control.

Two-speed fan motors, in conjunction with fan cycling, can double the number of steps of capacity control, when compared to fan cycling alone. This is particularly useful on single-fan motor units which would have only one step of capacity control by fan cycling. Two-speed fan motors are commonly used on cooling towers as the primary method of capacity control and also to provide the added advantage of reduced energy consumption at reduced load conditions.

Modulating dampers in the fan discharge of centrifugal blower fans are used for cooling tower capacity control, as well as for energy management. In many cases modulating dampers are used in conjunction with two-speed motors.

Condenser water bypass is another method used to control condenser-cooling tower capacity. This can be done by using a bypass valve between the condenser discharge and inlet.

4.4.7 Algorithm for Simulating the Performance of a Cooling Tower

Energy is consumed in driving the fan or fans required to achieve proper air movement through a cooling tower. The pump head of a cooling tower also contributes to the energy expended in the operation of the condenser water pump.

The algorithm assumes that the cooling tower has a two-speed fan motor and that the condenser water pump operates at constant volume. It determines the temperature of water leaving the tower and the power consumed by the fan motor in satisfying the cooling tower load. The following data are required.

Ambient Air Data

Dry bulb temperature of ambient air, t_{amb} (^{o}C)
Wet bulb temperature of ambient air, $t_{sl,amb}$ (^{o}C)

Barometric pressure, p_b (kPa)

Water Chiller Data

Chiller heat rejection load, QC (kW)
Condenser water pump motor input power, PCWP (kW)
Efficiency of condenser water pump η_{cwp}

Cooling Tower Data

Factor of Merit, FOM
Temperature of water entering the tower, t_{wi} (^{o}C)
Tower fan motor input power at full load, PCTF (kW)
Volumetric flow rate of ambient air through tower at full load V_{af} (m^3/s)
Mass flow rate of water entering the tower, m_w (kg/s)

Calculation Steps

1) Compute cooling tower load, QCT

$QCT = QC + (PCWP \times \eta_{cwp})$

2) Compute temperature of water leaving the tower, t_{wo}

$$t_{wo} = t_{wi} - \frac{(QCT)}{(m_w \times c_{pw})}$$

3) Compute reference water-air ratio, WAR

Compute S_{wi} and S_{ai} using Equations 3.4, 3.7, 3.25 and 3.26

$$WAR = \frac{S_{wi} - S_{ai}}{c_{pw}\ (t_{wi} - t_{sl,amb})}$$

4) Compute water efficiency, η_w using Equation 4.41a. Substitute $t_{sl,amb}$ for t_{slai}

5) Compute tower capacity factor, R

If $FOM > \eta_w$ (implying $R > 1$), solve the equation

$FOM = (R\,\eta_w)^R$ for R by using the Newton-Raphson method. Use the value of

$R = 1/\eta_w - 1/FOM + 1$ as a first guess.

If $FOM \leqslant \eta_w$ (implying $R \leqslant 1$), then $R = \frac{\ln \eta_w}{\ln FOM}$

6) Compute mass flow rate of air through tower, m_a to satisfy the load.

$$m_a = \frac{m_w}{R \times WAR}$$

7) Compute the specific volume of the ambient air, ν_a using Equations 3.14 and 3.15

8) Compute volumetric flow rate, V_a corresponding to m_a

$V_a = m_a \quad \nu_a$

9) Compute part load ratio PLR

$$PLR = \frac{V_a}{V_{af}}$$

10) Compute power consumed by the fan motor, PCT. Generally at part load, the fan cycles to meet the tower load. It is assumed that the volume of air discharged by the fan at low speed is half that discharged at high speed, and from fan laws, the power consumed by the fan motor at low speed is one-eighth that consumed at high speed.

Thus if PLR = 0.5, FFLP = 0.125

If PLR $\leq$ 0.5, the fan cycles between off and low speed operating conditions.

PLRLO = 0.0, PLRHI = 0.5

FFLPLO = 0.0, FFLPHI = 0.125

If 0.5 < PLR $\leq$ 1.0, the fan cycles between low and high speed operating conditions.

PLRLO = 0.5, PLRHI = 1.0

FFLPLO = 0.125 FFLPHI = 1.0

The fraction of the hour that the fan operates at the higher speed, RUNTIME is given by:

$$RUNTIME = \frac{PLR - PLRLO}{PLRHI - PLRLO}$$

The fraction of full load power, FFLP for the part load operating condition is given by:

$$FFLP = (RUNTIME \times FFLPHI) + (1.0 - RUMTIME)\ FFLPLO$$

Thus,

$$PCT = FFLP \times PCTF$$

4.5 PUMPS

A pump is a device that circulates liquids through piping systems. It provides the pressure necessary to overcome the resistance to flow of a liquid in a piping system. Pumps can be classified in two groups according to the way they develop this pressure; either by positive displacement or centrifugal force. In the first group are included reciprocating, gear, vane, screw, and rotary pumps. They are used only in specialized cases in HVAC work. The centrifugal pump is the type most widely used in circulating water in HVAC systems.

Centrifugal pumps are used in heating and air conditioning for four major applications (Ref. 1):

1) Condenser Water
2) Chilled Water
3) Hot Water
4) Boiler Feed and Condensate

4.5.1 Pump Performance

The centrifugal pump increases the pressure of the liquid by first increasing its velocity, and then converting that velocity energy to pressure energy.

The items of major importance in the performance of a pump are the pressure (head) it will develop, the volumetric flow rate it will deliver, the power required to drive the pump and its efficiency. These are called pump characteristics. The characteristics are usually presented in the form of curves for each pump, and can be used to select the correct pump for an application. The general shape of these curves is similar for all centrifugal pumps.

For a water pump, the power output is the power transmitted to the water. The power output, P_o, is related to the head developed by the pump, H_w and the volumetric flow rate, V_w by the formula

$$P_o = \rho_w \times g' \times H_w \times V_w / 1000.0 \qquad (4.52)$$

where:

P_o = pump power output (kW)
ρ_w = density of water (kg/m^3)
g' = acceleration due to gravity (m/s^2)
H_w = total pump head (m of water)
V_w = volumetric flow rate (m^3/s)

The power input to a pump is always greater than the power output because of friction and other unavoidable losses. The efficiency of a pump is defined as

$$\eta_p = \frac{\text{power output}}{\text{power input}} \times 100 = \frac{P_o}{P_i} \times 100 \qquad (4.53)$$

In general pumps are operated as constant volume, cycling or variable flow (Ref. 27).

The fraction of full load power, FFLP, for a pump is related to the part load ratio by the formula:

$$FFLP = a + b \times PLR + c \times PLR^2 + d \times PLR^3 \qquad (4.54)$$

a, b, c and d are part load model coefficients

$$PLR = \frac{\text{Heating or cooling load}}{\text{Heating or cooling capacity}} \qquad (4.55)$$

If the pump is a constant volume pump which is on whenever there is a load then

$$a = 1, \quad b = c = d = 0.0$$

If the pump is cycled in response to a load then

$$a = 0, \quad b = 1, \quad c = d = 0.0$$

If the pump is a variable speed pump, the part load model coefficients can be determined by applying regression analysis to the experimental or manufacturers' catalogue data. In the case the part load ratio, PLR is the ratio of the volumetric flow rate discharged by the pump at part load to that discharged at full load.

The power input to the pump at part load, P_i, is related to that required at full load, P_{if} by the formula:

$$P_i = FFLP \times P_{if} \qquad (4.56)$$

The temperature rise of the water stream, t_w, due to pump gains is given by:

$$\Delta t_w = \frac{P_o}{\rho_w V_w c_{pw}} \qquad (4.57)$$

REFERENCES FOR CHAPTER 4

1) ASHRAE "ASHRAE Handbook, 1983 Equipment", ASHRAE.

2) PITA, E. G. Air Conditioning Principles and Systems: An Energy Approach", 1981, Published by John Wiley and Sons, Inc.

3) BRATLEY, J.G. "The Computer Simulation of Boilers and Heat Pumps", M.Sc. Thesis, Cranfield Institute of Technology, September 1984.

4) PATTISON, J.R. SHARMA,V. "The Selection of Gas-Fired Boiler Plant for the Heating of Commercial Premises", Building Services Engineering, Research and Technology, 1980, Volume 1, No. 1, pp. 10-16.

5) EVANS, R.B "Improving the Operating Efficiency of High Thermal Capacity Gas Central Heating Boilers", Watson House Bulletin, May/June 1981, Volume 45, No. 318 pp. 98-105.

6) DON, W.A. "The Efficiency of Domestic Oil Burning Boilers at Reduced Loading", Energy World, January 1976, pp 6-10.

7) CHI, J. "Computer Simulation of Fossil Fuel-Fired Boilers", Proceedings of the Conference on Improving Efficiency and Performance of HVAC Equipment and Systems for Commercial and Industrial Buildings, Held at Purdue University from April 12-14, 1976. Volume 2, Paper No. C2 pp. 336-346.

8) HOLMES, M. "Part Load Efficiency of Gas and Oil-Fired Boilers", BSRIA Technical Note 1/76.

9) MCNAIR, H.P. "Energy Saving and Boiler Load Factor", Building Research Practice, Nov/Dec. 1983, Volume 11, No. 6 pp. 359-361.

10) ADAM, W. "The Selection of Boiler Installations from the Energy Conservation Point of View", Klimaatbeheersing, February 1980, Volume 9, No. 2 pp, 58-64 and 73-77.

11) "In-Use Efficiencies of Modern Gas Boilers", Watson House Bulletin, 1983, Volume 47, No. 2, pp. 7-9.

12) PAYNE, G.A. "The Energy Manager's Handbook", pp. 32.

13) ALLEN, J.J. HAMILTON, J.F. "Characterization of Water Chillers", Ray W Herrick Laboratory Report No. HL 80-22, Purdue University, 1980.

14) ALLEN, J.J. HAMILTON, J.F. "Comparison of Wate Chiller Models", Ray W. Herrick Laboratory Report No. HL 80-34, Purdue University, 1980.

15) ALLEN, J.J. HAMILTON, J.F. "Steady State Reciprocating Water Chiller Models", ASHRAE Transactions 1983, Volume 89 Part 2A, pp. 398-407.

16) STOECKER, W.F. "Procedures for Simulating the Performance of Components and Systems for Energy Calculations", Third Edition 1975. Published by ASHRAE.

17) ARI "Standards for Reciprocating Water Chilling Packages", ANSI/ARI 590 - 1981.

18) ASHRAE "Methods of Testing Liquid Chilling Packages", ASHRAE 30 - 1978.

19) LEVERENZ, D.J. BERGAN, N.E. "Development and Validation of a Reciprocating Chiller Model for Hourly Energy Analysis Programs", ASHRAE Transactions 1983, Volume 89, Part 1A pp. 156-174.

20) PITA, E.G. "Refrigeration Principles and Systems: An Energy Approach", 1984, Published by John Wiley and Sons, Inc.

21) YORK INT'L "50 Hz Hermetic Reciprocating Packaged Liquid Chillers", 1976 Published by Borg-Warner Corporation.

22) WALKER, W.H.
LEWIS, W.K.
MCADAMS, W.H. "Principles of Chemical Enegineering", 1923, Published by McGraw-Hill Book Company, New York.

23) MERKEL, F. "Verdunstungskuhlung", VDI Forschungsarbeiten No. 275, Berlin 1925.

24) SUTHERLAND, J.W. "Analysis of Mechanical-Draught Counterflow Air/Water Cooling Towers", Journal of Heat Transfer August 1983, Volume 105, pp 576-583.

25) WHILLIER, A. "A Fresh Look at the Calculation of Performance of Cooling Towers". ASHRAE Transactions 1976, Volume 82, Part 1 pp. 269-282.

26) WHILLIER, A. "Predicting the Performance of Forced-Draught Cooling Towers", Journal of the Mine Ventilation Society of South Africa, January 1977, Volume 30 No. 1, pp. 2-25.

27) KNEBEL, D.E. "Simplified Energy Analysis Using the Modified Bin Method", Prepared for ASHRAE, 1983

CHAPTER 5

SIMULATION OF THE PERFORMANCE OF HVAC SYSTEMS AND CENTRAL PLANT

NOMENCLATURE

Symbol	Description	Unit
APP	approach	K
F_k	kth constraint value	Various
FFLP	fraction of full load power	
FPOW	fan absorbed power	kW
g_{ai}	moisture content of air entering node	kg/kg
g_{ao}	moisture content of air leaving node	
g_{ma}	moisture content of mixed air	kg/kg
g_{oa}	moisture content of outside air	kg/kg
g_{ra}	moisture content of return air	kg/kg
h_{ai}	specific enthalpy of air entering node	kJ/kg
h_{ao}	specific enthalpy of air leaving node	kJ/kg
m_{ai}	mass flow rate of air entering node	kg/s
m_{ao}	mass flow rate of air leaving node	kg/s
m_{ma}	mass flow rate of mixed air	kg/s
$m_{oa,min}$	minimum mass flow rate of outside air	kg/s
PLR	part load ratio	
RNG,RNGN	range	K
r_i	fresh air fraction of air entering node	
r_o	fresh air fraction of air leaving from node	
TWBOA	wet bulb temperature of outside air (sling)	^oC
TWC1,TWC2	temperatures of water entering and leaving the condenser respectively	^oC
TWE1,TWE2	temperatures of water entering and leaving the evaporator respectively	^oC
TWICT,TWOCT	temperatures of water entering and leaving the cooling tower respectively	^oC
t_{ma}	temperature of mixed air	^oC
t_{oa}	temperature of outside air	^oC
t_{ra}	temperature of return air	^oC
t_z	zone air dry bulb temperature	^oC
$t_{z,min}$, $t_{z,max}$	minimum and maximum values of t_z respectively	
V_a	volumetric flow rate of air	m^3/s

5.1 INTRODUCTION

Stoecker (Ref. 1) has defined system simulation as predicting the operating quantities within a system (such as pressures, temperatures, energy-and fluid-flow rates) at the condition where all energy and material balances, all equations of state of working substances, and all performance characteristics of individual components are satisfied. For our purposes, system simulation can be classified into quasi-steady state and dynamic analysis.

Quasi-steady state system simulation assumes that over the time interval of interest, typically one hour, the operating variables are relatively constant but may change over the next time interval. Dynamic analysis is used for the study of performance of systems subject to frequent changes in the operating variables and has been applied to the thermal analysis of buildings, the stability and dynamic response of HVAC control systems. Reference 1 states that since the dynamic response of HVAC systems is much more rapid than that of the building, a steady state simulation of the system is adequate for most energy calculations.

As mentioned in Chapter 2, two basic approaches currently used in the computer simulation of building energy systems are the fixed schematic technique and the component based modelling technique. While the fixed schematic with options technique has been used by most of the building energy analysis programs developed in the last decade, advances in system simulation and increased interest in special and innovative systems have led to the development of the component based modelling approach. For simulating a given HVAC system, computer programs using the fixed schematic technique may be quicker and cheaper to run; however they lack the flexibility of the computer programs using the component based modelling approach.

5.2 COMPONENT BASED SYSTEM MODELLING

The HVAC system and central plant may be considered to be composed of a number of component modules. Therefore, the first step towards modelling the building energy system is to develop a model for each of the components. Each of the models is placed in a library for use in contructing systems.

Two techniques used for the component based performance simulation of building energy systems are the sequential and simultaneous calculation methods.

The sequential calculation method has resulted from the formulation of the component models on an input/output basis and presumes that a suitable starting point can be found to proceed with the simulation. Using input information (for the system schematic and its components), the output from the first component can be calculated and this forms the input to the next component. Using this and any other relevant input data this procedure is repeated for all the components; this leads to the determination of the performance of the entire system.

One advantage of the sequential modelling approach is that simple or complex component models can be used; these can be upgraded as technical knowledge improves thus allowing for further development of the computer simulation program. Component based system simulation programs making use of the sequential modelling approach include TRNSYS **(Ref. 2)** which has been developed for the transient simulation of solar energy systems and AMBER **(Ref. 3)** which uses the quasi-steady state approach.

In TRNSYS each component model is formulated as a separate FORTRAN subroutine. The components are described by either algebraic or differential equations. The transfer of information into and out of a component is shown in Fig. 5.1 which indicates the ordering of inputs, outputs and parameters for a mixing box operating in the minimum outdoor air control mode.

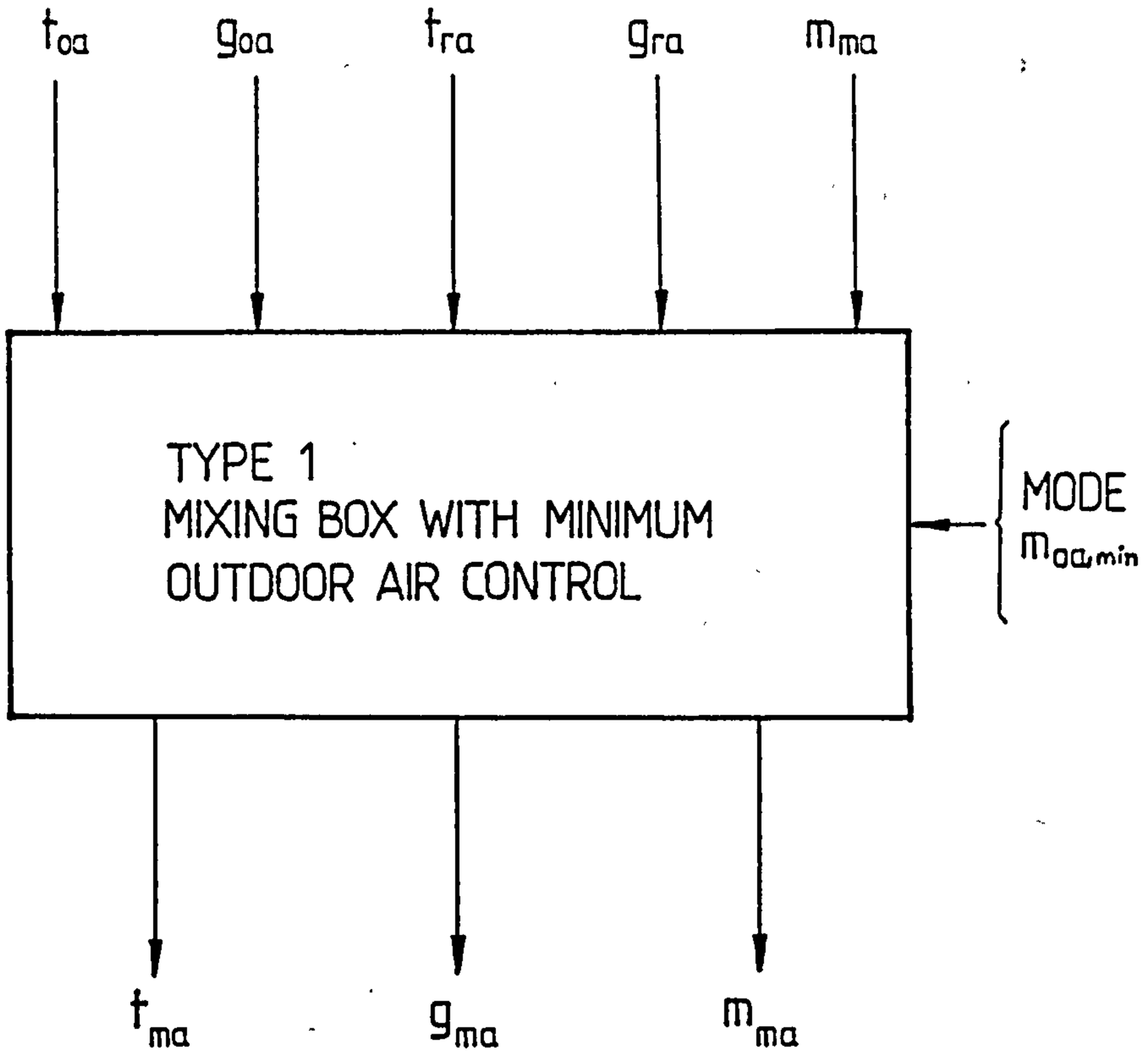

INFORMATION FLOW DIAGRAM
INPUTS 5
OUTPUTS 3
PARAMETERS 2

CHARACTERISTIC DESCRIPTION
PARAMETERS
1. MODE
2. $m_{oa,min}$

FIG. 5·1 COMPONENT DIAGRAM FOR MIXING BOX OPERATING IN MINIMUM OUTDOOR AIR CONTROL MODE.

The mixing box component receives data such as t_{oa}, g_{oa}, t_{ra}, g_{ra}, $m_{oa,min}$ and m_{ma} and computes t_{ma} and g_{ma}; these output data as well as m_{ma} are transmitted to other components. Once all the mathematical models of the components have been formulated, the next step is to construct a system information flow diagram.

An information flow diagram is a schematic representation of the flow of information between each of the system components. In the diagram each component is represented by a component diagram like Fig. 5.1. The information flow diagram of a system is constructed by joining all of the diagrams of the system components. TRNSYS recognizes the position of each component in the information flow diagram by the user assigning to each component a unique UNIT number. The input and output variables of each of the component models are then identified and their functional relationships determined. Solving the set of simultaneous algebraic and differential equations which describe the component models leads to the determination of the performance of the system.

The alternative approach to component based system simulation is the simultaneous calculation method.

Silverman et. al. **(Ref. 4)** have used a network modelling approach to simulate the performance of HVAC systems. With this method, the building and its energy systems can be viewed as a number of "nodes" connected by "arcs". Each node is of a particular type, e.g. fan, heating coil, cooling coil or air-conditioned zone. Each arc carries a fluid, e.g. air or water, and has certain properties such as mass flow rate, enthalpy, moisture content and fresh air fraction. Each node type implies certain "constraints" which must be enforced. For example a mixing box (collector) must obey the laws of conservation of mass, conservation of energy, conservation of water vapour and conservation of the fresh air component. These constitute equality constraints on the arc variables entering and leaving the node. They are written in the form:

$$F_k = m_{ao} - \Sigma\, m_{ai} \qquad (5.1)$$

$$F_k = m_{ao}\, h_{ao} - \Sigma\, m_{ai}\, h_{ai} \qquad (5.2)$$

$$F_k = m_{ao}\, g_{ao} - m_{ai}\, g_{ai} \qquad (5.3)$$

$$F_k = m_{ao}\, r_o - m_{ai}\, r_i \qquad (5.4)$$

In Equations 5.1 to 5.4, F_k is the kth constraint value (forced to zero in the solution process). The subscripts i and o represent the node "in" and "out" respectively, while m_a, h_a, g_a and r respresent air mass flow rate, enthalpy, moisture content and fresh air fraction respectively.

Some node types also imply inequality constraints. For example, a node representing an air-conditioned zone requires that the temperature in the leaving arc not violate high or low bounds. This is written as:

$$F_k = t_{z,max} - t_z \qquad (5.5)$$

$$F_k = t_z - t_{z,min} \qquad (5.6)$$

where $t_{z,max}$ and $t_{z,min}$ are the zone upper and lower temperaure bounds, and t_z the actual zone leaving air temperature. The F's here are again constraint values but are forced to be greater than or equal to zero, rather than strictly equal to zero, during the solution process. Typically, a particular node type implies several constraints of both equality and inequality types. This is summarised in Table 5.1. Table 5.1a shows a list of the different node types necessary to model a large class of systems. Table 5.1b shows a list of different kinds of constraints. The right column of Table 5.1a indicates the constraint which must be enforced for each type of node.

TABLE 5.1a

Node Type Definitions

Node Type	Description	Constraints Invoked
1	Outside air intake	None
2	Collector	2, 3, 4, 5
3	Fan	17
4	Cooling coil	6, 16, 19
5	Heating coil	18
6	Zone	10, 11, 12, 13, 14, 15
7	Distributor	7
8	Exhaust air outlet	None

TABLE 5.1b

Constraint Definitions

Constraint Type	Description	Type
2	Collector mass conservation	Equality
3	Collector energy conservation	Equality
4	Collector moisture conservation	Equality
5	Collector fresh air conservation	Equality
6	Cooling coil not allowed to heat	Inequality
7	Distributor mass conservation	Equality
10	Zone temperature lower bound	Inequality
11	Zone temperature upper bound	Inequality
12	Zone relative humidity upper bound	Inequality
13	Zone fresh air lower bound	Inequality
14	Zone moisture conservation	Equality
15	Zone energy conservation	Equality
16	Cooling coil moisture removal	Equality
17	Fan energy conservation	Equality
18	Heating coil not allowed to cool	Inequality
19	Cooling coil capacity limit	Inequality

Some arc variables are determined by external factors such as weather data, occupancy schedules and are defined as exogenous, meaning that these variables are external to the solution process.

The network definition of a HVAC system is accomplished by making use of four arrays ARCTAB, NODTYP, EXO and RNODE. The ARCTAB array represents, by reference to the constraints invoked for each node, a set of equations or inequalities which must be satisfied. The EXO array represents inputs which fix certain of the variables in ARCTAB. The RNODE array carries information about the nodes, e.g., capacities, parameters for the node constraint equations, etc.

Component models developed for the network modelling approach do not have distinct inputs and outputs. Rather each component is represented by one or more "constraints", which are simply functions of the arc variables.

At the solution point, the constraint is "satisfied", meaning that the function is either zero (equality constraint) or within the specified limits (inequality constraints). The approach to programming is therefore to select a proposed set of solution values, evaluate the constraints (as implied by the nodes present) for the proposed solution values, and repeat until all constraints are satisfied.

The solution algorithm utilised by Silverman et.al. to achieve this and solve the network is the Generalized Reduced Gradient Method (Ref. 5). After the network is solved the mass flow rates, enthalpies, humidities and fresh air fractions are known throughout. Other quantities of interest, for example temperatures, heat addition/removal rates at coil, etc. can be determined with auxiliary relationships.

The program developed by Silverman et.al. is limited in several ways. It optimises only over a single time period, allows only for single-fluid networks thus preventing analysis of generalised central plants and does not allow direct inclusion of conventional HVAC controls.

Sowell et. al. (Ref. 6) have expanded and refined the work carried out by Silverman et. al to include analysis of conventional HVAC proportional controls. The network description of the HVAC system is obtained using the concepts proposed by Silverman et. al.; however graph theory is employed to select a suitable set of equations and develop an algorithm for their solution. The network solution algorithm generated on the mainframe is downloaded to a microcomputer on which it becomes part of a tool for building energy analysis.

Despite the automatic determination of a very efficient computational sequence, including iterative calculations if necessary, several limitations remain. The microcomputer implementation of the solution algorithm examines only a single operational point and currently available component models deal primarily with the airside of HVAC systems. The water side of HVAC systems and central plant components are not modelled.

However, the authors indicate that further developments of the program will cater for these limitations.

A non-proprietary computer program, HVAC SIM+, (Ref. 7) which accounts for the dynamic interactions between the building shell, HVAC systems and equipment, and control systems is being developed at the National Bureau of Standards. The program employs advanced equation solving techniques and a hierarchical, modular approach to simulate the dynamic performance of entire building/HVAC/control systems. Such a simulation exercise involves the simultaneous solution of a large number of algebraic and differential equations over a large time period using time steps on the order of seconds or smaller. This is because the dynamics of systems within a building take place on a time scale on the order of seconds for actions involving local control loops to a time scale on the order of minutes for changes in zone conditions.

Potential research applications for the program of particular interest are to evaluate the energy conservation benefits of various advanced control strategies and algorithms, to examine the dynamic interactions among building subsystems, and to explore ways of optimising the annual energy performance of entire buildings considered as single systems. However, the authors warn that HVACSIM+ is not intended as a software that can be easily used by the general public or even design engineers.

The computer program, SYSPAN, developed to simulate the thermal performance of HVAC systems and central plant in this thesis uses the sequential modelling approach and is described in the next section.

5.3 SIMULATION METHODOLOGY OF COMPUTER PROGRAM SYSPAN

SYSPAN uses a component based sequential modelling approach to simulate the thermal performance of HVAC systems and central plant. Each component of a building energy system is formulated as a separate subroutine with distinct inputs and outputs using the models developed in Chapters 3 and 4.

SYSPAN has the following features:

Component modules are defined so as to include their associated controls. For the frequencies under consideration the response of most of the components is essentially steady state and thus a quasi-steady state modelling approach to predicting the energy usage of the heating and cooling plant is adequate.

The HVAC systems and equipment are configured using available component models.

The state of the air is determined at the inlet and outlet ports of each component of the HVAC system. From this the thermal loads on the coils and the electrical power requirement of the fan motor can be calculated. The coil thermal loads are passed to the central plant simulation program to determine the energy consumed by the primary system components to satisfy the loads.

The simulation of a system consists of setting the functional relationships between the components and then solving the resulting set of simultaneous relationships. Since each of the functions is formulated as a FORTRAN subroutine, SYSPAN calls these function modules or subroutines in order to solve the simultaneous equations. The order in which the subroutines are called depends on the available information at the system model generation stage. This is illustrated for the following applications:

For HVAC systems employing 100% outdoor air at all times, SYSPAN works its way through the system by starting from the outside air port, assuming the mass flow rate of conditioned air is known. Since all components of the system have been identified at the configuration stage, the relevant subroutines are called in sequence and the "balance point" of system operation is determined.

For recirculating air conditioning systems in which the mass flow rate of supply air, the state of return air and/or the desired temperature of mixed air is known, a convenient starting point for the simulation process is the mixing box (for outside and return air) and no iterations around the system loop is required.

For recirculating air conditioning systems where the starting point for simulation is not obvious or all the input data necessary to model any component is not available, SYSPAN sets up iterative calculations around the system loop. Iterative methods used to obtain a solution for the state of the system are the successive substitution or secant methods. The methods consist of starting with an initial value (successive substitution method) or two values (secant method) for the solution, calling all of the model subroutines (thus obtaining a new set of state variables), checking the new state against the old state, and iterating until convergence is achieved. The speed of convergence is, of course, dependent on the initial value(s) assumed and the convergence criteria.

Applications for which iterative calculations are necessary include recirculating systems serving zones where the internal conditions are floating, for example, zone air temperatures are known but the relative humidities are allowed to float between lower and upper limits. A suitable starting point for simulating such systems is the point where return air from all zones meet. Since the system return air temperature can be determined from the mixing box model, a value can be assumed for the return air relative humidity; this leads to determining the state of system return air. Iterative calculations are then setup around the system loop using the techniques outlined above in order to obtain a solution for the state of the system.

5.4 APPLICATION OF SYSPAN FOR SIMULATING THE PERFORMANCE OF HVAC SYSTEMS

The suite of computer programs, collectively referred to as SYSPAN, has been implemented on a VAX11/750 minicomputer to simulate the Collins Building Variable Air Volume (VAV) system as specified by IEA Annex 10 Working Group.

Two configurations of the VAV system serving the third floor of the penthouse suite of the Collins Building in Glasgow were specified in Annex 10 document AN85 0220-01 **(Refs. 8 and 9).**

In this thesis, only VAV system configuration 1 as shown in Fig 5.2 is modelled. The system comprises a mixing box (economiser), spray type humidifier, axial fans, cooling coil, heating coil and supply duct. The system is to be simulated under different control schemes and zone conditions. Data for the simulation exercises are given below and in Appendix A5.

5.4.1 Weather Data

Hourly values of dry bulb temperature and relative humidity for two days, namely September 7 and November 4, in 1981 are given in Appendix A5.6. The barometric pressures for September 7 and November 4 are 114.9 kPa and 94.3 kPa respectively.

5.4.2 Controls

5.4.2.1 Coils

The water mass flow rate through both coils is controlled by a temperature sensor at point 'A'. The control scheme is as follows (see Fig. 5.3):

If temperature at A is greater than or equal to 12^{o}C then,
    no water flow through heating coil
    full water flow through cooling coil
If temperature at A is between 11.25 and 10.75^{o}C then,
    no water flow through heating coil
    no water flow through cooling coil
If temperature at A is less than or equal to 10^{o}C then,
    full water flow through heating coil
    no water flow through cooling coil

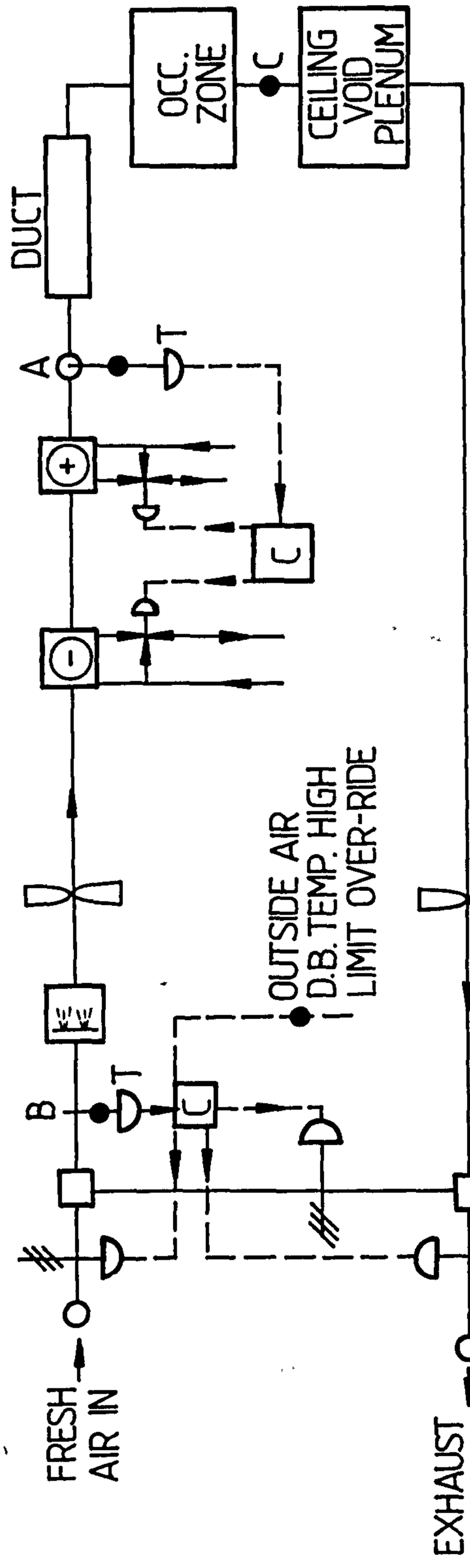

FIG. 5·2 VARIABLE AIR VOLUME SYSTEM CONFIGURATION 1

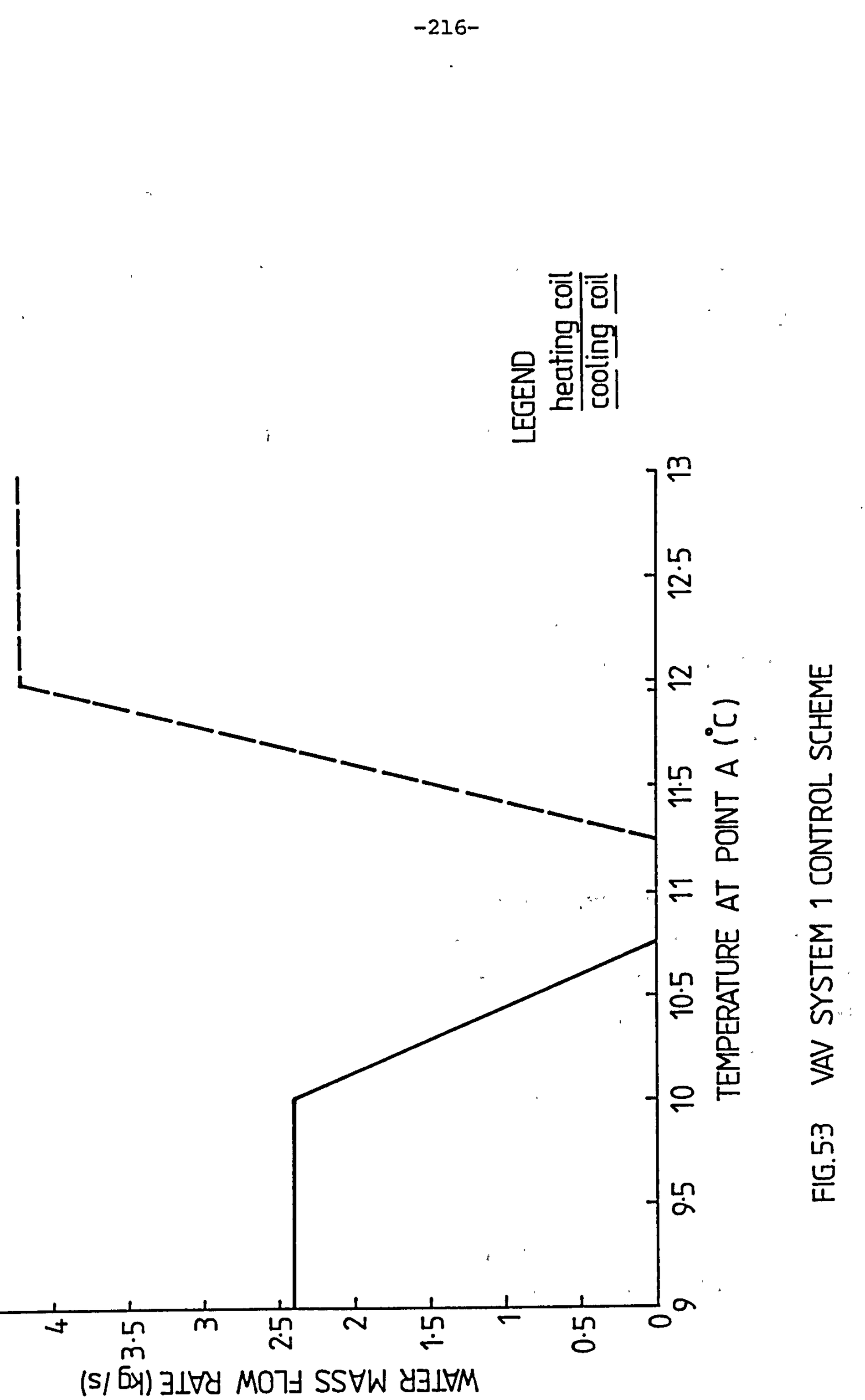

FIG.5:3 VAV SYSTEM 1 CONTROL SCHEME

5.4.2.2 Fresh Air Control

When in use the fresh air controller (economiser) responds to an outside air temperature sensor and a temperature sensor located at point 'B'. The controller works as follows:

If outside air temperature is greater than or equal to 16^{o}C then,

fresh air fraction is 10%

If outside air temperature is greater than or equal to 10^{o}C and less than 16^{o}C then,

fresh air fraction is 100%

If outside air temperature is less than 10^{o}C then,

fresh air fraction is adjusted to give a temperature of 10^{o}C at point 'B'

The fresh air fraction is considered to apply to mass flow rates.

5.4.2.3 VAV Box Control

The VAV box uses a simplified control scheme. Maximum air supply flow rate (6.2m^3/s) occurs when the zone temperature is greater than or equal to 22.1^{o}C. Minimum air supply (1.24m^3/s) occurs when the zone temperature is less than or equal to 20.1^{o}C. A linear proportional controller modulates the flow between these temperatures. The volumetric flow rates should be converted to mass flow rates by taking the density of air as 1.2kg/m^3.

5.4.2.4 Humidifier

The humidifier is controlled by an on/off device. It is on when the outside air temperature is less than 14^{o}C and the room relative humidity is less than 60%.

5.4.2.5 Fan

A blade pitch controller maintains 1 kPa in the entrance to the duct. The design pressure drop (i.e. at maximum air flow rate) of the VAV system is 0.5kPa.

This controller need not be modelled; the fan characteristic data given in Appendix A5.4 can be used.

5.4.3 Simulation Exercises

5.4.3.1 Exercise 1.1

In this exercise, the VAV system operates with 100% fresh air and constant zone conditions of 21°C, 55% RH. The ceiling void plenum is at a constant temperature of 22°C (for all exercises).

5.4.3.2 Exercise 1.2

In this exercise, the conditions are the same as for Exercise 1.1 except that the economiser is operating. Since the return air fan is not modelled for all exercises, it is assumed that air at room temperature is mixed with fresh air in the economiser.

5.4.3.3 Exercise 1.3

In this exercise, the VAV system operates with 100% fresh air and varying room conditions given in Appendix A5.7.

5.4.3.4 Exercise 1.4

In this exercise, the conditions are the same as for Exercise 1.3 except that the economiser is operating.

Each simulation exercise is to be conducted for the 24 hourly values of dry bulb temperature and relative humidity given for September 7 and November 4.

5.4. Simulation Technique

The following component models, formulated as separate FORTRAN subroutines have been used to simulate the VAV system (as specified in the various exercises). They are:

1) VAV Control Box Model: A direct linear routine models the VAV control box and determines the volumetric flow rate of air corresponding to zone temperature. From this, the mass flow rate of conditioned air is determined since the density of air is known.

2a) Mixing Box Model Type 2: This models the all outdoor air control system.

2b) Mixing Box Model Type 3: This models the economiser or the proportional outdoor air control system.

3) Humidifier Model Type 1: This models the wetted cell humidifier using recirculating water.

4) Fan Model Type 5: This models the axial fan with variable blade pitch angle control. By applying regression analysis to the fan characteristic data given in Appendix A5.4, an expression relating fan absorbed power, FPOW, to the volumetric flow rate of air, V_a has been obtained. This expression is:

$$FPOW = -2.576121 + 5.230758 \times V_a - 2.406034 \times V_a^2 + 0.76756 \times V_a^3 - 0.11094 \times V_a^4 + 6.176272E\text{-}03 \times V_a^5 \quad (5.7)$$

5a) Cooling Coil Model Type 1: This models the cooling coil with variable water flow rate.

5b) Cooling Coil Model Type 2: This models the cooling coil with fixed water flow rate.

6a) Heating Coil Model Type 1: This models the heating coil with variable water flow rate.

6b) Heating Coil Model Type 2: This models the heating coil with fixed water flow rate.

7) Duct Model: This models the thermal interaction between a duct and its surroundings.

After determining the mass flow rate of supply air, SYSPAN calls the relevant subroutines starting from the mixing box and solves the system sequentially; no iterative calculations are set up around the system loop. However, when modelling the heating and cooling coils, iterative calculations are necessary. The state of the air at the inlet and outlet ports of each component of the system, mass flow rates and temperatures of water leaving the coils, coil thermal loads, power input to the water pump motor and fan motor are determined. The last three variables mentioned are passed to the central plant simulation sub-program in order to calculate the energy consumed by the components of the primary system.

5.4.5 Results of the Simulation Exercises

The results obtained for the simulation exercises are presented as graphs of:

Dry bulb temperature of air leaving each component against time
Moisture content of air leaving each component against time
Mass flow rates of water through heating and cooling coils against time
Coil thermal loads against time

The graphs for Exercises 1.1 and 1.4 (for September 7 and November 4) are presented in the following pages (see Figs. 5.4a to 5.19) while those for Exercises 1.2 and 1.3 are presented in Appendix 5 (see Figs. A5.1a to A5.16).

For inter-model comparisons, the results obtained for the simulation exercises by one participant in the I E A Annex 10 Working Group are also

presented (see Figs. 5.4b to 5.18b and Figs. A5.1b to A5.15b) Morant (Ref.10) used the computer program TRNSYS to simulate the VAV system. As TRNSYS is basically designed for the transient simulation of solar energy systems, steady state mathematical models were developed for the VAV system components and included in the standard TRNSYS library.

In these graphs, the labels have the following meaning:

O - value of outside air
M - value after the mixing box
H - value after the humidifier
FS - value after the axial fan (supply air fan)
Cl - value after the cooling coil
Hl - value after the heating coil
D - value after the supply air duct
R - value of the room or zone
mwcc - mass flow rate of water through cooling coil (kg/s)
mwhc - mass flow rate of water through heating coil (kg/s)
qcs - sensible cooling load (kW)
qcl - latent cooling load (kW)
qct - total cooling load (kW)
qht - heating load (kW)

5.4.6 Analysis of the Results of the Simulation Exercises

The following notation explains the labelling adopted for the graphs:
Fig. 5. Xa is a graphical representation of the results obtained for the simulation exercises using SYSPAN.

Fig. 5. Xb is a graphical representation of the results obtained for the simulation exercises by Morant (Ref. 10).

For the graphs presented in Appendix A5, the corresponding notation is Fig. A5. Xa and Fig. A5. Xb respectively.

Generally, it can be seen that very good agreement exists between the two sets of results presented. Although this cannot be interpreted as a full scale validation of the algorithms used by SYSPAN, nevertheless it serves as a fairly good basis for evaluating the computer program.

Before analysing the results of the simulation exercises, it will be useful, here, to discuss how the VAV system is controlled.Simultaneous heating and cooling is eliminated by sequencing the operation of the heating and cooling coils and maintaining a dead band between their control bands (see Fig. 5.3). This is a positive control feature of the system. The operation of the humidifier is independent of the operation of the cooling coil. Thus, there exists the possibility of the two components operating simultaneously. This actually occurs, for some hours, with the result that the cooling coil, when dehumidifying, reduces the moisture content of the airstream below that entering the humidifier. Thus energy is wasted in operating the humidifier water pump and chiller simultaneously, although the power consumption of the former is relatively negligible. This is a negative feature of the control strategy used the VAV system.

For exercise 1.1, Figs. 5.4a and 5.5a show the dry bulb temperature and mositure content profiles for various 'points' around the system for September 7th simulation while Figs. 5.4b and 5.5b show the same profiles as obtained by Morant. Figs. 5.6a and 5.6b show the hourly variation of the mass flow rate of water through the heating and cooling coils and Fig. 5.7 shows the hourly variation of the coil thermal loads. It can be seen that the heating coil is not operating, the cooling coil negates the operation of the humidifier and the cooling coil total load varies from 12.92kW to 66.03kW. For the same exercise but for November 4th simulation (see Figs. 5.8a to 5.11), the heating coil operates between the 1st and 11th hour and between the 20th and 24th. At the 12th and 19th hour, neither the heating coil nor cooling coil operates because the temperature at control point 'A' falls in the dead band region. The maximum heating coil load is 17.26kW and the maximum cooling coil load is 24.53kW. The cooling coil performs sensible cooling only.

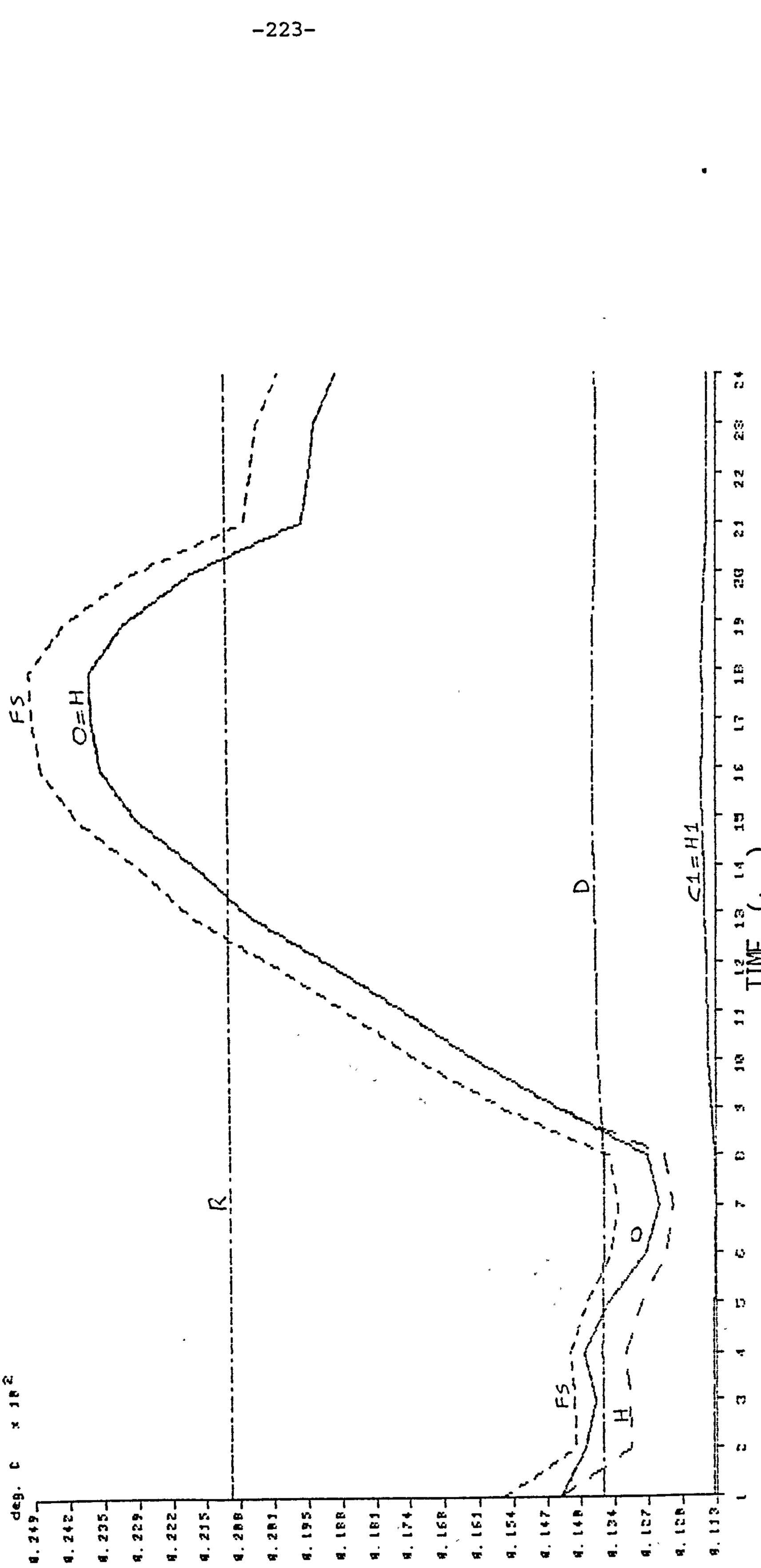
DRY BULB TEMPERATURE PROFILES - EXERCISE 1.1 SEPTEMBER 7
TIME (hour)
TEMPERATURE
deg. C x 10^2
FS
H
R
D
O
C1=H1
FS
H

FIG. 5.4A

Ex 1.1. Sept. 7 - temperatures

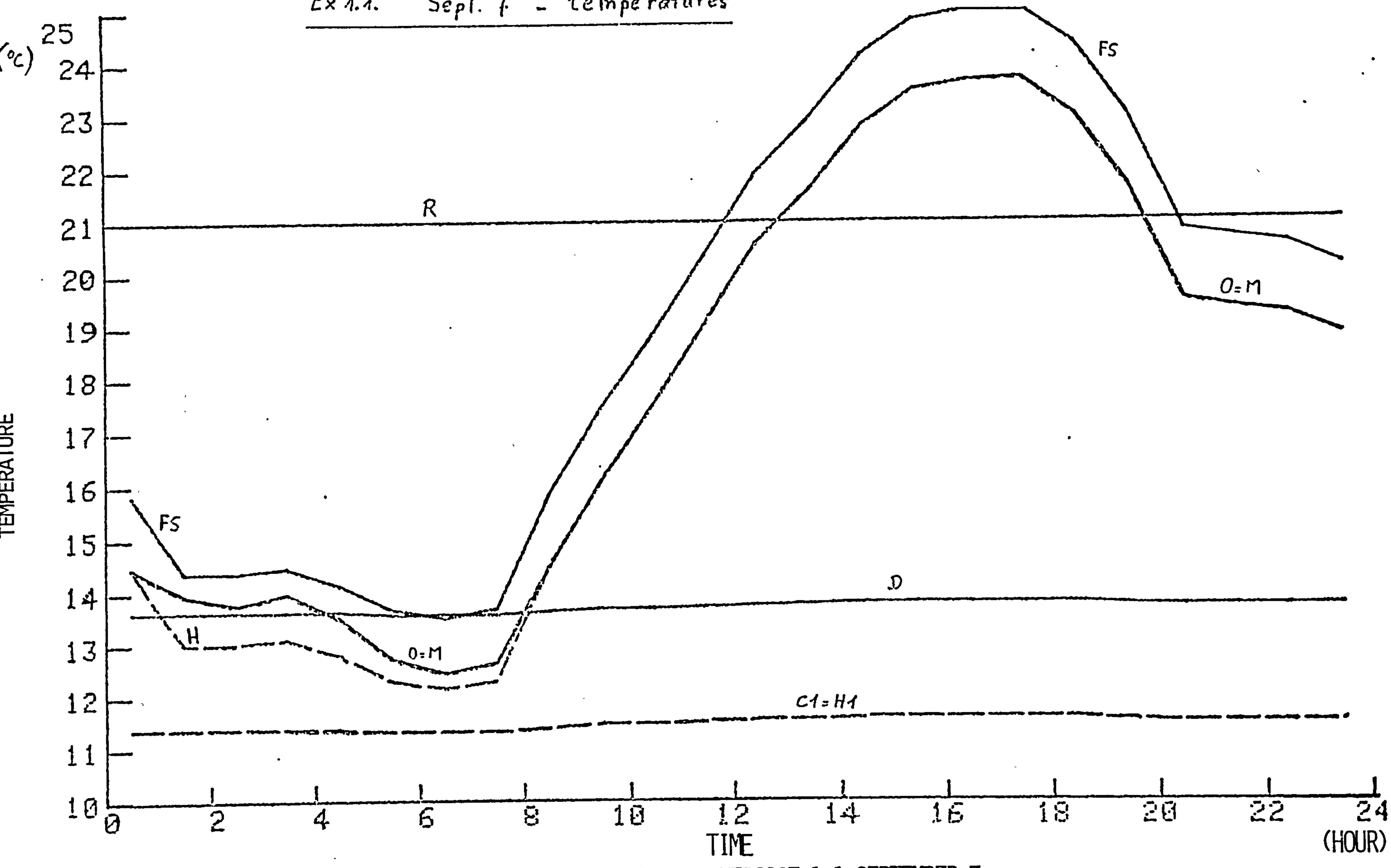

FIG. 5.4B DRY BULB TEMPERATURE PROFILES - EXERCISE 1.1 SEPTEMBER 7

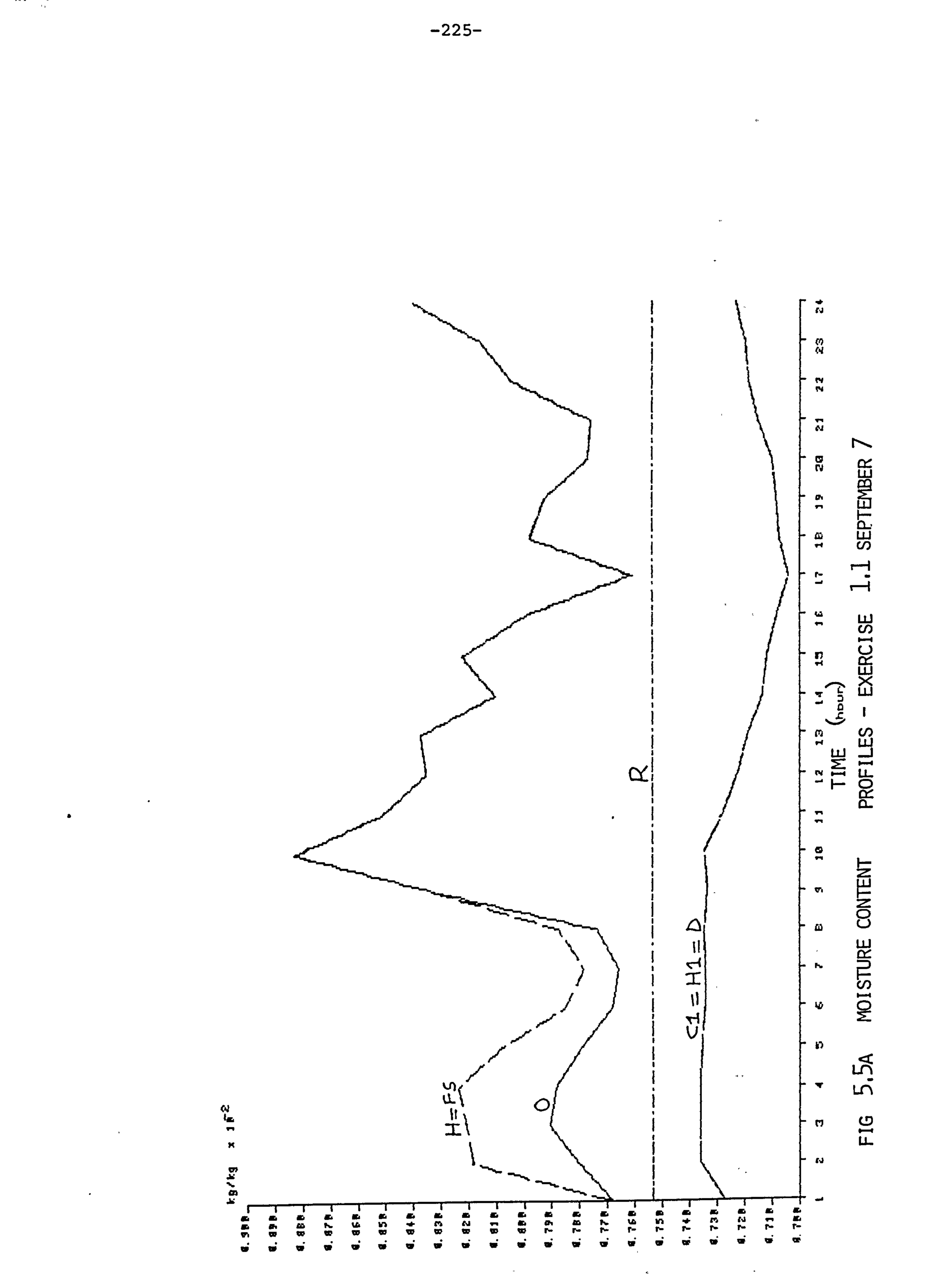

FIG 5.5A MOISTURE CONTENT

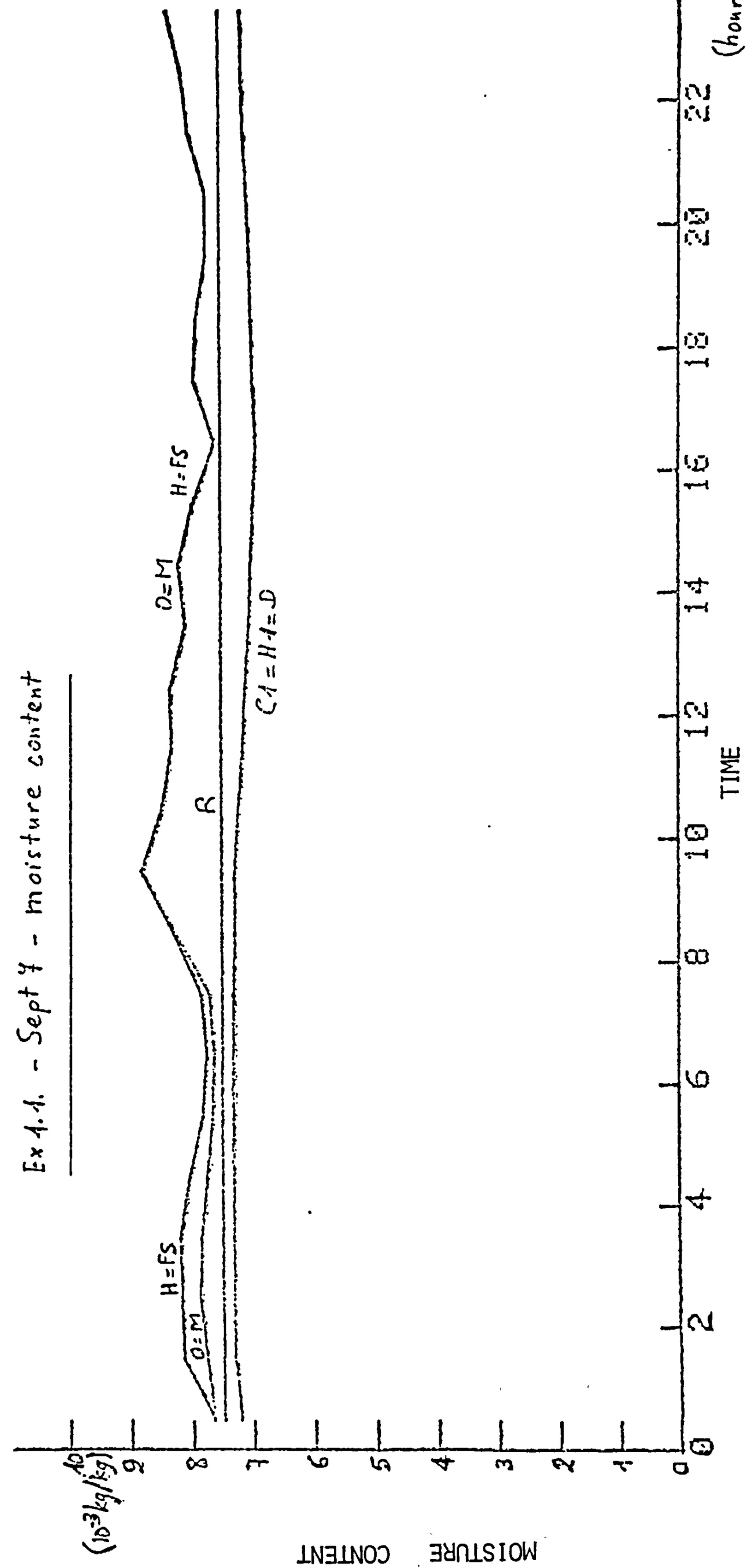

FIG. 5.5B MOISTURE CONTENT PROFILES - EXERCISE 1.1 SEPTEMBER 7

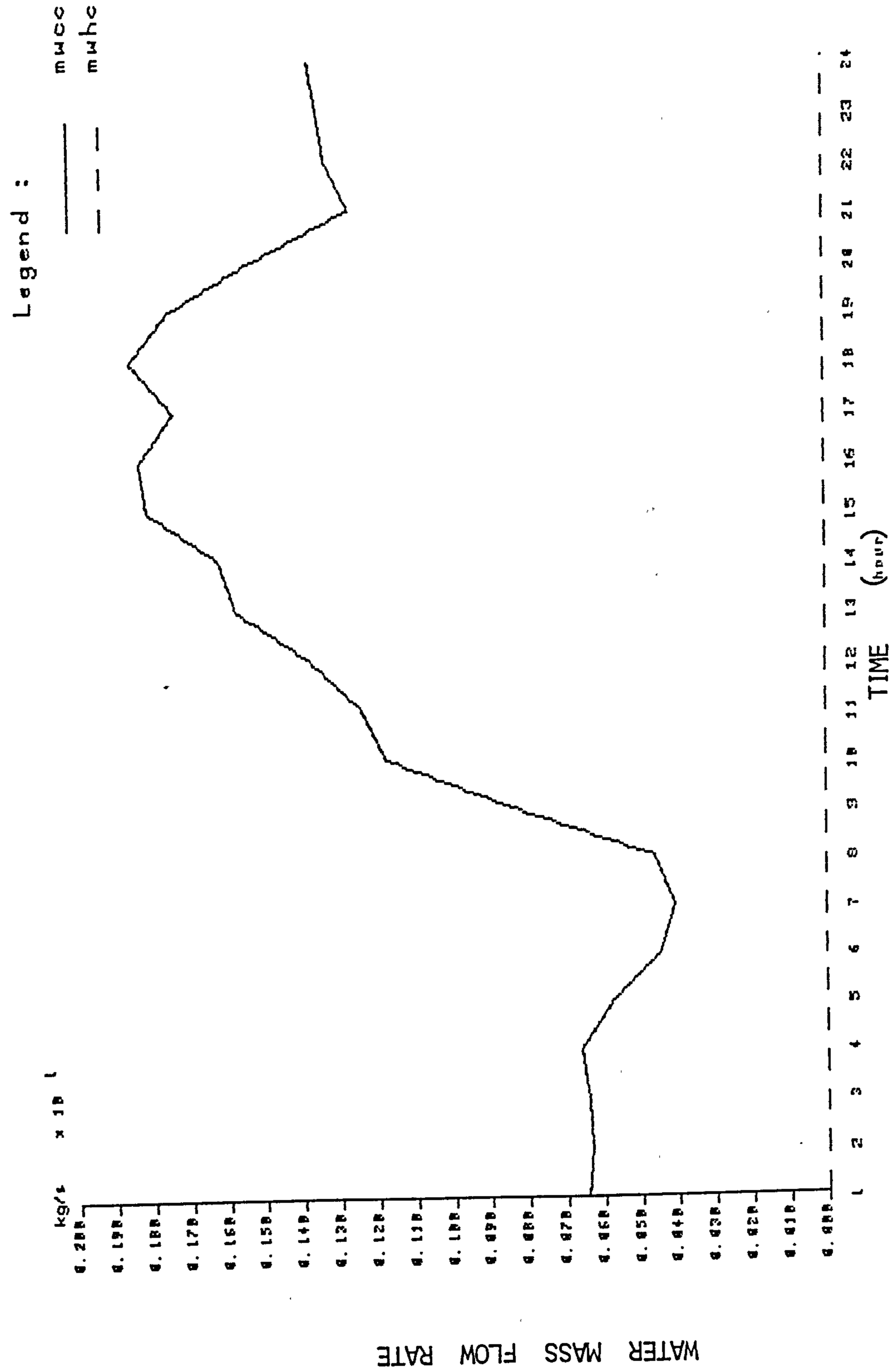

FIG 5.6A MASS FLOW RATES OF WATER THROUGH COILS - EXERCISE 1.1 SEPTEMBER 7

Ex 1.1- Sept 7- water flow rates

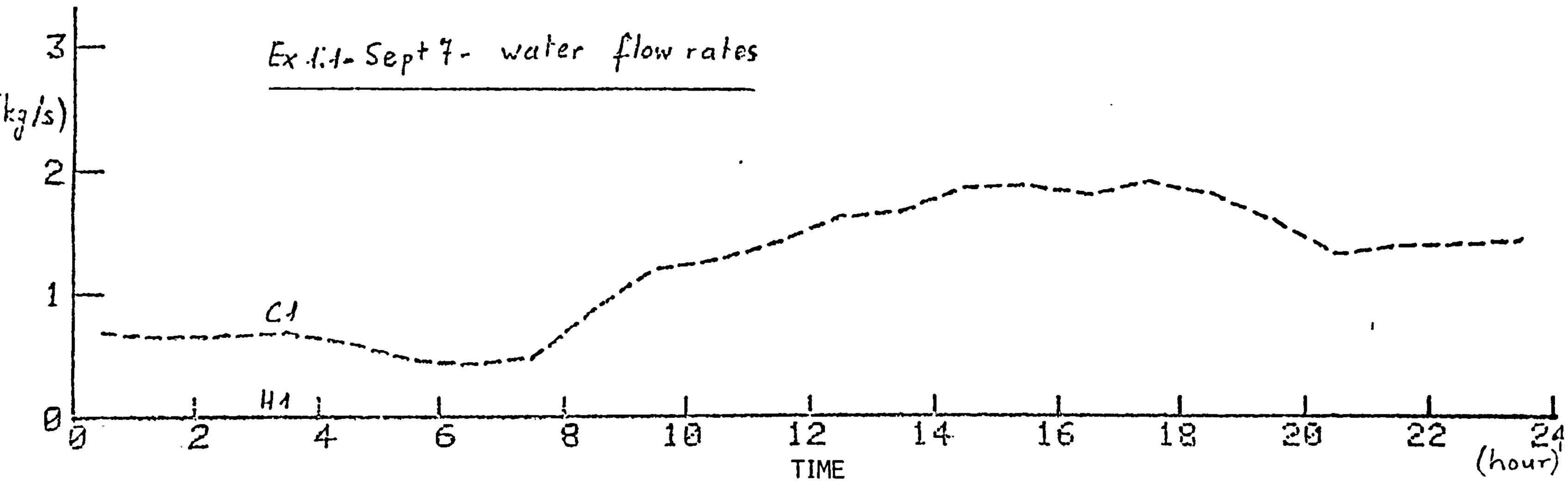

FIG. 5.6B. MASS FLOW RATES OF WATER THROUGH COILS - EXERCISE 1.1 SEPTEMBER 7

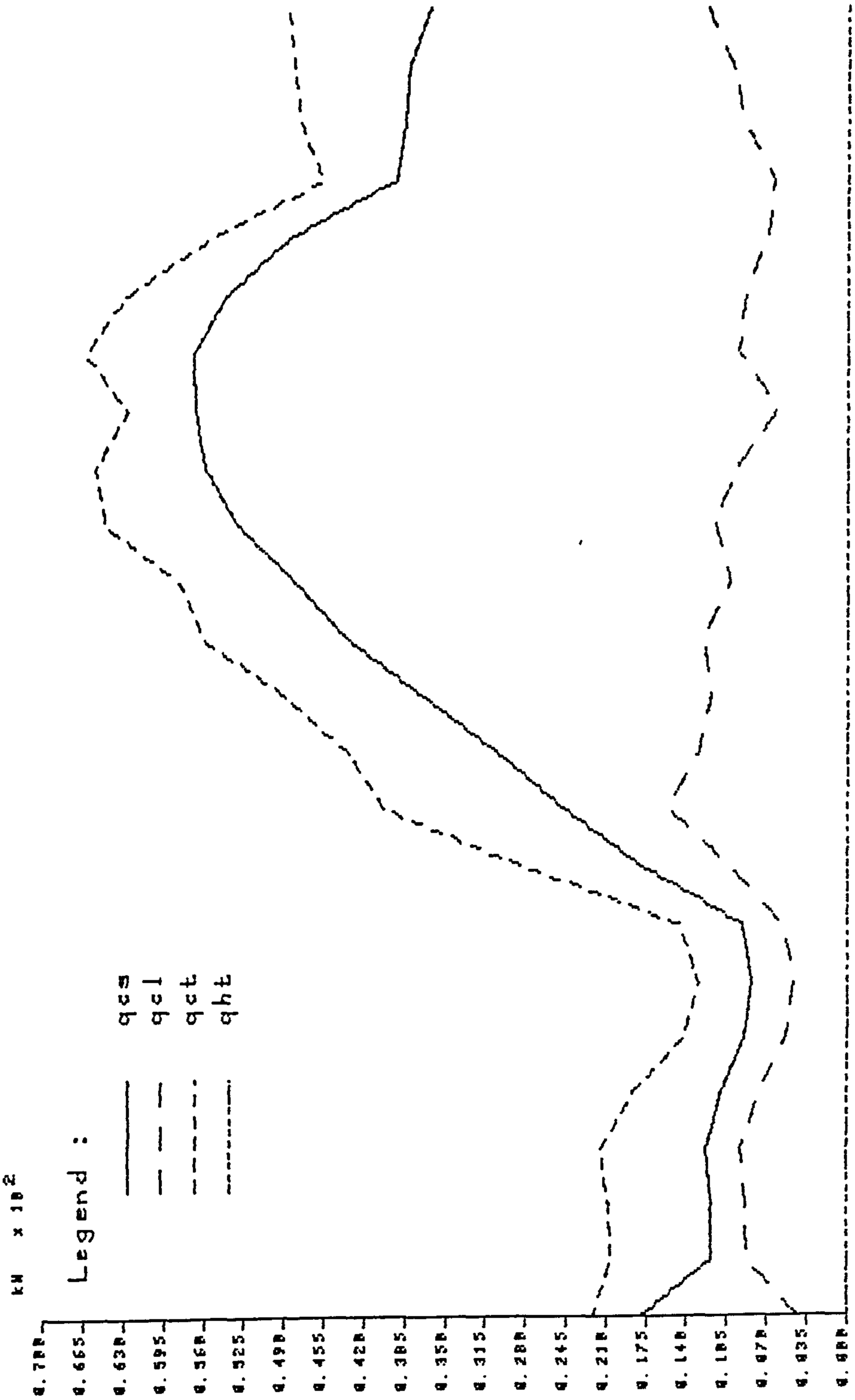

FIG. 5.7. COILS' THERMAL LOAD PROFILES - EXERCISE 1.1 SEPTEMBER 7

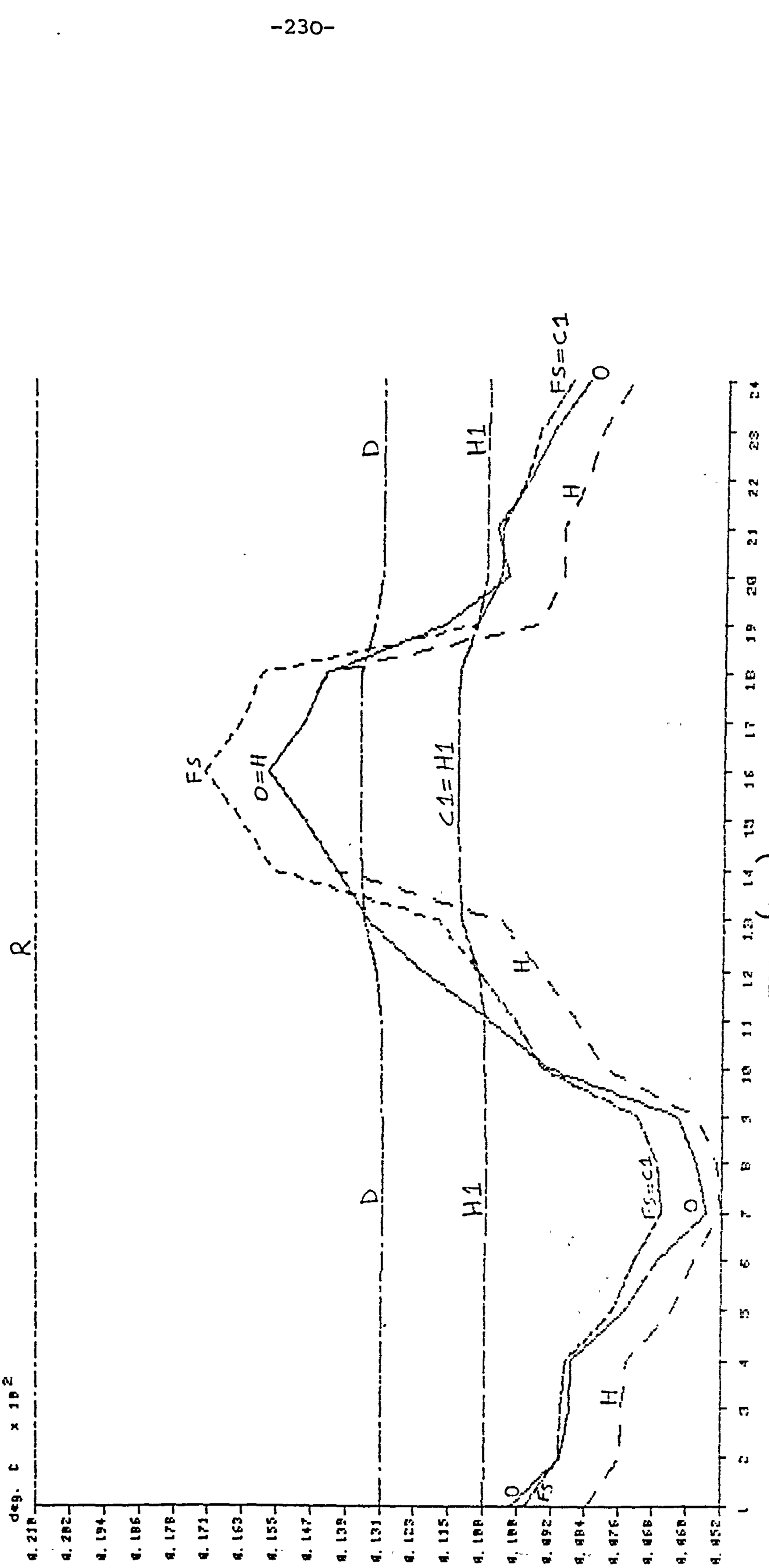
R
D
H1
C1=H1
FS=C1
O=H
FS
O
H
H1
D
H1
FS
O
H
TEMPERATURE
deg. C x 10^2
TIME (hours)
DRY BULB TEMPERATURE PROFILES - EXERCISE 1.1 NOVEMBER 4

FIG. 5.8A

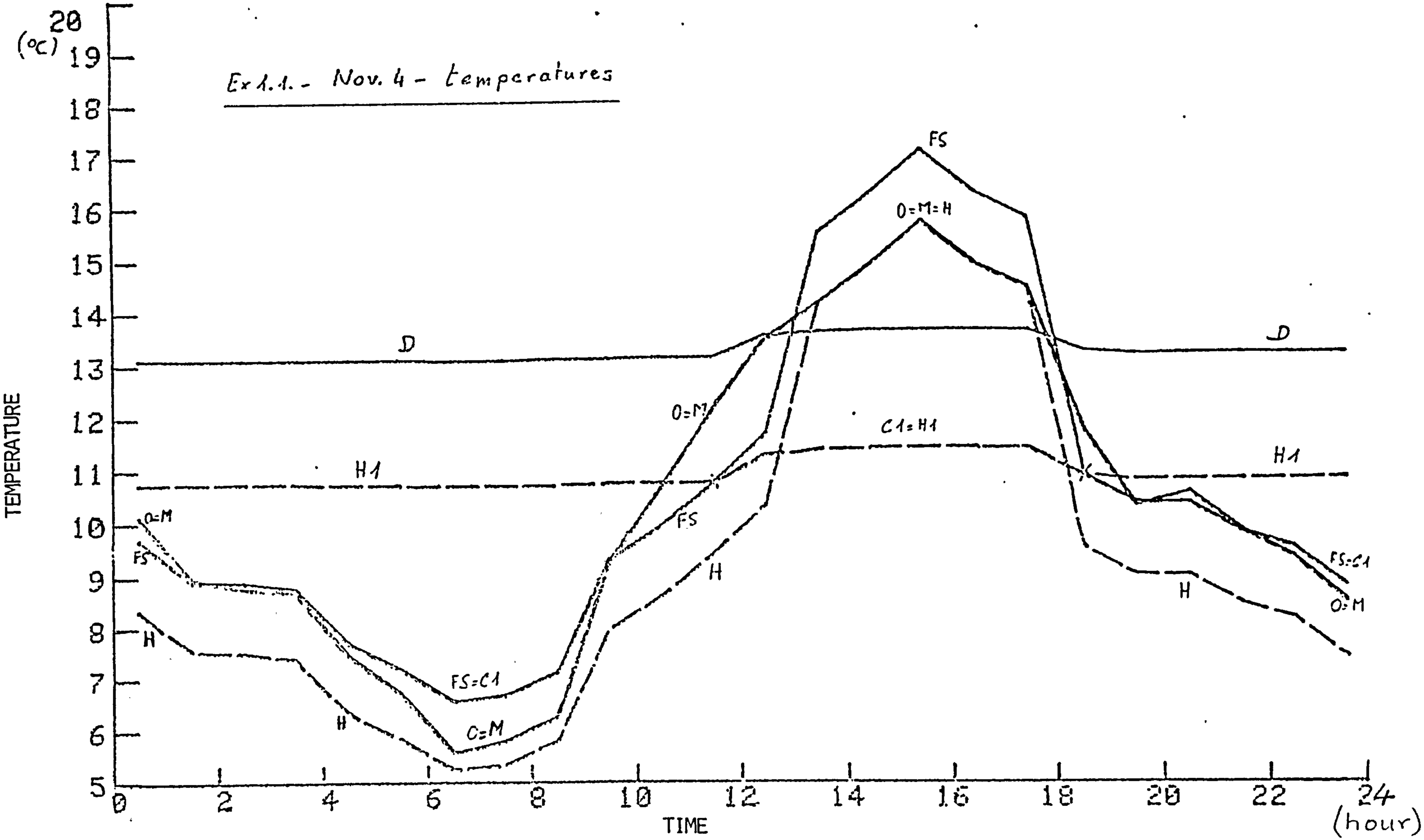

FIG. 5.8B DRY BULB TEMPERATURE PROFILES - EXERCISE 1.1 NOVEMBER 4

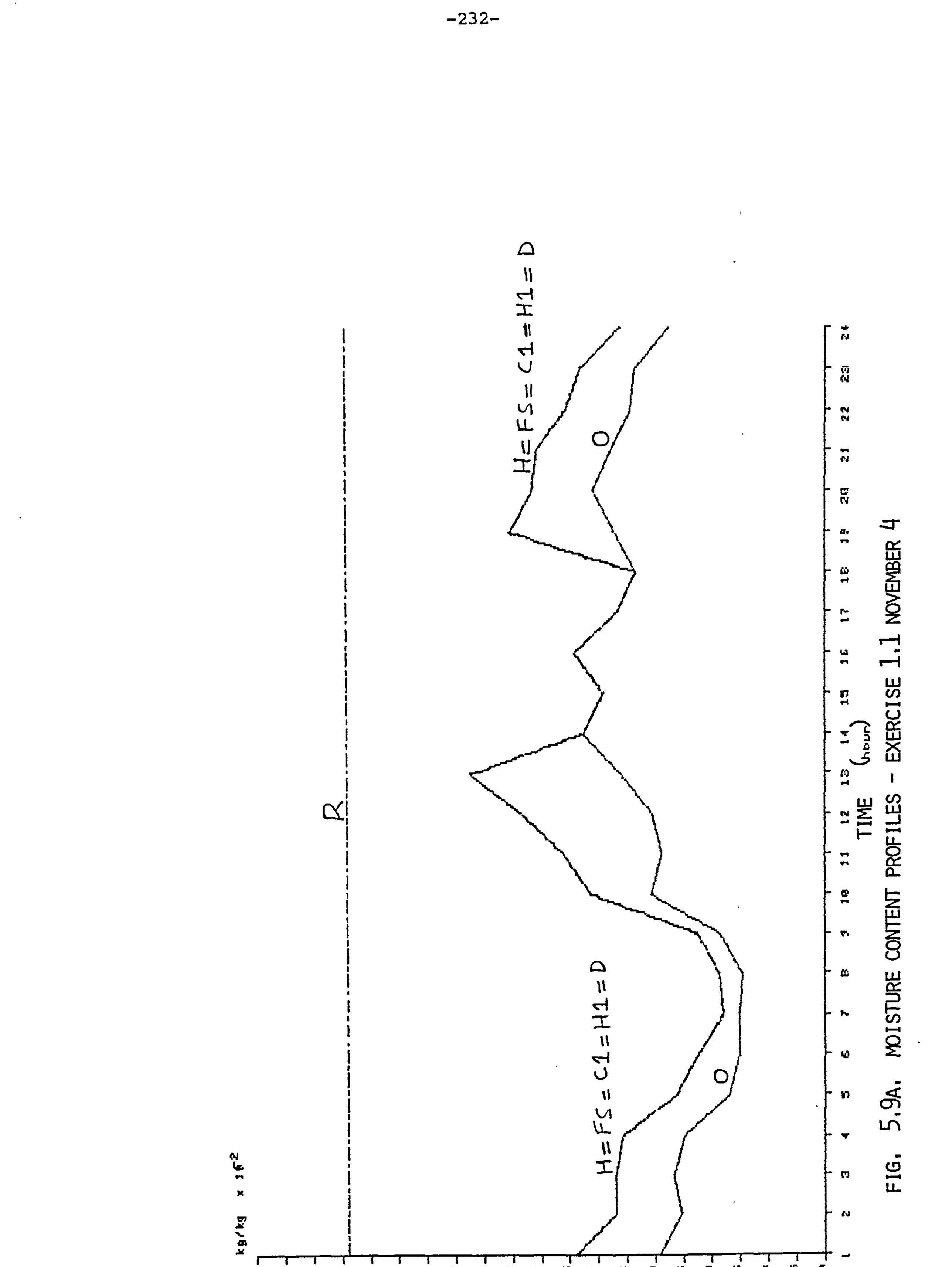

FIG. 5.9A. MOISTURE CONTENT PROFILES – EXERCISE 1.1 NOVEMBER 4

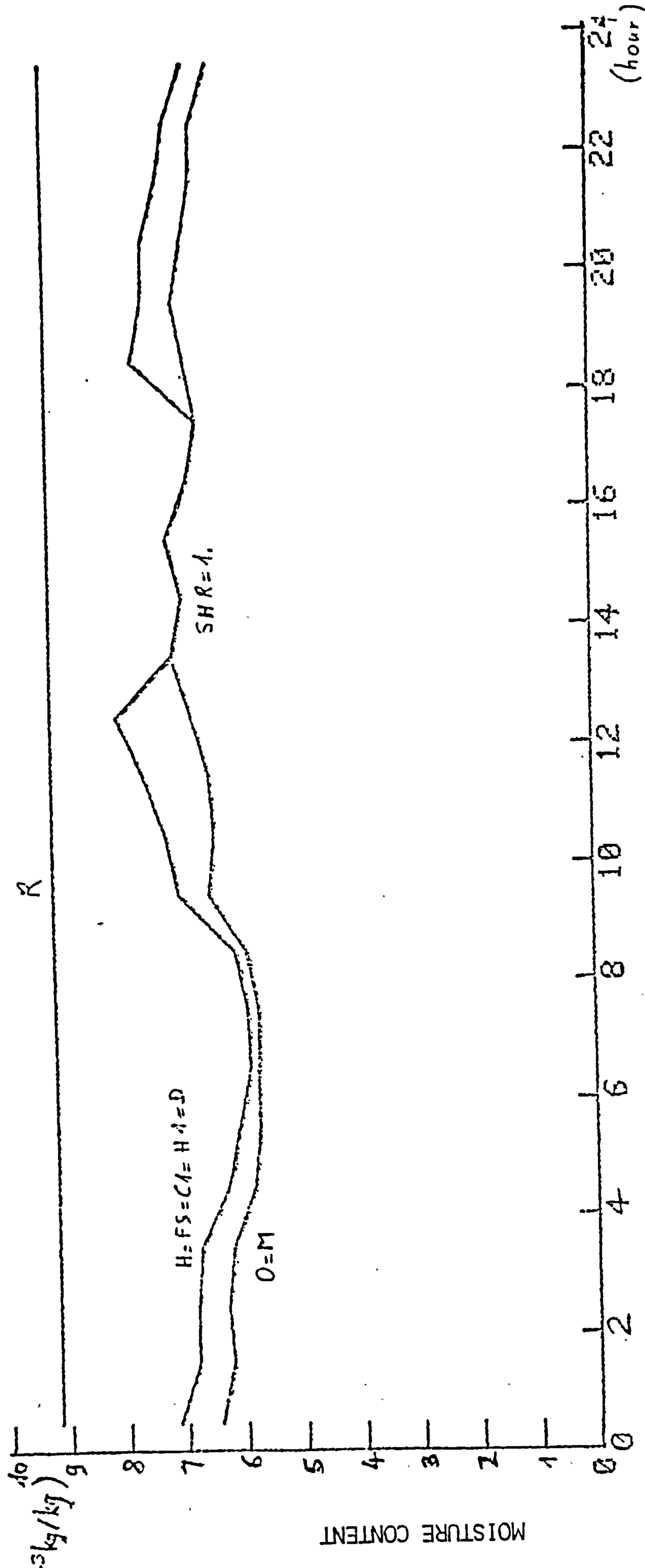

FIG. 5.9B. MOISTURE CONTENT PROFILES - EXERCISE 1.1 NOVEMBER 4

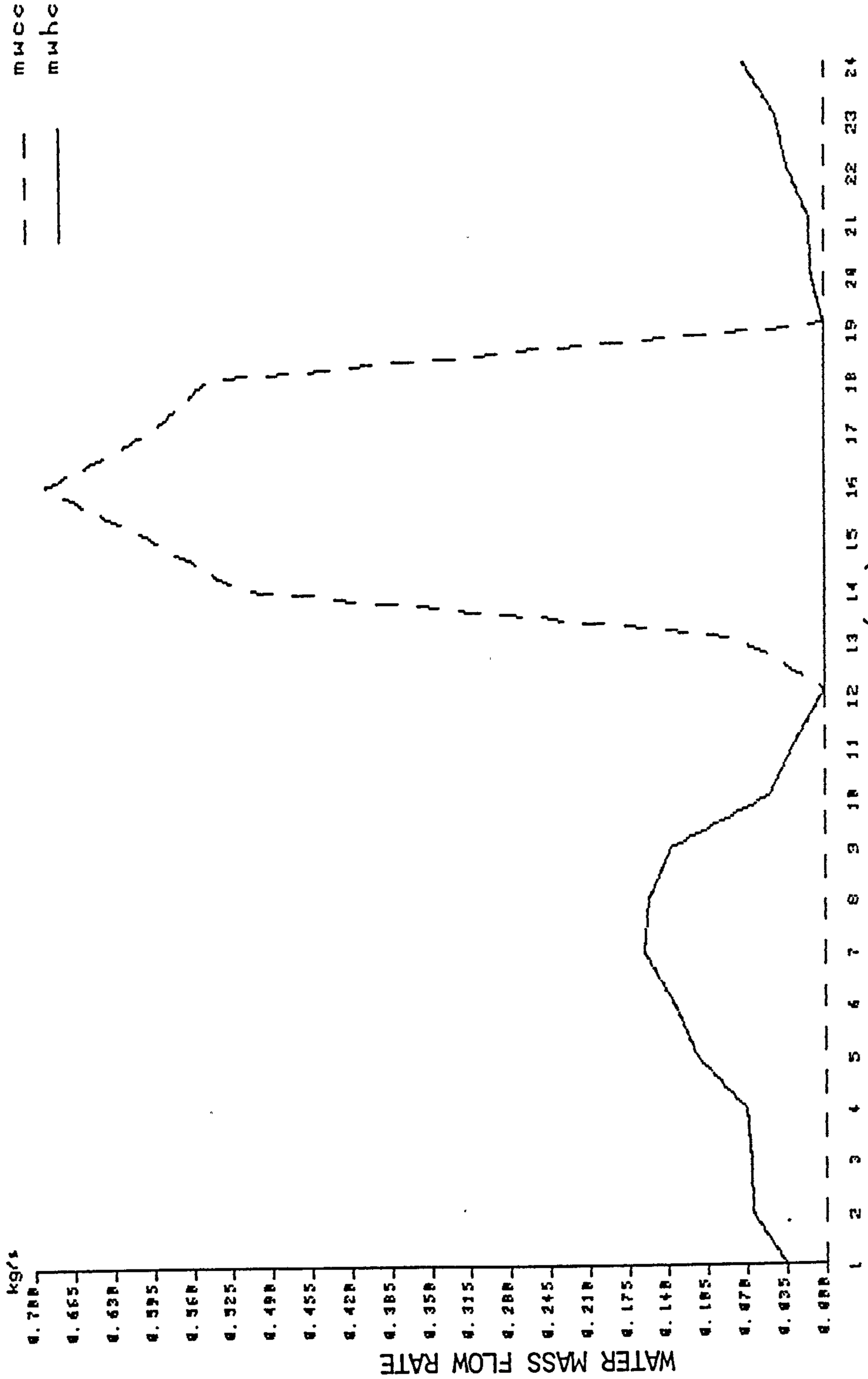

FIG. 5.10A MASS FLOW RATES OF WATER THROUGH COILS-EXERCISE 1.1 NOVEMBER 4

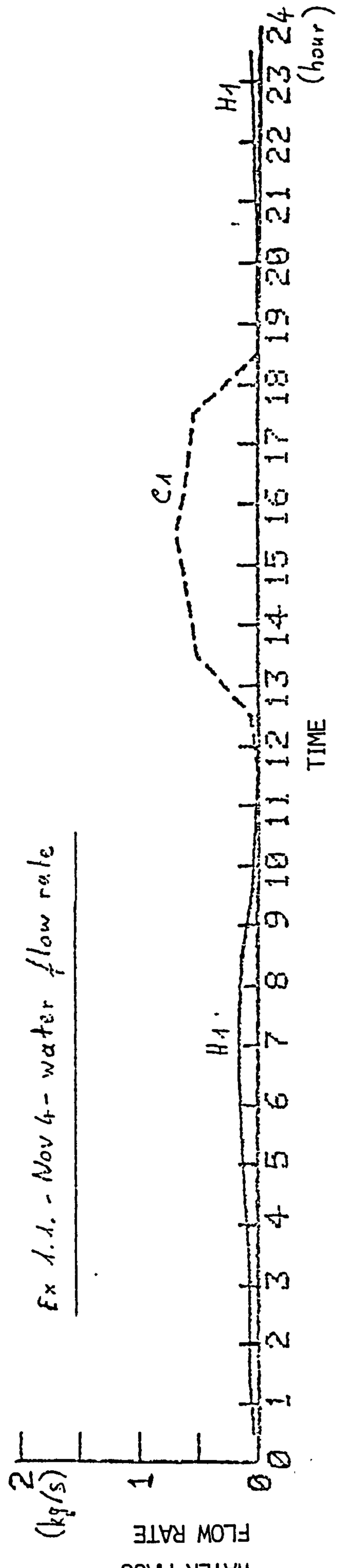
Ex 1.1. - Nov 4 - water flow rate
WATER MASS FLOW RATE (kg/s)
2
1
0
0 1 2 3 4 5 6 7 8 9 10 11 12 13 14 15 16 17 18 19 20 21 22 23 24 (hour)
TIME
MASS FLOW RATES OF WATER THROUGH COILS-EXERCISE 1.1 NOVEMBER 4
H1
C1
H1

FIG. 5.10B

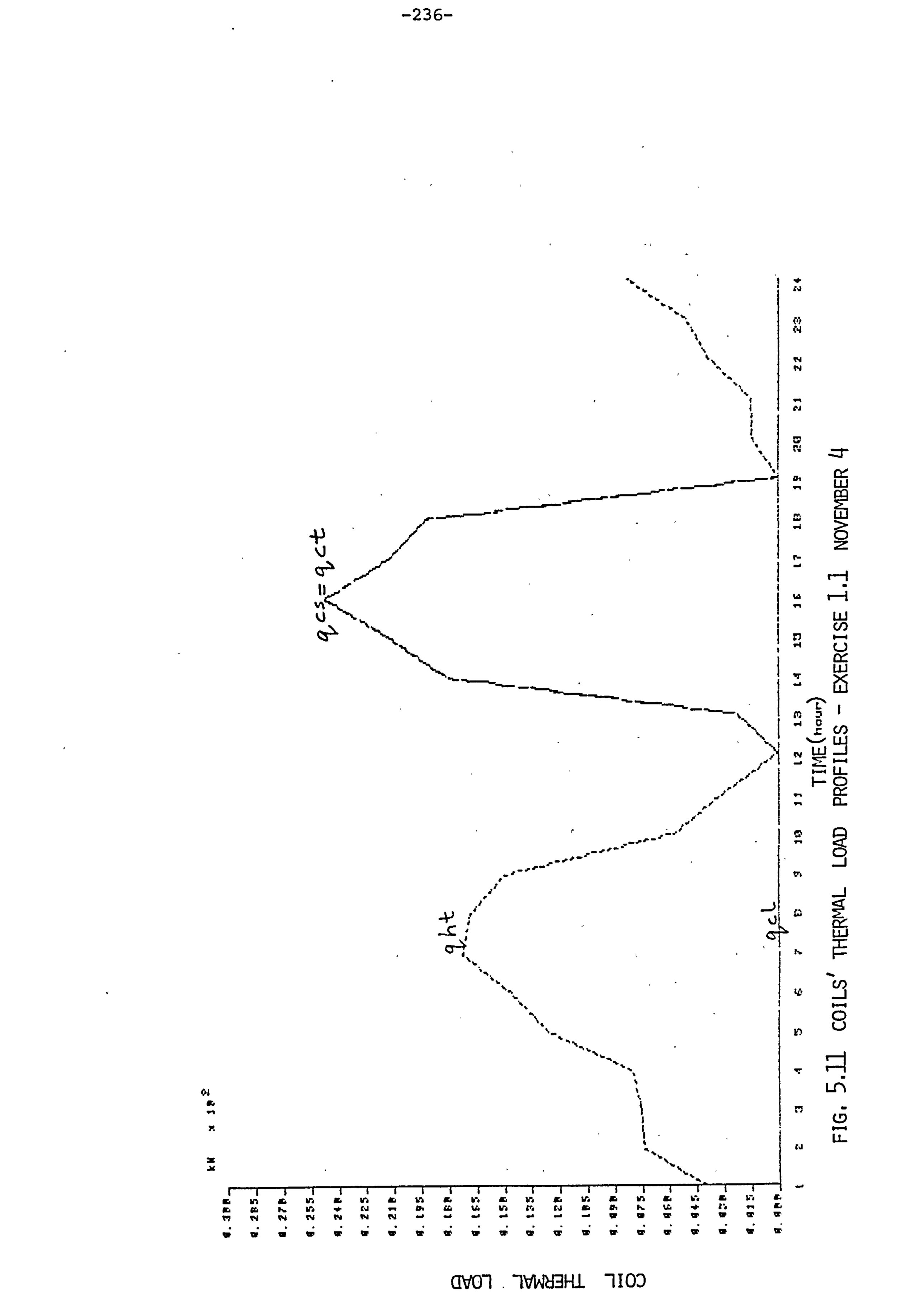

FIG. 5.11 COILS' THERMAL LOAD PROFILES - EXERCISE 1.1 NOVEMBER 4

Comparing September 7th simulation results for exercises 1.1 and 1.2, it can be seen that the maximum cooling load for the former (66.03kW) exceeds that of the latter (51.31kW). This reduction in the maximum cooling coil load is attributed to the economiser minimising the proportion of fresh air in the supply air to the zone for outside air temperatures greater than or equal to 16°C. Comparing November 4 simulation results for exercises 1.1 and 1.2, it can be seen from Figs. 5.11 and A5.8 that the hourly heating coil load for the former generally exceeds that of the latter. This is due to the economiser limiting the proportion of fresh air in the supply air to the zone when the outside air temperature is less than 10°C.

For exercises 1.3 and 1.4, we have variable zone conditions and the mass flow rate of supply air varies with the zone temperature according to the VAV Box control scheme. From the results of the simulation exercises 1.1 and 1.3 for September 7, it can be seen that anytime the supply air mass flow rate for the latter exceeds that for the former, the cooling coil load follows likewise. The reverse is also true, that is, the cooling coil load for exercise 1.3 is smaller than that for exercise 1.1 if the supply air mass flow rate for the former is smaller than that for the latter. These statements are also applicable to the results of the simulation exercises 1.1 and 1.3 for November 4 for both heating and cooling coils.

The results of the simulation exercise 1.4 for September 7, show that the cooling coil load varies from 7.44 kW to 145.6kW and for the same day, the results for exercise 1.3 indicate that the cooling load varies from 7.44kW to 114.7kW. For exercise 1.4 and using the weather data for November 4, the heating coil operates between the 1st and 6th hour and between the 20th and 24th hour, while the cooling coil operates between the 7th and 18th hour. At the 19th hour, neither the heating coil nor cooling coil operates due to the temperature at the control point falling in the dead band region.

It can be seen from Fig 5.14a that the mass flow rate of water through the cooling coil reaches its maximum value of 4.1kg/s between the 10th and 15th hours.

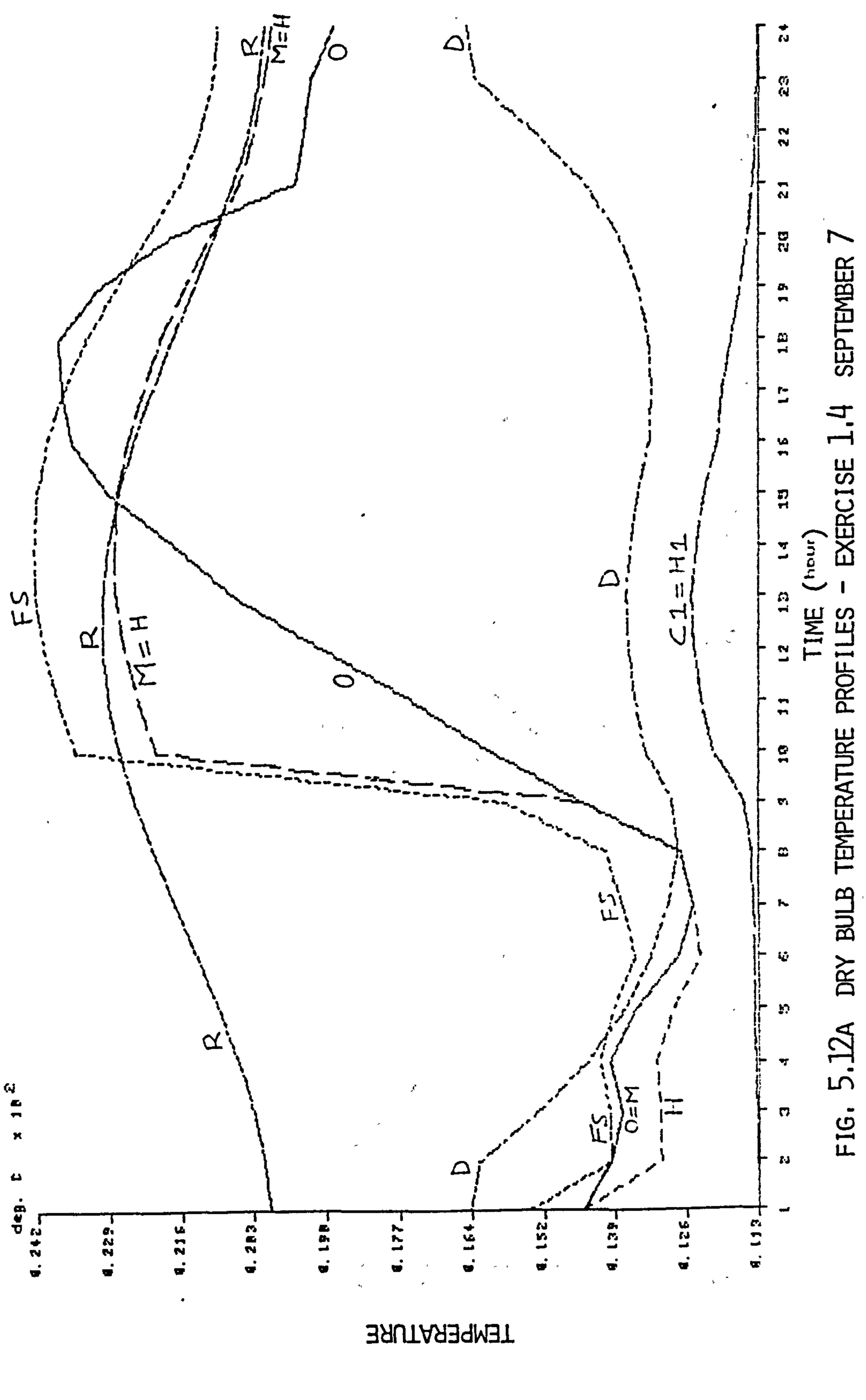

FIG. 5.12A DRY BULB TEMPERATURE PROFILES – EXERCISE 1.4 SEPTEMBER 7

Ex. 1.4. -Sept. 1- Temperatures

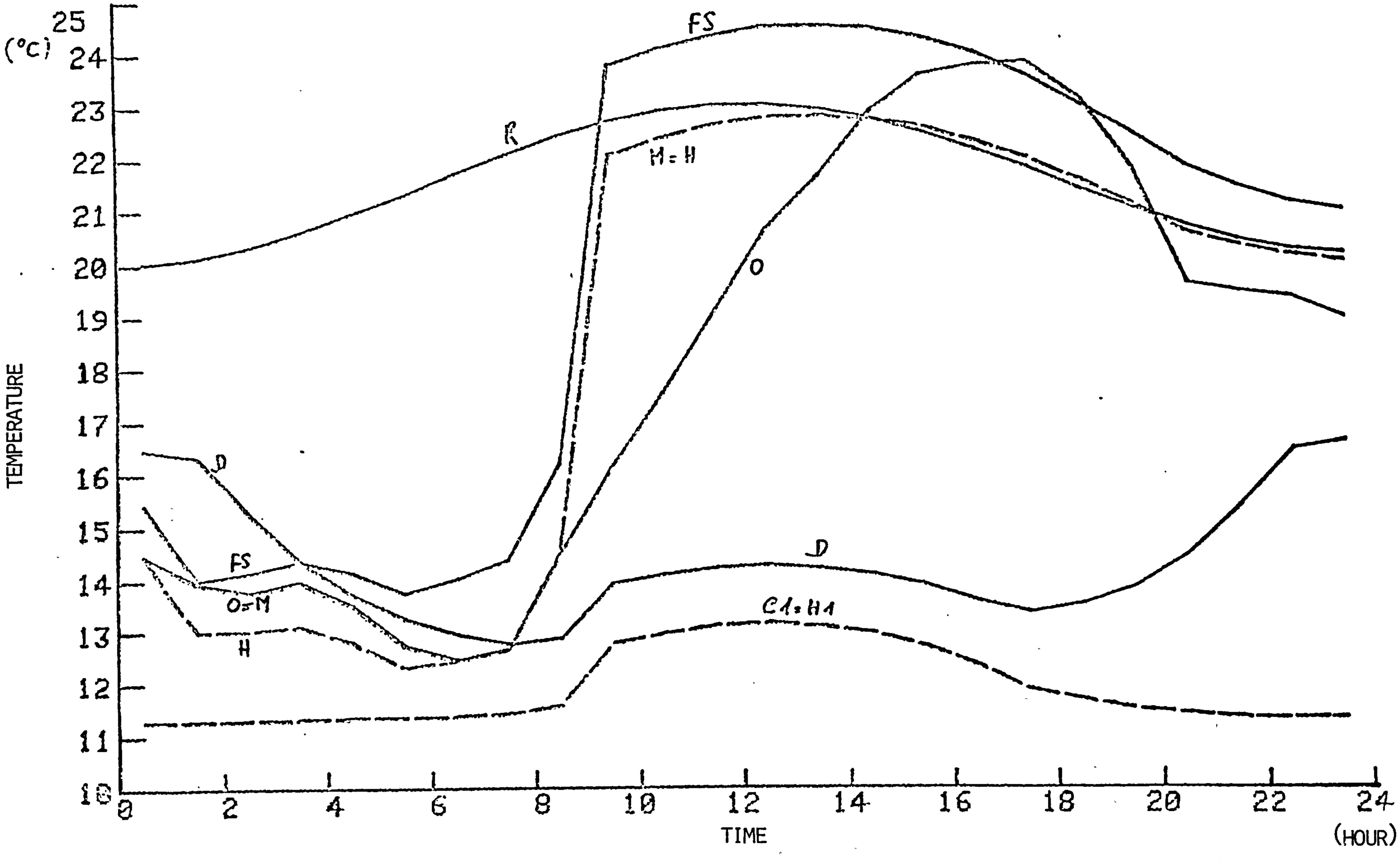

FIG. 5.12B DRY BULB TEMPERATURE PROFILES - EXERCISE 1.4 SEPTEMBER 7

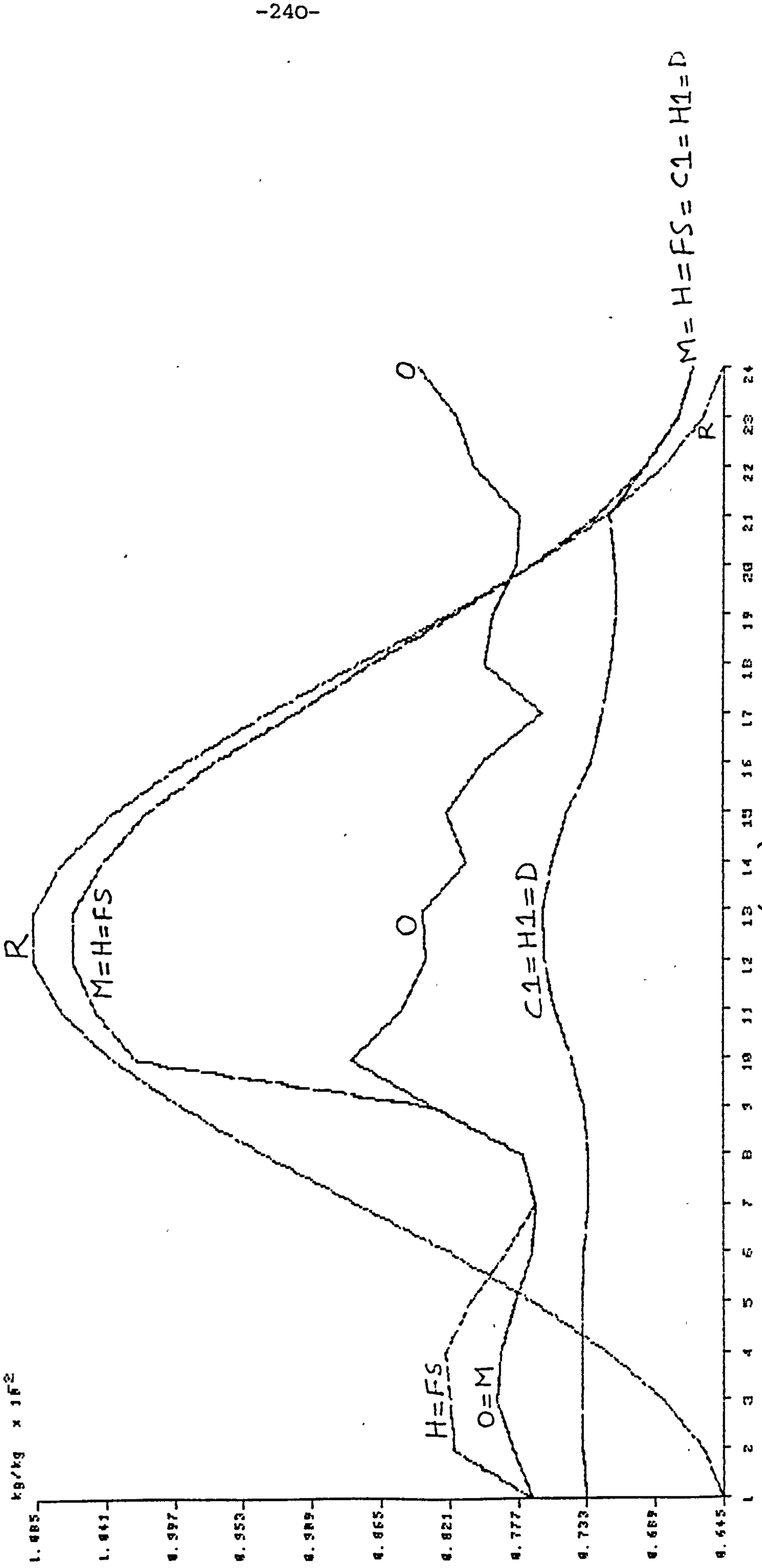

FIG. 5.13A MOISTURE CONTENT PROFILES - EXERCISE 1,4 SEPTEMBER 7

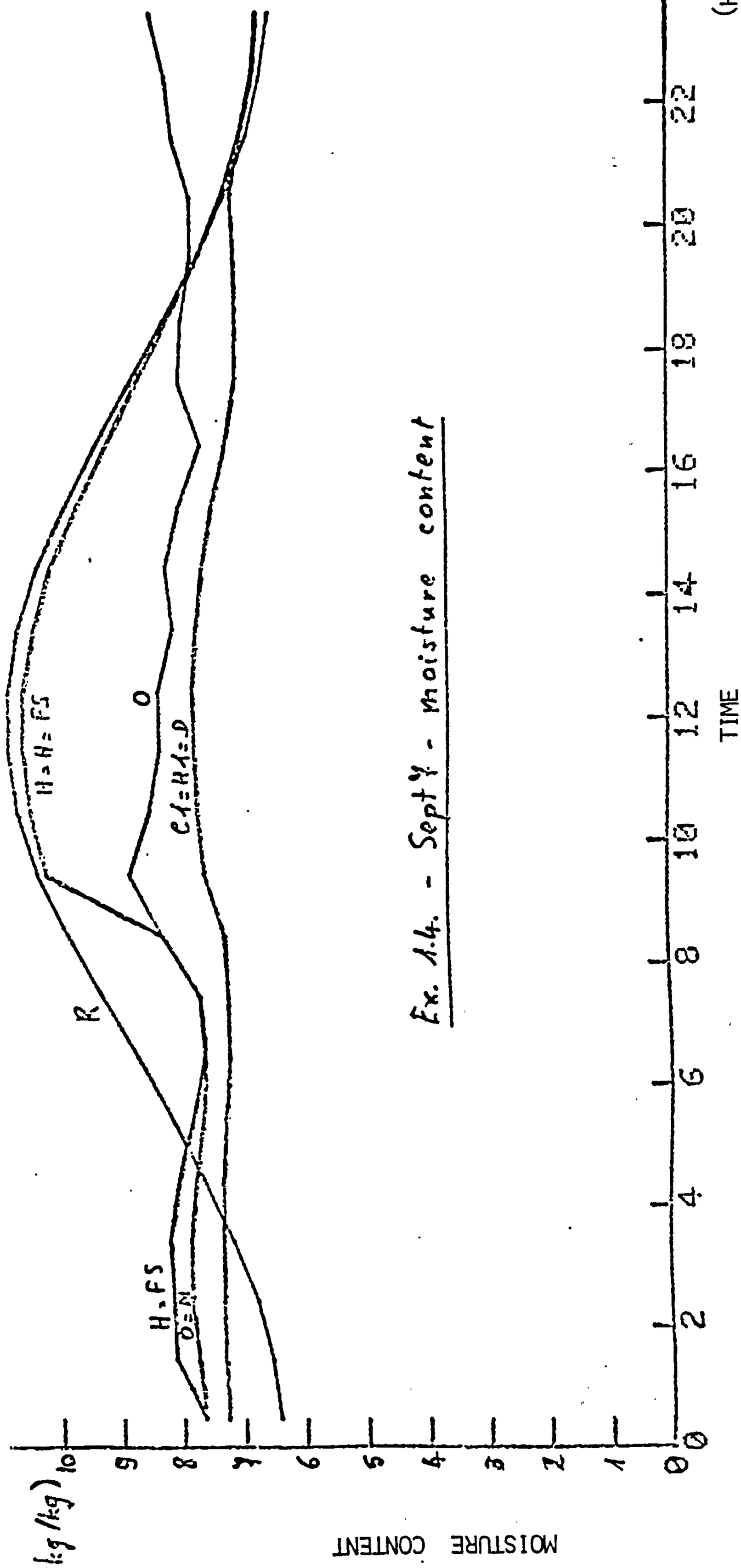

FIG. 5.13B MOISTURE CONTENT PROFILES - EXERCISE 1.4

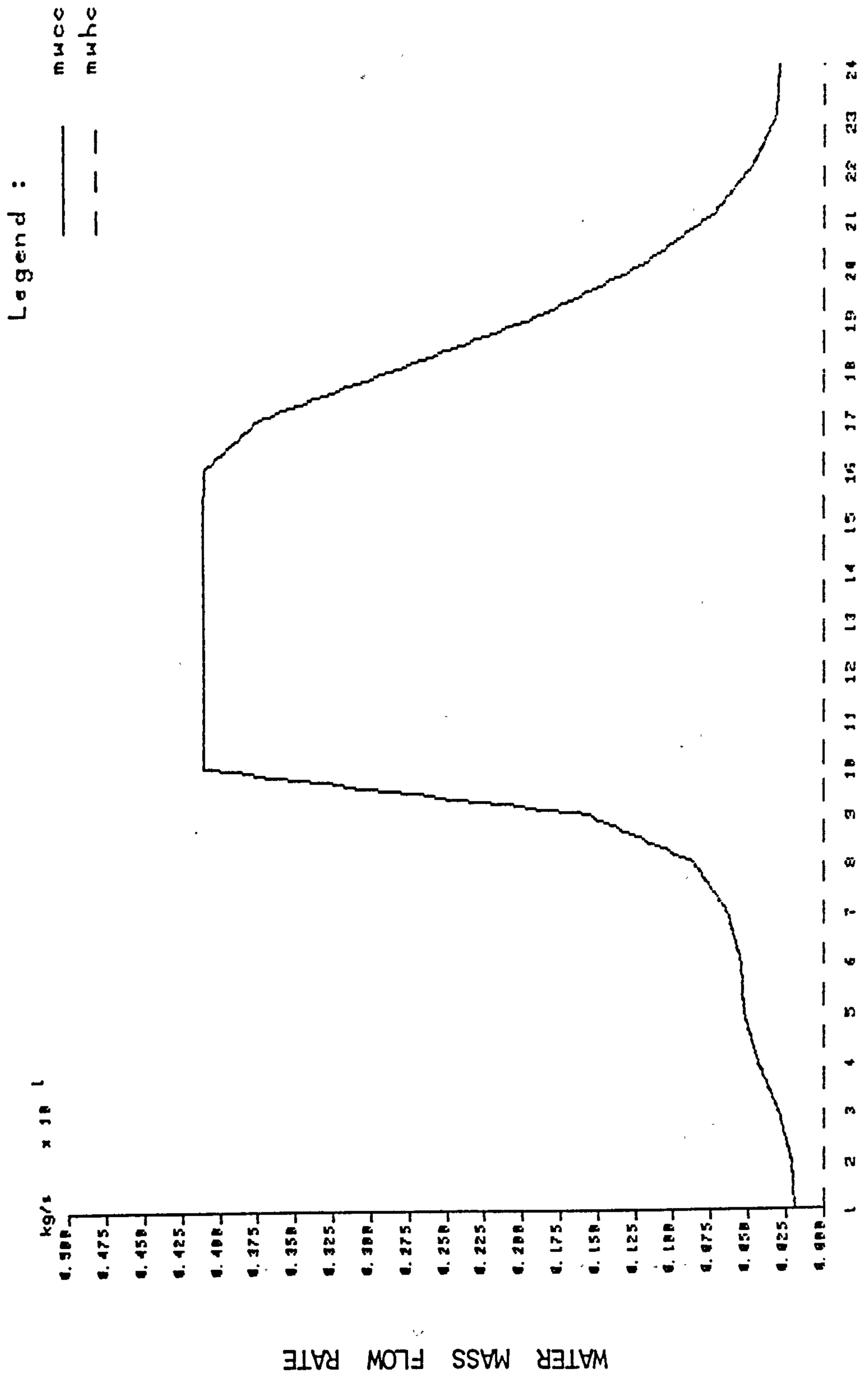

FIG. 5.14A MASS FLOW RATES OF WATER THROUGH COIL

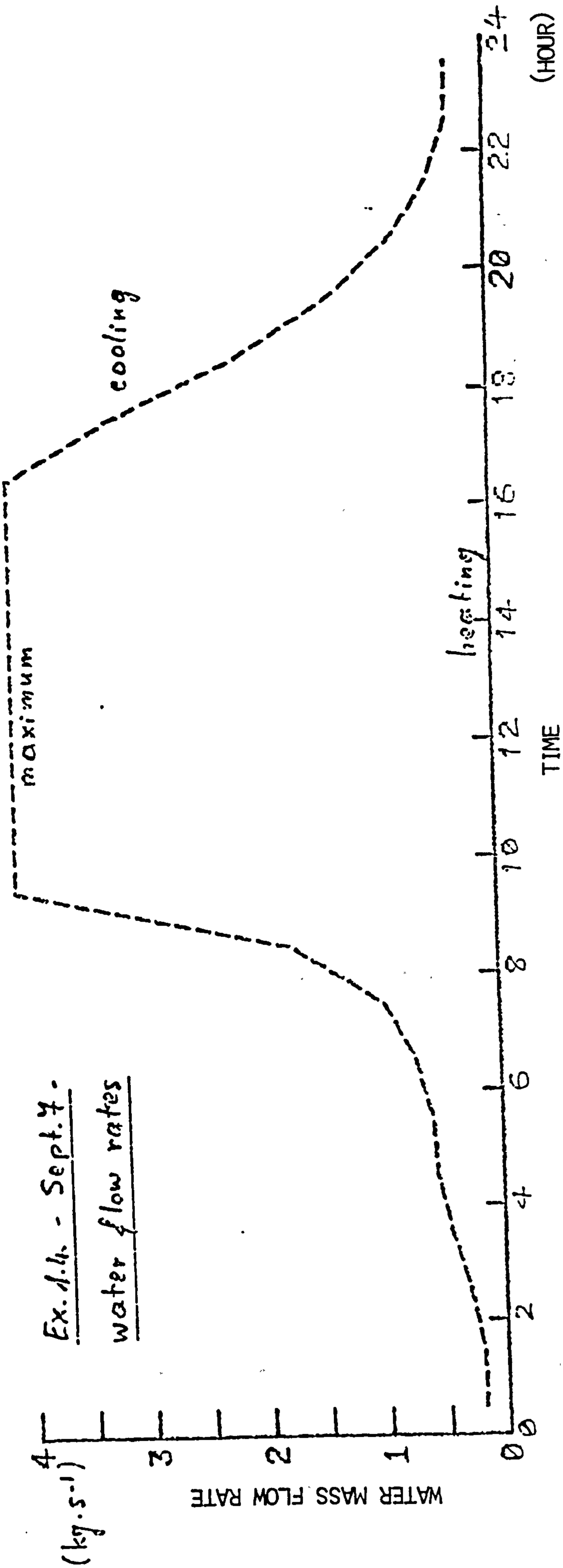

FIG. 5.14B MASS FLOW RATES OF WATER THROUGH COILS-EXERCISE 1.4 SEPTEMBER 7

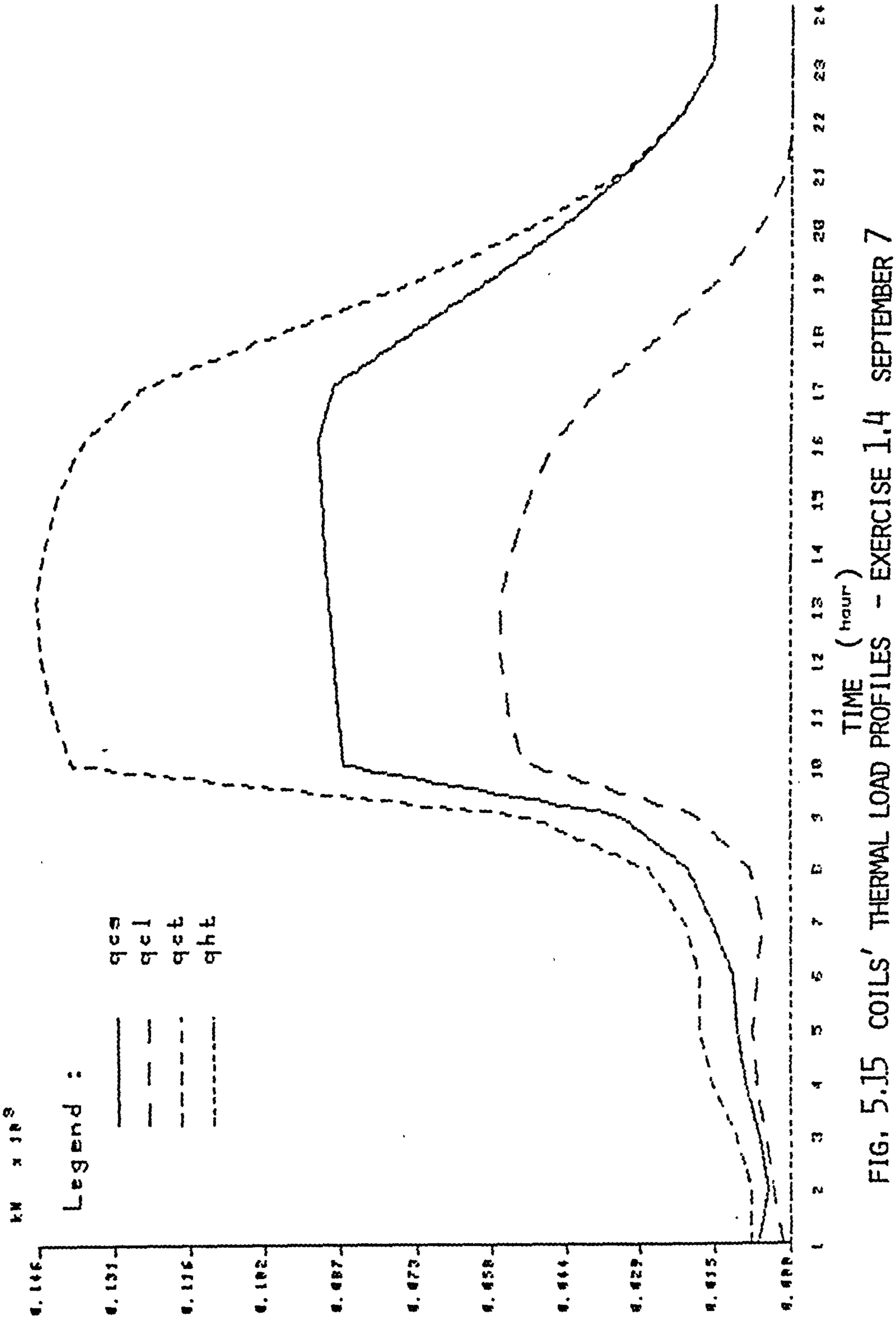

FIG. 5.15 COILS' THERMAL LOAD PROFILES - EXERCISE 1.4 SEPTEMBER 7

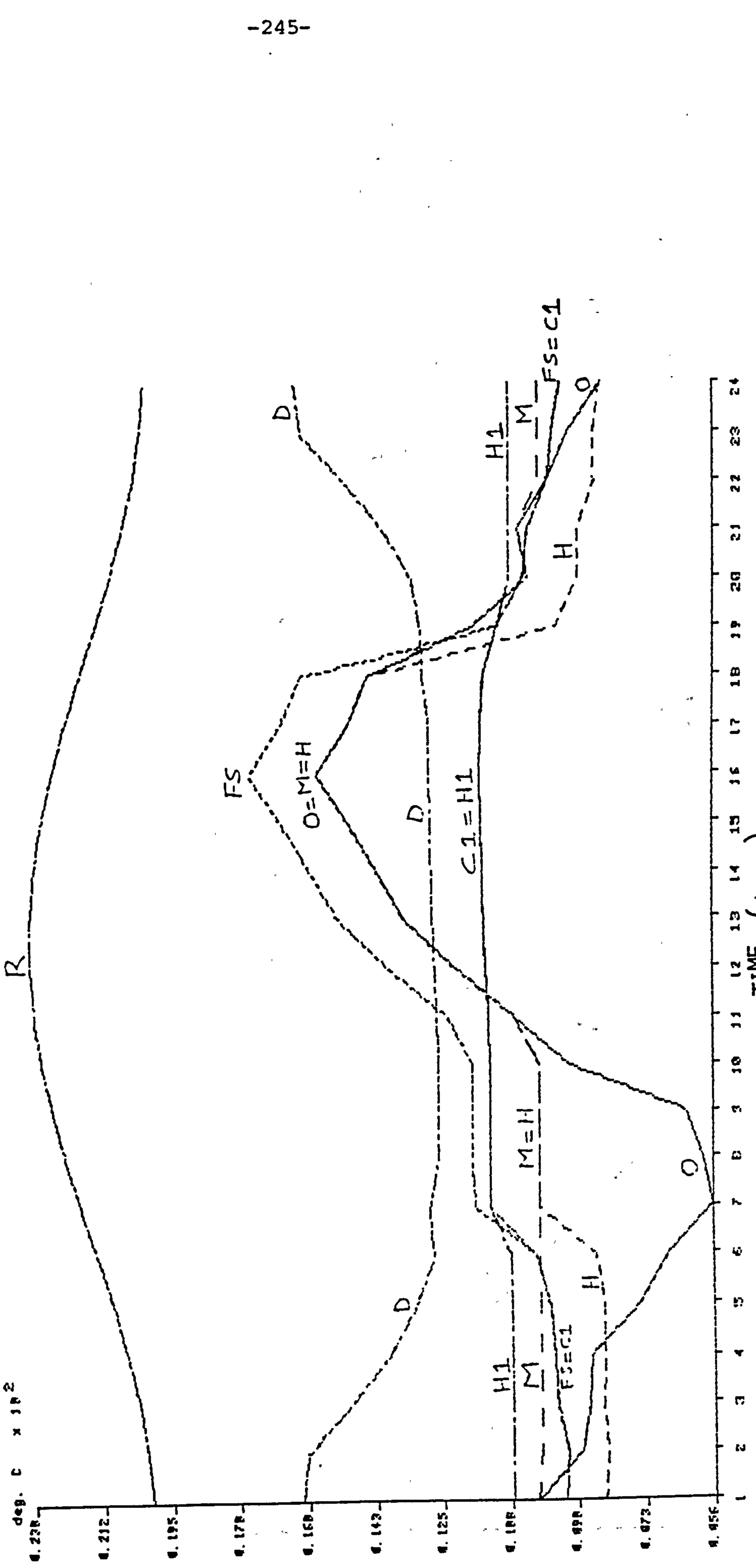

FIG. 5.16A DRY BULB TEMPERATURE PROFILES - EXERCISE 1,4 NOVEMBER 4

Ex. 1.4. - Nov. 4 - Temperatures

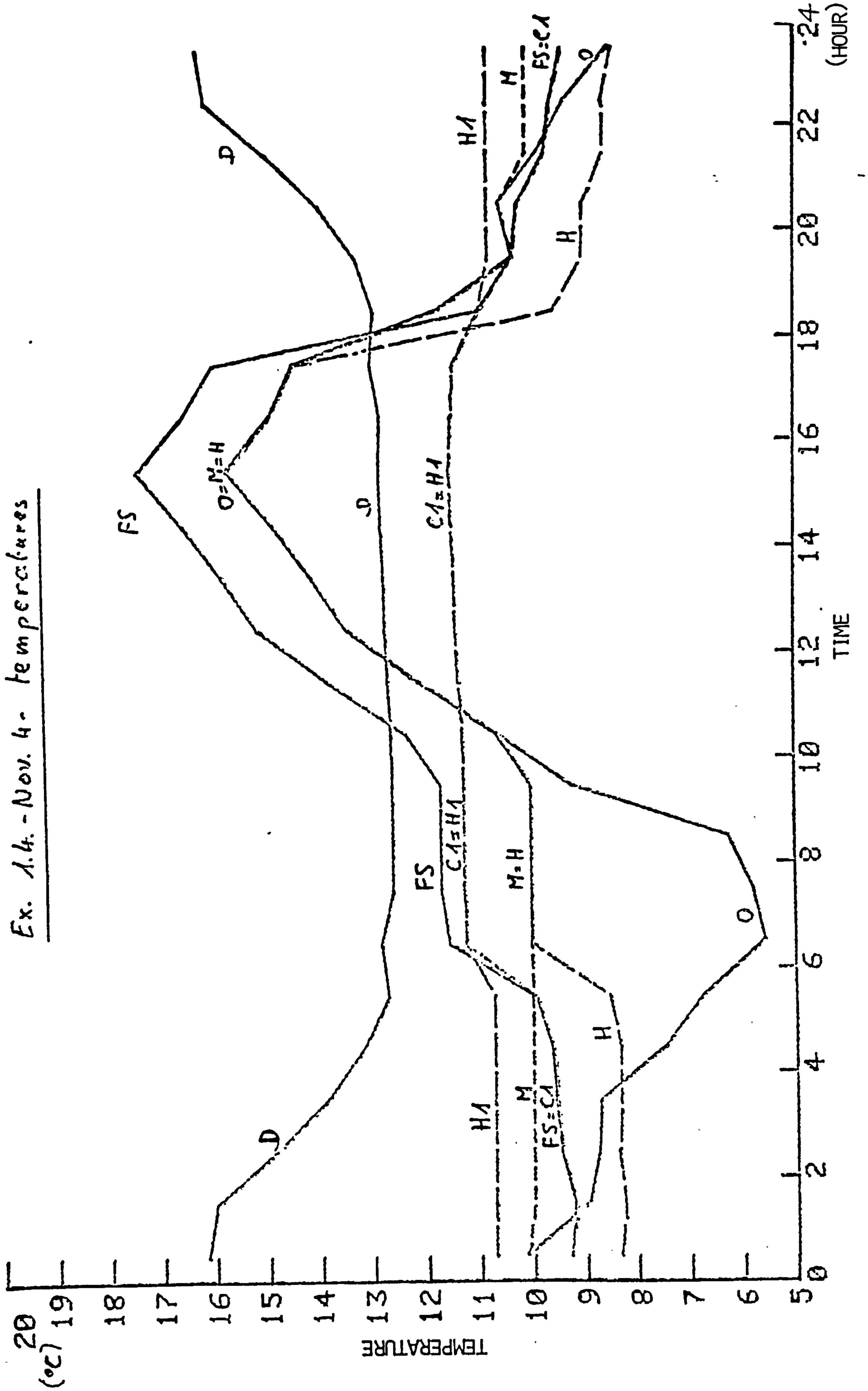

FIG. 5.16B DRY BULB TEMPERATURE PROFILES - EXERCISE 1.4 NOVEMBER 4

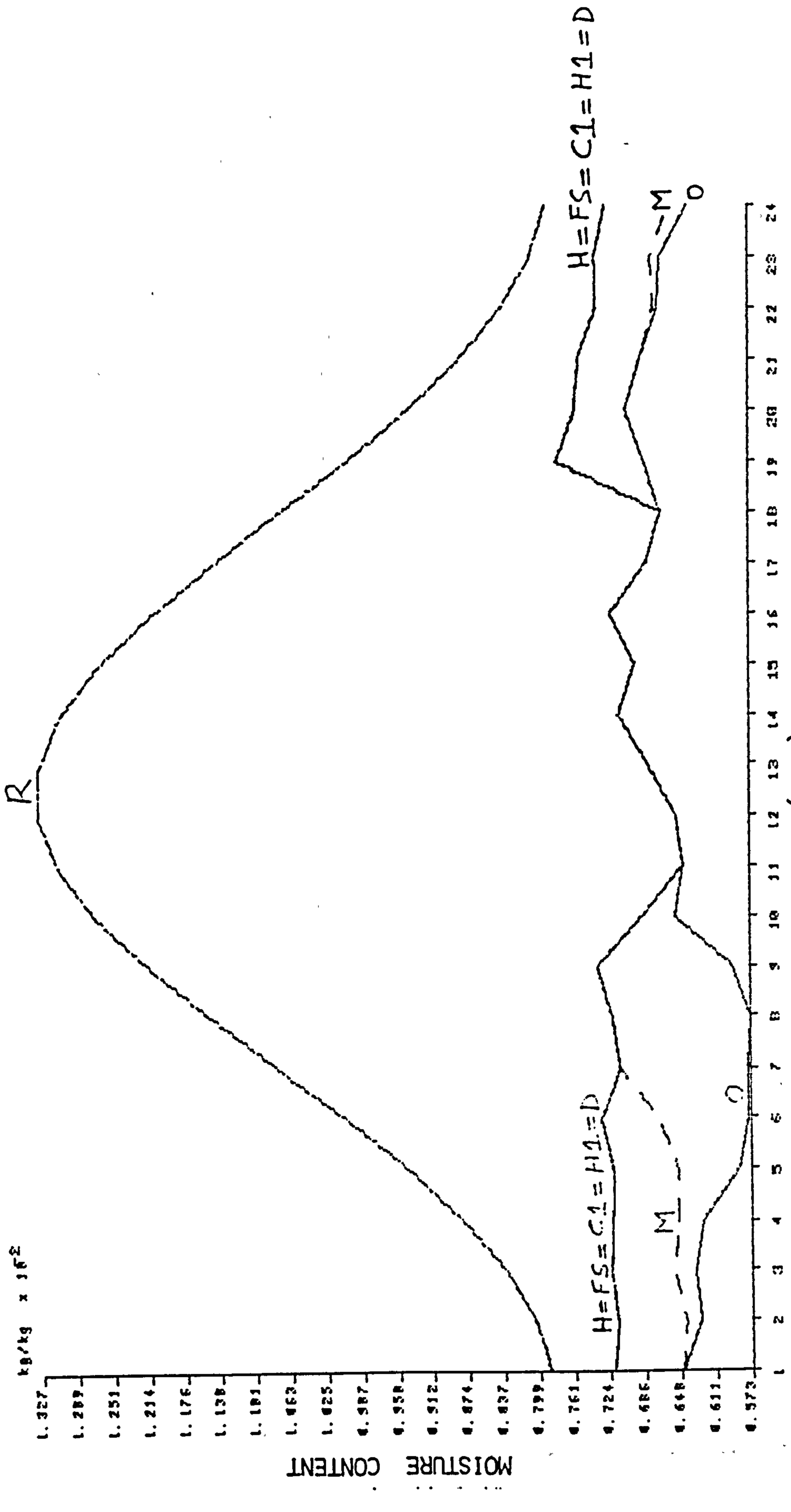

FIG. 5.17A MOISTURE CONTENT PROFILES - EXERCISE 1.4 NOVEMBER 4

Ex. 1.4 - Nov. 4 - moisture content

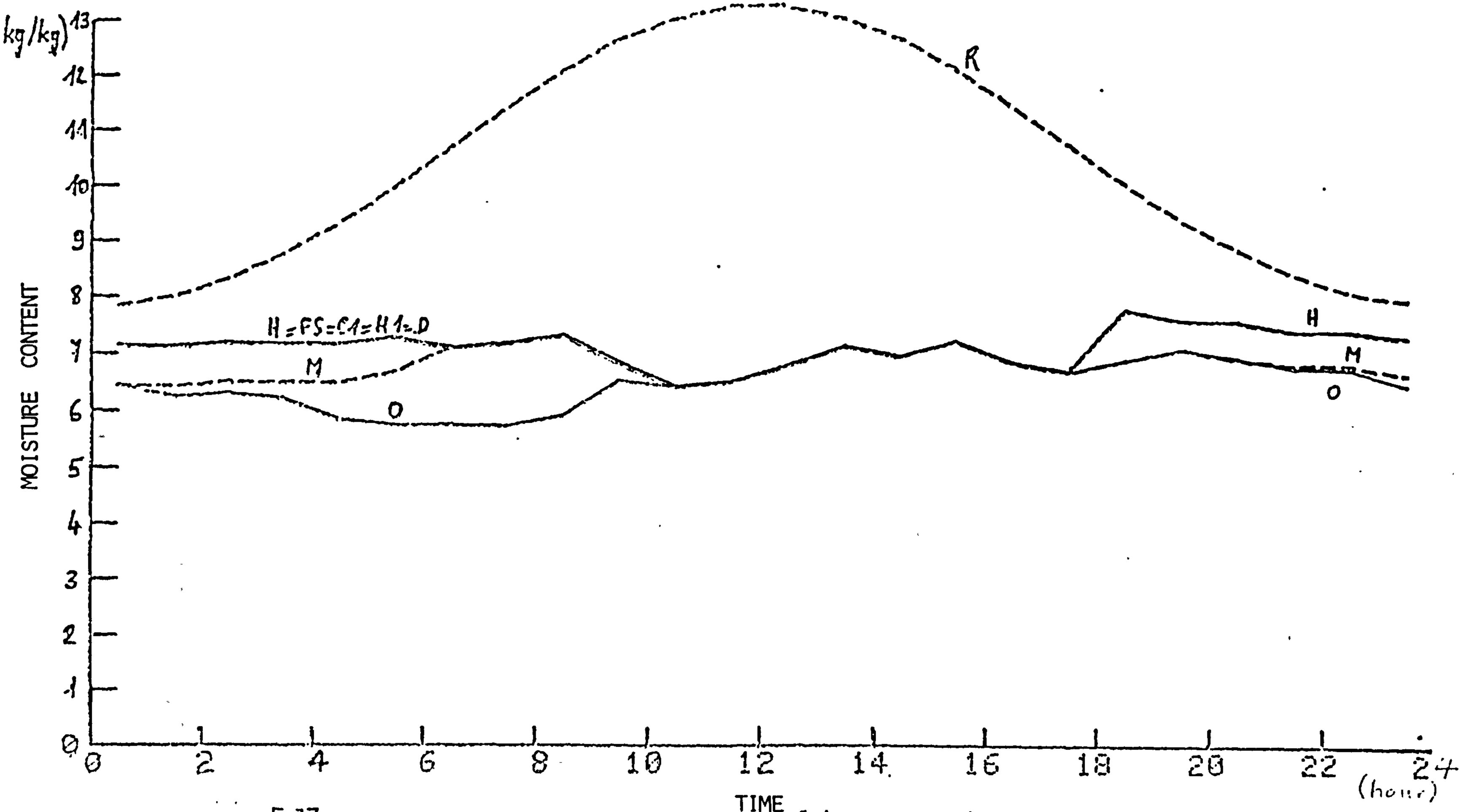

FIG. 5.17B MOISTURE CONTENT PROFILES - EXERCISE 1.4 NOVEMBER 4

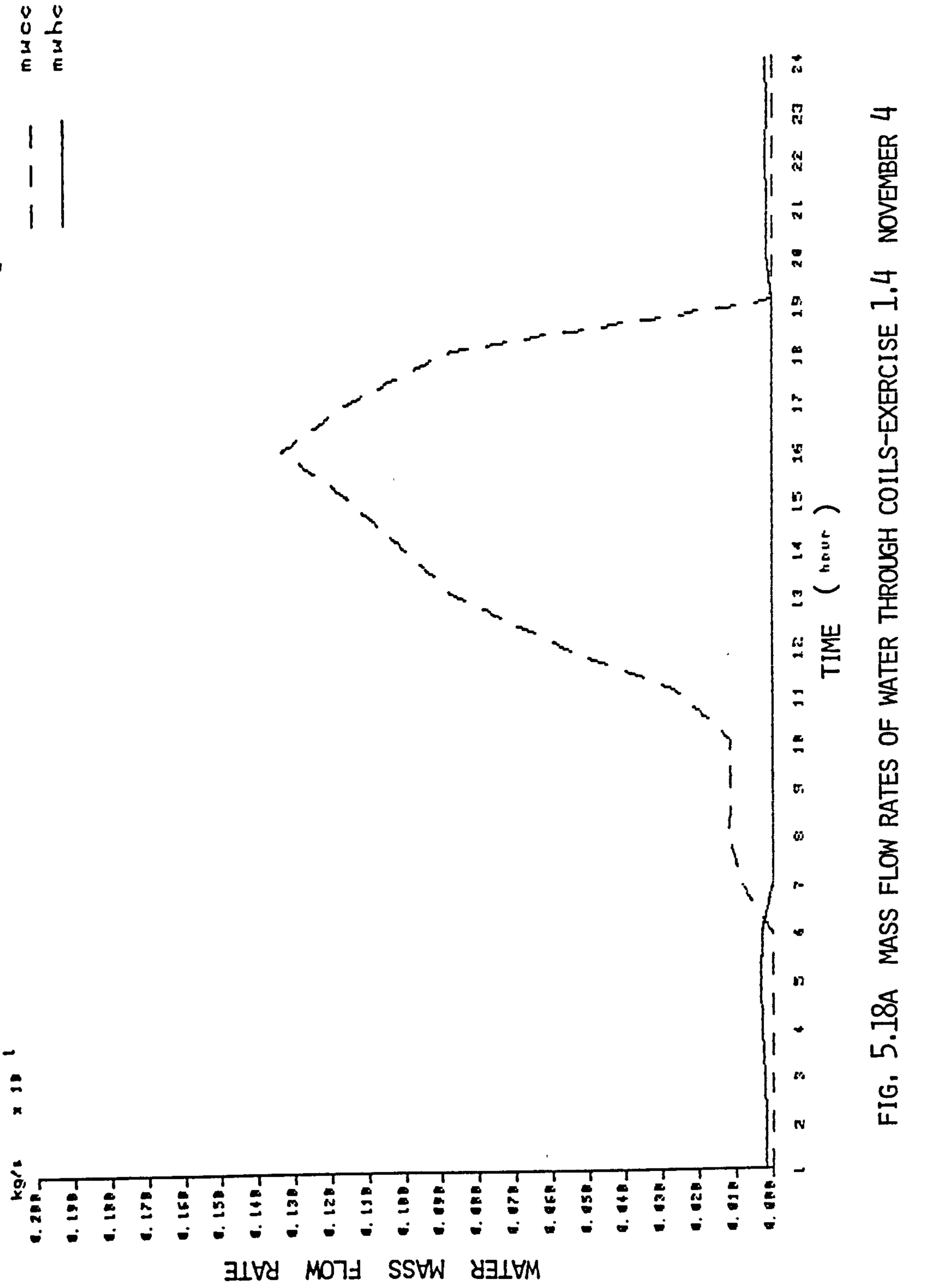

FIG. 5.18A MASS FLOW RATES OF WATER THROUGH COILS-EXERCISE 1,4 NOVEMBER 4

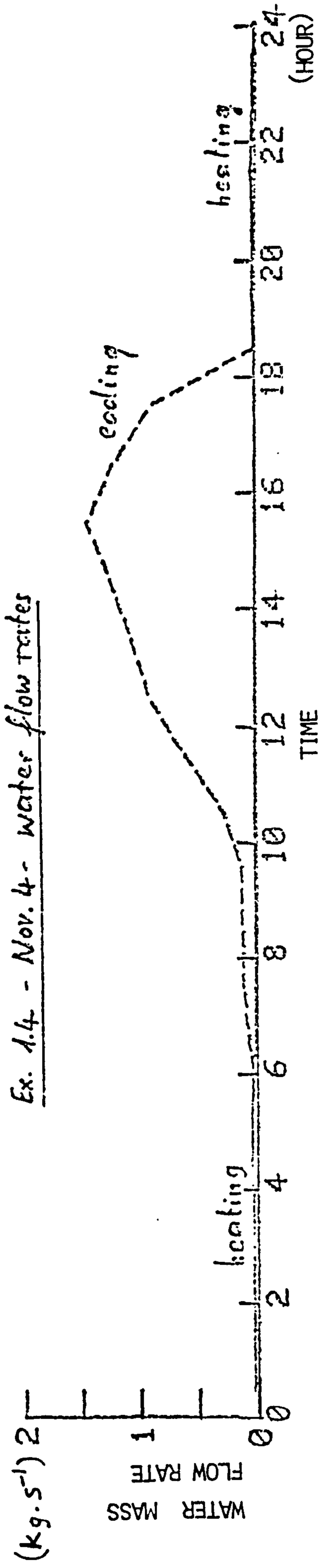

FIG. 5.18B MASS FLOW RATES OF WATER THROUGH COILS - EXERCISE 1.4 NOVEMBER 4

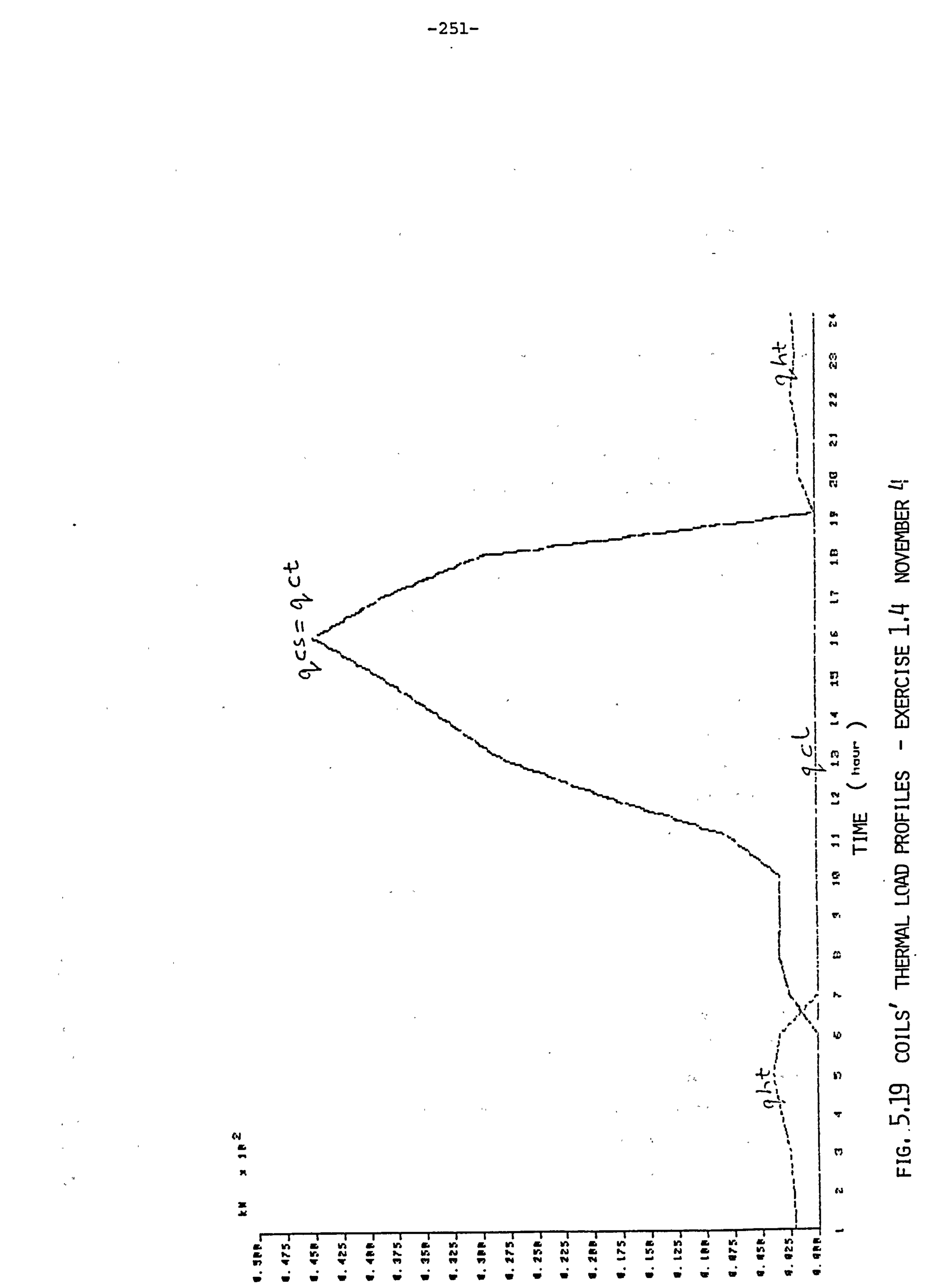

FIG. 5.19 COILS' THERMAL LOAD PROFILES - EXERCISE 1.4 NOVEMBER 4

From Fig. A5.11a, the mass flow rate of water through the cooling coil reaches this value between the 15th and 16th hours. It can also be observed that the maximum cooling load occurs during these time periods for each exercise.

5.5 APPLICATION OF SYSPAN FOR SIMULATING THE PERFORMANCE OF CENTRAL PLANT

The Collings Building System Simulation Exercises 1 and 2 do not include the simulation of the performance of the central plant; because of this no specifications have been made for the components of the central plant.

However, for illustrative purposes, a central cooling plant has been designed to meet the thermal requirement of the VAV system using the weather data of September 7, although this day does not represent a typical design day.

SYSPAN has been used to simulate the performance of this plant and determine the electrical power required to drive the components of the plant. The cooling plant comprises a water cooled reciprocating water chiller, chilled and condenser water pumps and a cooling tower (see Fig. 5.20). The cooling plant performance data are given below.

5.5.1 Cooling Plant Performance Data

5.5.1.1 Chiller

The chiller selected is a 50Hz York LCH50W (Ref. 11) water cooled hermetic reciprocating water chiller having a nominal capacity of 175.84kW. The chiller's compressor has four cylinders and rotates at a speed of 1470r.p.m. The capacity control mechanism operated by a thermostat sensing the temperature of the water entering the chiller, unloads cylinders down to minimum capacity in 4 steps by use of solenoid valves.

Applying regression analysis to the performance data given in Ref. 11, the full load model coefficients for the chiller are determined as:

For capacity

B1 = 143.82809 B2 = 15.47111
B3 = - 0.6777865 B4 = 0.4576413
B5 = - 0.02433473 B6 = - 0.5681095
B7 = 0.039002 B8 = 7.240383E-03
B9 = - 5.2034E-04

For power

B10 = 24.23438 B11 = - 1.614395
B12 = 0.098539 B13 = 0.308869
B14 = 1.876727E-03 B15 = 8.476418E-02
B16 = - 5.082313E-03 B17 = - 7.9379E-04
B18 = 6.350406E-05

To correspond with the chilled water flow temperature used for the simulation exercises, the chilled water supply temperature is assumed to be constant at 4.4°C. The design temperature of water leaving the condenser is 35°C.

The capacity reduction data for the reciprocating water chiller is shown in Table 4.1 which is reproduced here for convenience purposes.

Capacity Reduction Data

PLR	FFLP
1.00	1.00
0.75	0.80
0.50	0.61
0.25	0.40

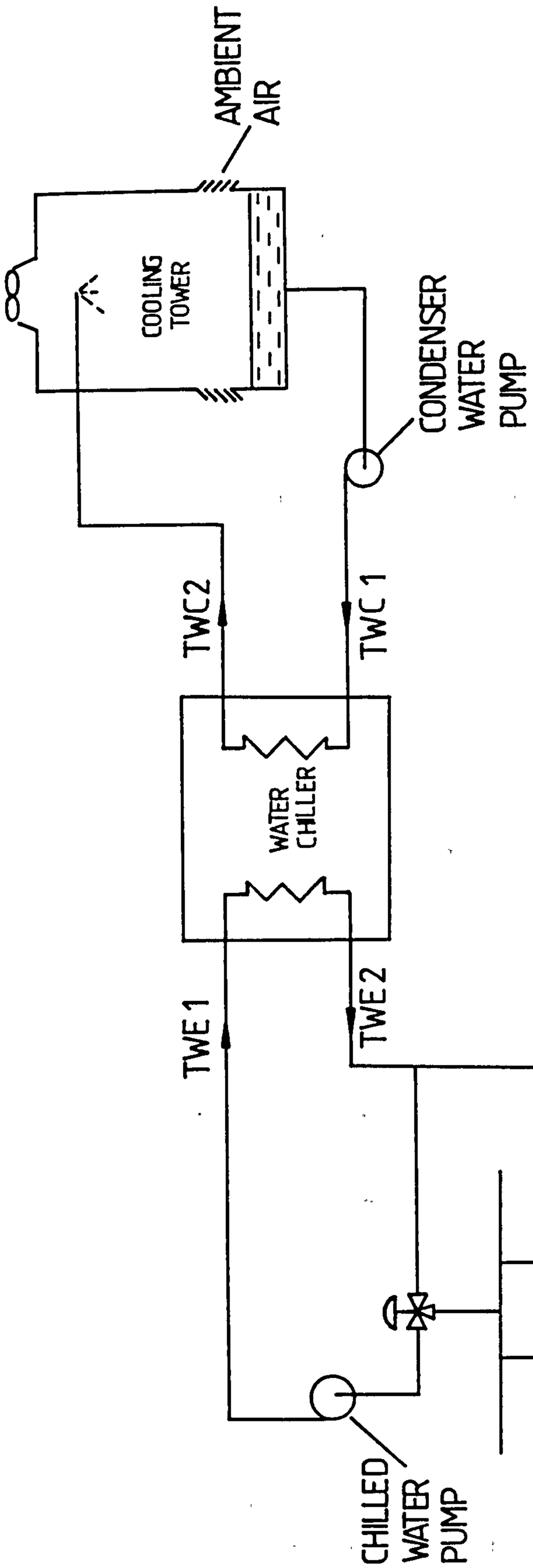

FIG. 5·20 COOLING SUBSYSTEM OF CENTRAL PLANT

5.5.1.2 Chilled Water Pump

This is a centrifugal pump which discharges a constant amount of water. The mass flow rate of chilled water is 4.1kg/s and the efficiency of the pump motor is 90%. The electrical power required to drive the pump motor is 0.9037kW.

5.5.1.3 Condenser Water Pump

This is a centrifugal pump which operates at constant volume. The mass flow rate of condenser water is 8.106kg/s and the efficiency of the pump motor is 90%. The electrical power consumption of the pump motor is 1.8073kW.

5.5.1.4 Cooling Tower

The cooling tower is an induced-draught counterflow type. Capacity control is provided by cycling the fan which operates at two speeds. The temperature of water leaving the cooling tower floats with the wet bulb temperature of ambient air subject to a fixed approach and is not allowed to fall below 18.333^{o}C.

Performance data for the cooling tower is as follows:
Factor of merit = 0.6
Full load volumetric flow rate of ambient air = 2.3909m^{3}/s
Power required to drive the cooling tower fan motor at full load = 1.958kW
The volumetric flow rate of ambient air at low speed is half of that at high speed and the power consumption of the fan motor at low speed is one-eighth of that at high speed.

5.5.2 Simulation Technique

The simulation of the performance of the cooling plant involves determining the energy consumed by the various components of the plant to satisy the VAV system thermal loads.

Equations 4.23 and 4.24 indicate that the capacity and full load power of a water cooled reciprocating water chiller depend on the temperatures TWE2 and TWC2. Since TWC2 is not readily known, the capacity,power requirement of the chiller and the load on the cooling tower cannot be determined. Thus, it is necessary to set up iterative calculations around the water loop of the condenser and cooling tower in order to determine the balance point of operation of the cooling plant, since the temperature of the chilled water supplied to the cooling coil is assumed constant.

Using the successive subtitution technique the performance of the cooling plant can be simulated. The calculational procedure is as follows:

1) Compute the temperature of water leaving the cooling tower, TWOCT.
   TWOCT = Maximum of {(TWBOA + APP) and 18.333}
   where TWBOA is the wet bulb temperature of outside air and APP is the approach (which can be determined from the design simulation run).

2) Assume a value for the range, RNG and determine the temperature of water entering the cooling tower, TWICT.
   TWICT = TWOCT + RNG

   Assuming losses in the piping from the condenser to cooling tower is negligible, the temperature of water leaving the condenser, TWC2 is equal to TWICT.

3) Use the reciprocating water chiller subroutine to determine the chiller power consumption and the condenser heat rejection load.

4) Use the cooling tower subroutine to determine a new value for range, RNGN. If RNGN and RNG are within a specified tolerance, go to step 5. Otherwise RNG = RNGN and go to step 2.

5) Determine the electrical power required to operate the cooling plant and its components.

6) Exit.

5.5.3 Results of the Central Plant Simulation Exercises

The simulation exercises comprise determining the performance of the central cooling plant in satisfying the thermal loads of the VAV system (for Exercises 1.1 to 1.4) using the weather data of September 7. The results are presented as graphs of:

Electrical power consumption against time

Part load ratio against time

In these graphs, the labels have the following meaning:

P	-	power consumption of the chiller's compressor (kW)
CTFKW	-	power consumption of the cooling tower fan motor (kW)
CPKW	-	power consumption of the cooling plant (sum of electrical power required to drive the chiller's compressor, cooling tower fan, chilled and condenser water pumps) (kW)
FMPOW	-	power consumption of the VAV system supply fan motor (kW)
WPPOW	-	power consumption of the VAV system humidifier water pump motor (kW)
TCPKW	-	total power consumption of the HVAC system and central cooling plant components (kW)
PLRCH	-	part load ratio for chiller
PLRCTF	-	part load ratio for cooling tower fan

5.5.4 Analysis of the Results of the Central Plant Simulation Exercises

Generally for all the exercises, the total VAV system and central plant power consumption (TCPKW) profile is similar to that of the total cooling load (qct).

For exercise 1.1, TCPKW varies from 12.723kW at the 7th hour to 29.723kW at the 18th hour (see Fig.5.21). The total energy consumption for the day is 533.002kWh. The part load ratio for the chiller varies from 0.0846 at the 7th hour to 0.4133 at the 17th hour (see Fig. 5.22). The minimum unloading ratio for the reciprocating water chiller is 0.25.

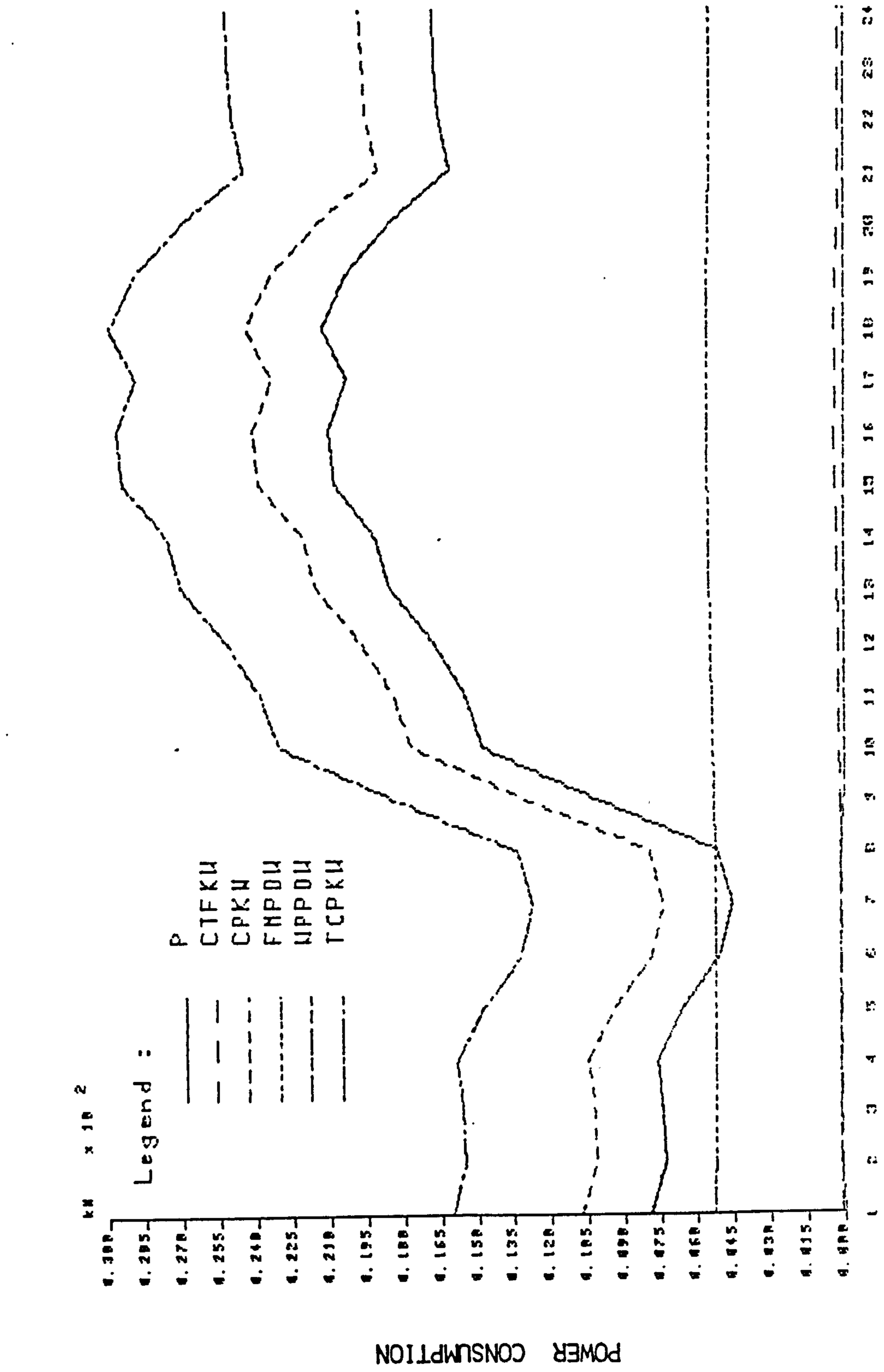
POWER CONSUMPTION
kW x 10 2
Legend :
P
CTFKU
CPKU
FMPOU
UPPOU
TCPKU
TIME (hour)
POWER CONSUMPTION PROFILES - EXERCISE 1.1 SEPTEMBER 7

FIG. 5.21 P

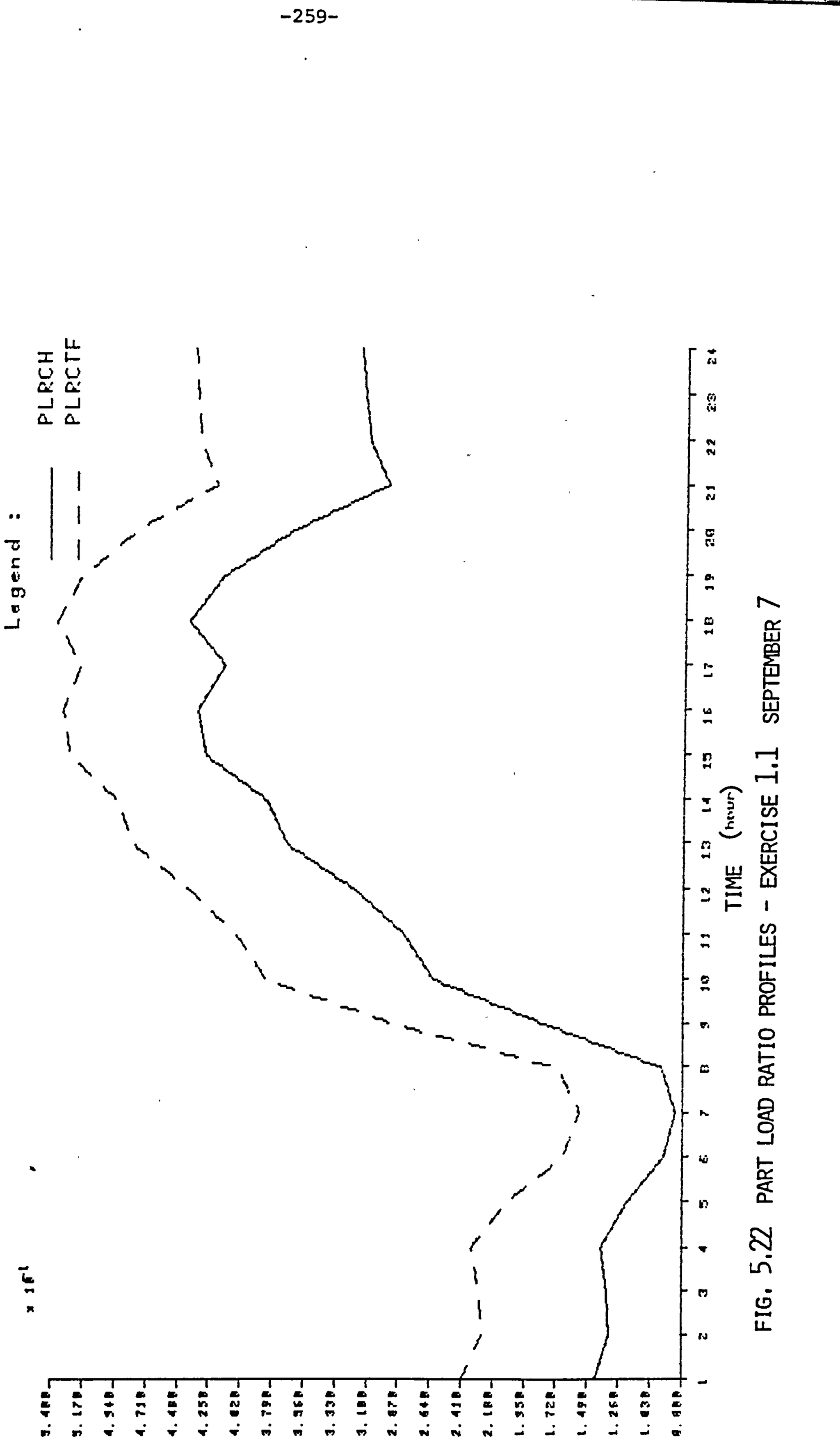

FIG. 5.22 PART LOAD RATIO PROFILES - EXERCISE 1.1 SEPTEMBER 7

Frequent or prolonged operation of chillers at capacities below the last step of unloading without the aid of a hot gas bypass mechanism is inadvisable. Thus for this chiller, such a mechanism which bypasses a portion of the hot discharge gas from the condenser to the evaporator inlet should be installed. This produces an artificial load on the evaporator and permits capacity reduction to as low as 5%.

For exercise 1.2, TCPKW varies from 12.713kW to 26.24kW. The total energy consumed by the primary and secondary system for the day is 519.291kWh. Thus compared to exercise 1.1, the reduction in energy use due to the operation of the economiser is 13.711 kWh or 2.572%. The part load ratio for the chiller varies from 0.0844 to 0.3407 with the chiller operating at part load ratios below the minimum unloading ratio for the first 9 hours (see Fig. 5.24).

For exercise 1.3, the energy consumption of the VAV system and central plant increases considerably (over the previous two) mainly because of the higher cooling load imposed on the cooling plant and increased fan power consumption. Over the 24 hour period, the energy consumption is 638.723 kWh. TCPKW varies from 7.199 kW at the 1st hour to 47.821 kW at the 16th hour while the part load ratio of the chiller varies from 0.0520 to 0.7713 for the same hours respectively (see Figs. 5.25 and 5.26).

For exercise 1.4, the total energy consumption of the VAV system and central plant for the day is 716.295 kWh. Compared to exercise 1.3, the increase in energy use is 77.572 kWh or 12.145%. This increase is mainly due to the higher cooling loads imposed on the cooling plant. Compared to exercise 1.2, the increase in energy use is 197.004 kWh or 37.9%. However, the chiller operates at part load ratios below the minimum unloading ratio for 12 hours (see Fig. 5.28).

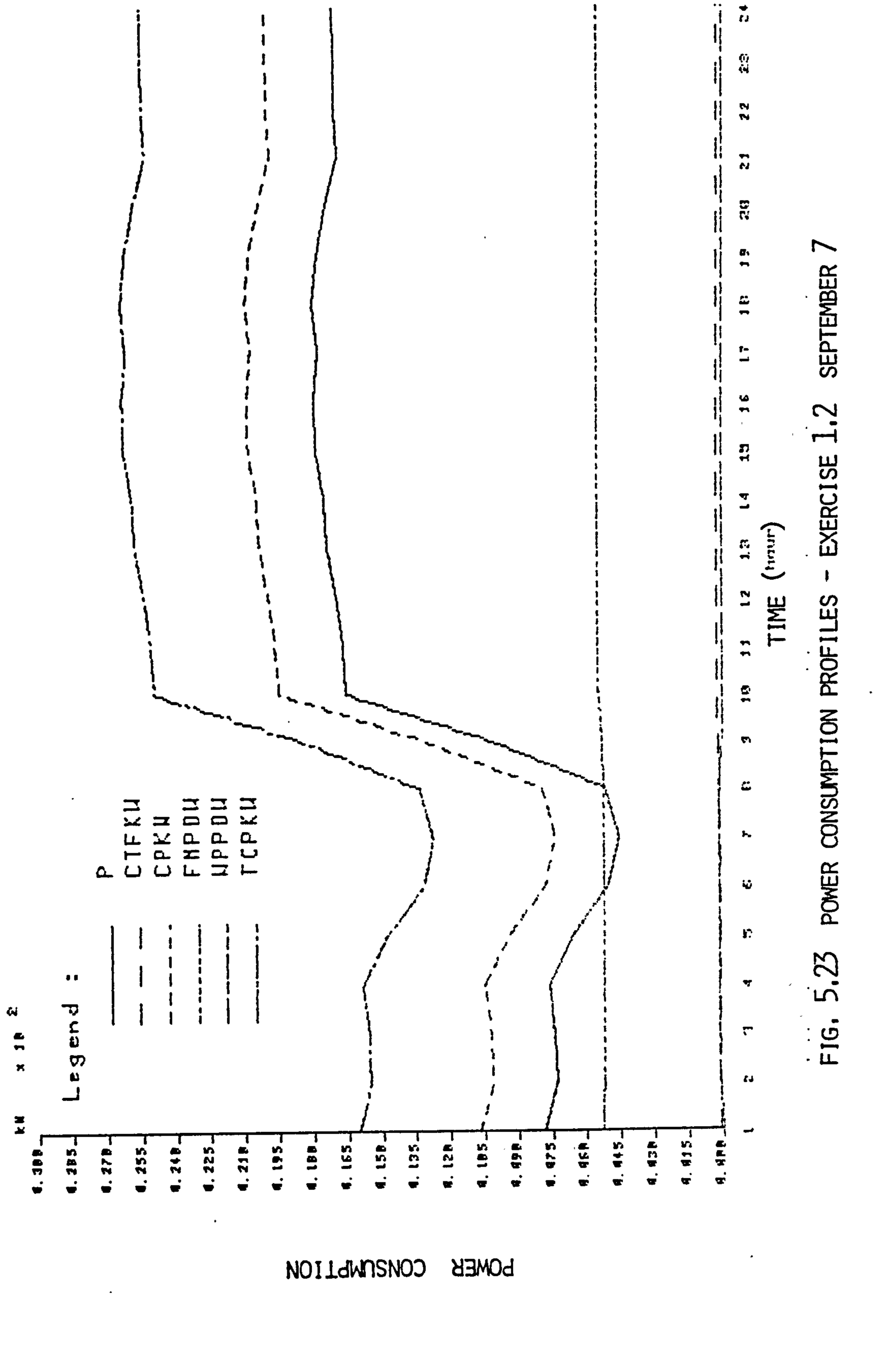

FIG. 5.23 POWER CONSUMPTION PROFILES - EXERCISE 1.2 SEPTEMBER 7

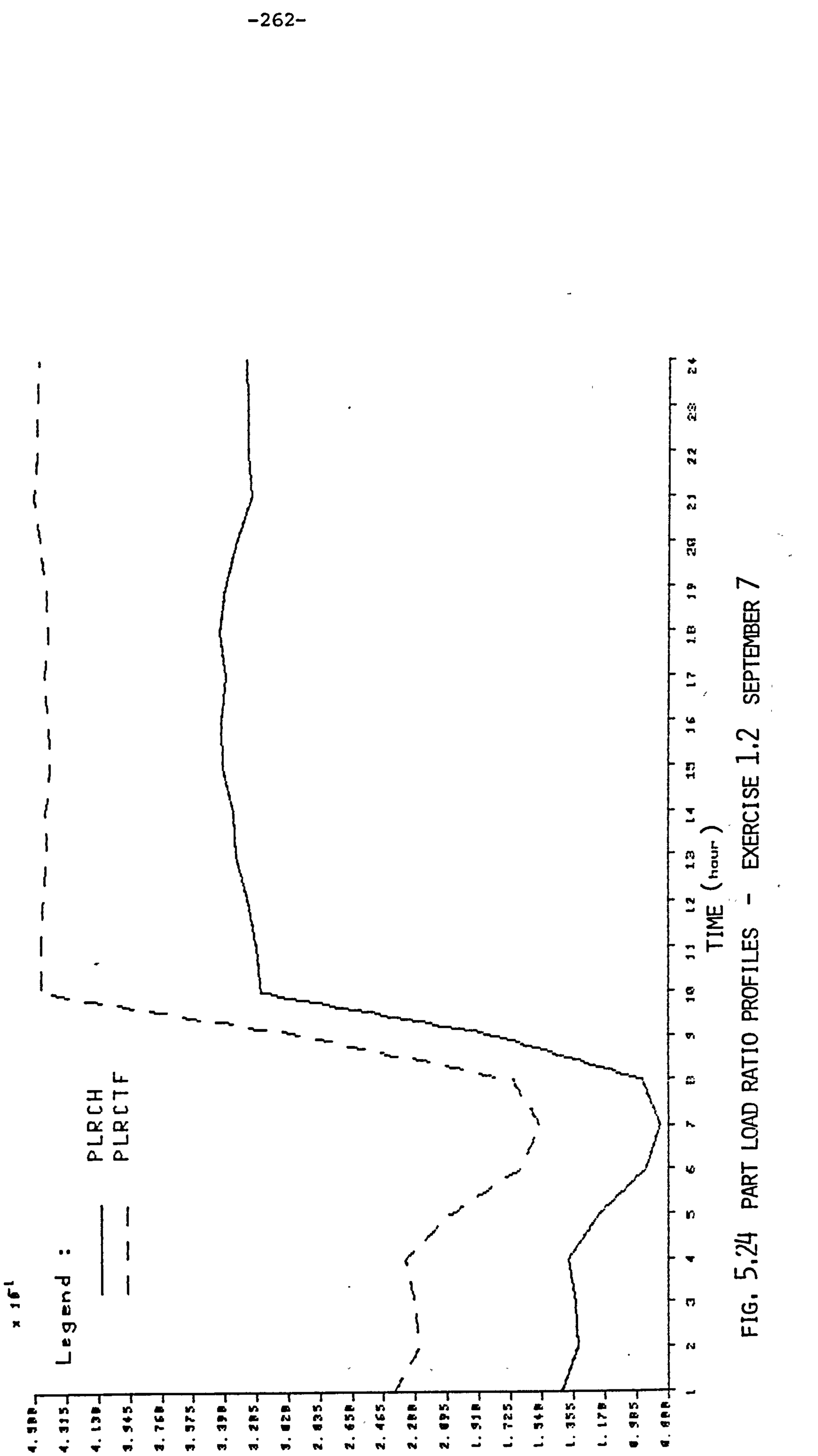

FIG. 5.24 PART LOAD RATIO PROFILES - EXERCISE 1.2 SEPTEMBER 7

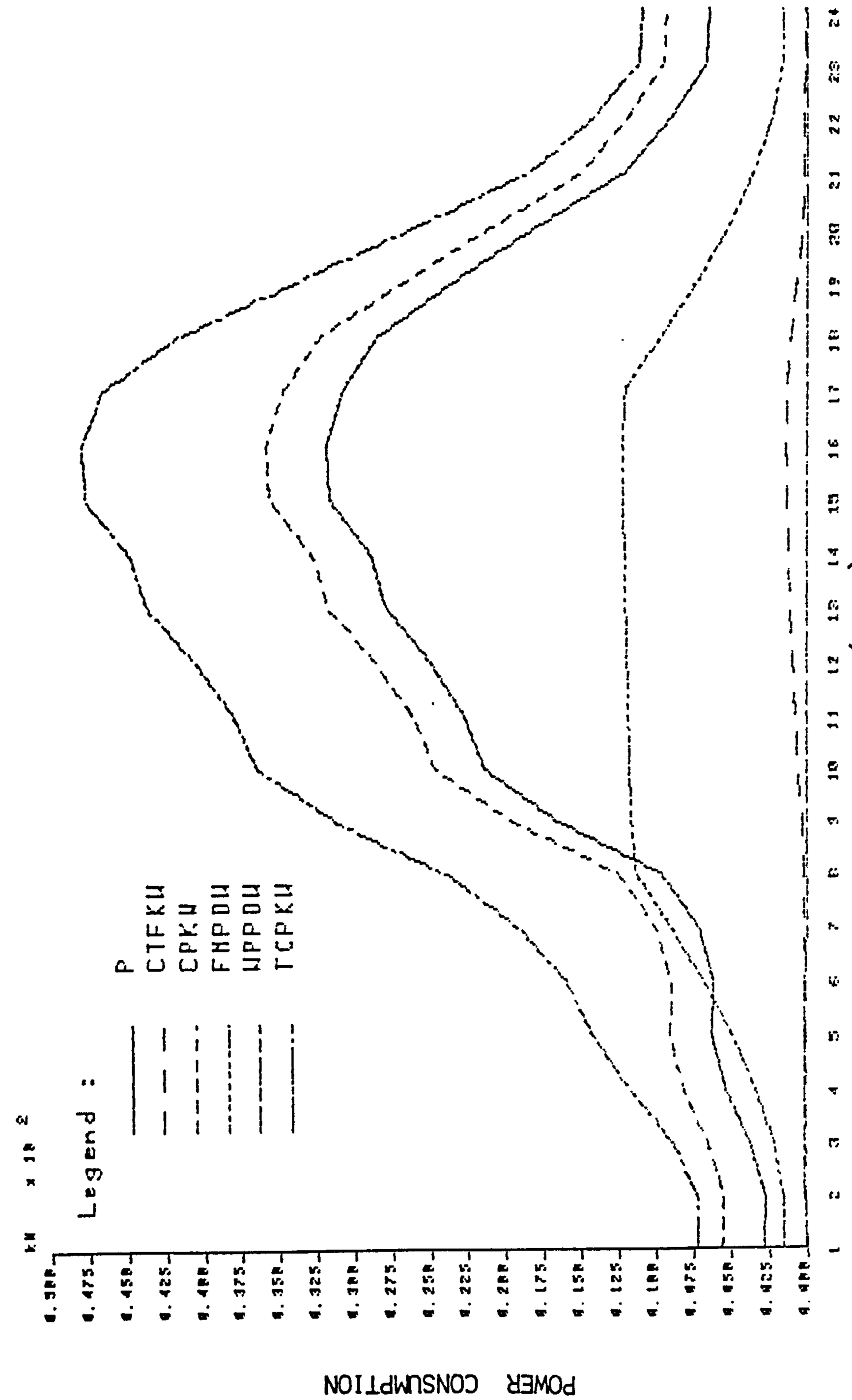

FIG. 5.25 POWER CONSUMPTION PROFILES - EXERCISE 1,3 SEPTEMBER 7

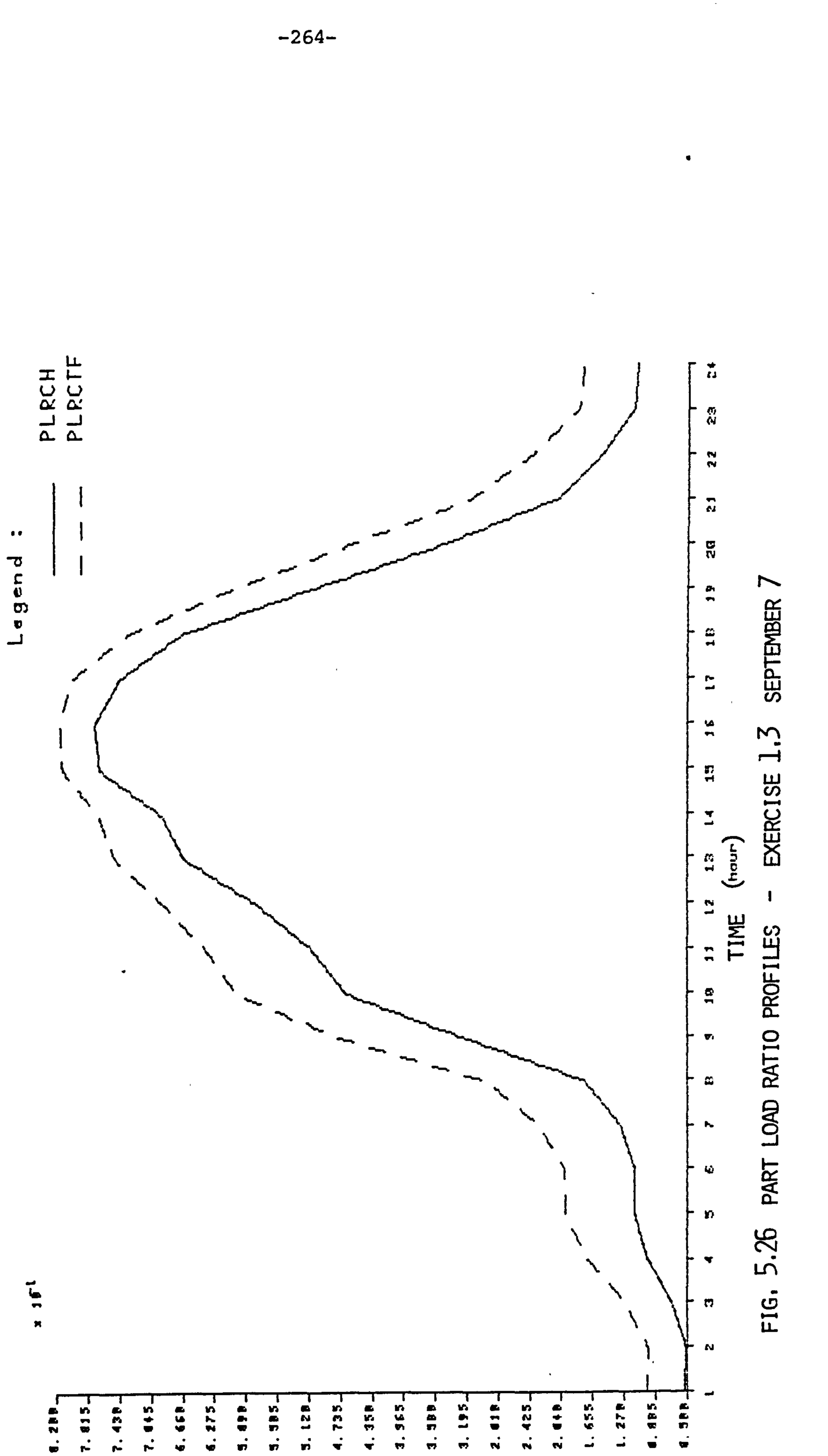

FIG. 5.26 PART LOAD RATIO PROFILES - EXERCISE 1.3 SEPTEMBER 7

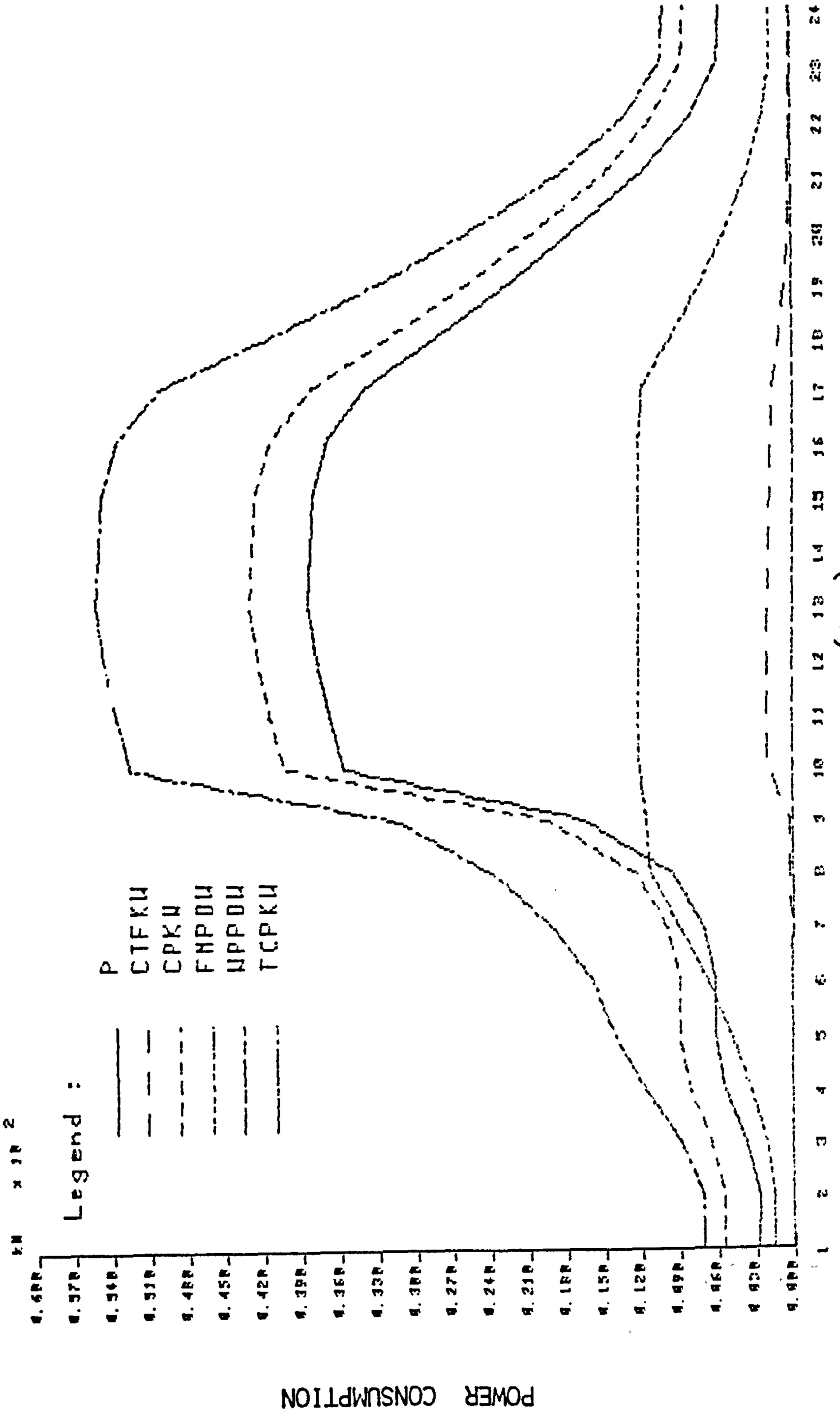
POWER CONSUMPTION
kW x 10 ^ 2
Legend :
P
CTFKU
CPKU
FNPOU
UPPOU
TCPKU
TIME (hour)
FIG. 5.27 POWER CONSUMPTION PROFILES - EXERCISE 1.4 SEPTEMBER 7

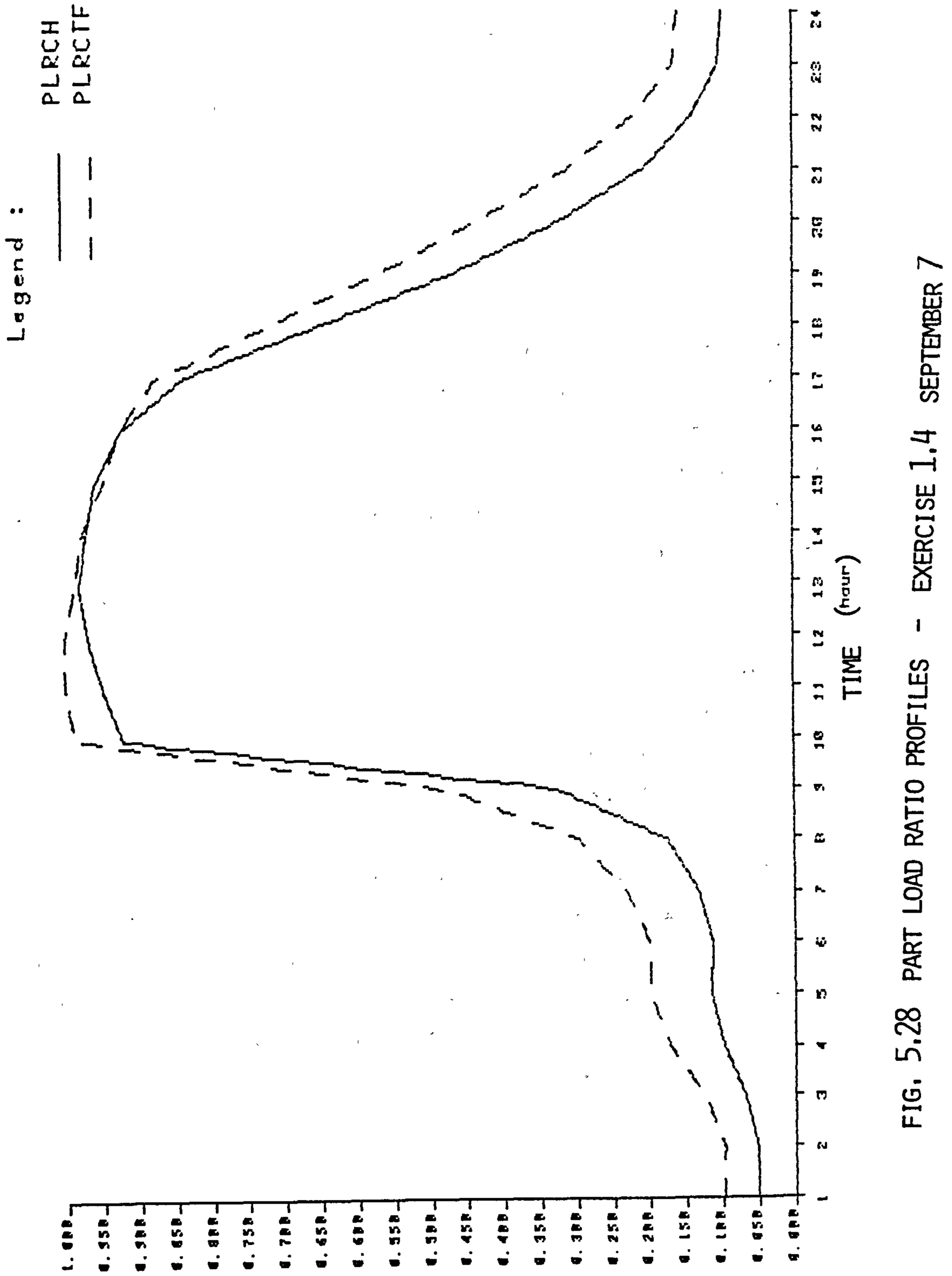

FIG. 5.28 PART LOAD RATIO PROFILES - EXERCISE 1.4 SEPTEMBER 7

5.6 VALIDATION OF SYSPAN

Wiltshire (Ref. 12) has reviewed the issue of validation and building energy simulation models and defined validation as the testing of a model's theoretical basis and its ability to reproduce the observed behaviour of the building or system. According to him, a full scale validation of a model will require the use of the following investigatory techniques:

Theoretical Examination
Analytical Verification
Comparative Studies
Empirical Validation

Theoretical Examination - The first stage of any validation verification study should begin with a rigorous theoretical examination of the fundamental principles embodied in the model. This requires the availability of good documentation in which there is a clear technical exposition of the physical and engineering assumptions; the analytical and numerical techniques that have been employed and a full explanation of the formulation of the associated algorithms.

Analytical Verification - With this technique, the models (and submodels) are evaluated against carefully designed problems with known analytical soutions. These problems can be chosen to test the most important individual and combined heat transfer mechanisms in the models.

Comparative Studies - With this technique, the results from the simulation of a hypothetical building or system by two or more models are compared. In the case where the models have been through the verification process, this procedure gives some indication of whether the use of the model introduces differences in the solution. If the verification process is omitted, there is less certainty in explaining the discrepancies between the results.

Empirical Validation - This is the ultimate stage of validation in which the correspondence between the model's solution and the real, physical world (building or system) is assessed. Only at this stage does it become clear whether the assumptions,approximations and operation of the model are adequate to match reality with a sufficient degree of accuracy.

From his review, Wiltshire proposed that greather emphasis in validation studies should be placed upon the theoretical examination of models and the development of scientifically rigorous analytical verification techniques since these are capable of identifying problems at all stages of model formulation. He suggests that a structured approach to validation is required in which the four validation techniques mentioned above have a role to play.

Since SYSPAN uses a component based simulation technique, the problem of its validation is largely reduced to the validation of its individual component models. The models formulated in SYSPAN use fundamental heat and mass transfer principles, laws of conservation of mass and energy and in some cases empirical data. Although there could be refinements to some of the models (e.g. cooling coil) to enhance their modelling capabilities, however they are suitably adequate for the purpose of steady state analysis of HVAC systems and building energy calculations.

As indicated in Section 5.4.6, the results obtained for the VAV system simulation exercises using SYSPAN were in very good agreement with those obtained by Morant. Although this cannot be regarded as a full scale validation of the algorithms used by SYSPAN, nevertheless it goes a long way towards satisying the comparative study validation technique elucidated by Wiltshire.

An empirical validation of these algorithms will require the use of a fully instrumented HVAC test facility where clearly defined and carefully monitored experiments can be carried out. Such a test facility has been designed and installed at Construction Engineering Research Laboratory, Champaign, Illinois in the United States of America (Refs. 13 and 14).

The components of the HVAC test facility could be configured and controlled to represent the more commonly used HVAC systems such as variable air volume, terminal reheat, dual duct constant volume, dual duct variable volume systems, etc. However, a number of problems were encountered in the course of conducting experiments to determine the performance of components and systems. The major problem was the failure of the various components and control systems to match the manufacturers' performance specifications. Efficient performance of most of the equipment was achieved only after field adjustment. The major recommendation of their study was that more research and development is needed to improve the reliability and maintainability of HVAC components and systems.

According to Kusuda (Ref. 15), most of the past validation efforts in building energy calculation have been directed toward the comparison of calculated and metered gross annual fuel/electricity. Although several attempts have been made to measure the detailed performance of HVAC systems of large buildings by extensive instrumentation, none of the results of these efforts have been useful for the comprehensive validation of the HVAC system simulation calculation procedures. Thus, one sees that the validation of building energy calculation procedures is an expensive and time consuming task. A proposal by Kusuda is to select a typical set of commonly used HVAC systems, equipment, and control schemes for sample problems for which solutions based upon the most accurate engineering analysis are available, for a limited number of operating conditions. With the use of these sample problems, at least the algorithmic accuracy of various simulation procedures can be evaluated for most of the conventional systems.

REFERENCES FOR CHAPTER 5

1) STOECKER, W.F. (ed) "Procedures for Simulating the Performance of Components and Systems for Energy Calculations" ASHRAE Task Group on Energy Requirements for Heating and Cooling of Buildings, ASHRAE 1975.

2) KLEIN, S.A. et. al. "TRNSYS, A Transient Simulation Program," University of Wisconsin-Madison, Engineering Experiment Station Report 38-11, Version 11.1, April 1981.

3) QUICK, J.P.
IRVING,S.J. "Computer Simulations for Predicting Energy Use," Proceedings of the 3rd CIB Symposium on Energy Conservation in the Built Environment, Dublin, April 1982.

4) SILVERMAN, G.J.
JUROVICS, S.A.
LOW, D.W.
SOWELL, E.F. "Modelling and Optimization of HVAC Systems Using Network Concepts," ASHRAE Transactions 1981, Volume 87 Part 2, pp. 585-597.

5) LASDON, L.S.
WARREN, A.D.
JAIN, A.
RATNER, M. "Design and Testing of a Generalized Reduced Gradient Code for Nonlinear Programming," ACM Transactions on Mathematical Software, Volume 4 No. 1, March 1978, pp.34-50.

6) SOWELL, E.F.
TAGHAVI, K.
LEVY, H. "Generation of Building Energy System Models," ASHRAE Transactions 1984, Volume 90 Part 1, pp. 573 - 586.

7) KELLY, G.E.
PARK, C.
CLARK, D.R.
MAY, W.B.
"HVAC SIM+, A Dynamic Building/HVAC/Control Systems Simulation Program, Paper No. 14, Proceedings of the Workshop on HVAC Controls Modelling and Simulation, Held at the Georia Institute of Technology, Georgia, U.S.A. from February 2-3, 1984.

8) HANBY, V.I.
"Collins Building System Simulation: Revised Specification for Exercises 1 and 2,", IEA Annex 10 Document Reference AN10850220-01.

9)
"General Geometrical Data," IEA Annex 10 Document Reference AN10850410-10.

10) MORANT, M.A.
"Exercises 1 and 2: the VAV System Report," IEA Annex 10 Document Reference AN10850620-01, June 1985.

11) YORK INTERNATIONAL
"50Hz Hermetic Reciprocating Packaged Liquid Chillers - Model LCH," Published by Borg - Warner Corporation, 1976.

12) WILTSHIRE, T.J.
"Validation and Building Energy Simulation Models," Sun at Work in Britain, June 1983, pp. 19-26.

13) HITTLE, D.C.
DOLAN, W.H.
LEVERENZ, D.J.
RUNDUS, R.
"Theory Meets Practice in a Full-Scale Heating, Ventilating and Air-Conditioning Laboratory," ASHRAE Journal, November 1982, Volume 24 No. 11, pp. 36-41.

14) DOLAN, W.H.
"Validation Data for Mechanical System Algorithms Used in Building Energy Analysis Programs," Technical Report E-177 (Report No. AD-A115182) U.S Army Construction

Engineering Research Laboratory, February 1982.

15) KUSUDA, T. "Standards Criteria for HVAC Systems and Equipment Performance Simulation Procedures," ASHRAE Journal, October 1981, Volume 23 No. 10, pp. 25-28.

CHAPTER 6

CONCLUSIONS AND RECOMMENDATIONS FOR FURTHER WORK

6.1 CONCLUSIONS

The need to design energy efficient buildings, improve the thermal performance of existing building stock and the availability of powerful digital computers have led to the development of building energy analysis computer programs. Energy analysis plays an important role in developing an optimum HVAC system and equipment, architectural design of new buildings and in determining cost effective modifications to existing buildings.

Generally, the first stage in the building design process is to determine an optimum shape/form of the envelope, suitable construction materials and the appropriate layer by layer composition of the building elements (walls, floors, roofs, etc.). This requires the use of a thermal loads analysis computer program which can determine accurately the effects of the changes in building design variables on the heating and cooling loads of the building.

The choice of an adequate HVAC system to satisfy the heating and cooling loads and maintain the building internal conditions requires a system simulation program which enables comparative studies of alternative systems to be made. Component based simulation methods seek to give the designer this flexibility by enabling a system to be defined by specifying its individual components and their connections.

A modular system simulation computer program requires the availability of mathematical models which can accurately analyse the thermal performance of the components comprising the system and evaluate the effects of various control strategies on system operation. Component models of HVAC systems and central plant developed in this thesis make use of fundamental heat and mass transfer principles, laws of conservation of mass and energy and where appropriate emprical data.

They are basically steady state and address those physical variables used in the selection and design of HVAC components.

The computer program SYSPAN, developed in this thesis, utilises the component based sequential modelling approach to simulate the performance of HVAC systems and central plant. A wide variety of HVAC systems can be configured and simulated by SYSPAN using available component models. Since each of the component models are formulated as separate FORTRAN subroutines, SYSPAN calls the relevant subroutines in order to determine the balance point of system operation. The order in which the subroutines are called depends on the available information at the system model generation stage. The simulation of the performance of the HVAC system involves determining the state of the air at the inlet and outlet ports of each component of the system and other relevant variables such as coil thermal loads, fan power consumption, etc.

The energy consumed by the central plant component in satisfying the thermal requirements of the HVAC system is determined with the aid of the central plant simulation subprogram. The performance of the components of building energy systems at part load must be accounted for if a reasonably accurate calculation of the energy consumption is to be obtained. This is because these components operate at part load conditions for most of the time.

It can be seen from the results of the simulation exercises (for VAV system and central plant) that SYSPAN can be used as an energy analysis tool by building services designers or operators. As the state of the air is determined throughout the circuit, a thorough analysis of the performance of the HVAC system can be made. Thus, the effects of various control strategies on system performance can be investigated. Also, the hourly part load ratios at which the components are operating are presented. This information can be used to devise an effective energy management program for scheduling the operation of the system and central plant.

6.2 RECOMMENDATIONS FOR FURTHER WORK

One of the major problems encountered in this study is the lack of sufficient full and part load performance data of the components of HVAC systems and equipment in the public domain. Thus, there exists the need to produce comprehensive quality data sets of the performance of these components which can be used to validate algorithms employed by component models or aid in component model development. The efforts of the IEA Working Group on System Simulation in Buildings (Annex 10) in this direction are noted; however, their work will be more useful if they liaise with the major manufacturers of HVAC components or include proficient building services designers in their group.

For the purpose of determining performance data and checking manufacturers' specification of components, a fully instrumented HVAC test facility should be set up. Using this full scale test facility, various components can be configured and controlled to represent a wide variety of HVAC systems. Experiments can be conducted to determine the performance of the various systems, obtain data for the individual components and investigate the effects of various control schemes on system performance. Reliable data obtained from such clearly defined and carefully monitored experiments can be used to validate the algorithms employed by system simulation computer programs.

In order to fully utilise the flexibility provided by the modular simulation program, SYSPAN, an improved user interface which makes the input and editing of complex system models easier and faster should be developed and linked to it.

BIBLIOGRAPHY

1) HOLMES, M.J. "The Simulation of Heating and Cooling Coils for Performance Analysis," Proceedings of an International Conference on System Simulation in Buildings, Held at the University of Liege, Liege, Belgium from December 6-8, 1982; pp. 245-280.

2) HOLMES, M.J. "System Simulation Techniques for Calculation of Energy Consumption," BSRIA Project Report 15/111, 1978.

3) ELMAHDY, A.H. "Analytical and Experimental Multi-Row Finned-Tube Heat Exchanger Performance During Cooling and Dehumidifying Process," Ph.D. Thesis, Carleton University, Ottawa, Canada, December 1975.

4) "Environmental Engineering in South African Mines," Published by the Mine Ventilation Society of South Africa, 1982.

5) IRVINE, F.T.
LILEY, P.E. "Steam and Gas Tables with Computer Equations," Published by Academic Press, Inc. 1984.

6) HITTLE, D.C. "An Algorithm for Modelling a Direct Expansion Air-Cooled Condensing Unit," ASHRAE Transactions 1982, Volume 88 Part 2, pp. 655-676.

7) DUMOUCHEL, P.
SANDER, D. M. "Simulation of HVAC Systems and Controls," Proceedings of the Third

International Symposium on the Use of Computers for Environmental Engineering Related to Buildings, Held at Banff,Alberta, Canada from May 10 - 12, 1978; pp. 479-489.

8) WOOLDRIDGE, M. J.
MOLLER, S.K.
"BUNYIP - A New Building Energy Use Investigation Package," Proceedings of the Fourth International Symposium on the Use of Computers for Environmental Engineering Related to Buildings, pp. 470-477.

9) KLEIN, S.A.
BECKMAN, W.A.
DUFFIE, J.A.
"TRNSYS - A Transient Simulation Program," ASHRAE Transactions 1976, Volume 82 Part 1, pp. 623-633.

10) CONTE, S.D.
BOOR, C. de
"Elementary Numerical Analysis: An Algorithmic Approach," Third Edition 1983, Published by McGraw-Hill International Book Company.

11) STOECKER, W.F.
JONES, J.W.
"Refrigeration and Air Conditioning," Second Edition 1982, Published by McGraw-Hill Book Company.

12) STOECKER, W.F.
"Design of Thermal Systems," Second Edition 1980, Published by McGraw-Hill Book Company.

13) HODGE, B.K.
"Analysis and Design of Energy Systems," 1985, Published by Prentice Hall, Inc. Englewood Cliffs, New Jersey, United States of America.

14) LITTLER, J.G.F. "Validation of Simulation Models," Sun at Work in Britain, June 1983, pp. 27-34.

15) STAMPER, E.
GREENBERGER, M. "Simulation of a Multicylinder Reciprocating Refrigeration System with Chilled Water Coil and Evaporative Condenser," Proceedings of the Symposium on the Use of Computers for Enviromental Engineering Related to Buildings, Held at the National Bureau of Standards Gaithersburg, Maryland, United States of America from November 30- December 2, 1970; pp. 545-555.

16) ELMAHDY, A.H.
MITALAS, G.P. "A Simple Model for Cooling and Dehumidifying Coils for Use in Calculating Energy Requirements for Buildings," ASHRAE Transactions 1977, Volume 83 Part 2, pp. 103 - 117.

17) KUSUDA, T.
ISHII, K. "Energy Analysis for a Sample Building by the Proposed ASHRAE Simplified Method," Report No. DOE/CS/20057-T4, DE81 027189; Natural Bureau of Standards, Washington D.C. USA; January 1981.

18) YORK, D.A.
CAPPIELLO, C.C (eds) "DOE2 Engineers Manual (Version 2.1A)," Report No. DE83 004575, LBL-11353, November 1, 1981.

19) SAMUEL, A.E.
CHIA, T.H. "Simulation of the Full and Part Load Energy Consumption of HVAC System of Building," Building and Environment, Volume 18, No. 4, pp. 207-218, 1983.

20) HASELTINE, J.D.
QVALE, E.B.

"Comparison of Power and Efficiency of Constant Speed Compressors Using Three Different Capacity Reduction Methods," ASHRAE Transactions 1971, Volume 77 Part 1, pp. 158-162.

APPENDICES

APPENDIX A3.1

Derivation of Equations 3.52 and 3.53b

Consider an incremental area of a counterflow hot water coil surface as shown in Fig. A 3.1. The rate of heat transfer over the area dA_o can be expressed in three ways as follows:

$$dq_h = U_o \, \theta \, dA_o \qquad (1)$$

$$dq_h = - m_w \, c_{pw} \, dt_w \qquad (2)$$

$$dq_h = - m_a \, c_{pma} \, dt_a \qquad (3)$$

The reason for the negative signs in Equations 2 and 3 is that for increasing heat exchanger area, temperatures t_w and t_a are decreasing in value. Let $m_w \, c_{pw}$ be the smaller thermal capacity, then the definitions of NTU, C and E are

$$NTU = \frac{U_o \, A_o}{m_w \, c_{pw}}, \qquad C = \frac{m_w \, c_{pw}}{m_a \, c_{pma}}, \qquad E = \frac{t_{wi} - t_{wo}}{t_{wi} - t_{ai}}$$

From Equations 2 and 3 we have,

$$dq_h = - m_w \, c_{pw} \, dt_w = - m_a \, c_{pma} \, dt_a$$

$$m_w \, c_{pw} \, dt_w = m_a \, c_{pma} \, dt_a \qquad (4)$$

Now $\theta = t_w - t_a \quad \therefore \; d\theta = dt_w - dt_a$

$$\therefore \; m_w \, c_{pw} \, (dt_w - dt_a) = m_w \, c_{pw} \, dt_w - m_w \, c_{pw} \, dt_a$$

Substituting for $m_w \, c_{pw} \, dt_w$ using Equation 4 we get,

$$m_w \, c_{pw} \, (dt_w - dt_a) = m_a \, c_{pma} \, dt_a - m_w \, c_{pw} \, dt_a$$
$$= dt_a \, (m_a \, c_{pma} - m_w \, c_{pw})$$

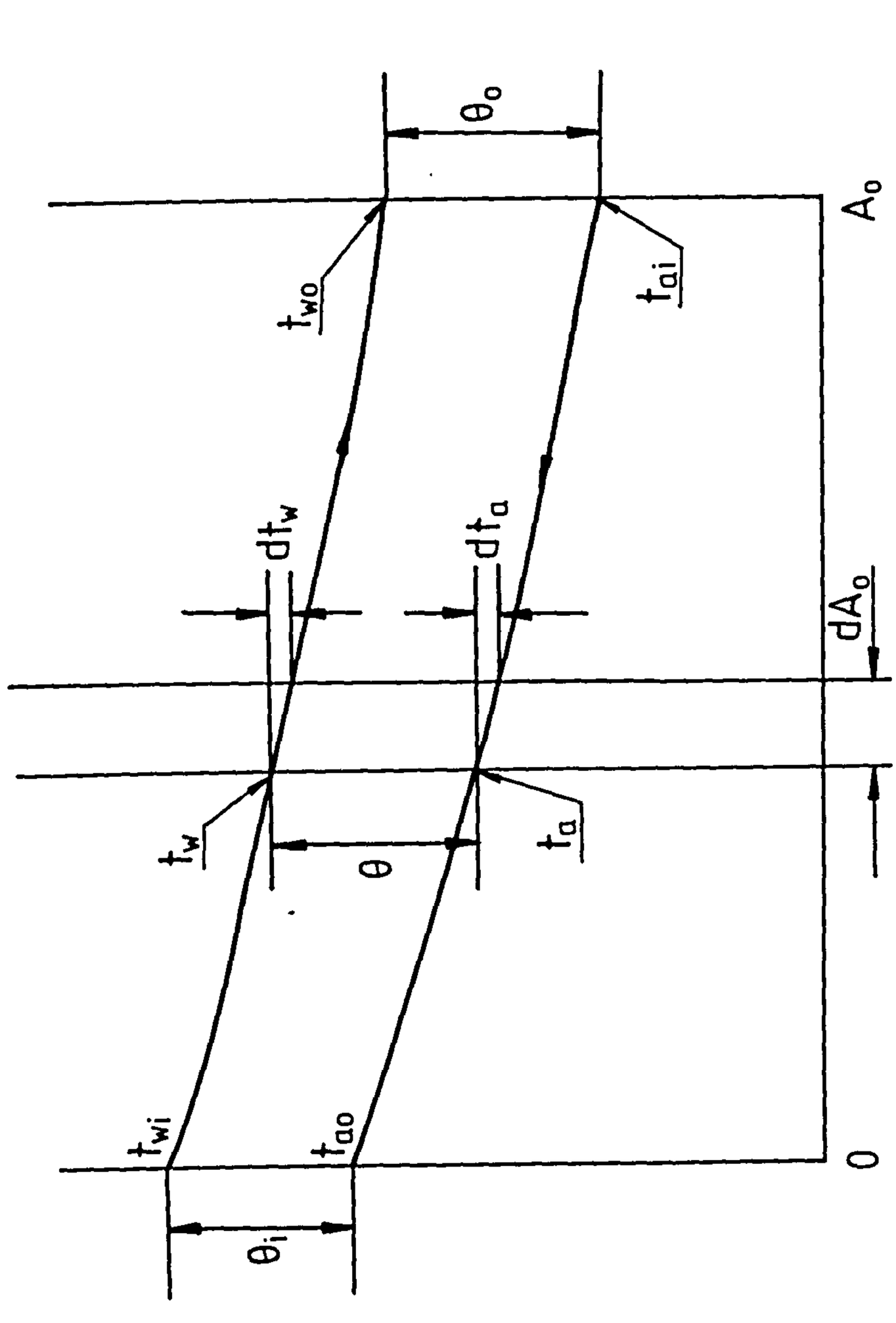

FIG. A 3·1 TEMPERATURE DISTRIBUTION IN A COUNTER FLOW HOT WATER COIL

Using Equation 3, dt_a may be eliminated to give,

$$m_w\ c_{pw}\ (dt_w - dt_a) = \frac{-dq_h}{m_a\ c_{pma}}\ (m_a\ c_{pma} - m_w\ c_{pw})$$

$$m_w\ c_{pw}\ (dt_w - dt_a) = -\ dq_h\ (1 - C)$$

Using Equation 1 to eliminate dq_h gives

$$dt_w - dt_a = \frac{-\ U_o\ \theta\ dA_o\ (1 - C)}{m_w\ c_{pw}}$$

$$\text{Thus}\quad \frac{d\theta}{\theta} = \frac{-\ U_o\ (1 - C)\ dA_o}{m_w\ c_{pw}}$$

Integrating we get,

$$\int_{\theta_i}^{\theta_o} \frac{d\theta}{\theta} = \frac{-\ U_o\ (1 - C)}{m_w\ c_{pw}} \int_{0}^{A_o} dA_o$$

$$\ln \frac{\theta_o}{\theta_i} = \frac{-\ U_o\ A_o}{m_w\ c_{pw}}\ (1 - C) = -\ NTU\ (1 - C)$$

$$\text{Thus}\quad \frac{\theta_o}{\theta_i} = \exp\ (-\ NTU\ (1 - C))$$

$$\text{But}\ \frac{\theta_o}{\theta_i} = \frac{t_{wo} - t_{ai}}{t_{wi} - t_{ao}} = \frac{t_{wi} - t_{ai} - (t_{wi} - t_{wo})}{t_{wi} - t_{ai} - (t_{ao} - t_{ai})} \qquad (5)$$

From the definition of E we have

$$t_{wi} - t_{wo} = E\ (t_{wi} - t_{ai}) \qquad (6)$$

Also from heat balance

$$m_a\ c_{pma}\ (t_{ao} - t_{ai}) = m_w\ c_{pw}\ (t_{wi} - t_{wo}) = m_w\ c_{pw}\ E(t_{wi} - t_{ai})$$

$$\text{Thus}\ t_{ao} - t_{ai} = \frac{m_w\ c_{pw}\ E\ (t_{wi} - t_{ai})}{m_a\ c_{pma}}$$

Using the definition of C we get,

$$t_{ao} - t_{ai} = CE\ (t_{wi} - t_{ai}) \qquad (7)$$

Using Equations 6 and 7 in Equation 5 we get,

$$\frac{\theta_o}{\theta_i} = \frac{(t_{wi} - t_{ai})\ (1 - E)}{(t_{wi} - t_{ai})\ (1 - CE)}$$

Thus

$$\frac{\theta_o}{\theta_i} = \frac{1 - E}{1 - CE} = \exp\ (-\ NTU\ (1 - C)) \qquad (8)$$

$$1 - E = (1 - CE)\ \exp\ (-\ NTU\ (1 - C))$$

$$1 - \exp\ (-\ NTU\ (1 - C)) = E\ (1 - C\ \exp\ (-\ NTU\ (1 - C))$$

$$\therefore\quad E = \frac{1 - \exp\ (-\ NTU\ (1 - C))}{1 - C\ \exp\ (-\ NTU\ (1 - C))} \qquad (9)$$

If C = 1, Equation 9 becomes indeterminate. For this case Equation 7 becomes

$$t_{ao} - t_{ai} = E\ (t_{wi} - t_{ai}) \qquad (10)$$

From Equation 6,

$$t_{wi} - t_{wo} = E\ (t_{wi} - t_{ai})$$

$$\therefore\quad t_{ao} - t_{ai} = t_{wi} - t_{wo}$$

$$\therefore\quad t_{wo} - t_{ai} = t_{wi} - t_{ao} \qquad (11)$$

Thus

$$Q = U_o\ A_o\ (t_{wi} - t_{ao}) = m_w\ c_{pw}\ (t_{wi} - t_{wo})$$

$$\therefore\quad t_{wi} - t_{wo} = \frac{U_o\ A_o}{m_w\ c_{pw}}\ (t_{wi} - t_{ao})$$

$$\therefore\quad t_{wi} - t_{wo} = NTU\ (t_{wi} - t_{ao}) \qquad (12)$$

From the definition of E we have

$$\underline{E} = \frac{t_{wi} - t_{wo}}{t_{wi} - t_{ai}} = \frac{t_{wi} - t_{wo}}{(t_{wi} - t_{wo}) + (t_{wo} - t_{ai})} \qquad (13)$$

Using Equations 11 and 12, Equation 13 becomes

$$E = \frac{NTU\ (t_{wi} - t_{ao})}{NTU\ (t_{wi} - t_{ao}) + (t_{wi} - t_{ao})}$$

$$E = \frac{NTU}{NTU + 1}$$

APPENDIX A3.2

Derivation of Equations 3.106 and 3.107b

Consider an incremental area of a counterflow chilled water coil surface as shown in Fig. A3.2. The rate of heat transfer over the area dA_o can be expressed in three ways as follows:

$$dq_{ct} = U'_o \, \theta \, d \, A_o \qquad (1)$$

$$dq_{ct} = -m_w \, c_{pw} \, dt_w \qquad (2)$$

$$dq_{ct} = \frac{- m_a \, c_{pma} \, dt_a}{SHR} \qquad (3)$$

The reason for the negative signs in Equations 2 and 3 is that the rate of change of temperatures t_w and t_a with heat exchanger area is negative.

Let $\frac{m_a \, c_{pma}}{SHR}$ be the smaller thermal capacity, then

the definitions of NTU_c, C_c and E_c are

$$NTU_c = \frac{U'_o \, A_o \, SHR}{m_a \, c_{pma}} \qquad C_c = \frac{m_a \, c_{pma}}{SHR \, m_w \, c_{pw}} \qquad E_c = \frac{t_{ai} - t_{ao}}{t_{ai} - t_{wi}}$$

From Equations 2 and 3 we have,

$$dq_{ct} = - m_w \, c_{pw} \, dt_w = \frac{- m_a \, c_{pma} \, dt_a}{SHR}$$

$$\therefore \quad m_w \, c_{pw} \, dt_w \, SHR = m_a \, c_{pma} \, dt_a \qquad (4)$$

Now $\theta = t_a - t_w \qquad \therefore \quad d\theta = dt_a - dt_w$

$$m_a \, c_{pma} \, (dt_a - dt_w) = m_a \, c_{pma} \, dt_a - m_a \, c_{pma} \, dt_w$$

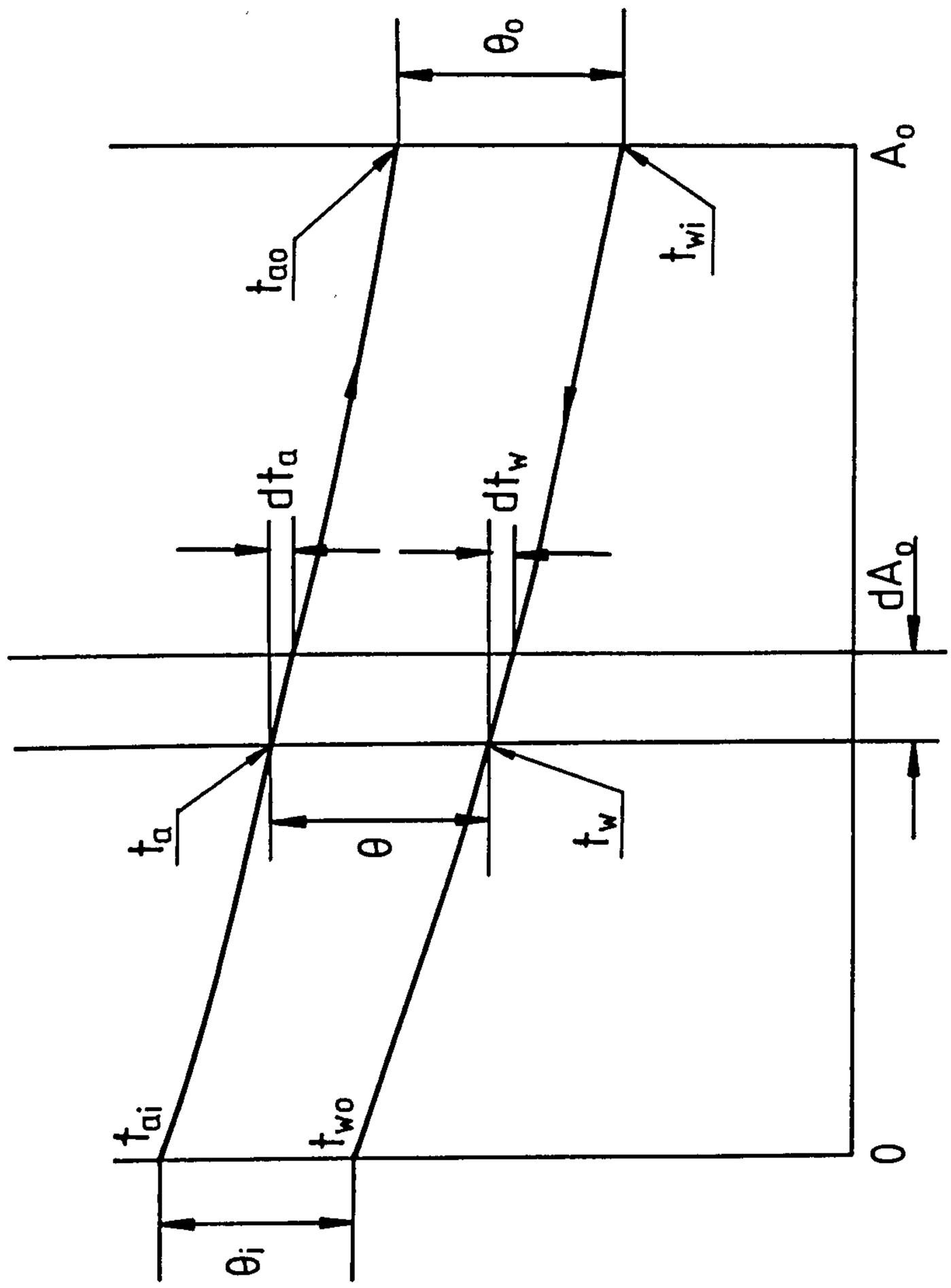

FIG. A3·2 TEMPERATURE DISTRIBUTION IN A COUNTERFLOW CHILLED WATER COIL

Using Equation 4 we get,

$$m_a\ c_{pma}\ (dt_a - dt_w) = m_w\ c_{pw}\ dt_w\ SHR - m_a\ c_{pma}\ dt_w$$
$$= dt_w\ (m_w\ c_{pw}\ SHR - m_a\ c_{pma})$$

Using Equation 2, dt_w may be eliminated to give

$$m_a\ c_{pma}\ (dt_a - dt_w) = -\ dq_{ct}\ \left(\frac{m_w\ c_{pw}\ SHR - m_a\ c_{pma}}{m_w\ c_{pw}}\right)$$

$$m_a\ c_{pma}\ d\theta = -\ dq_{ct}\ SHR\ \left(1 - \frac{m_a\ c_{pma}}{SHR\ m_w\ c_{pw}}\right)$$

$$m_a\ c_{pma}\ d\theta = -\ dq_{ct}\ SHR\ (1 - C_c)$$

Using Equation 1 to eliminate dq_{ct} gives

$$d\theta = \frac{-U_o'\ \theta\ dA_o}{m_a\ c_{pma}}\ SHR\ (1 - C_c)$$

$$\text{Thus}\quad \frac{d\theta}{\theta} = \frac{-U_o'\ SHR\ (1 - C_c)}{m_a\ c_{pma}} \times dA_o$$

Integrating we get

$$\int_{\theta_i}^{\theta_o} \frac{d\theta}{\theta} = \frac{-U_o'\ SHR\ (1 - C_c)}{m_a\ c_{pma}} \int_0^{A_o} dA_o$$

$$\ln \frac{\theta_o}{\theta_i} = \frac{-U_o'\ SHR\ (1 - C_c)\ A_o}{m_a\ c_{pma}} = -\ NTU_c\ (1 - C_c)$$

$$\text{Thus}\quad \frac{\theta_o}{\theta_i} = \exp\ (-\ NTU_c\ (1 - C_c)) \qquad (5)$$

$$\text{But}\quad \frac{\theta_o}{\theta_i} = \frac{t_{ao} - t_{wi}}{t_{ai} - t_{wo}} = \frac{(t_{ai} - t_{wi}) - (t_{ai} - t_{ao})}{(t_{ai} - t_{wi}) - (t_{wo} - t_{wi})} \qquad (6)$$

From the definition of E_c we have

$$t_{ai} - t_{ao} = E_c (t_{ai} - t_{wi}) \qquad (7)$$

From heat balance

$$\frac{m_a c_{pma} (t_{ai} - t_{ao})}{SHR} = m_w c_{pw} (t_{wo} - t_{wi})$$

$$\text{Thus } t_{wo} - t_{wi} = \frac{m_a c_{pma}}{SHR\ m_w c_{pw}} (t_{ai} - t_{ao})$$

Using the definition of C_c and Equation 7 we get

$$t_{wo} - t_{wi} = C_c E_c (t_{ai} - t_{wi}) \qquad (8)$$

Using Equations 7 and 8 in Equation 6 we get

$$\frac{\theta_o}{\theta_i} = \frac{(t_{ai} - t_{wi})(1 - E_c)}{(t_{ai} - t_{wi})(1 - C_c E_c)}$$

Thus

$$\frac{\theta_o}{\theta_i} = \frac{1 - E_c}{1 - C_c E_c} = \exp (- NTU_c (1 - C_c))$$

$$\therefore\ 1 - E_c = (1 - C_c E_c) \exp (- NTU_c (1 - C_c))$$

$$1 - \exp (- NTU_c (1 - C_c)) = E_c (1 - C_c \exp (- NTU_c (1 - C_c))$$

$$\therefore\ E_c = \frac{1 - \exp (- NTU_c (1 - C_c))}{1 - C_c \exp (- NTU_c (1 - C_c))} \qquad (9)$$

If $C_c = 1$, Equation 9 becomes indeterminate. For this case Equation 8 becomes

$$t_{wo} - t_{wi} = E_c (t_{ai} - t_{wi}) \qquad (10)$$

From Equation 7,

$$t_{ai} - t_{ao} = E_c (t_{ai} - t_{wi})$$

$$t_{wo} - t_{wi} = t_{ai} - t_{ao} \qquad (11a)$$

$$t_{ao} - t_{wi} = t_{ai} - t_{wo} \qquad (11b)$$

Thus

$$Q = U_o' A_o (t_{ai} - t_{wo}) = \frac{m_a c_{pma} (t_{ai} - t_{ao})}{SHR}$$

$$t_{ai} - t_{ao} = \frac{U_o' A_o (t_{ai} - t_{wo}) SHR}{m_a c_{pma}}$$

$$\therefore \quad t_{ai} - t_{ao} = NTU_C (t_{ai} - t_{wo}) \qquad (12)$$

From the definition of E_C we have

$$E_C = \frac{t_{ai} - t_{ao}}{t_{ai} - t_{wi}} = \frac{t_{ai} - t_{ao}}{(t_{ai} - t_{wo}) + (t_{wo} - t_{wi})} \qquad (13)$$

Using Equations 11a, 11b and 12, Equation 13 becomes

$$E_C = \frac{NTU_C (t_{ai} - t_{wo})}{(t_{ai} - t_{wo}) + NTU_C (t_{ai} - t_{wo})}$$

$$E_C = \frac{NTU_C}{NTU_C + 1}$$

APPENDIX A4.1

DERIVATION OF EQUATION 4.8

Consider a boiler equipped with on-off control of the fuel burner. The nominal full load steady state boiler efficiency measured with the burner operating continuously is η_{bf}.

Consider a time period θ_o during which the boiler is on and being controlled by a thermostat. This is represented in Fig. A4.1.

Let θ_u be the time that the burner must operate to provide the useful heat required by the HVAC system.

Let θ_s be the time that the burner must operate to compensate for the heat losses which occur during the period that the burner does not operate usefully.

Let θ_f be the total functioning time.

The part load ratio, PLR, is given by

$$PLR = \frac{\theta_u}{\theta_o} \qquad (1)$$

From the definition of stop loss factor, SLF, we have for a given period θ_o,

$$SLF = \frac{QBI \times \theta_s}{QBI \times (\theta_o - \theta_u)} = \frac{\theta_s}{\theta_o - \theta_u} \qquad (2)$$

From Equation 4.6, $PLEF = \frac{\eta_{bp}}{\eta_{bf}}$

But,

$$\eta_{bp} = \frac{\text{Heating energy delivered to HVAC system at part load}}{\text{Total heating energy consumed by burner at part load}}$$

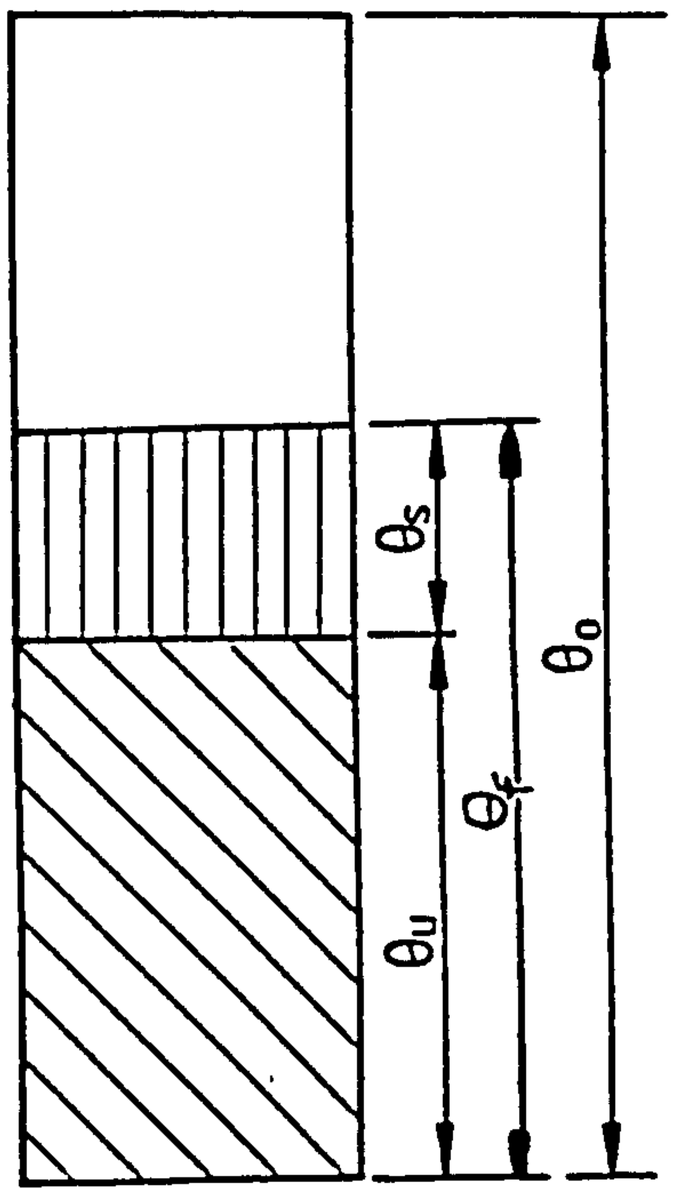

FIG. A 4·1 REPRESENTATION OF BOILER MATHEMATICAL MODEL

$$\eta_{bp} = \frac{\theta_u \ QBI}{\theta_f \ QBI} \cdot \eta_{bf}$$

$$\text{Thus } \eta_{bp} = \frac{\theta_u}{\theta_f} \cdot \eta_{bf} \qquad (3)$$

$$\text{Thus PLEF} = \frac{\eta_{bp}}{\eta_{bf}} = \frac{\theta_u}{\theta_f} \qquad (4)$$

From Equation 2,

$$SLF = \frac{\theta_s}{\theta_o - \theta_u} = \frac{\theta_f - \theta_u}{\theta_o - \theta_u}$$

$$\text{Thus, SLF } (\theta_o - \theta_u) = \theta_f - \theta_u \qquad (5)$$

$$\text{From Equation 1, } \theta_o = \frac{\theta_u}{PLR}$$

$$\text{From Equation 4, } \theta_f = \frac{\theta_u}{PLEF}$$

Substituting for θ_o and θ_f in Equation 5 we get,

$$SLF\left(\frac{\theta_u}{PLR} - \theta_u\right) = \frac{\theta_u}{PLEF} - \theta_u$$

Dividing throughout by θ_u we get,

$$SLF\left(\frac{1}{PLR} - 1\right) = \frac{1}{PLEF} - 1$$

Thus

$$\frac{1}{PLEF} = 1 + SLF\left(\frac{1}{PLR} - 1\right)$$

$$\text{Thus PLEF} = \frac{1}{1 + SLF\left(\frac{1}{PLR} - 1\right)}$$

APPENDIX A4.2

BOILERS

GUIDE TO FULL LOAD EFFICIENCY AND STOP LOSS FACTOR

On/off control only.

Ref.	TYPE OF BOILER	FULL LOAD EFFICIENCY	SLF
	Small natural-draught gas boilers 80°C maintained	72.0 - 79.0	0.025-0.055
10	Large natural-draught gas boilers 80°C maintained	76.2	0.023
	Large forced-draught gas boilers 80°C maintained	80.9	0.007
6	Oil pressure jet	74.0	0.04
	Wall flame oil	70.0	0.06
7	Gas 88 kW on off	77.0	0.04
	Concord	75.0	Not
11	Fuelsaver	76.5	Available
	Average efficiency 1981	77.0	
9	Low thermal capacity (small boiler)	75.5 - 76.5	0.014-0.022
	High thermal capacity (small boiler)	71.2	0.02
4	Sectional CI forced draught gas	76.6	0.02
	Sectional CI natural draught gas	73.1	0.04
8	Average gas and oil fired boilers domestic to large	Not Available	0.05

12	Shell type oil fired boiler	77.6	0.03

Efficiencies fall between 70.0% and 80%

SLF fall between 0.01 and 0.06

APPENDIX A4.3

TABLE 1

Catalogue Data for 70.3 kW Reciprocating Water Chiller (Full Load)

TWC1 (^{o}C)	TWE2 (^{o}C)	QE (kW)	P (kW)
23.9	4.4	70.3	19.4
23.9	5.6	72.8	19.7
23.9	6.7	75.6	19.9
23.9	7.8	77.7	20.1
23.9	8.9	79.5	20.3
23.9	10.0	81.6	20.6
26.7	4.4	68.2	20.0
26.7	5.6	70.7	20.3
26.7	6.7	73.5	20.5
26.7	7.8	75.6	20.7
26.7	8.9	77.7	21.0
26.7	10.0	79.5	21.2
29.4	4.4	66.1	20.7
29.4	5.6	68.9	21.0
29.4	6.7	71.4	21.1
29.4	7.8	73.8	21.4
29.4	8.9	75.9	21.7
29.4	10.0	78.1	21.9
32.2	4.4	64.0	21.4
32.2	5.6	66.5	21.7
32.2	6.7	69.3	21.9
32.2	7.8	71.7	22.3
32.2	8.9	73.8	22.6
32.2	10.0	76.3	22.8
35.0	4.4	61.9	22.2
35.0	5.6	64.3	22.5
35.0	6.7	67.2	22.8
35.0	7.8	69.6	23.2
35.0	8.9	72.1	23.5
35.0	10.0	74.5	23.8

TABLE 2

Experimental Part Load Data for 70.3 kW Reciprocating Water Chiller

TWC1 (^{o}C)	TWE2 (^{o}C)	QEPL (kW)	PPL (kW)
24.3	6.6	70.0	19.0
24.0	7.0	63.6	17.6
25.4	6.6	61.2	17.7
29.8	6.6	51.0	17.9
28.4	7.4	49.2	17.3
27.8	7.8	40.8	15.9
27.9	7.4	40.4	15.3
28.3	7.6	34.8	13.9
26.1	8.5	19.7	9.2

Tables 1 and 2 are taken from Ref. 19

APPENDIX A4.4

TABLE 1 Factors of Merit for Forced-Draught Cooling Towers

Type of Cooling Tower		Typical values of Factor of Merit FOM
Sprays located in a horizontal tunnel, with no packing	Single-stage Two-stage Three-stage	0.4 to 0.5 0.45 to 0.55 0.55 to 0.65
Vertical spray-filled tower, no packing	High water loading Low water loading	0.5 to 0.6 0.6 to 0.7
Vertical, with packing	High water loading Low water loading	0.55 to 0.65 0.65 to 0.75
Industrial packed towers		0.6 to 0.7
Industrial, densely packed towers having perhaps a high pressure loss		0.7 to 0.8
Natural-draught large cooling towers as used by ESCOM at power stations		0.65 to 0.75

Table 1 is taken from Ref. 26

APPENDIX A5

SPECIFICATION OF VAV SYSTEM COMPONENTS

A5.1 HEATING COIL

Geometrical Data

Heat exchanger consists of circular tubes with continuous fins having the following characteristic data:

Surface designation: 7.75 - 5/8T

Tube arrangement : staggered

Tube vertical spacing	38.1mm
Tube horizontal spacing	44.45mm
Tube outside diameter	17.17mm
Tube inside diameter	15.17mm
Fin spacing	3.227mm
Fin thickness	0.406mm
Hydraulic diameter	3.86mm
Free flow area/Face area	0.4812
Fin area/Air side area	0.95

Coil Data

Face area	$2.4m^2$
Air side area	$118.8m^2$
Water side area	$6.0m^2$
No. of water circuits	40
No. of rows of tubes	2

Heat Transfer Performance

Air side heat transfer coefficient, h_o, can be calculated using Equation 3.77 with C_1 and C_2 having the values 0.1036 and - 0.35804 respectively.

Water side heat transfer coefficient, h_w, can be calculated using Equation 3.80 for laminar flow and Equation 3.81 for turbulent flow.

Other Data

Water flow temperature	40.6°C
Maximum water mass flow rate	2.4 kg/s

A5.2 COOLING COIL

Geometrical Data

as for heating coil

Coil Data

Face area	$2.88m^2$
Air side area	$284.70m^2$
Water side area	$14.40m^2$
No. of water circuits	40
No. of rows of tubes	4

Heat Transfer Performance

Compute the air and water side heat transfer coefficients as for the heating coil.

Other Data

Water flow temperature	4.4°C
Water maximum mass flow rate	4.1kg/s

A5.3 HUMIDIFIER

The humidifier is of the wetted cell type and can be considered to have a constant effectiveness of 0.9. The water pump electrical consumption is 0.120kW when humidifier is on.

A5.4 SUPPLY AIR FAN

The supply air fan is of the axial flow type. The fan motor efficiency is assumed to be 90%. The fan has the following characteristic data:

FAN CHARACTERISTICS

VOLUME FLOW RATE (m^3/s)	ABSORBED POWER (kW)
1.24	1.431
1.5	1.930
2.0	2.824
2.5	3.729
3.0	4.701
3.5	5.759
4.0	6.897
4.5	8.092
5.0	9.337
5.5	10.678
6.0	12.233
6.2	12.953

A5.5 SUPPLY AIR DUCT

The supply air duct is assumed to have an overall UA value of 1.002 kW/K.

A5.6.1 OUTSIDE AIR TEMPERATURE AND RELATIVE HUMIDITY FOR SEPTEMBER 7 1981

Time (h)	Outside Air Temperature (°C)	Relative Humidity (%)
1	14.463	84.635
2	13.938	88.951
3	13.750	91.256
4	13.963	89.712
5	13.495	91.422
6	12.725	94.790
7	12.463	96.134
8	12.675	95.780
9	14.495	91.338
10	16.100	87.440

Time (h)	Outside Air Temperature (°C)	Relative Humidity (%)
11	17.488	77.203
12	19.038	68.761
13	20.588	62.601
14	21.625	56.881
15	22.825	53.625
16	23.499	50.083
17	23.675	47.201
18	23.725	49.302
19	23.025	51.095
20	21.675	54.384
21	19.493	62.117
22	19.338	64.988
23	19.225	66.341
24	18.813	70.030

A5.6.2 OUTSIDE AIR TEMPERATURE AND RELATIVE HUMIDITY FOR NOVEMBER 4 1981

Average values on the hour

TIME (h)	OUTSIDE AIR TEMPERATURE (°C)	RELATIVE HUMIDITY (%)
1	10.100	78.141
2	8.950	81.862
3	8.750	83.833
4	8.713	82.863
5	7.475	84.531
6	6.725	87.565
7	5.563	94.925
8	5.800	92.934
9	6.263	93.080
10	9.225	83.645
11	10.638	75.062
12	12.150	68.734
13	13.438	65.901

TIME (h)	OUTSIDE AIR TEMPERATURE (°C)	RELATIVE HUMIDITY (%)
14	14.125	65.945
15	14.863	61.325
16	15.688	60.236
17	14.863	60.247
18	14.388	60.698
19	11.688	74.352
20	10.250	84.000
21	10.513	80.736
22	9.775	82.738
23	9.262	85.198
24	8.425	86.147

A5.7 ROOM CONDITIONS

Average values on the hour

TIME (h)	DRY BULB TEMPERATURE (°C)	RELATIVE HUMIDITY (%)
1	20.02	50.11
2	20.12	50.79
3	20.31	52.09
4	20.59	53.93
5	20.93	56.18
6	21.30	58.70
7	21.70	61.30
8	22.07	63.82
9	22.41	66.07
10	22.69	67.91
11	22.88	69.21
12	22.98	69.89
13	22.98	69.89
14	22.88	69.21

TIME (h)	DRY BULB TEMPERATURE (°C)	RELATIVE HUMIDITY (%)
15	22.69	67.91
16	22.41	66.07
17	22.07	63.82
18	21.70	61.30
19	21.30	58.70
20	20.93	56.18
21	20.59	53.93
22	20.31	52.09
23	20.12	50.79
24	20.02	50.11

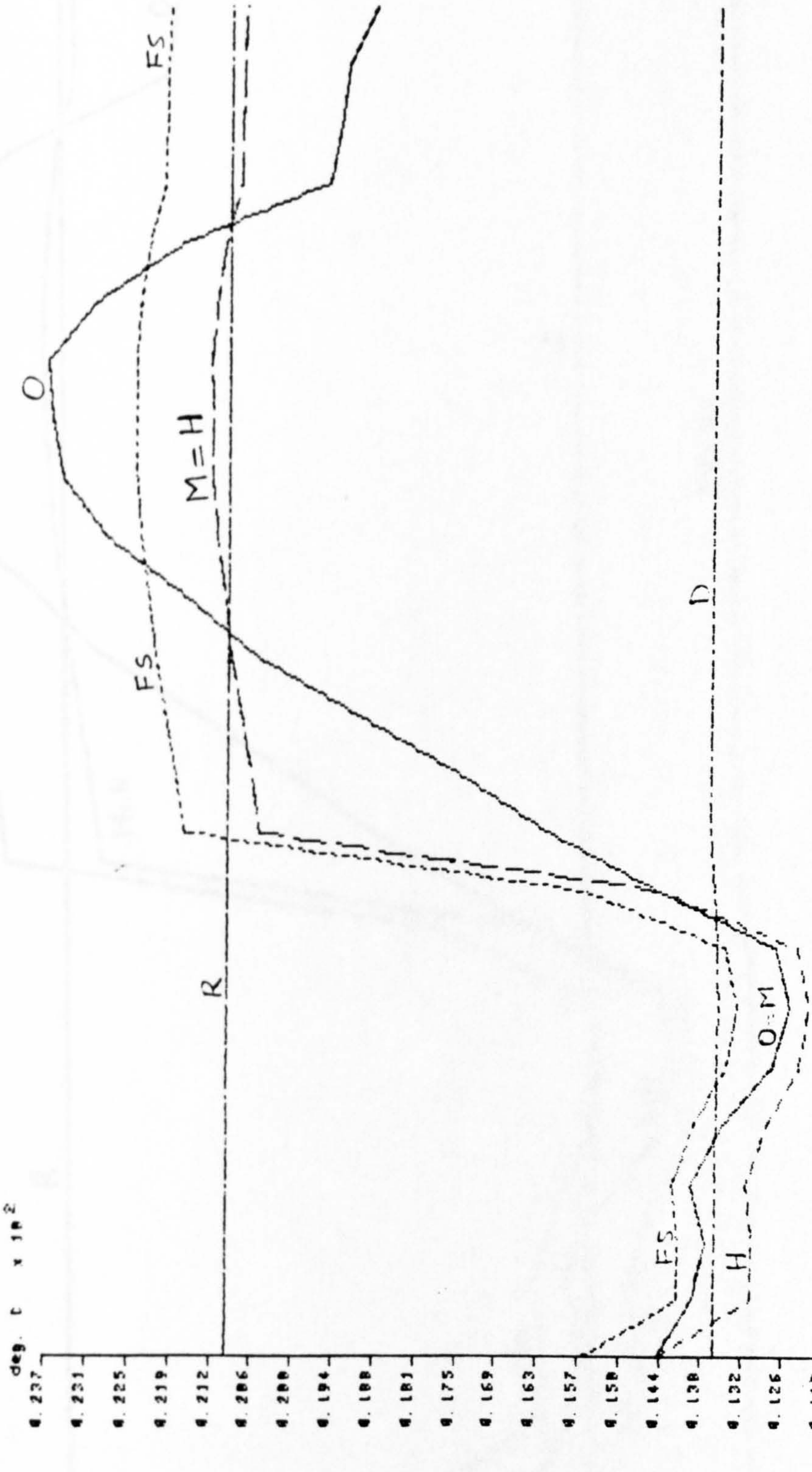

FIG. A5.1A DRY BULB TEMPERATURE PROFILES - EXERCISE 1.2 SEPTEMBER 7

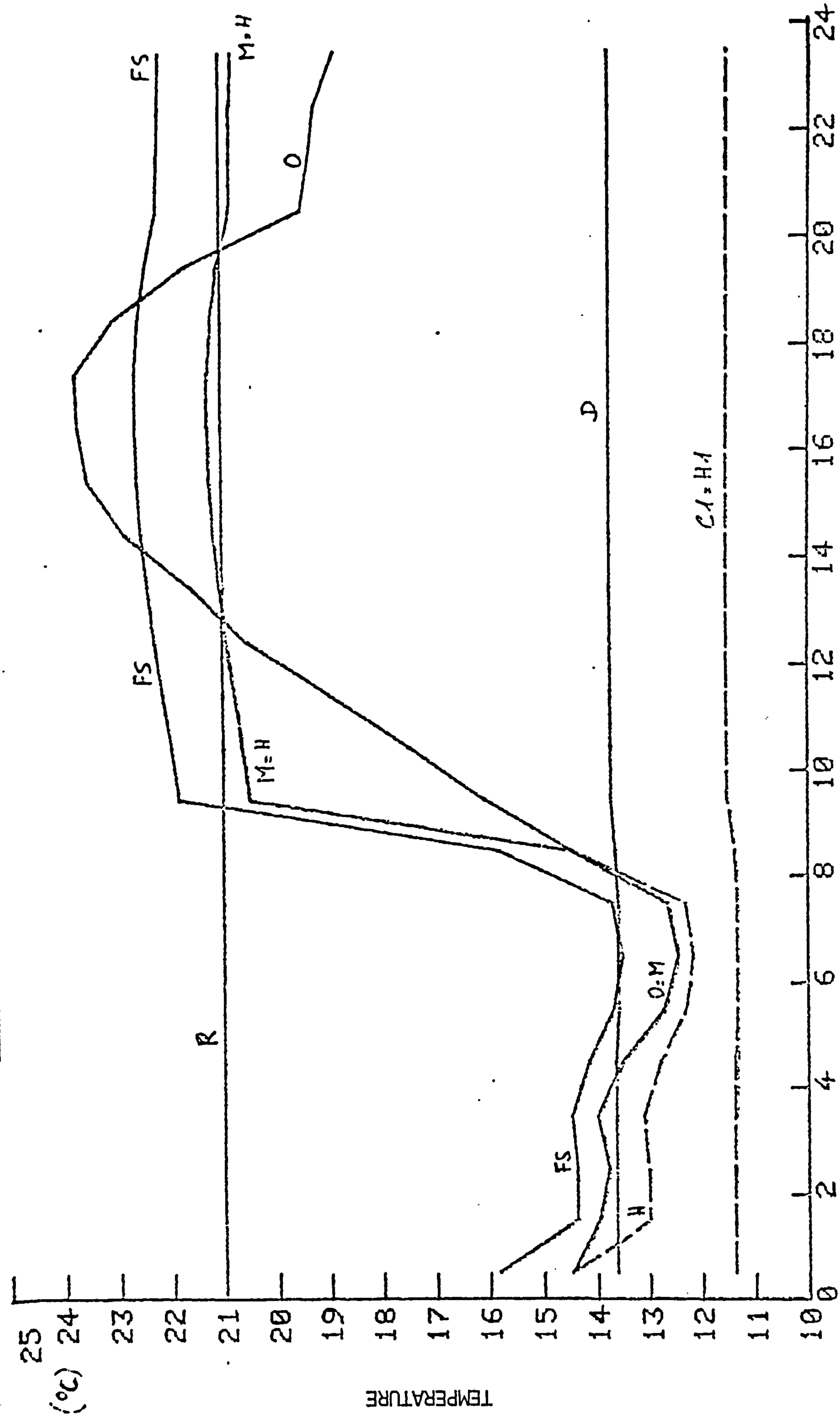

FIG. A5.1B DRY BULB TEMPERATURE PROFILES - EXERCISE 1.2 SEPTEMBER 7

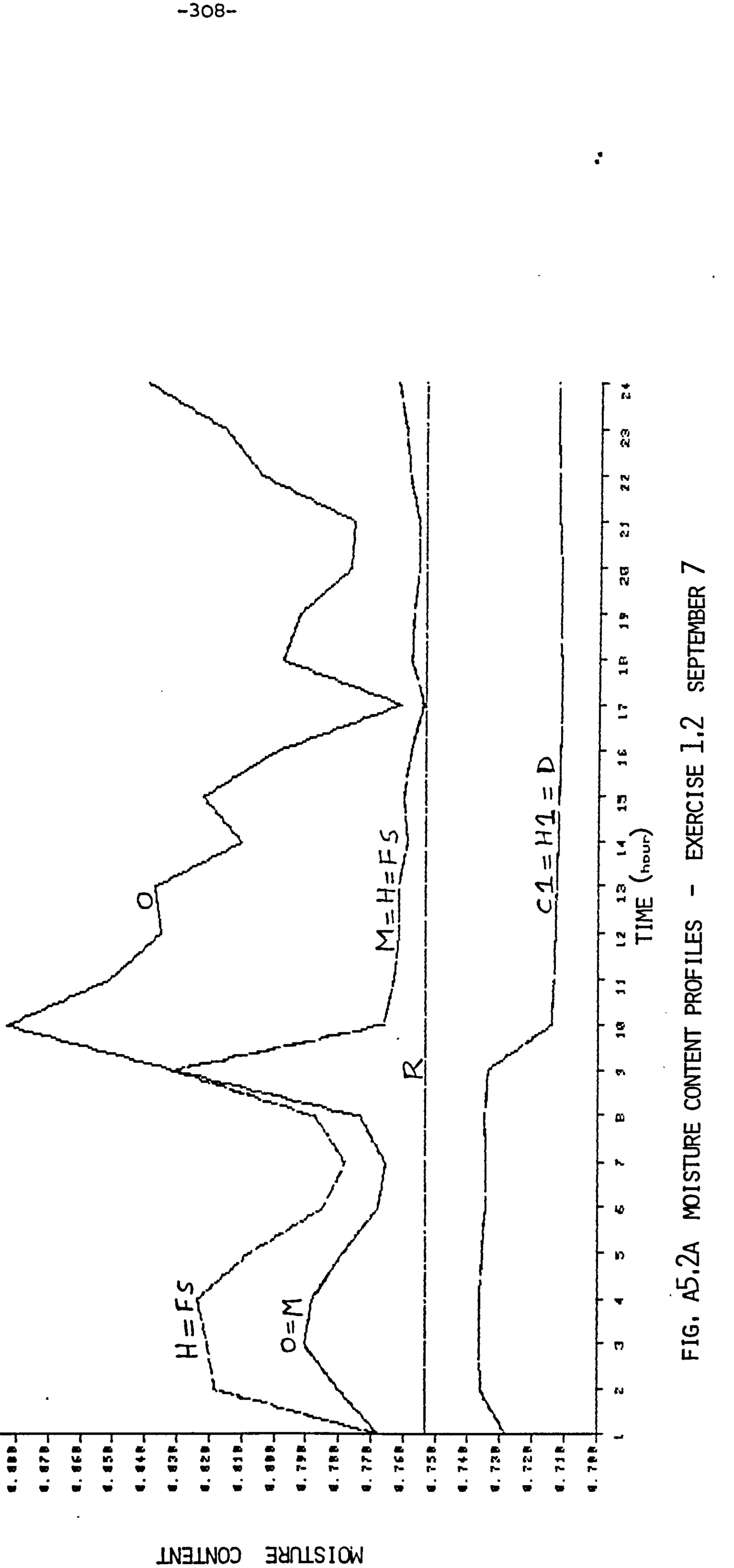

FIG. A5.2A MOISTURE CONTENT PROFILES - EXERCISE 1.2

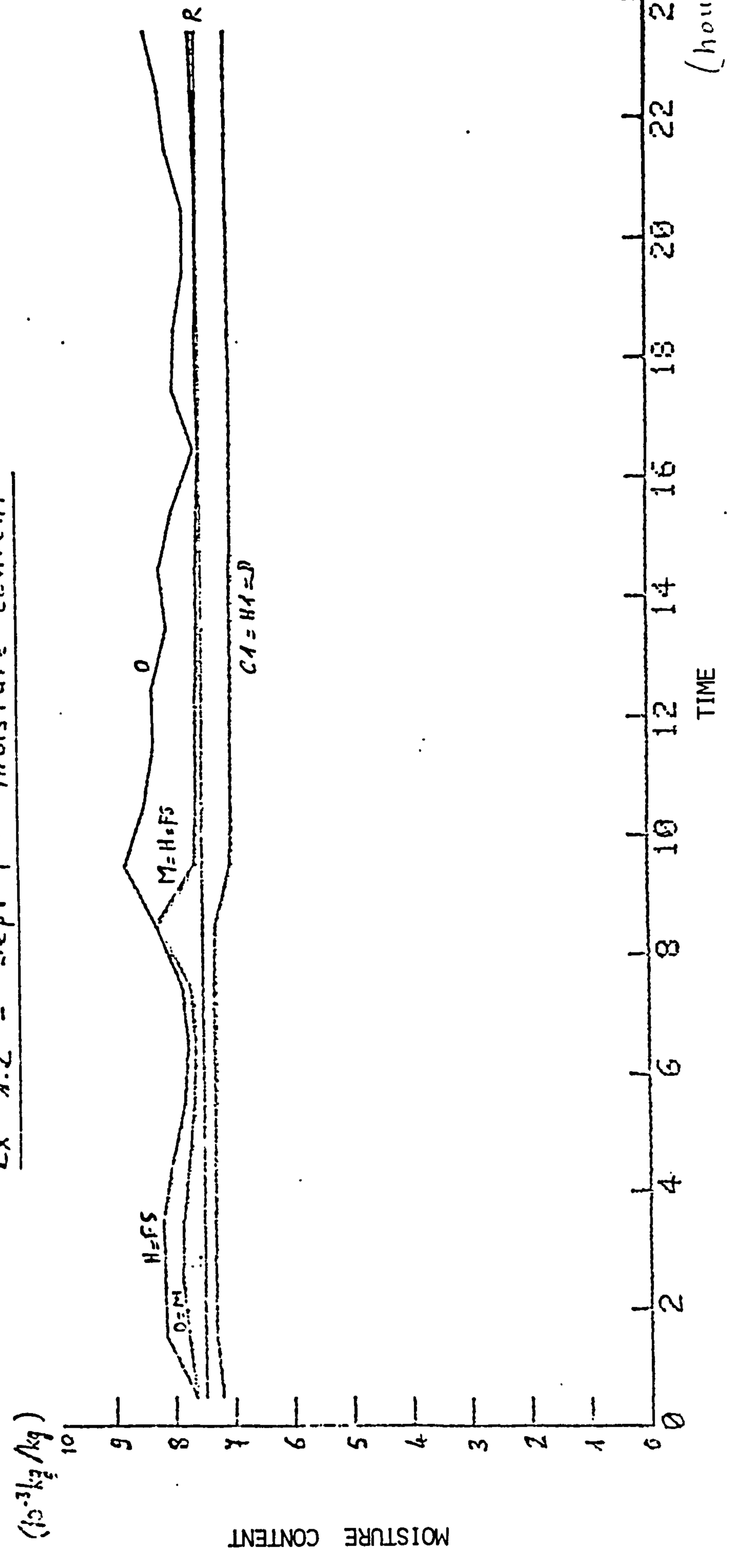

FIG. A5.2B MOISTURE CONTENT PROFILES - EXERCISE 1.2 SEPTEMBER 7

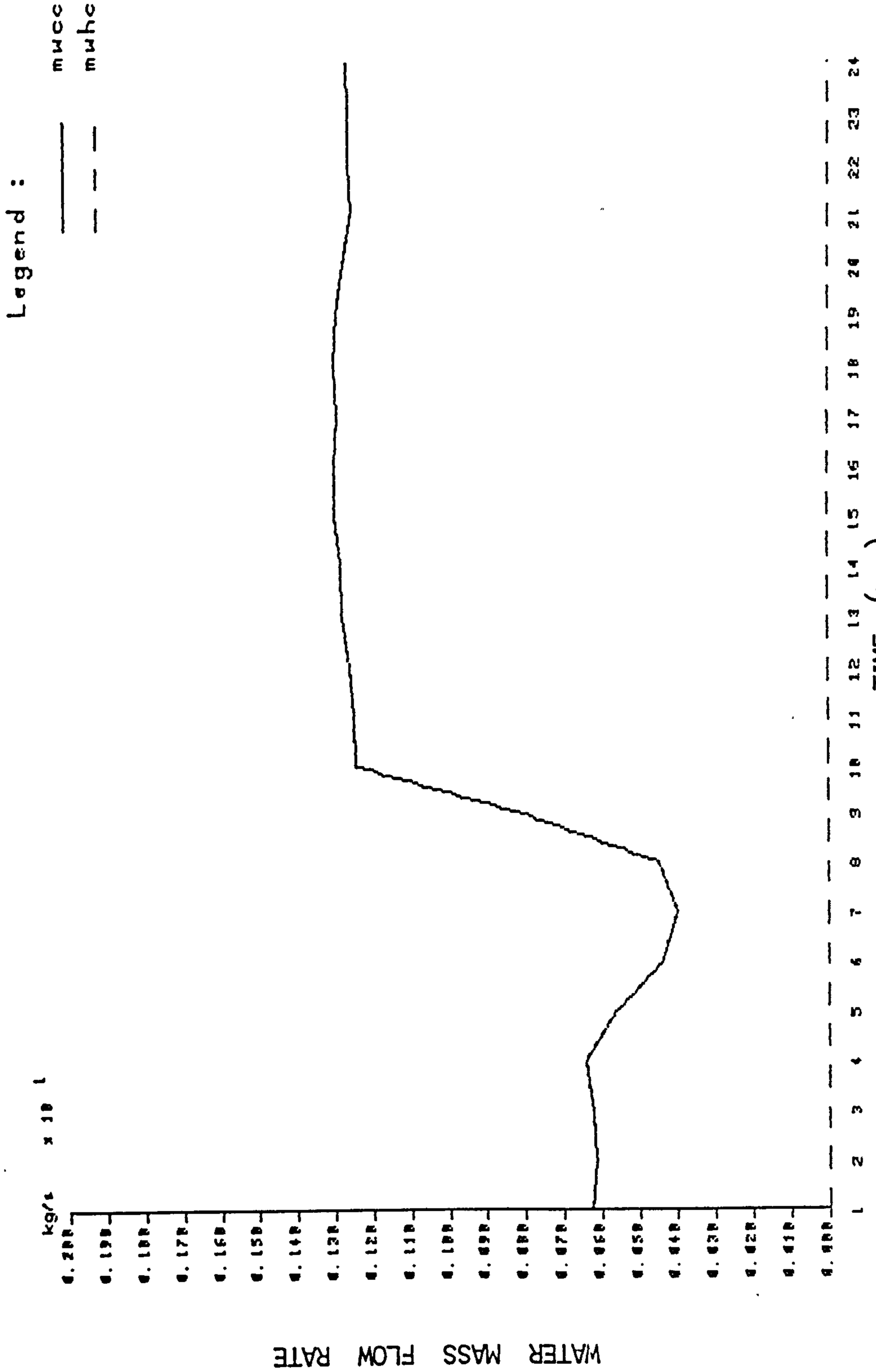

FIG. A5.3A MASS FLOW RATES OF WATER THROUGH COILS - EXERCISE 1.2 SEPTEMBER 7

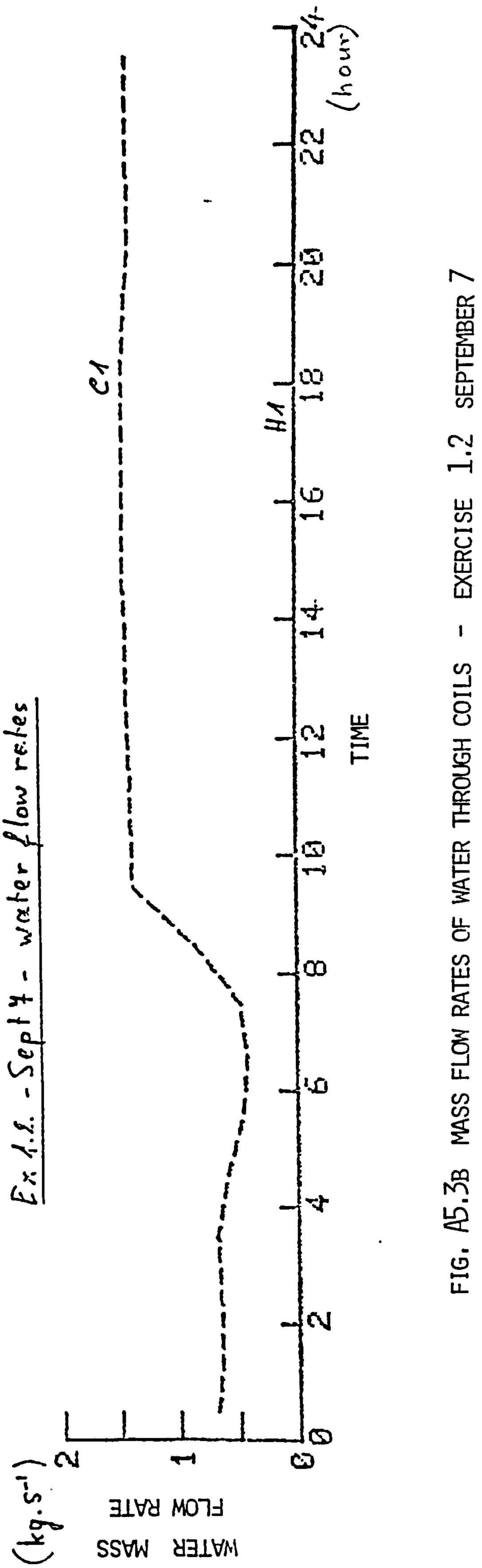

FIG. A5.3B MASS FLOW RATES OF WATER THROUGH COILS - EXERCISE 1.2 SEPTEMBER 7

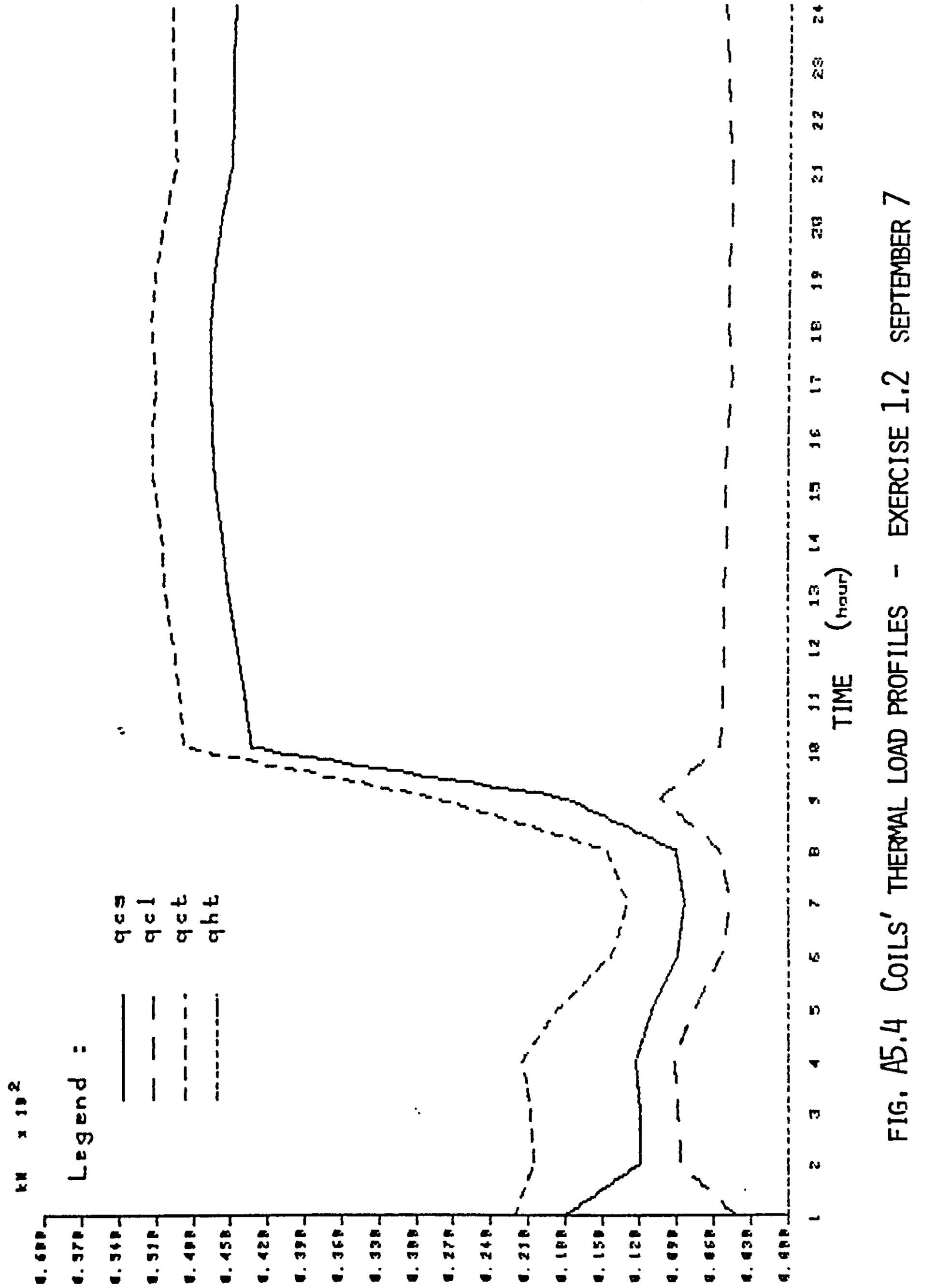

FIG. A5.4 COILS' THERMAL LOAD PROFILES - EXERCISE 1.2 SEPTEMBER 7

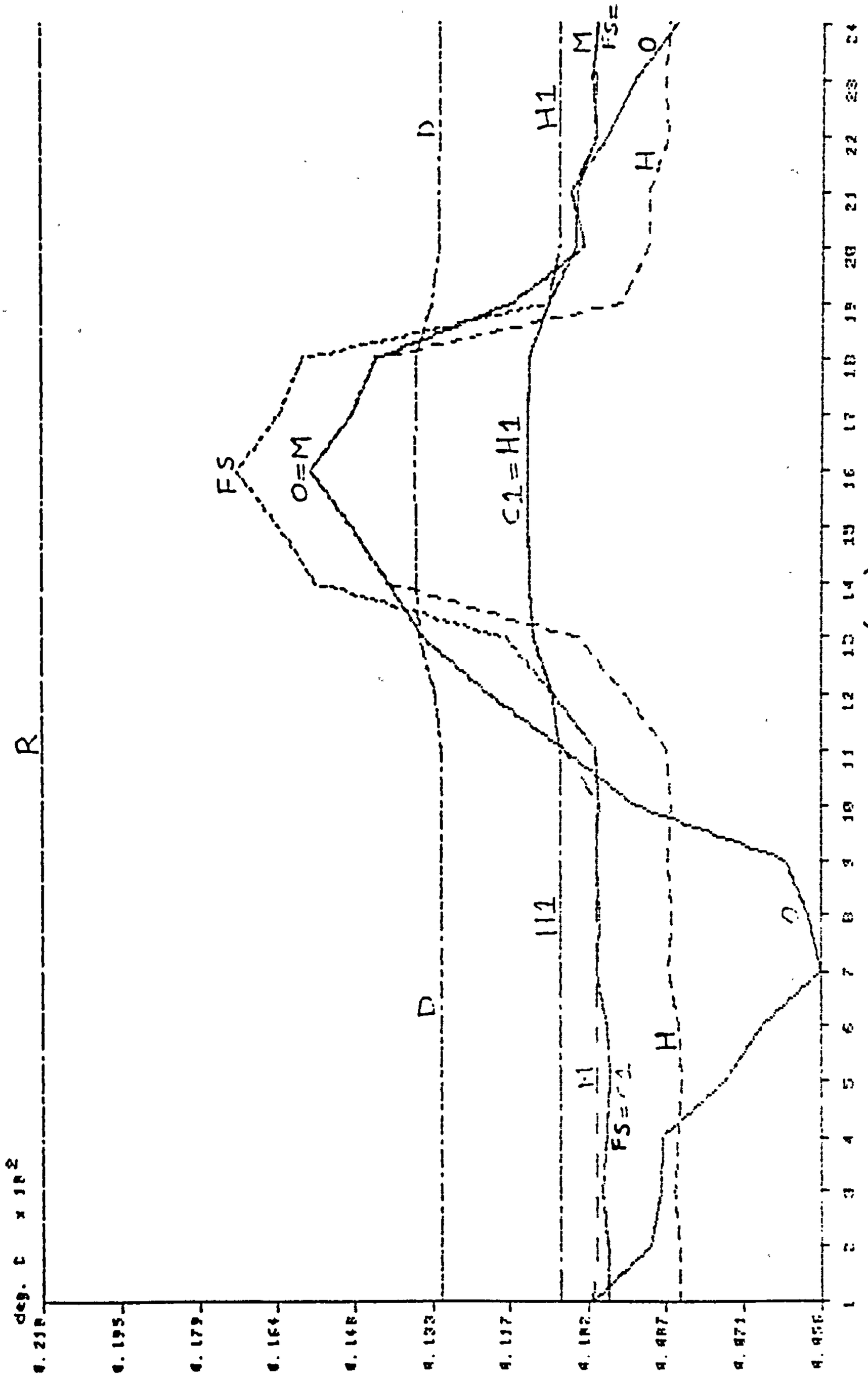
DRY BULB TEMPERATURE PROFILES - EXERCISE 1.2 NOVEMBER 4
TIME (hour)
TEMPERATURE
deg. C x 10^2
FS
O=M
C1=H1
D
H1
H
R
C
1-1
FS=C1

FIG. A5.5A

Ex. 1.2. - Nov. 4 - temperatures

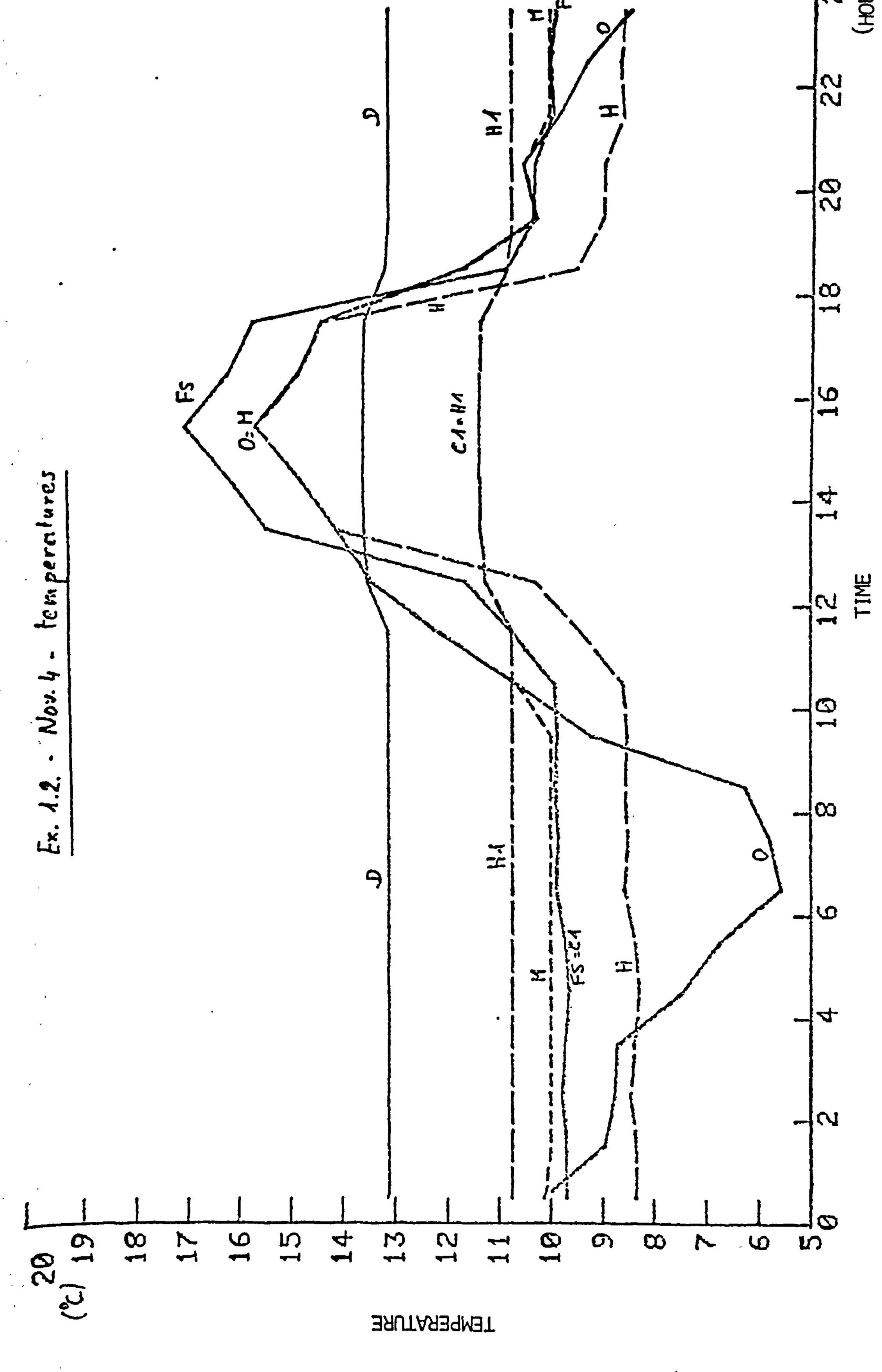

FIG. A5.5B DRY BULB TEMPERATURE PROFILES - EXERCISE 1.2 NOVEMBER 4

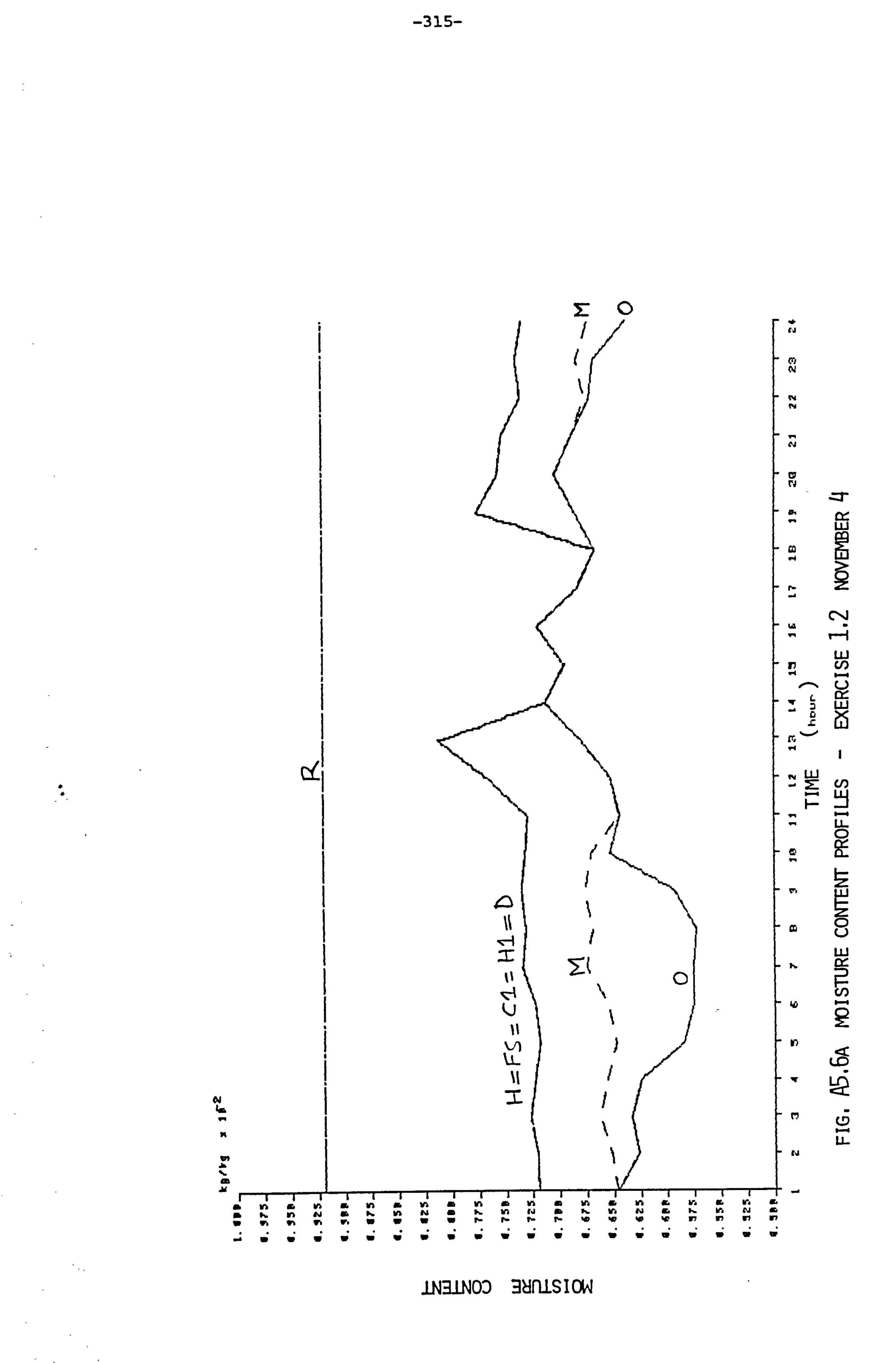

FIG. A5.6A MOISTURE CONTENT PROFILES - EXERCISE 1.2 NOVEMBER 4

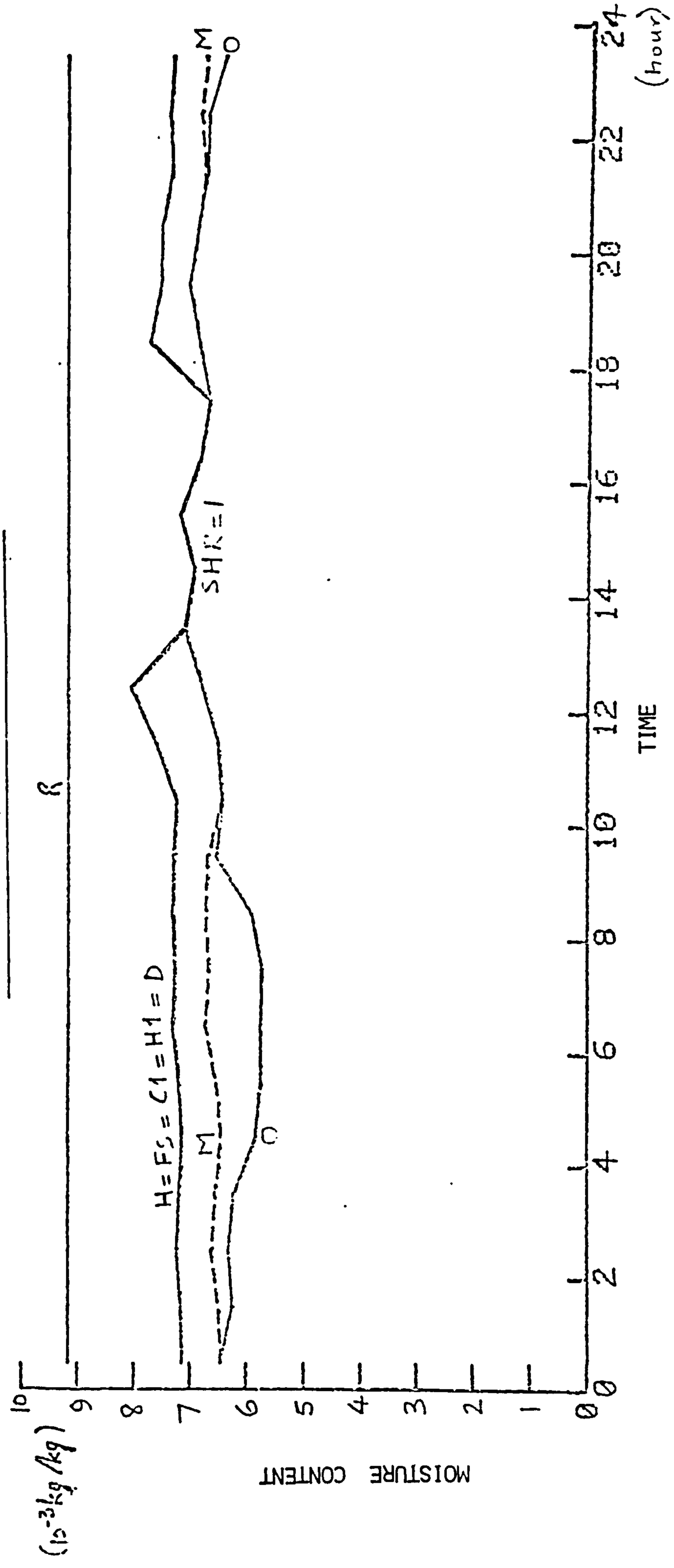

FIG. A5.6B MOISTURE CONTENT PROFILES - EXERCISE 1.2 NOVEMBER 4

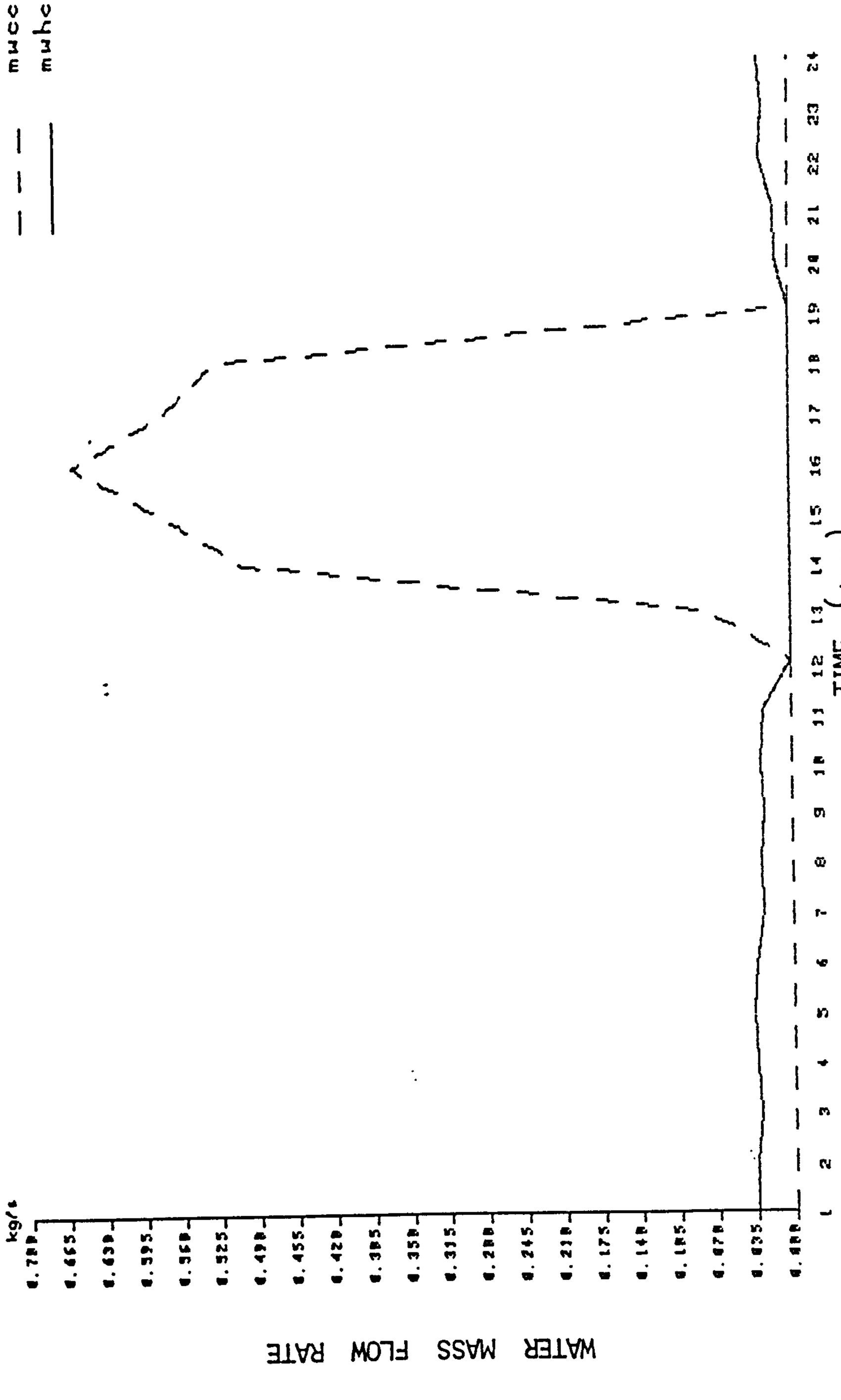

FIG. A5.7A MASS FLOW RATES OF WATER THROUGH COILS - EXERCISE 1,2 NOVEMBER 4

Ex. 1.2 - Nov. 4 - water flow rates

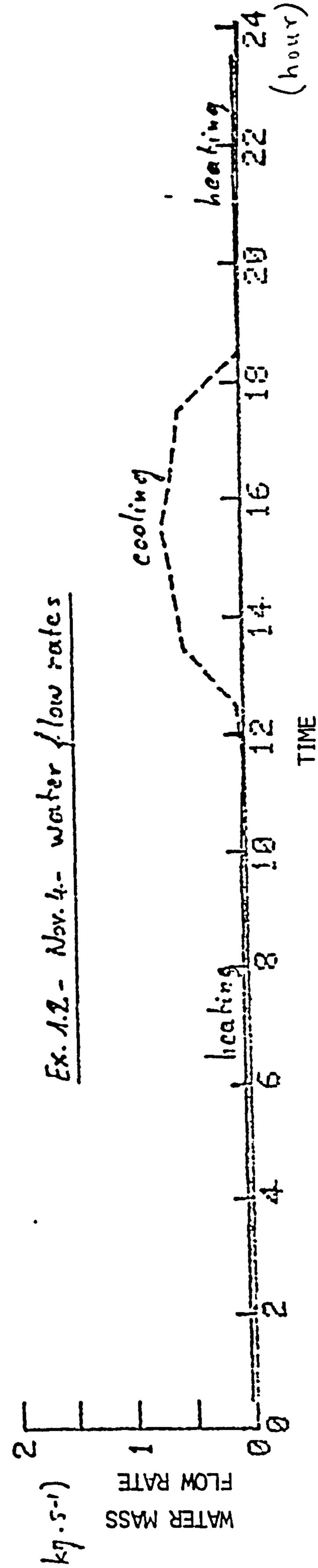

FIG. A5.7B - EXERCISE 1.2 NOVEMBER 4 - MASS FLOW RATES OF WATER THROUGH COILS

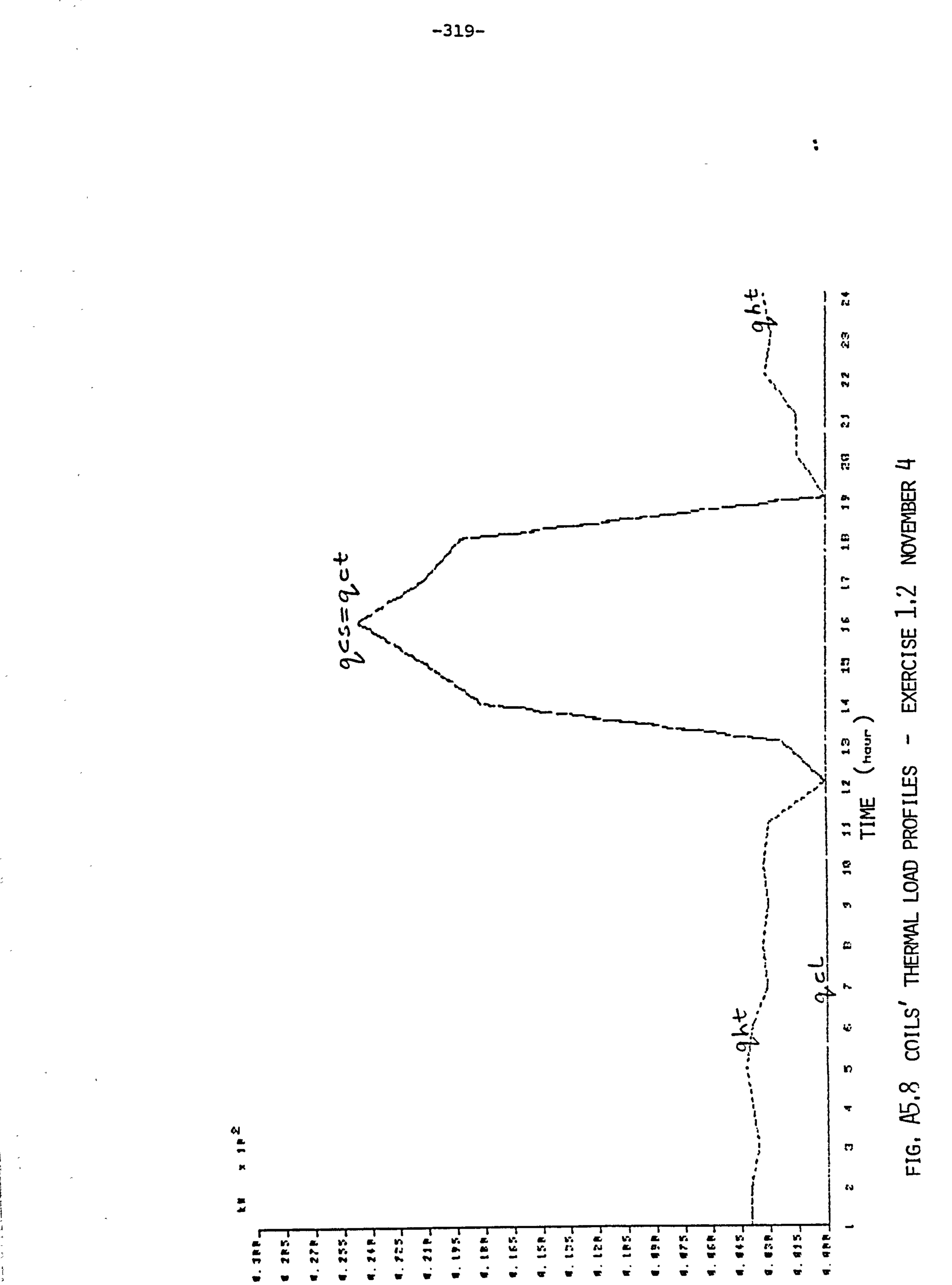

FIG. A5.8 COILS' THERMAL LOAD PROFILES - EXERCISE 1,2 NOVEMBER 4

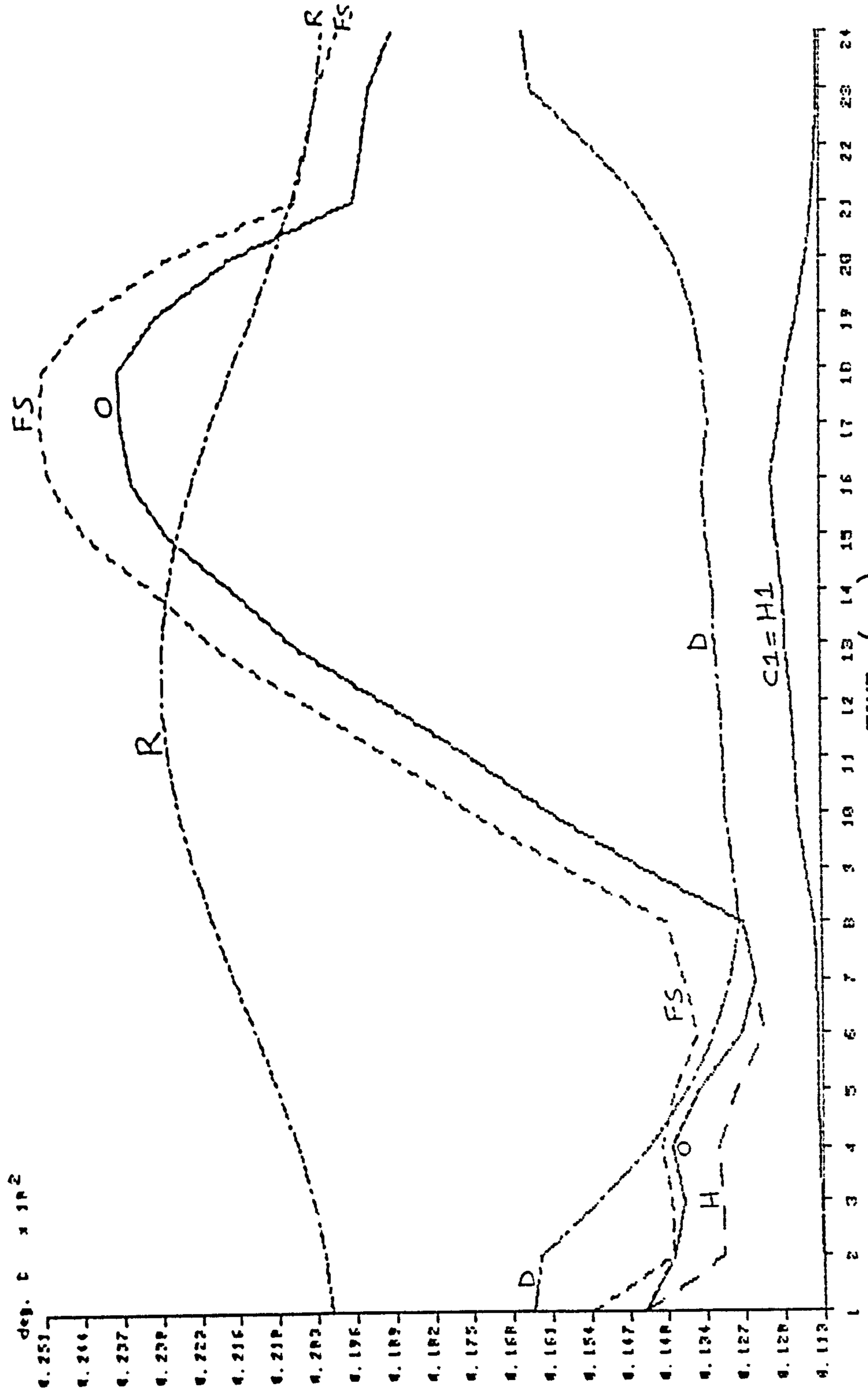

FIG. A5.9A DRY BULB TEMPERATURE PROFILES - EXERCISE 1.3 SEPTEMBER 7

Ex. 1.3. - Sept. 7 - temperatures

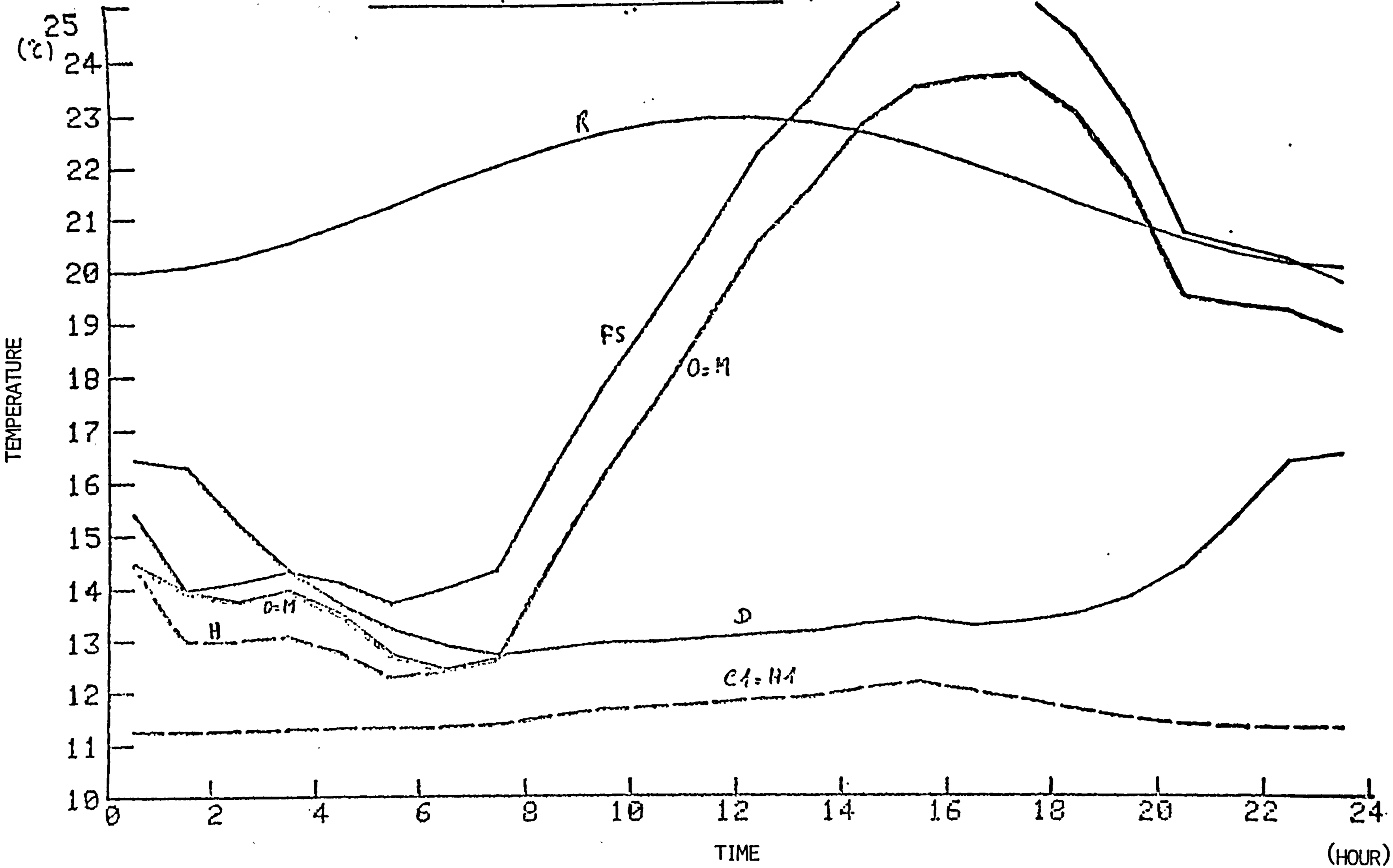

FIG. A5.9B DRY BULB TEMPERATURE PROFILES - EXERCISE 1.3 SEPTEMBER 7

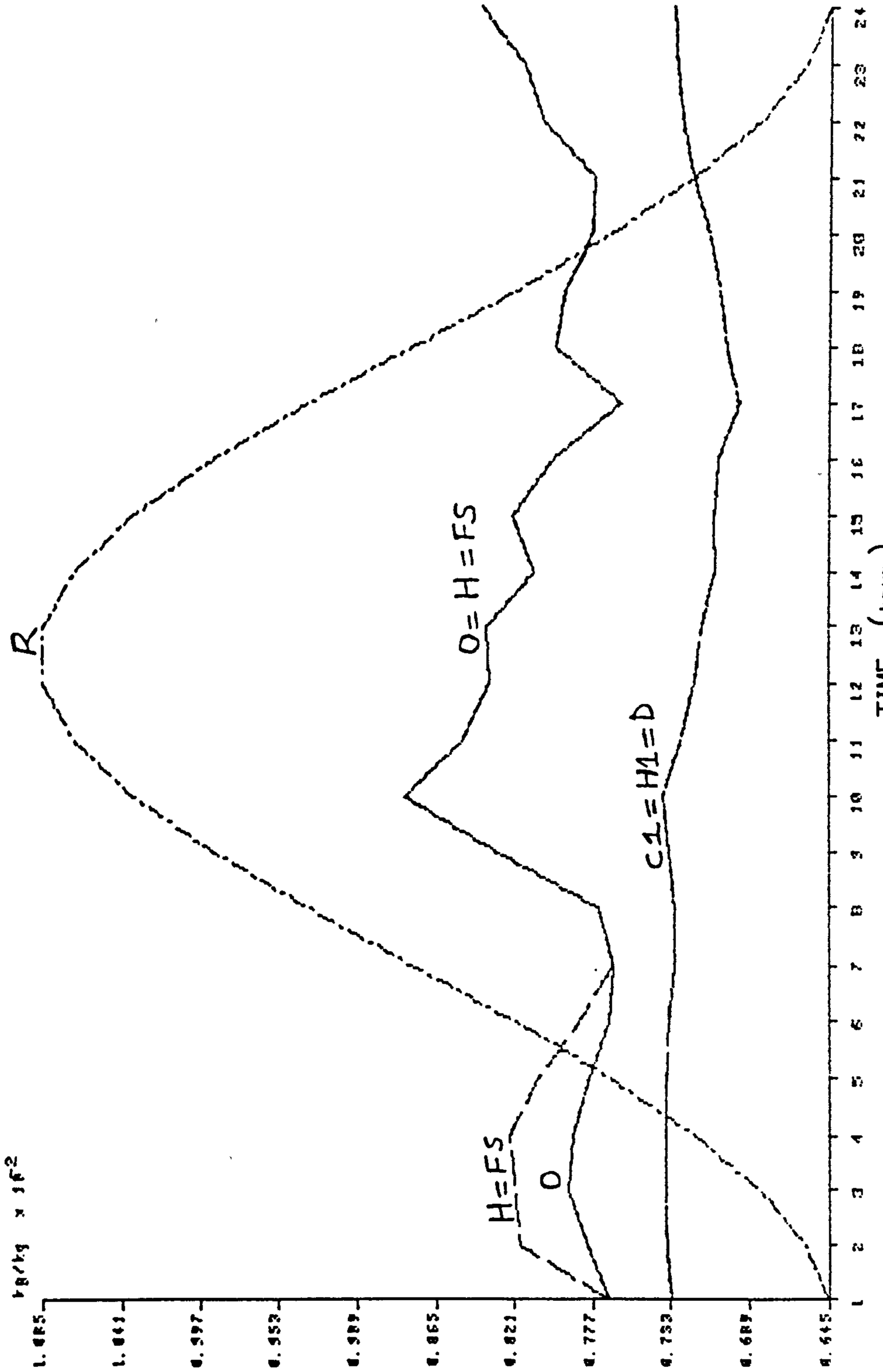

FIG. A5.10A - EXERCISE 1,3 SEPTEMBER 7

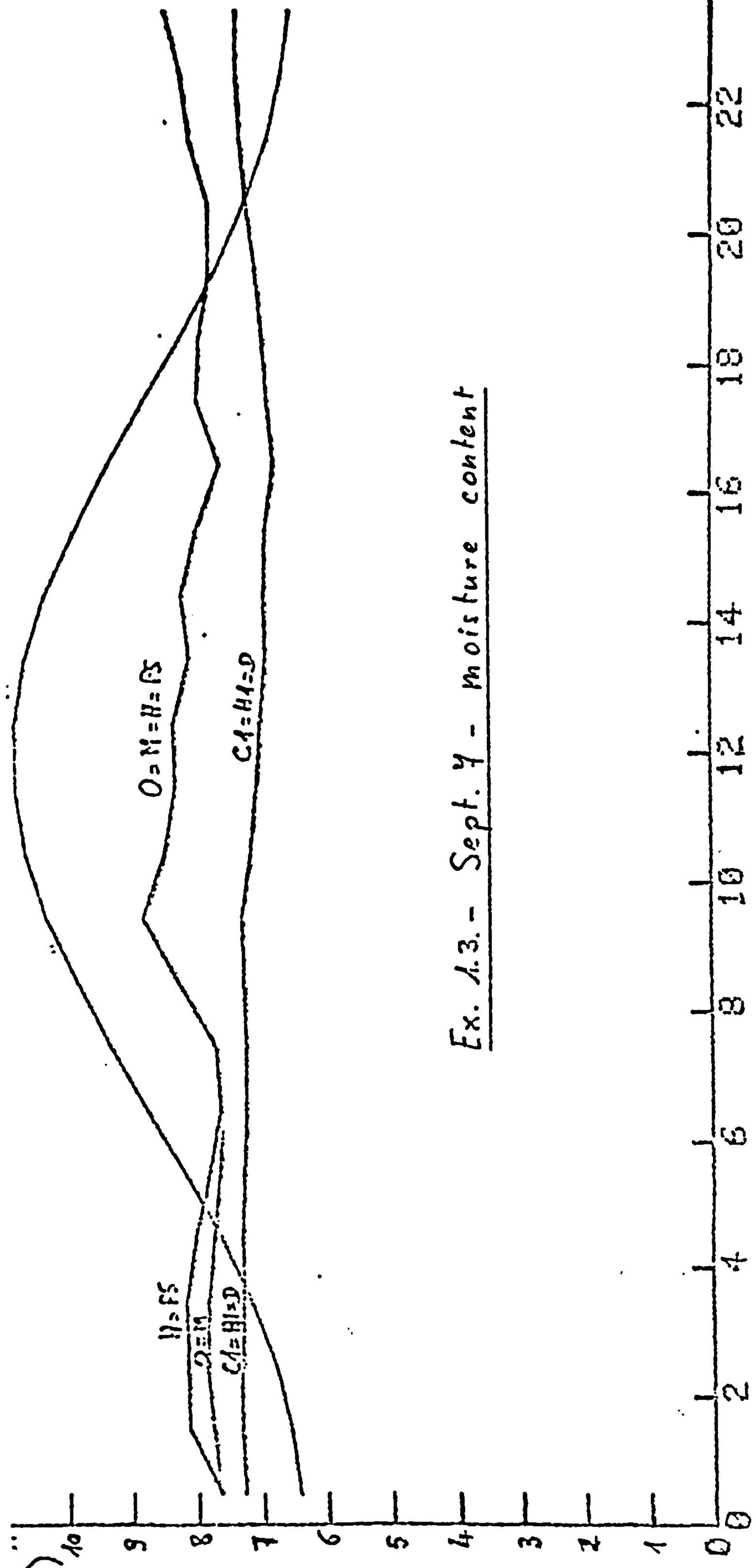

FIG. A5.10B MOISTURE CONTENT PROFILES - EXERCISE 1.3 SEPTEMBER 7

FIG. A5.11A MASS FLOW RATES OF WATER THROUGH COILS - EXERCISE 1,3 SEPTEMBER 7

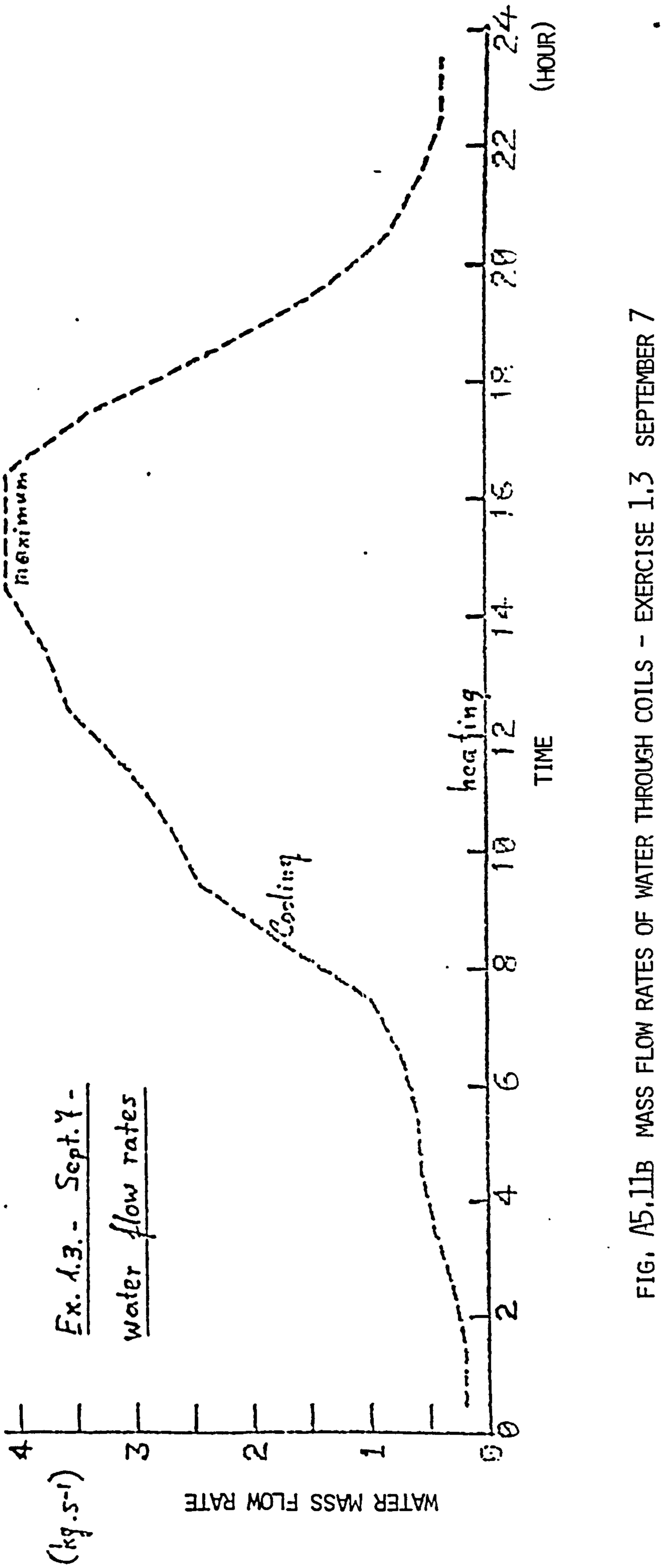

FIG. A5.11B MASS FLOW RATES OF WATER THROUGH COILS - EXERCISE 1.3 SEPTEMBER 7

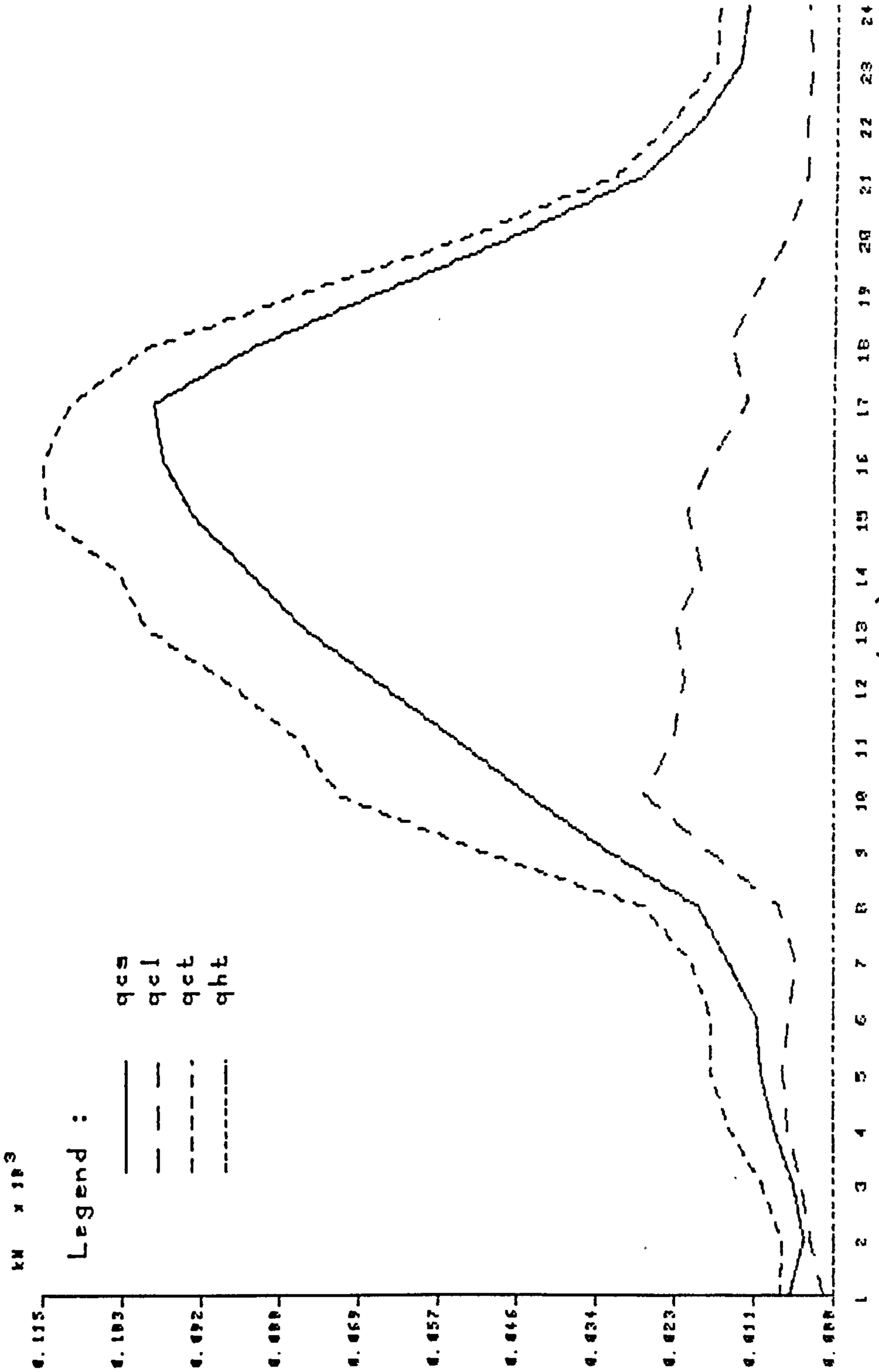
COILS' THERMAL LOAD PROFILES - EXERCISE 1,3 SEPTEMBER 7
TIME (hour)
COIL THERMAL LOAD
kW x 10^3
Legend :
qcs
qcl
qct
qht

FIG. A5.12 C

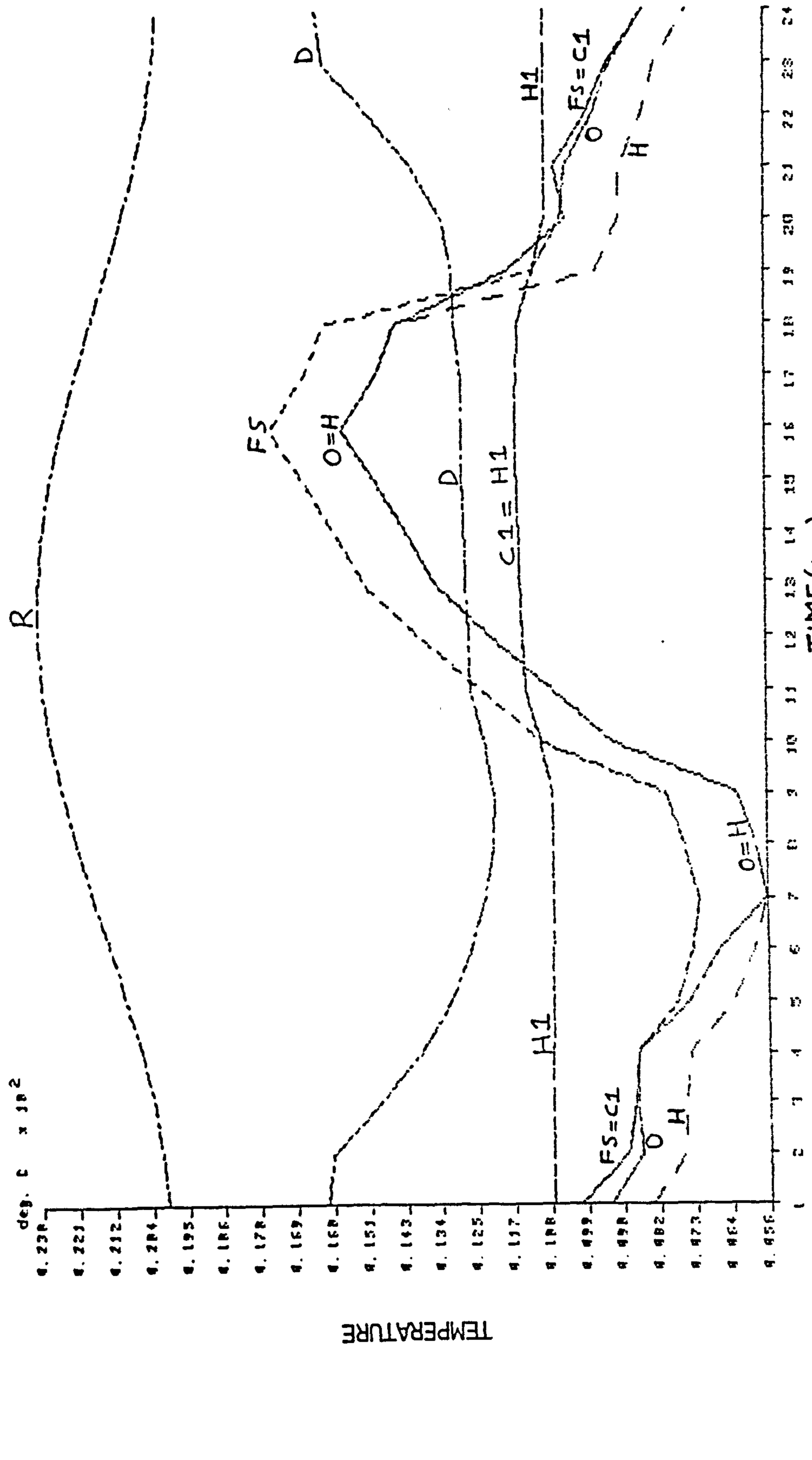

FIG. A5.13A DRY BULB TEMPERATURE PROFILES - EXERCISE 1.3 NOVEMBER 4

Ex. A.3. - Nov. 4 - temperatures

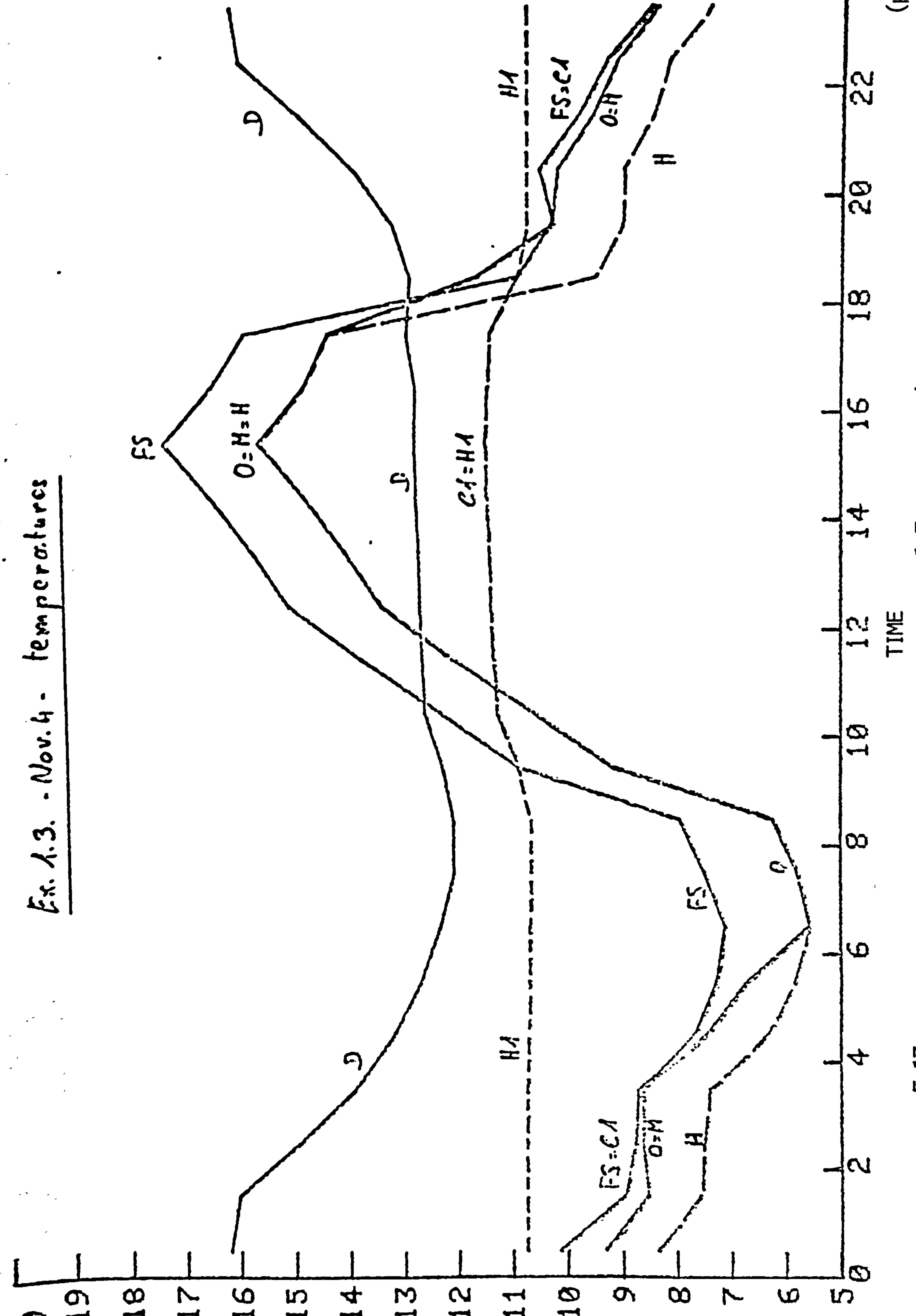

FIG. A5.13B DRY BULB TEMPERATURE PROFILES-EXERCISE 1,3 NOVEMBER 4

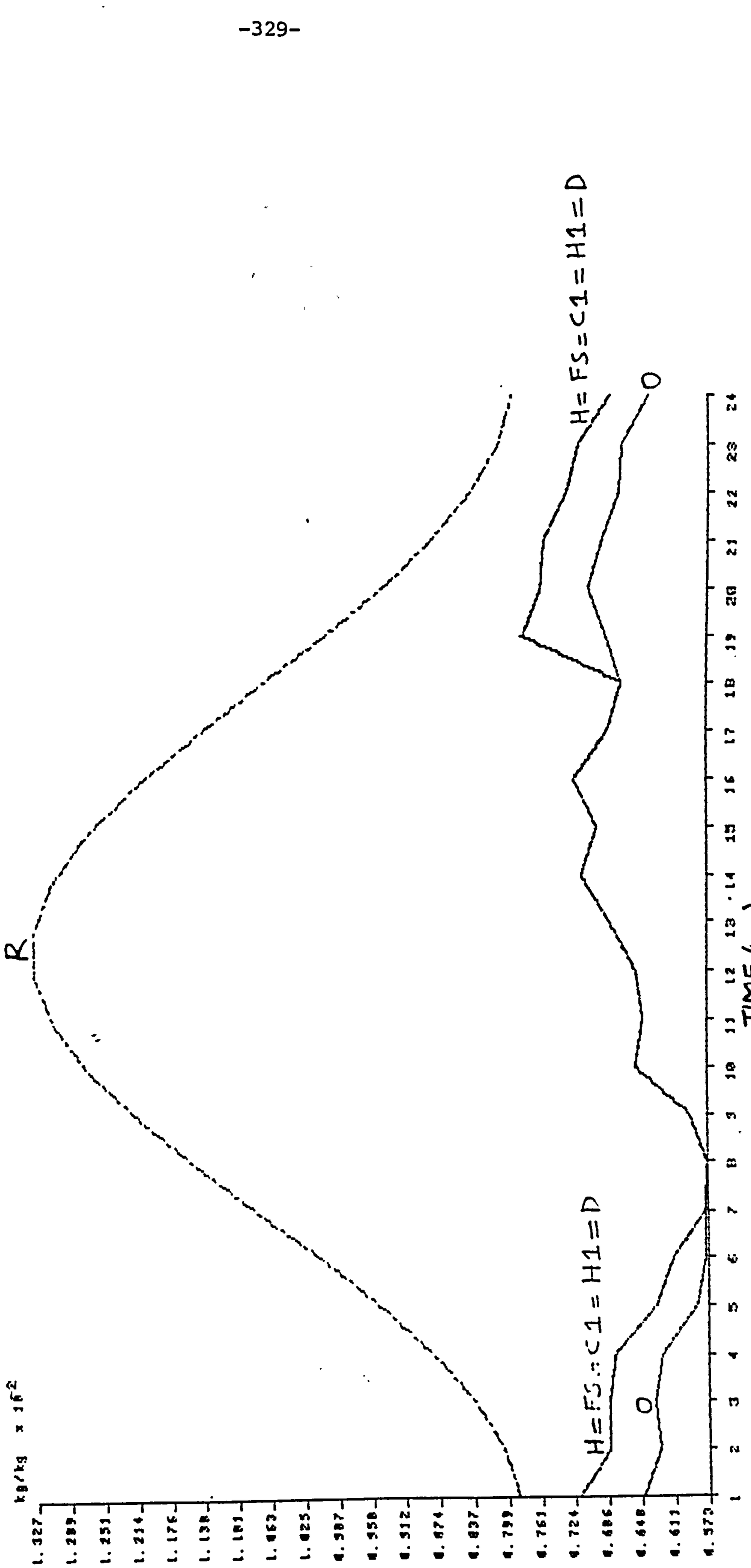

FIG. A5.14A MOISTURE CONTENT PROFILES - EXERCISE 1,3 NOVEMBER 4

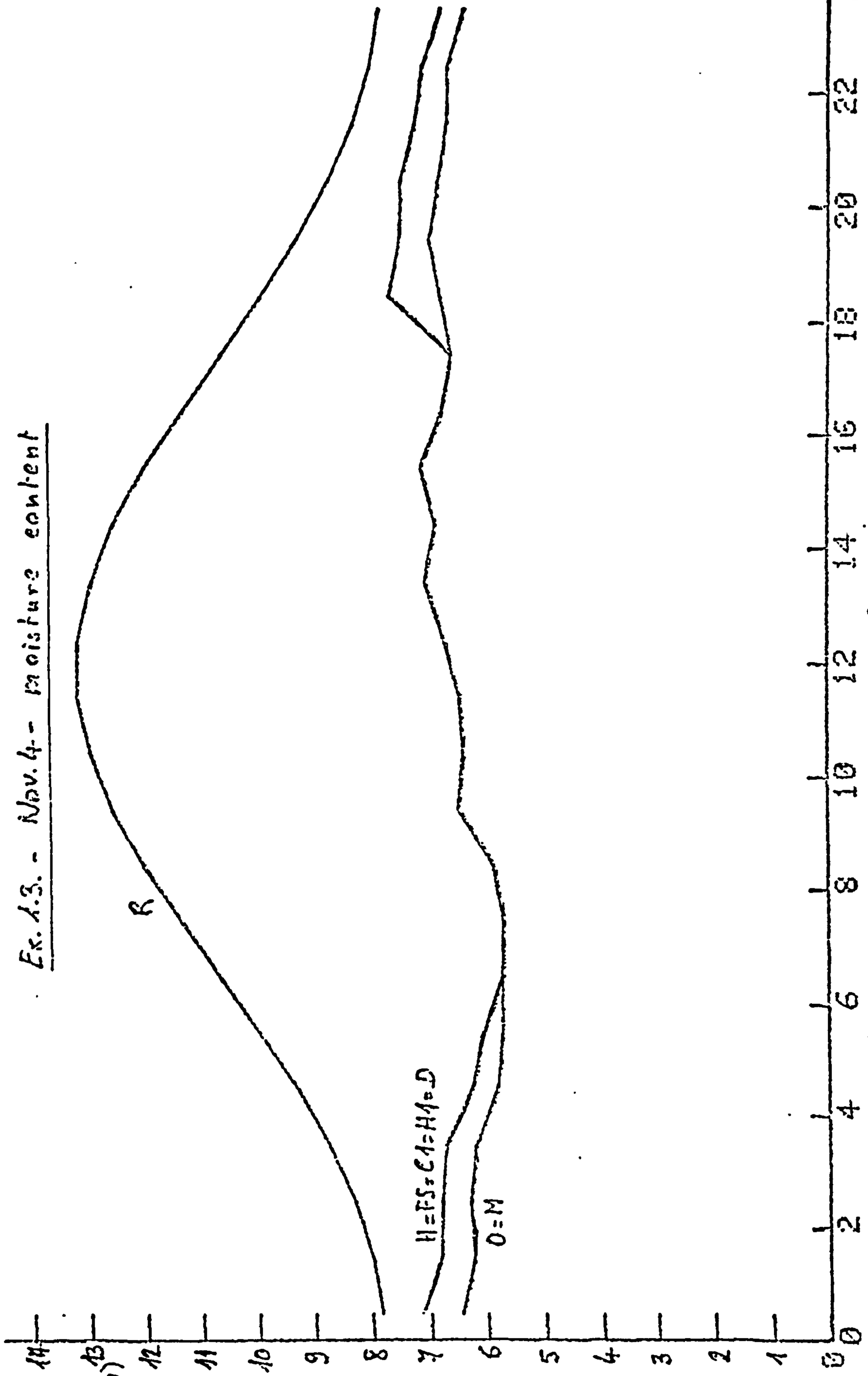

FIG. A5.14B MOISTURE CONTENT PROFILES - EXERCISE 1.3 NOVEMBER 4

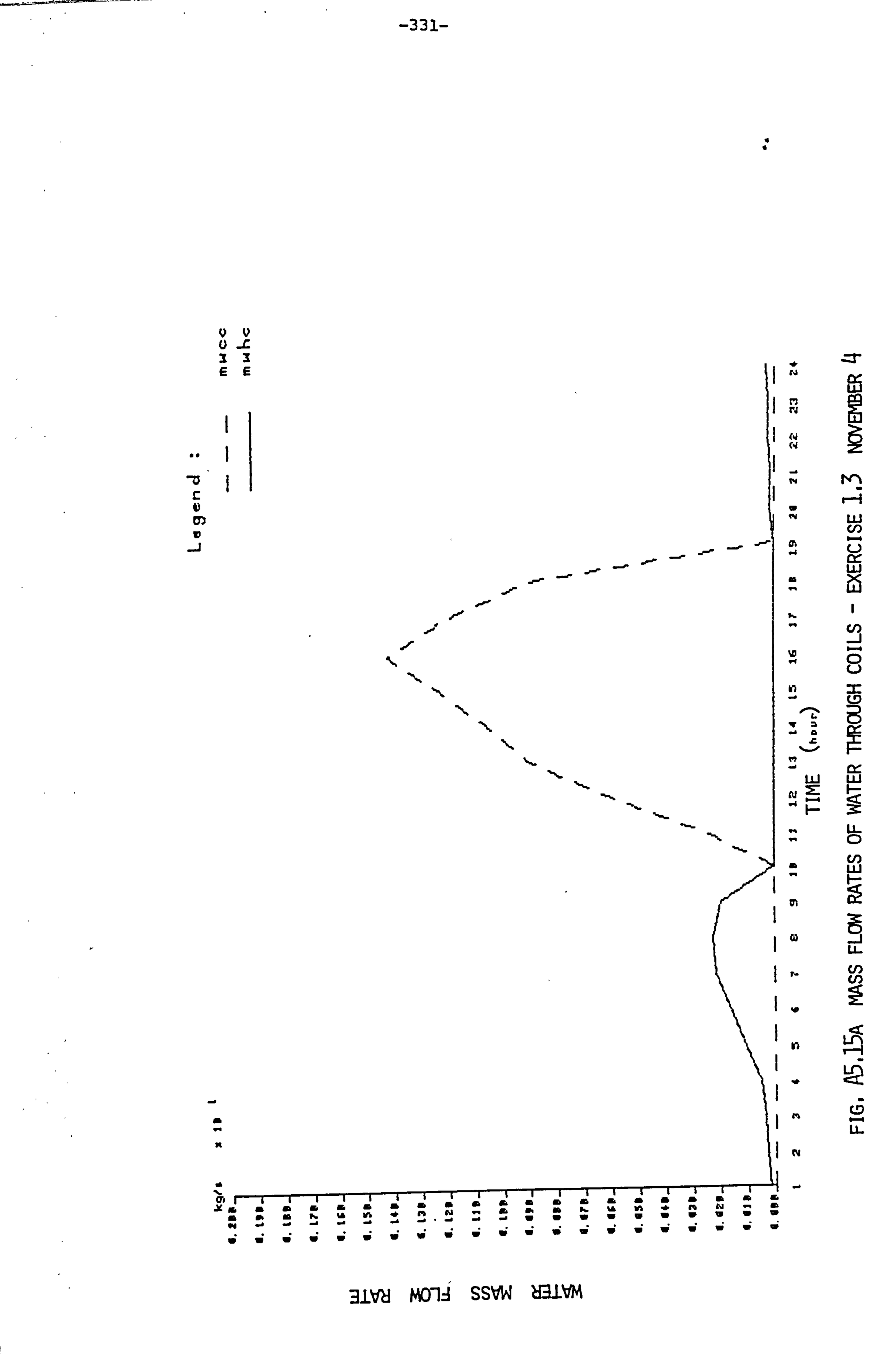

FIG, A5,15A MASS FLOW RATES OF WATER THROUGH COILS - EXERCISE 1.3 NOVEMBER 4

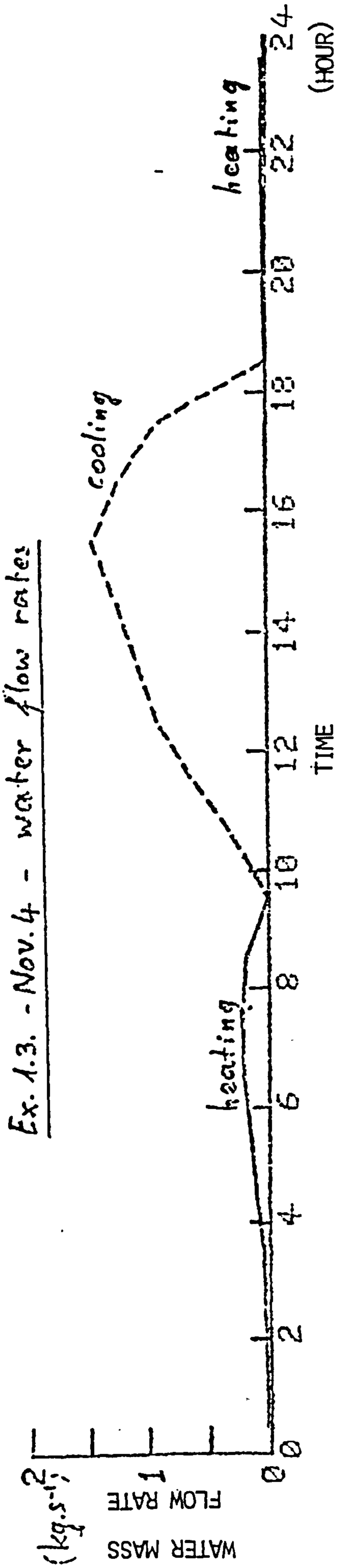

FIG. A5.15B MASS FLOW RATES OF WATER THROUGH COILS - EXERCISE 1.3 NOVEMBER 4

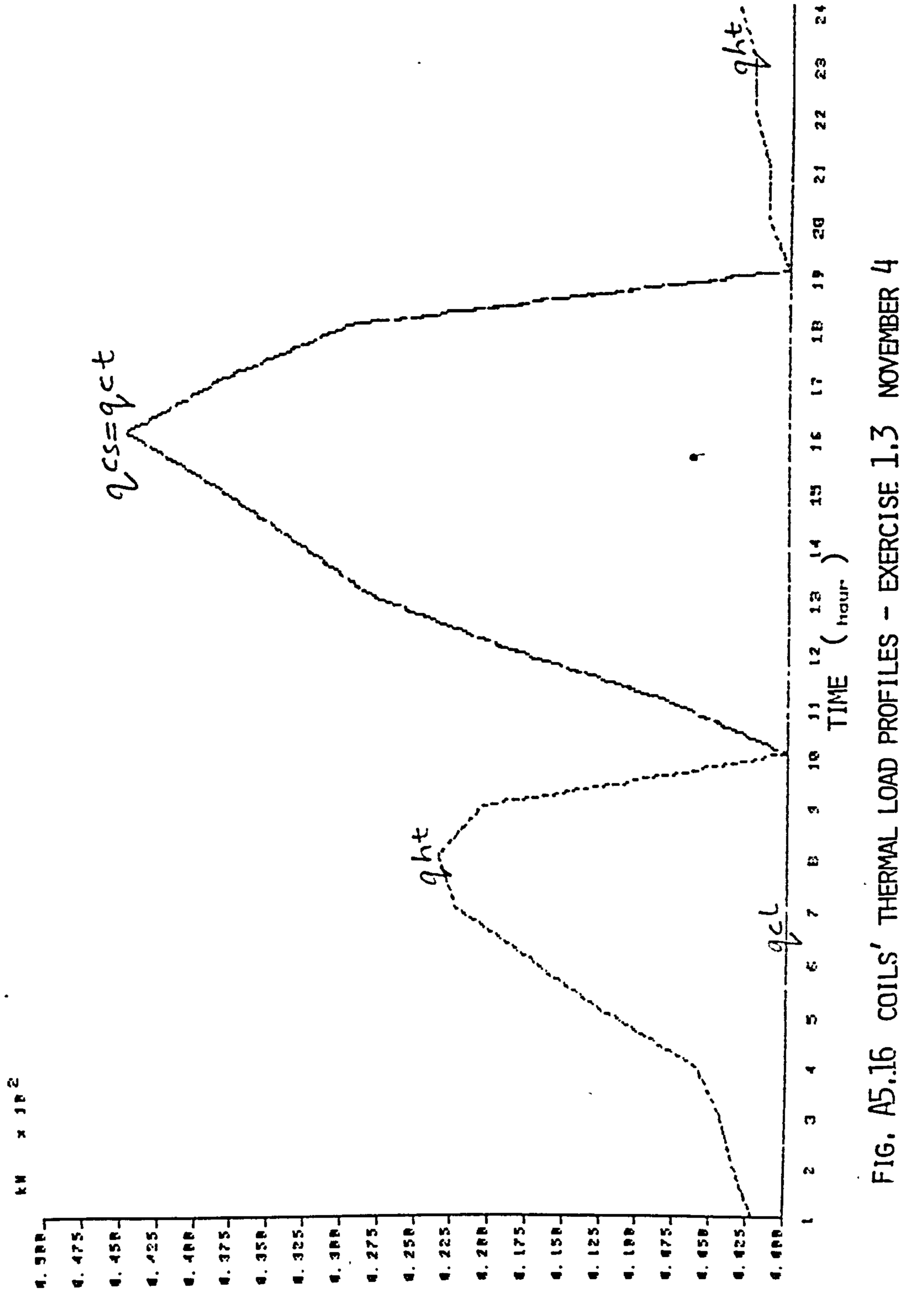

FIG. A5.16 COILS' THERMAL LOAD PROFILES - EXERCISE 1.3